Characterization of *Saccharomyces cerevisiae* Pseudohyphal Development

by
Carlos Joaquín Gimeno
B.A. University of California at Berkeley (1990)

Submitted in partial fulfillment of the
requirements for the degree of Doctor of Philosophy

at the
Massachusetts Institute of Technology
May 1994

Signature of Author_____
Department of Biology
May 1994

Certified by_____
Gerald R. Fink
Thesis Supervisor

Accepted by_____
Frank Solomon
Chairperson, Departmental
Committee on Graduate Studies

Characterization of *Saccharomyces cerevisiae* Pseudohyphal Growth

by Carlos Joaquín Gimeno

Submitted to the Department of Biology
in May 1994 in partial fulfillment of the
requirements for the Degree of Doctor of Philosophy

Abstract:

When starved for nitrogen, *MAT**a**/α Saccharomyces cerevisiae* cells undergo a dimorphic transition to pseudohyphal growth (PHG). Pseudohyphae are filaments of elongated incompletely separated cells that grow by budding, often invasively. PHG may be a foraging mechanism: pseudohyphal cells may be vectors that deliver ellipsoidal cells to new substrates. PHG is a *MAT**a**/α*-diploid-specific dimorphic transition. Mating type locus regulation may occur because the mating type locus programs the polar budding pattern of newborn *MAT**a**/α* cells that is required for PHG.

Mutations in *SHR3* cause cells to inappropriately enter the pseudohyphal pathway when growing on media where proline is sole nitrogen source. This probably occurs because *shr3/shr3* strains have impaired proline uptake so that when they grow on proline medium they are nitrogen starved. The constitutively active *RAS2^{val19}* allele inappropriately activates PHG while overexpression of cAMP phosphodiesterase 2 inhibits PHG. The latter mutation is epistatic to the former suggesting that the RAS-cAMP pathway may directly regulate PHG.

PHD1 overexpression enhances PHG and also induces PHG on rich medium. PHD1 is a nuclear protein and has a DNA binding motif similar to the DNA binding domains of the SWI4 and MBP1 transcription factors and a region of StuA, suggesting that PHD1 is a transcription factor. StuA is an

Aspergillus nidulans protein that regulates two PHG-like cell divisions. *phd1/phd1* strains undergo normal PHG when starved for nitrogen. Overexpression of *PHD1* induces *DAL81* and *POL2*. *DAL81* encodes a transcriptional inducer of nitrogen catabolic genes and *POL2*, a gene regulated by MBP1, encodes a S phase-specific DNA polymerase. These results raise the possibility that PHD1 may regulate nitrogen metabolism and the cell cycle, two processes with logical connections to PHG.

SOK2 is a PHD1 homolog (80% identity over the DNA binding motif) that may participate in the RAS-cAMP pathway. Mutant *sok2/sok2* strains undergo greatly enhanced PHG. Mutant *phd1/phd1 sok2/sok2* strains exhibit moderately enhanced PHG revealing a genetic interaction between *PHD1* and *SOK2*. PHD1 and SOK2 may act together to integrate and transduce signals that control PHG.

Thesis supervisor: Dr. Gerald R. Fink, American Cancer Society Professor of Genetics and Director of the Whitehead Institute for Biomedical Research

Acknowledgments

I would like to first thank my advisor and mentor Gerald Fink for making the laboratory portion of my graduate education comprehensive, exciting, and rewarding.

I also would like to express my gratitude to the members of my thesis committee, Phillips Robbins, Terry Orr-Weaver, Jun Liu, and John Chant, for their time and valuable input into my thesis.

I would also like to thank Cora Styles and my mentor and collaborator Per Ljungdahl for sharing their knowledge and enthusiasm with me.

I also feel indebted to Judy Bender, Chip Celenza, Jan-Huib Franssen, Julia Koehler, Steve Kron, Hans-Ulrich Mösch, and David Pellman for their help and encouragement.

I would also like to thank those people with whom I collaborated, interacted, or both and all of the people with whom I coincided in the Fink lab for helping to make my graduate career a success.

Finally, I would like to thank Ruth Hammer and my parents, Joaquín and Rosalie Gimeno, for their support and encouragement.

Table of Contents

Chapter 1:

Genetic Regulation of *Saccharomyces cerevisiae* Pseudohyphal Growth

Introduction

This chapter reviews and integrates recently published information about *Saccharomyces cerevisiae* pseudohyphal growth. For a discussion of older work on pseudohyphal growth and related issues, readers are referred to several excellent articles and books (Barnett, 1992; Barnett et al., 1979; Guilliermond, 1920; Kendrick, 1985; Mortimer and Johnston, 1986; Scherr and Weaver, 1953; van der Walt, 1970; von Wettstein, 1983).

The dimorphic transition to pseudohyphal growth is *MAT***a**/α diploid-specific and is induced by nitrogen starvation (Gimeno et al., 1992). Pseudohyphal growth can be divided into at least three distinct phases. In the first phase, an ellipsoidal yeast cell buds an elongated pseudohyphal cell (Gimeno et al., 1993). In the second phase, the elongated daughters bud identical elongated cells that compose the backbone of the pseudohypha. In the third phase, the elongated cells of the pseudohypha, with the exception of those very near the growing tip of the filament, bud vegetative ellipsoidal yeast cells. The net result is that pseudohyphal growth disperses asexually produced vegetative ellipsoidal yeast cells to new and otherwise inaccessible growth substrates. This has been interpreted to mean that pseudohyphal growth is a foraging mechanism.

Component processes of pseudohyphal growth include the diploid-specific polar budding pattern of newborn cells, cell elongation, invasive growth into substrates, and the incomplete separation of pseudohyphal mother and daughter cells (Gimeno et al., 1992). With the exception of the polar budding pattern, a property of all wild-type *MAT***a**/α diploid newborn cells, these processes are induced by nitrogen starvation. The *MAT* and

RSR1/BUD1 genes affect pseudohyphal growth because they regulate one of these processes, polar budding (Bender and Pringle, 1989; Chant and Herskowitz, 1991). *MAT***a**/α diploid cells have the polar budding pattern that permits pseudohyphal growth, whereas *MAT***a** and *MAT*α haploid cells have the axial pattern that precludes pseudohyphal growth (Chant and Pringle, 1991; Freifelder, 1960). The *RSR1/BUD1* gene is also required for the polar budding pattern; a Bud1$^-$ diploid has a random budding pattern (Chant and Herskowitz, 1991; Ruggieri et al., 1989) that impairs pseudohyphal growth (Gimeno et al., 1992).

The *SHR3* gene indirectly regulates pseudohyphal growth by a mechanism understood in some molecular detail (Gimeno et al., 1993; Ljungdahl et al., 1992). Shr3$^-$ strains inappropriately induce pseudohyphal growth when grown on proline as the sole nitrogen source. SHR3, a component of the endoplasmic reticulum (ER), is required for amino acid permeases, including the proline permease PUT4, to exit the endoplasmic reticulum and reach the plasma membrane. Thus, Shr3$^-$ strains have impaired proline uptake that results in nitrogen starvation, which consequently leads to induction of pseudohyphal growth when proline is the sole nitrogen source.

Several other genes have been reported to affect pseudohyphal growth directly or indirectly. These include protein phosphatase 2A, *ELM1*, *PAM1*, *PDE2*, *PHD1*, *RAS2*, *SOK2*, *STE7*, *STE11*, *STE12*, and *STE20*. Mutations in genes encoding any of the three subunits of protein phosphatase 2A can cause filamentous growth (Blacketer et al., 1993; Healy et al., 1991; Ronne et al., 1991; van Zyl et al., 1992) and some of these mutations interact with mutant alleles of the *PAM1* or *ELM1* genes (Blacketer et al., 1993; Hu and Ronne, 1994). The PAM1 protein is unrelated to proteins in databases while

ELM1 is related to protein kinases. *PHD1* and *SOK2* encode putative transcription factors that strongly enhance pseudohyphal growth when overexpressed and disrupted, respectively (Gimeno, 1994; Gimeno and Fink, 1994; Ward and Garrett, 1994). The PHD1 and SOK2 proteins are homologous to *Aspergillus nidulans* StuA, a regulatory protein that controls two pseudohyphal growth-like cell divisions during conidiogenesis (Timberlake, 1991). The *RAS2* and *PDE2* genes encode components of the RAS-cAMP signal transduction pathway (Broach and Deschennes, 1990). Ectopic activation of *RAS2* induces pseudohyphal growth under inappropriate conditions while *PDE2* overexpression inhibits pseudohyphal growth (Gimeno et al., 1992; Gimeno et al., 1993). *STE7*, *STE11*, *STE12*, and *STE20* encode components of a signal transduction pathway that regulates mating-specific genes and some genes linked to either transposon Ty or the repeated element sigma (Sprague and Thorner, 1992). Loss of function of any of these four genes causes impaired pseudohyphal growth (Liu et al., 1993). The mechanisms by which these varied genes regulate pseudohyphal growth are not yet clear and their elucidation is the next frontier in the pseudohyphal growth field.

Genes and Proteins that Directly or Indirectly Regulate Pseudohyphal Growth

SHR3 and Amino Acid Permeases

SHR3 is the gene whose mechanism of pseudohyphal growth regulation is understood in most detail. *SHR3* was identified as a gene that when mutated confers upon yeast cells resistance to 30 mM histidine (Ljungdahl et al., 1992). Mutant *shr3* strains have pleiotropically impaired amino acid uptake (Gimeno et al., 1993; Ljungdahl et al., 1992) and the *shr3* mutation is synthetically lethal with several mutations that cause amino acid auxotrophies. In addition, *shr3* strains constitutively induce the translation of *GCN4*, a gene encoding a positive regulator of amino acid biosynthetic genes that is only translated under conditions of amino acid starvation (Hinnebusch, 1988).

Cloning and sequencing of *SHR3* revealed that its predicted protein product is not homologous to known proteins and is probably an integral membrane protein and other experiments showed that it is a component of the ER membrane. The impaired amino acid transport observed in *shr3* strains occurs because many amino acid permeases fail to exit the ER and reach the plasma membrane, where they are functionally expressed. The permeases are found to be at least partially inserted into the ER membrane but do not assume their normal topology. This phenomenon appears to be specific to amino acid permeases because several other secretory proteins including the plasma membrane [H+]ATPase, α factor, **a** factor, invertase, and the vacuolar enzyme carboxypeptidase Y are secreted normally in *shr3* strains.

Haploid *shr3* strains grow slowly when they utilize proline as sole nitrogen source because of their proline uptake defect. Diploid *shr3/shr3* strains not only grow slowly on proline, but also ectopically enter the pseudohyphal growth pathway (Gimeno et al., 1992). It seems likely that the nitrogen starvation experienced by *shr3* strains utilizing proline as sole nitrogen source induces them to undergo pseudohyphal growth. Thus, *SHR3* affects pseudohyphal growth indirectly by controlling the secretion of amino acid permeases.

The Mating Type Locus and *BUD* Genes

The polar budding pattern of newborn diploid cells is regulated by a cell's ploidy as reflected by its genotype at the mating type (*MAT*) locus and is the only component process of pseudohyphal growth that is not induced by nitrogen starvation. Only *MAT**a**/α* diploids and not *MAT**a*** or *MATα* haploids or *MAT**a**/**a*** or *MATα/α* diploids show pseudohyphal growth, indicating that the *MAT* locus controls this dimorphic transition (Gimeno et al., 1992). The *MAT* locus also controls the budding pattern of yeast strains (Chant and Pringle, 1991; Herskowitz, 1989). Cells expressing only *MAT**a*** or *MATα* bud in the axial pattern whereas cells expressing both *MAT**a*** and *MATα* bud in a polar manner (see Table 1 in Chapter 2). The axial pattern leads to budding at the junction of two cells and cannot extend the filament. Only the polar budding pattern of wild-type diploid cells in which new buds emerge from the daughter on the side opposite the junction to her mother is consistent with pseudohyphal growth. In fact, it has been clearly shown by time lapse photomicroscopy that pseudohyphae elongate by polar budding by newborn cells (Gimeno et al., 1992).

Budding pattern genes represented by *BUD1-BUD5* are required for selection of the proper bud site and consequently for establishing the proper axis of cell division (Bender and Pringle, 1989; Chant et al., 1991; Chant and Herskowitz, 1991; Park et al., 1993). *BUD1*, *BUD2*, and *BUD5* convert the default random budding pattern to bipolar and subsequent action of *BUD3* and *BUD4* converts bipolar to axial (Chant and Herskowitz, 1991). To explain the observed cell type specificity (diploids are bipolar, haploids axial) an elegant model was proposed that either or both *BUD3* and *BUD4* are repressed by the repressor a1α2 found only in *MAT**a**/α* cells (Chant and Herskowitz, 1991). That a *MAT**a**/α* diploid strain with a random budding pattern caused by a mutant allele of *BUD1* has impaired pseudohyphal growth demonstrated that *BUD* genes are important for pseudohyphal growth. This observation was recently expanded with the discovery that a *bud4* haploid strain that has the polar budding pattern undergoes pseudohyphal growth when starved for nitrogen (Sanders and Herskowitz, 1994).

The cell type specificity of pseudohyphal growth is best understood by considering the different roles of diploid and haploid cells in the *S. cerevisiae* life cycle (Gimeno and Fink, 1992). The diploid is the assimilative phase of *S. cerevisiae* and the predominant cell type found growing in nature (Lodder, 1970). Thus, the diploid phase must be specialized to deal with a variety of nutritional conditions and stresses. Diploids have two cell type-specific nutrient stress responses, sporulation and pseudohyphal growth. It has been proposed that the diploid polar budding pattern exists at least in part to allow one of these processes, pseudohyphal growth (Gimeno et al., 1992). In this model, diploid cells are specifically able to undergo pseudohyphal growth and foraging because they are the cell type that is specialized for assimilating nutrients.

The haploid phase is transient in the life cycle of *S. cerevisiae* and functions as a gamete. Haploid cells are specialized to rapidly reform the diploid phase immediately after ascospore germination. As I explain below, it is thought that haploids have the axial budding pattern, which precludes pseudohyphal growth, to enable them to perform mating efficiently (Nasmyth, 1982). The diploid phase is usually reconstituted when the two *MAT**a*** spores in the ascus mate with their two *MAT*α sister spores (Hicks et al., 1977). If an ascospore becomes separated from its mate, it uses its mating type interconversion system and axial budding pattern to efficiently reconstitute the diploid phase. The action of the mating type interconversion system results in two cells of ascospore-derived four celled microcolonies being *MAT**a*** and two cells being *MAT*α. The axial budding pattern causes the cells of opposite mating types to be juxtaposed allowing efficient mating. Thus haploid cells are specialized for mating and specifically have the axial budding pattern, which prevents pseudohyphal growth, to make mating more efficient. In this model, haploids do not need to be able to undergo pseudohyphal growth because the goal of their transient existence is to reform the pseudohyphal growth-competent diploid phase.

The RAS-cAMP Signaling Pathway

The RAS-cAMP signaling pathway regulates mitotic growth, sporulation, stationary phase, and pseudohyphal growth (Broach, 1991; Broach and Deschennes, 1990; Gimeno, 1994; Gimeno et al., 1992). The RAS1 and RAS2 proteins are low molecular weight GTP-binding proteins that are associated with the plasma membrane (Fig. 1.1). When they are bound to GTP they are active as signal transduction molecules, and when they are

Figure 1.1 The RAS-cAMP pathway. The RAS1 and RAS2 proteins are inactive as signal transducers when bound to GDP. CDC25 promotes the RAS proteins to undergo GDP-GTP exchange. When bound to GTP, RAS1 and RAS2 stimulate adenylate cyclase (CYR1) to convert ATP to cAMP. cAMP binds to the regulatory subunit of cAMP-dependent protein kinase (BCY1) releasing the catalytic subunits (TPK1, TPK2, TPK3) which are active protein kinases. IRA1 and IRA2 turn off RAS1 and RAS2 by promoting hydrolysis of RAS-bound GTP to GDP. The cAMP phosphodiesterases PDE1 and PDE2 turn off cAMP-dependent protein kinase by hydrolyzing cAMP to AMP. When intracellular cAMP levels decrease BCY1 releases cAMP and associates with the TPK proteins, inactivating them.

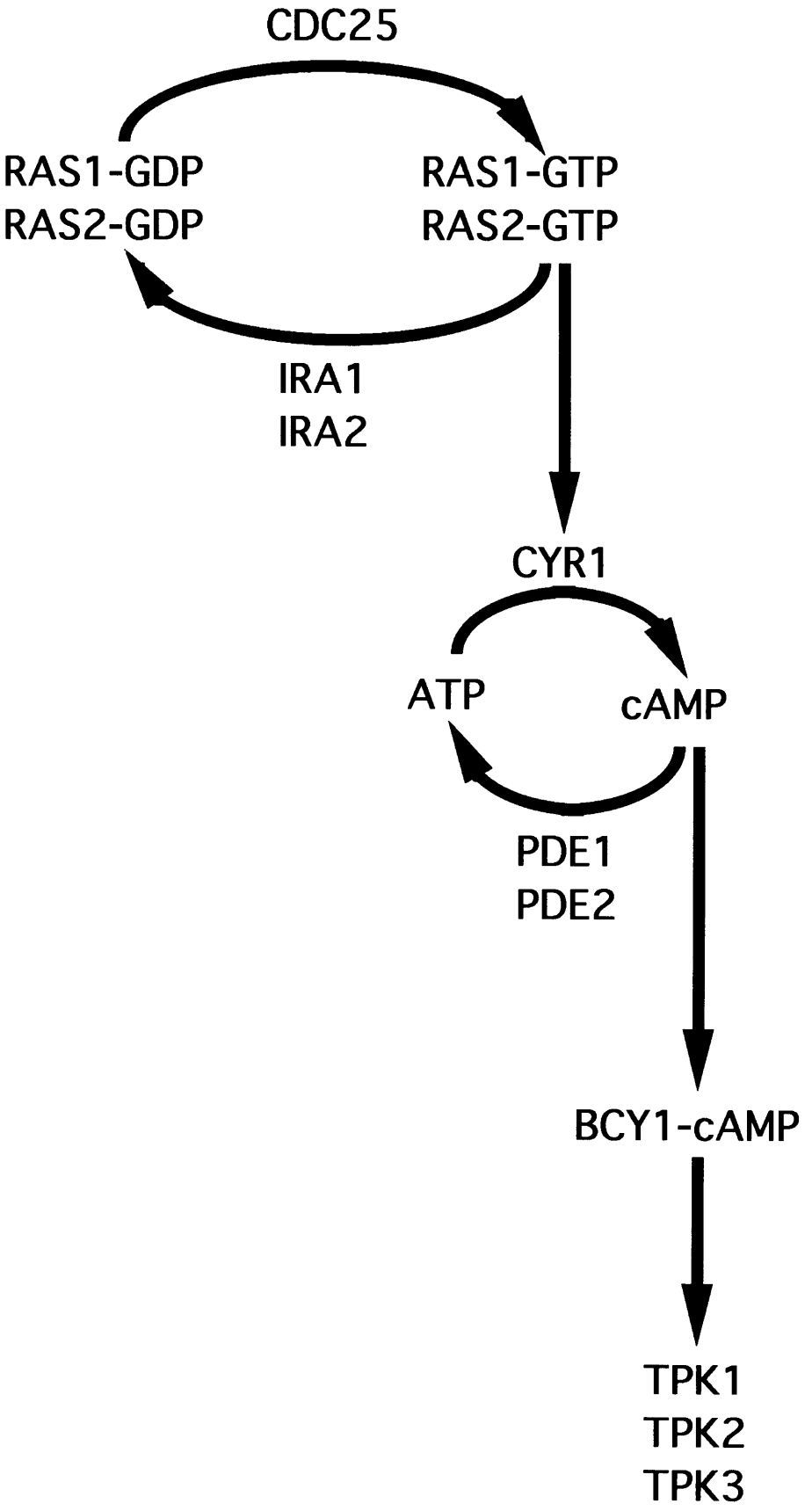
CDC25
RAS1-GDP
RAS2-GDP
RAS1-GTP
RAS2-GTP
IRA1
IRA2
CYR1
ATP
cAMP
PDE1
PDE2
BCY1-cAMP
TPK1
TPK2
TPK3

bound to GDP they are inactive. Regulation of the activity of the RAS proteins involves the CDC25 protein which promotes the exchange of GDP for GTP, and the functionally redundant IRA1 and IRA2 proteins which stimulate the intrinsic GTPase activity of the RAS proteins, causing their bound GTP to be converted to GDP. GTP-bound RAS proteins stimulate *CYR1*-encoded adenylate cyclase to convert ATP to cAMP, a second messenger molecule. cAMP acts by controlling the activity of cAMP-dependent protein kinase, an enzyme that, when inactive, exists in the cell as a heterotetramer composed of two regulatory subunits encoded by *BCY1* and two catalytic subunits encoded by three functionally redundant genes, *TPK1*, *TPK2*, and *TPK3*. When high levels of cAMP are generated in the cell, cAMP molecules bind to BCY1 proteins, and these complexes disassociate from the TPK proteins. Free TPK proteins are catalytically active serine-threonine protein kinases that regulate the activity of their substrates by phosphorylating them. Substrates are thought to include several enzymes involved in carbohydrate metabolism and some RAS-cAMP pathway components (Broach and Deschennes, 1990). At the level of cAMP, the RAS-cAMP pathway is downregulated by two genes, *PDE1* and *PDE2*, encoding low and high affinity phosphodiesterases, respectively. Other genes that may participate in the RAS-cAMP signaling pathway are known, but how they fit into the pathway is not well understood (Broach, 1991).

Strains that have an inactive RAS-cAMP pathway are inviable (Broach and Deschennes, 1990). Such strains include *cdc25* strains, *ras1 ras2* strains, *cyr1* strains, and *tpk1 tpk2 tpk3* strains. In general, strains that experience a sudden inactivation of the RAS-cAMP pathway arrest growth as unbudded cells if they are haploid and sporulate if they are diploid. Strains with a hypoactive RAS-cAMP pathway cannot grow on nonfermentable carbon

sources and accumulate carbohydrate reserves. *MAT**a**/α* strains that have a hypoactive RAS-cAMP pathway because they overexpress *PDE2* have severely inhibited pseudohyphal growth (Gimeno, 1994, Chapter 6). Strains that have a hyperactive RAS-cAMP pathway are hypersensitive to heat shock and nitrogen starvation, lose their carbohydrate reserves, and cannot sporulate efficiently. A *MAT**a**/α* yeast strain that has a hyperactive RAS-cAMP pathway because it carries the dominant constitutively active $RAS2^{val19}$ allele (Kataoka et al., 1984) exhibits enhanced pseudohyphal growth. Inhibition of pseudohyphal growth by *PDE2* overexpression is epistatic to enhancement of pseudohyphal growth by $RAS2^{val19}$, suggesting that $RAS2^{val19}$ enhances pseudohyphal growth by raising intracellular cAMP levels which probably then cause activation of cAMP-dependent protein kinase. Taken together, these results suggest that cells consider information transmitted by the RAS-cAMP signaling pathway when deciding whether or not to undergo pseudohyphal growth.

The only well characterized environmental signal that activates the RAS-cAMP pathway is the addition of glucose or a related fermentable sugar to yeast cells that are starved for glucose, have been growing on a nonfermentable carbon source, or are in stationary phase (Broach and Deschennes, 1990). Within two minutes of this treament, intracellular levels of cAMP rise 10 to 50 fold. Soon after this cAMP spike, cAMP levels fall to a basal level that is about two fold higher than the level of cAMP that existed in the cell when it was starved for carbon. Thus, upregulation of the RAS-cAMP pathway is associated with growth on a good carbon source and downregulation of the RAS-cAMP pathway correlates with carbon starvation. These relationships are consistent with the effects of perturbations in the RAS-cAMP pathway on carbohydrate reserves: upregulation of the RAS-cAMP

pathway causes depletion of carbohydrate reserves, whereas downregulation of the RAS-cAMP pathway causes accumulation of these reserves. These effects result because active cAMP-dependent protein kinase directly or indirectly activates enzymes that break down storage carbohydrates and inactivates enzymes that synthesize them. These facts suggest that one role of the RAS-cAMP pathway is to communicate information to the cell about the availability of carbon sources. As discussed in detail in Chapter 6, information about carbon status is relevant for a cell's decision to undergo pseudohyphal growth and this may explain why the RAS-cAMP pathway regulates pseudohyphal growth.

Putative Transcription Factors PHD1 and SOK2

PHD1 and *SOK2* are two related genes that have interesting pseudohyphal growth regulatory properties. *PHD1* was identified as a high copy number enhancer of pseudohyphal growth (Gimeno and Fink, 1994). *PHD1* overexpression causes *MAT**a**/α* strains to manifest prolific pseudohyphal growth earlier than wild-type controls. Also, the pseudohyphal cells of strains overexpressing *PHD1* are more elongated than wild-type pseudohyphal cells. Significantly, *PHD1* overexpression also induces pseudohyphal growth in *MAT**a**/α* cells growing on rich medium. As determined by indirect immunofluorescence, PHD1 protein localizes to the nucleus. The 366 amino acid PHD1 protein has a 100 amino acid DNA binding motif related to that of the *S. cerevisiae* transcription factors SWI4 and MBP1. These facts suggest that PHD1 may be a transcription factor. The DNA binding motif in PHD1 is about 70% identical to a region of *A. nidulans* StuA. This homology is interesting because StuA regulates the two pseudohyphal

growth-like cell divisions that occur during conidiophore morphogenesis (Miller et al., 1991; Miller et al., 1992; Timberlake, 1990; Timberlake, 1991). A *MAT**a**/α phd1/phd1* strain undergoes normal pseudohyphal growth in a qualitative pseudohyphal growth assay.

Insights into the possible cellular role of *PHD1* were gained by the identification of genes that are induced when *PHD1* is overexpressed (Gimeno, 1994, Chapter 5). Three essential and two probably nonessential genes that are induced by *PHD1* overexpression were identified. Two of these genes are *POL2* and *DAL81* and the three others have not been previously characterized. *POL2* is a DNA polymerase involved in DNA repair and chromosomal DNA replication (Budd and Campbell, 1993; Morrison et al., 1990; Wang et al., 1993). *POL2* is regulated by MBP1 (Johnston and Lowndes, 1992), a transcription factor whose DNA binding domain is related to the DNA binding motif in PHD1, which induces *POL2* expression during the G1 to S transition. This raises the interesting possibility that PHD1 may control the MBP1 regulon which includes genes that regulate cell elongation and cell separation, two component processes of pseudohyphal growth (Gimeno and Fink, 1994).

DAL81 is a transcriptional regulator required for the induced expression of several genes encoding enzymes that catabolize poor sources of nitrogen (Bricmont and Cooper, 1989; Bricmont et al., 1991; Coornaert et al., 1991). *DAL81* is induced by nitrogen starvation and *RAS2^{val19}* (Gimeno, 1994), two conditions that activate the pseudohyphal growth pathway (Gimeno et al., 1992). It is possible that *PHD1* is involved in the transduction of the nitrogen starvation signal, the *RAS2^{val19}* signal, or both to *DAL81*. *DAL81* appears not to be required for the pseudohyphal growth component processes of cell elongation, agar invasion, and incomplete cell separation. The absense of a

pseudohyphal growth phenotype in *dal81/dal81* mutants raises the possibility that *PHD1* may induce *DAL81* so that cells in the pseudohyphal growth mode have the catabolic enzymes they need to utilize the poor nitrogen sources that they are likely to encounter while foraging.

SOK2 was isolated by Mary Ward and Stephen Garrett as a high copy number suppressor of the temperature-sensitive growth defect of a *tpk1⁻ tpk2(ts) tpk3⁻* mutant (Ward and Garrett, 1994). Subsequently, deletion of *SOK2* was found to exacerbate the temperature sensitivity of the *tpk2(ts)* mutation. Together, these results suggest that SOK2 may function in the RAS-cAMP pathway downstream of cAMP-dependent protein kinase. *SOK2* is predicted to encode a 470 amino acid protein that contains a DNA binding motif that is 81.7% identical to the DNA binding motif found in PHD1. Because PHD1 and the RAS-cAMP pathway have been implicated in pseudohyphal growth control, the possible role of SOK2 in pseudohyphal growth was studied.

Overexpression of *SOK2* from a 2μm plasmid weakly enhances pseudohyphal growth and disruption of *SOK2* causes strongly enhanced pseudohyphal growth. *MAT**a**/α phd1/phd1 sok2/sok2* double mutants exhibit enhanced pseudohyphal growth that is less vigorous than that of *MAT**a**/α sok2/sok2* strains. Thus, the enhanced pseudohyphal growth manifested by *MAT**a**/α sok2/sok2* strains is partially *PHD1*-dependent. The bulk of these observations could be explained if one or more pseudohyphal growth genes were positively regulated by PHD1 and negatively regulated by SOK2 and if these two proteins competed for the same regulatory binding sites in the promoters of these pseudohyphal growth genes. Because *phd1/phd1* strains exhibit normal pseudohyphal growth and *sok2/sok2 phd1/phd1* strains exhibit moderately enhanced pseudohyphal growth, this model predicts that yeast

has at least one gene whose function is redundant with the pseudohyphal growth regulatory function of *PHD1*.

It is interesting that the RAS-cAMP pathway regulates pseudohyphal growth and genetically interacts with *SOK2* and that *SOK2* genetically interacts with *PHD1*. It is possible that SOK2 and PHD1 are members of a group of structurally related transcription factors that respond to and integrate the signals that influence a cell's decision to enter the pseudohyphal growth mode.

Pheromone Response Genes

Haploid *S. cerevisiae* cells have a signal transduction pathway that transmits the signal that a mating partner is nearby (Sprague and Thorner, 1992). At the apex of this pathway is a plasma membrane receptor (STE2 or STE3) that binds to a peptide pheromone (MFA1, MFA2, MFα1, and MFα2) secreted by a cells of the opposite mating type. The pheromone bound receptor interacts with a heterotrimeric G protein (GPA1, STE4, and STE18) that is thought to directly or indirectly activate a protein kinase (STE20) and a protein whose function is unknown (STE5). These proteins are thought to stimulate various protein kinases (STE11, STE7, KSS1, and FUS3) that directly or indirectly activate a transcription factor (STE12).

STE12 has several functions including the activation of mating-specific genes and some genes linked to transposon Ty (Errede and Ammerer, 1989). Additionally, STE12 probably regulates some genes linked to the repeated element sigma (Van Arsdell et al., 1987). STE12 protein activates mating-specific genes by binding to a specific DNA sequence present in their promoters (Errede and Ammerer, 1989). Ty contains this specific STE12

binding site so that it often puts genes into whose promoters it has transposed under the control of STE12 and upstream pheromone signaling pathway components (Ciriacy et al., 1991; Dubois et al., 1982; Errede et al., 1980; Taguchi et al., 1984). Interestingly, STE12 and other components of the pheromone signaling pathway are required for carbon source regulation of some Ty-linked genes (Taguchi et al., 1984).

Of the genes that encode the pheromone response pathway components mentioned in the preceding paragraph, only *KSS1*, *STE7*, *STE11*, *STE12*, and *STE20* are known to be expressed in *MAT**a**/α* cells (Liu et al., 1993; Sprague and Thorner, 1992). Mutations in *STE7*, *STE11*, *STE12*, and *STE20* but not mutations in *KSS1* impair pseudohyphal growth (Liu et al., 1993). Activated alleles of *STE11* and *STE12* enhance pseudohyphal growth and enhancement by active *STE11* requires *STE12*. Mutations in *STE2*, *STE3*, *STE4*, *STE18*, and *FUS3* do not affect pseudohyphal growth. It is not known whether mutations in *MFA1*, *MFA2*, *MFα1*, *MFα2*, or *GPA1* affect pseudohyphal growth. These results show that some of the pheromone signaling pathway components that are expressed in *MAT**a**/α* cells directly or indirectly regulate pseudohyphal growth. It would be interesting to know if these genes regulate pseudohyphal growth by activating mating-specific genes, Ty-linked genes, or by some other mechanism.

Protein Kinases, Protein Phosphatases, and Interacting Proteins

Recently a genetic screen was reported that identified haploid yeast mutants that are constitutively elongated (Blacketer et al., 1993). The *elm1*, *elm2*, and *elm3* mutants were the focus of this study. Mutations in *ELM1*, *ELM2*, or *ELM3* in *MAT**a**/α* strains constitutively induce invasive

pseudohyphal growth. Interestingly, strains that are heterozygous at the *ELM2* or *ELM3* loci have enhanced pseudohyphal growth on nitrogen starvation medium. *ELM1* was cloned and encodes a putative protein kinase. Deletion of *ELM1* in haploid strains caused cell elongation and incomplete cell separation while *elm1Δ/elm1Δ* diploids exhibited constitutive pseudohyphal growth.

Protein phosphatase 2A (PP2A) is one of four superfamilies of protein phosphatases (Cohen, 1989). In both yeast and higher organisms this enzyme is comprised of at least two regulatory subunits (A and B) and a catalytic subunit (C) (Cohen, 1989; Peng et al., 1991). The product of *TPD3* is thought to encode the A regulatory subunit of PP2A (van Zyl et al., 1992) while the product of the *CDC55* gene probably encodes the B regulatory subunit (Healy et al., 1991). Deletion of *TPD3* or *CDC55* causes a filamentous phenotype (Blacketer et al., 1993; Healy et al., 1991; van Zyl et al., 1992). The filamentous structures formed by $Tpd3^-$ or $Cdc55^-$ strains are elongated, multinucleate, and have constrictions and diffuse nuclei. Three redundant genes, *PPH3*, *PPH21*, and *PPH22*, have been reported to encode putative catalytic subunits (C subunits) of protein phosphatase 2A (Ronne et al., 1991). Interestingly, mutant alleles of these gene cause morphological phenotypes (Ronne et al., 1991) including cell elongation, which is caused by *PPH22* overexpression. There is evidence that PP2A is involved in carbohydrate metabolism. PP2A activates glycogen synthase *in vitro* by dephosphorylating it (Peng et al., 1991). This is particularly interesting because glycogen synthase is thought to be activated directly or indirectly by phosphorylation by cAMP-dependent protein kinase (Broach and Deschennes, 1990). Thus, PP2A and the RAS-cAMP pathway, which has been implicated in

pseudohyphal growth control (Gimeno, 1994, Chapter 6; Gimeno et al., 1992), may have a common target.

A gene called *PAM1* was isolated as a high copy number suppressor of the inviability of *pph3 pph21 pph22* triple mutants (Hu and Ronne, 1994). The *PAM1* product is predicted to be a hydrophilic 93 kD protein that contains two coiled coil motifs and has a basic carboxyl-terminal region. PAM1 is not significantly related to known proteins. Interestingly, overexpression of *PAM1* induces pseudohyphal growth (Hu and Ronne, 1994). The pseudohyphal cells in the *PAM1* overexpression-induced pseudohyphae are well separated and mononucleate.

Interestingly, the *ELM1* gene interacts with *CDC55* (Blacketer et al., 1993). Double *cdc55 elm1* mutants have a synthetic growth defect, have highly abnormal morphologies, have a defect in either or both cytokinesis and cell separation. This result suggests that *ELM1* and *CDC55* may be involved in the same cellular function. Other evidence that *CDC55* may be involved in pseudohyphal growth is that strains heterozygous for *CDC55* have enhanced pseudohyphal growth on nitrogen starvation medium and no pseudohyphal growth phenotypes on rich medium (Blacketer et al., 1993).

It should also be mentioned that the redundant PPZ1 and PPZ2 putative protein phosphatases have also been implicated in pseudohyphal growth control. PPZ1 and PPZ2 are thought to be involved in the PKC signaling pathway and *ppz1 ppz2* strains undergo pseudohyphal growth when grown in osmotically supported medium (Lee et al., 1993). Taken together, these results suggest that protein phosphorylation is important in regulating pseudohyphal growth. It is now important to systematically study the role of the genes discussed in this section in pseudohyphal growth regulation.

Conclusions

The genetic regulation of *S. cerevisiae* pseudohyphal growth promises to be complicated (Table 1.1). To date, research into this area has focused on the identification of genes whose mutation affects pseudohyphal growth. Only in the case of *SHR3* is the molecular mechanism of pseudohyphal growth control understood in some detail. The mating type locus and *BUD* genes control pseudohyphal growth most likely by programming the polar budding pattern of newborn cells. The molecular mechanism of this programming as well as how the *BUD* gene products determine budding pattern are active research areas. Genes directly involved in the well characterized RAS-cAMP and pheromone signal transduction pathways have been implicated in pseudohyphal growth control. Also, *PHD1* and *SOK2*, new genes whose products have interesting homologies to well characterized transcription factors and developmental regulators have also been implicated in pseudohyphal growth control. ELM1, a protein kinase of unknown function, protein phosphatases, and PAM1, a protein phosphatase interacting protein may also play direct roles in pseudohyphal growth control.

Now that a long list of possible direct regulators of pseudohyphal growth exists, it is possible to systematically determine each one's function in pseudohyphal growth control. In Chapter 7, possible systematic approaches to determine whether a gene whose mutation affects pseudohyphal growth directly affects this process are presented. Reagents and technical advances that would help the pseudohyphal growth field make rapid progress are also presented.

Literature Cited

Barnett, J. A. (1992). The taxonomy of the genus *Saccharomyces* Meyen *ex* Reess: a short review for non-taxonomists. Yeast *8,* 1-23.

Barnett, J. A., Payne, R. W., and Yarrow, D. (1979). A Guide to Identifying and Classifying Yeasts. (Cambridge: Cambridge University Press).

Bender, A., and Pringle, J. R. (1989). Multicopy suppression of the *cdc24* budding defect in yeast by *CDC42* and three newly identified genes including the ras-related gene *RSR1*. Proc. Natl. Acad. Sci. USA *86,* 9976-9980.

Blacketer, M. J., Koehler, C. M., Coats, S. G., Myers, A. M., and Madaule, P. (1993). Regulation of dimorphism in *Saccharomyces cerevisiae*: involvement of the novel protein kinase homolog Elm1p and protein phosphatase 2A. Mol. Cell. Biol. *13,* 5567-5581.

Bricmont, P. A., and Cooper, T. G. (1989). A gene product needed for induction of allantoin system genes in *Saccharomyces cerevisiae* but not for their transcriptional activation. Mol. Cell. Biol. *9,* 3869-3877.

Bricmont, P. A., Daugherty, J. R., and Cooper, T. G. (1991). The *DAL81* gene product is required for induced expression of two differently regulated nitrogen catabolic genes in *Saccharomyces cerevisiae*. Mol. Cell. Biol. *11,* 1161-1166.

Broach, J. R. (1991). *RAS* genes in *Saccharomyces cerevisiae*: signal transduction in search of a pathway. Trends Genet. *7,* 28-33.

Broach, J. R., and Deschennes, R. J. (1990). The function of *RAS* genes in *Saccharomyces cerevisiae*. Adv. Cancer Res. *54,* 79-139.

Budd, M. E., and Campbell, J. L. (1993). DNA polymerases ∂ and ε are required for chromosomal replication in *Saccharomyces cerevisiae.* Mol. Cell. Biol. *13,* 496-505.

Chant, J., Corrado, K., Pringle, J. R., and Herskowitz, I. (1991). Yeast *BUD5*, encoding a putative GDP-GTP exchange factor, is necessary for bud site selection and interacts with bud formation gene *BEM1*. Cell *65,* 1213-1224.

Chant, J., and Herskowitz, I. (1991). Genetic control of bud site selection in yeast by a set of gene products that constitute a morphogenetic pathway. Cell *65,* 1203-1212.

Chant, J., and Pringle, J. R. (1991). Budding and cell polarity in *Saccharomyces cerevisiae*. Curr. Opin. Genet. Dev. *1,* 342-350.

Ciriacy, M., Freidel, K., and Lohning, C. (1991). Characterization of trans-acting mutations affecting Ty and Ty-mediated transcription in *Saccharomyces cerevisiae*. Curr. Genet. *20,* 441-448.

Cohen, P. (1989). The structure and regulation of protein phosphatases. Annu. Rev. Biochem. *58,* 453-508.

Coornaert, D., Vissers, S., and André, B. (1991). The pleiotropic *UGA35* (*DURL*) regulatory gene of *Saccharomyces cerevisiae*: cloning, sequence, and identity with the *DAL81* gene. Gene *97,* 163-171.

Dubois, E., Jacobs, E., and Jauniaux, J.-C. (1982). Expression of the ROAM mutations in *Saccharomyces cerevisiae*: involvement of *trans*-acting regulatory elements and relation with the Ty1 transcription. EMBO J. *1,* 1133-1139.

Errede, B., and Ammerer, G. (1989). STE12, a protein involved in cell-type-specific transcription and signal transduction in yeast, is part of protein-DNA complexes. Genes Dev. *3,* 1349-1361.

Errede, B., Cardillo, T. S., Wever, G., and Sherman, F. (1980). ROAM mutations causing increased expression of yeast genes: their activation by signals directed toward conjugation functions and their formation by insertion of Ty1 repetitive elements. Cold Spring Harbor Symp. Quant. Biol. *45,* 593-602.

Freifelder, D. (1960). Bud position in *Saccharomyces cerevisiae.* J. Bacteriol. *80,* 567-568.

Gimeno, C. J. (1994). Characterization of *Saccharomyces cerevisiae* Pseudohyphal Development. (Ph.D. Thesis: Massachusetts Institute of Technology).

Gimeno, C. J., and Fink, G. R. (1992). The logic of cell division in the life cycle of yeast. Science *257,* 626.

Gimeno, C. J., and Fink, G. R. (1994). Induction of pseudohyphal growth by overexpression of *PHD1*, a *Saccharomyces cerevisiae* gene related to transcriptional regulators of fungal development. Mol. Cell. Biol. *14,* 2100-2112.

Gimeno, C. J., Ljungdahl, P. O., Styles, C. A., and Fink, G. R. (1992). Unipolar cell divisions in the yeast *S. cerevisiae* lead to filamentous growth: regulation by starvation and *RAS*. Cell *68,* 1077-1090.

Gimeno, C. J., Ljungdahl, P. O., Styles, C. A., and Fink, G. R. (1993). Characterization of *Saccharomyces cerevisiae* pseudohyphal growth. In Dimorphic Fungi in Biology and Medicine, H. Vanden Bossche, Odds, F. C., and Kerridge, D., eds. (New York, New York: Plenum).

Guilliermond, A. (1920). The Yeasts. (New York: John Wiley and Sons, Inc.).

Healy, A. M., Zolnierowicz, S., Stapleton, A. E., Goebl, M., DePaoli-Roach, A. A., and Pringle, J. R. (1991). *CDC55*, a *Saccharomyces cerevisiae* gene involved in cellular morphogenesis: identification, characterization, and homology to the B subunit of mammalian type 2A protein phosphatase. Mol. Cell. Biol. *11,* 5767-5780.

Herskowitz, I. (1989). A regulatory hierarchy for cell specialization in yeast. Nature *342,* 749-757.

Hicks, J. B., Strathern, J. N., and Herskowitz, I. (1977). Interconversion of yeast mating types III. Action of the homothallism (HO) gene in cells homozygous for the mating type locus. Genetics *85,* 395-405.

Hinnebusch, A. G. (1988). Mechanisms of gene regulation in the general control of amino acid biosynthesis in *Saccharomyces cerevisiae*. Microbiol. Rev. *52,* 248-273.

Hu, G.-Z., and Ronne, H. (1994). Overexpression of yeast *PAM1* gene permits survival without protein phosphatase 2A and induces a filamentous phenotype. J. Biol. Chem. *269,* 3429-3435.

Johnston, L. H., and Lowndes, N. F. (1992). Cell cycle control of DNA synthesis in budding yeast. Nucleic Acids Res *20,* 2403-2410.

Kataoka, T., Powers, S., McGill, C., Fasano, O., Strathern, J., Broach, J., and Wigler, M. (1984). Genetic analysis of yeast *RAS1* and *RAS2* genes. Cell *37,* 437-445.

Kendrick, B. (1985). The Fifth Kingdom. (Waterloo: Mycologue Publications).

Lee, K. S., Hines, L. K., and Levin, D. E. (1993). A pair of functionally redundant yeast genes (*PPZ1* and *PPZ2*) encoding type 1-related protein phosphatases function within the *PKC1*-mediated pathway. Mol. Cell. Biol. *13,* 5843-5853.

Liu, H., Styles, C. A., and Fink, G. R. (1993). Elements of the yeast pheromone response pathway required for filamentous growth of diploids. Science *262,* 1741-1744.

Ljungdahl, P. O., Gimeno, C. J., Styles, C. A., and Fink, G. R. (1992). SHR3: a novel component of the secretory pathway specifically required for localization of amino acid permeases in yeast. Cell *71,* 463-478.

Lodder, J. (1970). The Yeasts: a Taxonomic Study. (Amsterdam: North-Holland Publishing Co.).

Miller, K. Y., Toennis, T. M., Adams, T. H., and Miller, B. L. (1991). Isolation and transcriptional characterization of a morphological modifier: the *Aspergillus nidulans* stunted (*stuA*) gene. Mol. Gen. Genet. *227,* 285-292.

Miller, K. Y., Wu, J., and Miller, B. L. (1992). *StuA* is required for cell pattern formation in *Aspergillus*. Genes Dev. *6,* 1770-1782.

Morrison, A., Araki, H., Clark, A. B., Hamatake, R. K., and Sugino, A. (1990). A third essential DNA polymerase in *S. cerevisiae*. Cell *62,* 1143-1151.

Mortimer, R. K., and Johnston, J. R. (1986). Genealogy of principal strains of the yeast genetic stock center. Genetics *113,* 35-43.

Nasmyth, K. A. (1982). Molecular genetics of yeast mating type. Annu. Rev. Genet. *16,* 439-500.

Park, H.-O., Chant, J., and Herskowitz, I. (1993). BUD2 encodes a GTPase-activating protein for Bud1/Rsr1 necessary for proper bud-site selection in yeast. Nature *365,* 269-274.

Peng, Z. Y., Wang, W., Wilson, S. E., Schlender, K. K., Trumbly, R. J., and Reimann, E. M. (1991). Identification of a glycogen synthase phosphatase from yeast *Saccharomyces cerevisiae* as protein phosphatase 2A. J. Biol. Chem. *266,* 10925-10932.

Ronne, H., Carlberg, M., Hu, G. Z., and Nehlin, J. O. (1991). Protein phosphatase 2A in *Saccharomyces cerevisiae*: effects on cell growth and bud morphogenesis. Mol. Cell. Biol. *11,* 4876-4884.

Ruggieri, R., Bender, A., Matsui, Y., Powers, S., Takai, Y., Pringle, J. R., and Matsumoto, K. (1989). *RSR1*, a *ras*-like gene homologous to K*rev*-1/*smg*21A/*rap*1A: role in the development of cell polarity and interactions with the Ras pathway in *Saccharomyces cerevisiae*. Mol. Cell. Biol. *12,* 758-766.

Sanders, S., and Herskowitz, I. (1994). Personal communication.

Scherr, G. H., and Weaver, R. H. (1953). The dimorphism phenomenon in yeasts. Bacteriol. Rev. *17,* 51-92.

Sprague, G. F., and Thorner, J. W. (1992). Pheromone response and signal transduction during the mating process of *Saccharomyces cerevisiae*. In The Molecular and Cellular Biology of the Yeast *Saccharomyces*: Gene

Expression, E. W. Jones, Pringle, J. R., and Broach, J. R., eds. (Cold Spring Harbor, New York: Cold Spring Harbor Laboratory Press).

Taguchi, A. K. W., Ciriacy, M., and Young, E. T. (1984). Carbon source dependence of transposable element-associated gene activation in *Saccharomyces cerevisiae*. Mol. Cell. Biol. *4,* 61-68.

Timberlake, W. E. (1990). Molecular genetics of *Aspergillus* development. Annu. Rev. Genet. *24,* 5-36.

Timberlake, W. E. (1991). Temporal and spatial controls of *Aspergillus* development. Curr. Opin. Genet. Dev. *1,* 351-357.

Van Arsdell, S. W., Stetler, G. L., and Thorner, J. (1987). The yeast repeated element sigma contains a hormone-inducible promoter. Mol. Cell. Biol. *7,* 749-759.

van der Walt, J. P. (1970). Genus 16. *Saccharomyces* Meyen emend. Reess. In The Yeasts: a Taxonomic Study, J. Lodder, eds. (Amsterdam: North-Holland Publishing Co.).

van Zyl, W., Huang, W., Sneddon, A. A., Stark, M., Camier, S., Werner, M., Marck, C., Sentenac, A., and Broach, J. R. (1992). Inactivation of the protein phophatase 2A regulatory subunit A results in morphological and transcriptional defects in *Saccharomyces cerevisiae*. Mol. Cell. Biol. *12,* 4946-4959.

von Wettstein, D. (1983). Emil Christian Hansen Centennial Lecture: from pure yeast culture to genetic engineering of brewers yeast. (European Brewery Convention Congress: London). 97-119.

Wang, Z., Wu, X., and Friedberg, E. C. (1993). DNA repair synthesis during base excision repair in vitro is catalyzed by DNA polymerase ε and is influenced by DNA polymerases α and ∂ in *Saccharomyces cerevisiae*. Mol. Cell. Biol. *13*, 1051-1058.

Ward, M. P., and Garrett, S. (1994). Personal communication.

Chapter 2:

Initial Characterization of *Saccharomyces cerevisiae* Pseudohyphal Growth

Summary

This chapter will introduce the logic and results of the initial experiments of my pseudohyphal growth project. An appendix that contains some of these experiments is included as an aid to the reader. Results pertaining to the development of pseudohyphae are presented.

Microscopic analysis of pseudohyphal growth in diploid *MAT**a**/α* and *MAT**a**/α shr3/shr3 Saccharomyces cerevisiae* strains revealed that the first pseudohyphal cell in a pseudohypha originates by budding from an ellipsoidal mother. Mature pseudohyphae have a backbone of elongated pseudohyphal cells that typically invades the agar medium. Pseudohyphal cells that are located a few cells away from the growing tip of the filament often bud mitotic ellipsoidal cells. These vegetative ellipsoidal cells colonize the new substrates to which they have been delivered by the filament of pseudohyphal cells.

These observations have been used to formulate a model of how pseudohyphae forage for nitrogen. In this model, the elongated pseudohyphal cells and the ellipsoidal cells that together compose the pseudohypha have distinct roles in foraging. Pseudohyphal cells have the role of penetrating and exploring substrates. Their elongated shape aids in exploration because it increases the linear growth rate of the pseudohypha. This occurs because pseudohyphal cells are about 1.5 times longer than ellipsoidal cells and have a similar doubling time to them. Once the pseudohypha has penetrated a new substrate it begins to generate vegetative ellipsoidal cells. In the model it is the role of the ellipsoidal cells to colonize new substrates and assimilate the nutrients that are present in them. Thus,

pseudohyphal cells can be viewed as vectors that deliver mitotic ellipsoidal cells to new and otherwise inaccessible growth substrates.

Introduction

The logic and results of the initial experiments of my pseudohyphal growth project are important for the reader to put in perspective the body of work described in this thesis. For the reader's convenience, an appendix that contains most of the research on the *SHR3* gene described in this introduction is included at the end of the chapter. Research not presented in the Appendix is presented in Chapter 3. This introduction also describes my specific contributions to the Appendix to Chapter 2 and Chapter 3.

When I began my graduate studies, I started to work on *SHR3*, a previously uncharacterized gene. *SHR3* had been cloned and was being characterized by my mentor Per Ljungdahl and its product was unrelated to known proteins. *SHR3* was interesting because its mutation resulted in the impairment of the uptake of several different amino acids. Although several mutations that resulted in this phenotype had been described (Grenson and Hennaut, 1971; Lasko and Brandriss, 1981; McCusker and Haber, 1990; Sorsoli et al., 1964; Surdin et al., 1965), none of them had been molecularly characterized. Thus, the mechanism by which the mutation of a single gene pleiotropically affected amino acid uptake remained a mystery.

Histidine is a noncatabolizable nitrogen source that is toxic at media concentrations greater than 1 mM (Ljungdahl et al., 1992). *SHR3* had been identified by Per in a genetic selection called SHR (super high histidine-resistant) for genes whose mutation permitted a histidine auxotrophic yeast strain to grow on a synthetic medium that contained 30 mM histidine and had proline as sole nitrogen source (SPD plus 30 mM histidine). Proline was used as sole nitrogen source because at least three different permeases that take up histidine are expressed by yeast cells growing on this amino acid

(Ljungdahl et al., 1992). Thus, only mutations that affected the cellular target of histidine or that diminished histidine transport by all three histidine transport systems were expected to be isolated in the SHR screen. *shr3* mutations fit into the second class described above and caused an additional phenotype, slow growth on SPD medium that contained 0.2 mM histidine.

To learn more about the phenomenon of super high histidine-resistance and the *SHR3* gene, I studied whether some already characterized amino acid transport mutants were resistant to 30 mM histidine. I was especially interested in the *apf* mutant described by Grenson because it had pleiotropically impaired amino acid uptake and was biochemically well characterized (Grenson and Hennaut, 1971). Grenson had sent a *MAT*α *apf* strain derived from the Σ1278b genetic background called RA68 (Grenson and Hennaut, 1971) to Dr. Fink in 1971 and it had been entered into the Fink laboratory strain collection as F35. I obtained F35 from the strain collection and determined that it grew well on SPD plus 30 mM histidine medium and that it grew poorly on SPD plus 0.2 mM histidine medium. In these respects *apf* and *shr3* mutants behaved similarly. Thus, it seemed possible that *apf* and *shr3* were alleles of the same gene.

The fact that *apf* strains have impaired proline uptake (Grenson and Hennaut, 1971) suggested that F35 grew slowly on SPD plus 0.2 mM histidine, which has proline as sole nitrogen source, because it could not efficiently import its nitrogen source and consequently was nitrogen starved. When I examined the small colonies made by F35 on the SPD plus 1 mM histidine medium under the microscope I noticed that they had a fuzzy appearance. Closer examination of the colonies revealed that they had many filaments of elongated cells emanating away from them. Furthermore, these filaments actually invaded the agar medium on which they were growing. F35

was observed to make these filaments when grown on SPD plus 0.2 mM histidine medium but not on rich media that were tested, including SPD plus 0.2 mM histidine medium that had been supplemented with other nitrogen sources (Gimeno et al., 1992). Because of this result and because *apf* strains are known to have impaired proline uptake (Grenson and Hennaut, 1971), it seemed possible that the filamentous growth was caused by the nitrogen starvation that F35 probably experiences when it utilizes proline as sole nitrogen source.

These filaments of cells resembled the hyphae or filaments produced by filamentous fungi (Kendrick, 1985). After some library research, I found several yeast taxonomy books that reported that *Saccharomyces cerevisiae* makes filaments called pseudohyphae which are defined as chains of elongated yeast cells that have not completely separated and that elongate by budding growth (Guilliermond, 1920; Lodder, 1970). This definition perfectly described the filaments produced by F35 that I had observed. I realized that I was potentially working on a part of the *S. cerevisiae* life cycle that had never been studied by molecular geneticists.

Next, I wanted to demonstrate that F35 was a *S. cerevisiae* strain and not a contaminant and to do a complementation experiment to determine whether *apf* and *shr3* were allelic. I decided to do these experiments simultaneously by setting up a cross between F35 (reported to be *MAT*α *apf*) and a *MAT***a** *shr3* strain. The result of this and subsequent crosses was that F35 did not mate with either *MAT***a** or *MAT*α strains. This meant that F35 was either not a *S. cerevisiae* strain or that F35 had become diploid. I tested the latter possibility by subjecting F35 to a sporulation experiment. F35 sporulated and tetrad analysis showed that the four ascospores derived from F35 asci gave rise to nonmating strains that behaved just like F35. The

simplest explanation for this observation was that the *ho* allele of RA68 (*MATα apf ho*) had reverted to *HO* permitting a mitotic RA68 segregant to switch mating types and subsequently mate to its mother, producing a strain with the genotype *MAT**a**/α apf/apf HO/HO* (for a review of mating type switching see (Herskowitz, 1989)). Such a strain would sporulate and generate four *MAT**a**/α apf/apf HO/HO* meiotic segregant strains per ascus, just as F35 did.

To test this hypothesis, I sporulated F35 and mixed the resulting asci containing haploid ascospores with a haploid *ho* - *S. cerevisiae* strain that had an auxotrophic marker (strain MB758-5B, *MAT**a** ho ura3-52*) on rich media. I incubated the mixture of cells and ascospores at 30° C in the hope that after germination some of the ascospores would manage to mate with MB758-5B and not with their sister ascospores. After the incubation at 30° C, I replica plated the mating mix to a SPD plus 0.2 mM histidine plate to select for the diploid strains that resulted from the mating. This double selection works because F35 derived *apf* strains grow poorly on SPD plus 0.2 mM histidine and MB758-5B cells require uracil for growth. After several days, a few colonies had grown out of the patch of cells on the SPD plus 0.2 mM histidine plate. Tetrad analysis of a strain derived from one of these colonies (CGDY53) revealed that its genotype was *MAT**a**/α apf/APF ho/HO ura3-52/URA3*. This result proved that F35 was a *S. cerevisiae* strain with the genotype *MAT**a**/α apf/apf HO/HO*.

I went on to show that *apf* was allelic to *shr3* (Ljungdahl et al., 1992). One of the ways that I did this utilized a *MAT**a** ho apf ura3-52* strain (CGAS53-2E) that was an ascospore segregant of the CGDY53 strain described above. I transformed CGAS53-2E with a control plasmid and also with a plasmid from Per that contained the cloned *SHR3* gene. The CGAS53-2E control plasmid transformant grew on SPD plus 30 mM histidine medium while the CGAS53-

2E *SHR3* plasmid transformant did not: Thus the *SHR3* gene on a plasmid complemented the *apf* mutation.

This information proved useful because Per's molecular analysis of *SHR3* provided important information about how *SHR3* might regulate pseudohyphal growth. Per had shown that *SHR3* protein resides in the ER (Ljungdahl et al., 1992). This result immediately suggested that *SHR3* might be involved in the secretion of amino acid permeases. In this model, *shr3* mutants fail to secrete normal levels of amino acid permeases to the plasma membrane resulting in a pleiotropic defect in amino acid transport. Per's elegant experiments subsequently proved this model and contributed significantly to our understanding of nitrogen starvation regulation of pseudohyphal growth (Ljungdahl et al., 1992). These results suggested that *MAT**a**/α shr3/shr3* strains undergo vigorous pseudohyphal growth when utilizing proline as sole nitrogen source probably because abnormally low levels of functional proline permeases in these strains cause impaired proline uptake that results in nitrogen starvation.

In the course of these classical genetic experiments, three important facts about pseudohyphal growth became apparent to me. First, *MAT**a**/α shr3/shr3* diploid strains but not *MAT**a** shr3* or *MATα shr3* haploid strains undergo pseudohyphal growth when grown on proline medium (Gimeno et al., 1992). This result means that pseudohyphal growth in *S. cerevisiae* is a diploid-specific developmental pathway. This observation makes sense because in *S. cerevisiae* the diploid phase is the assimilative phase found in nature while the haploid phase has a transient existence in the life cycle (Gimeno and Fink, 1992).

The second fact was that strains of only some genetic backgrounds undergo pseudohyphal growth. I found that *MAT**a**/α shr3/shr3* Σ1278b

(Grenson et al., 1966) strains undergo vigorous pseudohyphal growth when grown on proline medium while the *MAT**a**/α shr3/shr3* strains that Per had been working with that were related to the S288c (Mortimer and Johnston, 1986) genetic background did not. Interestingly, a *MAT**a**/α shr3/shr3* hybrid strain that had one ∑1278b parent and one S288c parent did undergo vigorous pseudohyphal growth when grown on proline medium suggesting that S288c strains have cryptic recessive mutations in genes required for pseudohyphal growth (Gimeno et al., 1992).

The third and most important fact was that pseudohyphal growth is a latent developmental pathway of wild-type ∑1278b *MAT**a**/α* diploid *S. cerevisiae* strains. I first showed this by demonstrating that a wild-type *MAT**a**/α* diploid strain undergoes modest pseudohyphal growth when it is grown on proline medium (Gimeno et al., 1992). Proline is a well documented poor nitrogen source (Cooper, 1982) and thus it seemed likely that the yeast strain was moderately starved for nitrogen when growing on proline and thus induced modest pseudohyphal growth. I confirmed this result by developing SLAHD medium, a medium identical to SPD plus 0.2 mM histidine that instead of proline contains 0.05 mM ammonium sulfate as sole nitrogen source (as a comparison, standard synthetic complete SC medium contains 37.8 mM ammonium sulfate). This nitrogen starvation medium induces prolific and vigorous pseudohyphal growth in *MAT**a**/α* wild-type strains (Gimeno et al., 1992).

During this time I also performed many observational experiments with the technical help of Cora Styles. This work showed that pseudohyphal cells are morphologically distinct from ellipsoidal cells, that pseudohyphae elongate by budding, that a pseudohyphal cell can bud to produce another pseudohyphal cell or a mitotic ellipsoidal cell, and that newborn

pseudohyphal and sated ellipsoidal cells both have a unipolar budding pattern (Gimeno et al., 1992). This last result suggested that the role of the tightly regulated unipolar budding pattern of newborn *MAT***a**/α diploid cells may be to allow pseudohyphal growth (Gimeno and Fink, 1992; Gimeno et al., 1992). The finding that a mutant diploid yeast strain with the random budding pattern has impaired pseudohyphal growth confirmed that unipolar budding is important for pseudohyphal growth. In another genetic experiment, I showed that a constitutively active allele of *RAS2*, a central component of the RAS-cAMP signaling pathway, ectopically induces pseudohyphal growth. This experiment was important because it implicated a well characterized signal transduction pathway that regulates stress responses in pseudohyphal growth control. These experiments are presented in Chapter 3.

Additional observational experiments showed that the first pseudohyphal cell of a pseudohypha is formed by budding from an ellipsoidal mother cell and that the role of pseudohyphal cells in the pseudohypha is probably to deliver vegetative ellipsoidal cells to new substrates that they subsequently colonize. These experiments are the focus of this chapter and have been published (Gimeno et al., 1993).

After completing the work described above, I focused on studying the genetic regulation of pseudohyphal growth. My first step was to perform a screen for genes whose overexpression induces pseudohyphal growth (Chapter 4). One of these genes, *PHD1*, encodes a probable transcription factor related to a fungal protein that controls a pseudohyphal growth-like process. The focus of my work now became to study *PHD1* and how it might regulate pseudohyphal growth. In one line of experimentation, I isolated genes that are induced by *PHD1* overexpression (Chapter 5). This study raised the interesting possibility that *PHD1* may regulate the cell cycle and nitrogen metabolism, two processes that have clear connections to

pseudohyphal growth. In another series of experiments, I studied the role of *SOK2*, a *PHD1* homolog that may act in the RAS-cAMP pathway, in pseudohyphal growth (Chapter 6). This work showed that *SOK2* may repress pseudohyphal growth and that *SOK2* and *PHD1* interact genetically.

The work presented in this thesis has provided a strong foundation for the burgeoning pseudohyphal growth field. It provides authoritative technical and intellectual information on pseudohyphal growth to interested researchers. Scientists working on yeast, filamentous fungi, plants, and human cells are all using parts of my thesis research in their studies. I look forward to monitoring the progress of this field in the years to come.

Results

Pseudohyphal Cells Originate by Budding from Ellipsoidal Cells

The first pseudohyphal cell in a pseudohypha could originate in at least two ways. An ellipsoidal cell could initiate the growth of a pseudohypha by undergoing morphogenesis and changing its shape to the pseudohyphal morphology or it could retain its ellipsoidal morphology and produce a pseudohyphal cell by budding. To distinguish between these two models, I pregrew a Shr3$^-$ strain on rich medium, which supports the ellipsoidal morphology, transferred it to SPHD medium, which activates the PHG program in Shr3$^-$ strains, and, after a short period of time, analyzed 4-celled microcolonies microscopically (Fig. 2.1A). In these microcolonies, cell morphology can be unambiguously assigned only to the two cells with daughters because it is unknown what part of the cell cycle unbudded cells are in. The diploid polar budding pattern allows one to infer the mother-daughter relationships of the four cells in the microcolony (Gimeno et al., 1992). The cell with the ellipsoidal morphology indicated by the arrow is the progenitor of the microcolony and has retained its ellipsoidal shape. Its first daughter is an elongated pseudohyphal cell. Given that pseudohyphal cells form by budding in elongating pseudohyphae (Gimeno et al., 1992), this observation suggests that incipient pseudohyphae are initiated by ellipsoidal cells that bud to form pseudohyphal cells.

As Pseudohyphae Elongate They Become Covered with Ellipsoidal Cells

Elongated pseudohyphal cells give rise to either of two cell types (Gimeno et al., 1992): They divide to produce an elongated daughter with roughly the same final

dimensions as the mother cell or alternatively an ellipsoidal cell with roughly the dimensions of an ellipsoidal cell growing on rich medium. Both the elongated pseudohyphal cell and the ellipsoidal cell can be produced either apically or laterally (Gimeno et al., 1992). The ellipsoidal cells produced by the pseudohyphal cell may be a new cell type or they may be identical to ellipsoidal yeast cells growing on rich medium. These ellipsoidal cells are clearly proliferating because they can be observed to bud (visible in Fig. 2.1B indicated by a large arrow and in (Gimeno et al., 1992)). Interestingly, these ellipsoidal cells have not been observed to bud pseudohyphal cells and thus initiate new filaments. Pseudohyphae are often observed to invade the agar and subsequently begin budding ellipsoidal cells at the base of the pseudohypha (Figs. 2.1B and 2.1C). As long as the pseudohypha continues to grow, the first few cells at the growing tip are pseudohyphal cells. Pseudohyphae have a backbone of pseudohyphal cells that becomes covered with vegetative ellipsoidal cells. These ellipsoidal cells constitute the majority of the pseudohyphal biomass.

Figure 2.1 Origin and Development of *S. cerevisiae* Pseudohyphae. (A) A Shr3$^-$ strain, CGX19 (*MAT**a**/α shr3-102/shr3-102 ura3-52/ura3-52*), was pregrown overnight on YPAD medium and then streaked for single cells on a SPHD plus uracil plate. An incipient pseudohypha after 7 hours (A) and an invasive pseudohypha after 4.75 days (B) are shown. In (A), the arrow indicates the cell with the ellipsoidal morphology that initiated the pseudohypha. In (B) the large arrow indicates a mitotic ellipsoidal cell and the small arrow indicates a pseudohyphal cell. A wild-type strain, CGX68 (*MAT**a**/α*), was pregrown overnight on YPAD medium and then streaked for single cells on a SLAHD plate. A macroscopic invasive pseudohypha after 10.6 days is shown (C). The scale bars in Panels A, B, and C represent repectively 3, 10, and 30 μm.

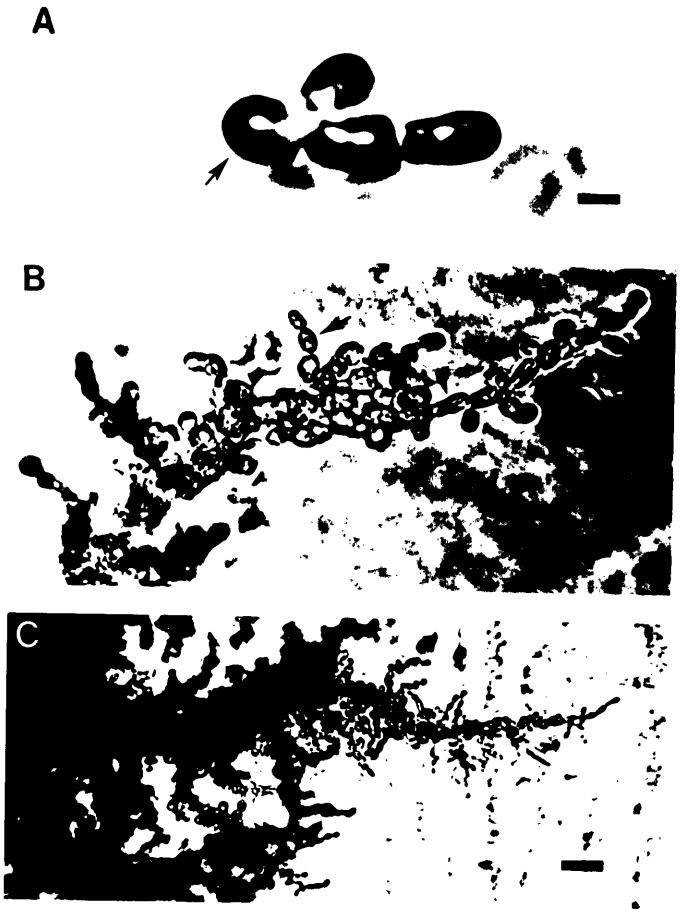
A
B
C

Discussion

Pseudohyphal Cells Deliver Yeast Cells to New Substrates

The growing tip of a mature elongating pseudohypha is composed of pseudohyphal cells. Pseudohyphal cells behind the growing tip often bud ellipsoidal cells that divide and colonize their new growth substrate. Thus, a pseudohypha is composed of a backbone of pseudohyphal cells that become covered with vegetative ellipsoidal cells as the pseudohypha grows. This phenomenon suggests that pseudohyphal cells are specialized to rapidly invade new substrates, like the interior of a grape, and deliver assimilative ellipsoidal cells to them. In this model it is the ellipsoidal cells, and not the pseudohyphal cells, that colonize new substrates and assimilate the majority of the nutrients present in them. Moreover, the elongated shape of pseudohyphal cells allows them to extend 1.5 times faster than if they had the ellipsoidal morphology, giving further support to the idea that these cells are specialized for exploration and foraging (Gimeno et al., 1992). These observations suggest that the pseudohyphal growth mode may be thought of as: ellipsoidal cell at one position →pseudohyphal cells →ellipsoidal cells at a new position.

Interestingly, apical growth predominates over lateral growth in pseudohyphae. The fact that pseudohyphal cells often laterally bud yeast cells contributes to apical growth because yeast cells are not observed to initiate pseudohyphal branches. This apical dominance may be advantageous because it prevents clonal pseudohyphae from competing with each other for nutrients and favors the exploration of new substrates.

Materials and Methods

Saccharomyces cerevisiae Strains

Construction of yeast strains used in this work, with the exception of CGX66, CGX68, CG143, and CG144 has been described elsewhere. Yeast strains used in this work are listed in Table 2.1. MB1000 and MB758-5B were crossed to construct diploid strain CGX66. CGX66 was sporulated, tetrads were dissected, and a *MAT**a*** segregant (CG143) and a *MAT*α segregant (CG144) were isolated. CG143 and CG144 were crossed to make diploid CGX68 that is congenic to the Σ1278b genetic background.

Media, Microbiological Techniques, and Light Microscopy

Standard *S. cerevisiae* media were prepared and yeast genetic manipulations were performed as previously described (Sherman et al., 1986). YPAD is a standard rich medium (Gimeno et al., 1992; Sherman et al., 1986). Other media and microbiological techniques have been described in detail elsewhere (Gimeno et al., 1992). In nonstandard media name abbreviations S represents synthetic, H represents histidine, and D represents dextrose (used at 2% weight per volume). In the following nonstandard media, sole nitrogen source name abbreviations are SLAHD (low ammonia, 0.05 mM ammonium sulfate as sole nitrogen source) and SPHD (proline added at a concentration of 1 gram per liter). Uracil may be added to SLAHD and SPHD media at the standard concentration of 0.2 mM. This concentration of uracil only minimally inhibits pseudohyphal growth. Light microscopy methods have been described in detail elsewhere (Gimeno et al., 1992).

Table 2.1 Yeast Strain List[a]

Strain Name	Genotype	Reference or Derivation
CGX19	*MAT**a**/α ura3-52/ura3-52 shr3-102/shr3-102*	(Gimeno et al., 1992)
MB1000	*MATα*	(Brandriss and Magasanik, 1979)
MB758-5B	*MAT**a** ura3-52*	(Siddiqui and Brandriss, 1988)
CGX66	*MAT**a**/α ura3-52/URA3*	MB1000 X MB758-5B
CG143	*MAT**a***	CGX66 meiotic segregant
CG144	*MATα*	CGX66 meiotic segregant
CGX68	*MAT**a**/α*	CG143 X CG144

[a] All *S. cerevisiae* strains are congenic to the Σ1278b genetic background (Grenson et al., 1966).

Literature Cited

Brandriss, M. C., and Magasanik, B. (1979). Genetics and physiology of proline utilization in *Saccharomyces cerevisiae*: enzyme induction by proline. J. Bacteriol. *140,* 498-503.

Cooper, T. G. (1982). Nitrogen metabolism in *Saccharomyces cerevisiae*. In The Molecular Biology of the Yeast Saccharomyces: Metabolism and Gene Expression, J. N. Strathern, Jones, E. W., and Broach, J. R., eds. (Cold Spring Harbor: Cold Spring Harbor Laboratory Press).

Gimeno, C. J., and Fink, G. R. (1992). The logic of cell division in the life cycle of yeast. Science *257,* 626.

Gimeno, C. J., Ljungdahl, P. O., Styles, C. A., and Fink, G. R. (1992). Unipolar cell divisions in the yeast *S. cerevisiae* lead to filamentous growth: regulation by starvation and *RAS*. Cell *68,* 1077-1090.

Gimeno, C. J., Ljungdahl, P. O., Styles, C. A., and Fink, G. R. (1993). Characterization of *Saccharomyces cerevisiae* pseudohyphal growth. In Dimorphic Fungi in Biology and Medicine, H. Vanden Bossche, Odds, F. C., and Kerridge, D., eds. (New York, New York: Plenum).

Grenson, M., and Hennaut, C. (1971). Mutation affecting activity of several distinct amino acid transport systems in *Saccharomyces cerevisiae*. J. Bacteriol. *105,* 477-482.

Grenson, M., Mousset, M., Wiame, J. M., and Bechet, J. (1966). Multiplicity of the amino acid permeases in *Saccharomyces cerevisiae* I. Evidence for a specific arginine-transporting system. Biochim. Biophys. Acta *127,* 325-338.

Guilliermond, A. (1920). The Yeasts. (New York: John Wiley and Sons, Inc.).

Herskowitz, I. (1989). A regulatory hierarchy for cell specialization in yeast. Nature *342,* 749-757.

Kendrick, B. (1985). The Fifth Kingdom. (Waterloo: Mycologue Publications).

Lasko, P. F., and Brandriss, M. C. (1981). Proline transport in *Saccharomyces cerevisiae.* J. Bacteriol. *148,* 241-247.

Ljungdahl, P. O., Gimeno, C. J., Styles, C. A., and Fink, G. R. (1992). SHR3: a novel component of the secretory pathway specifically required for localization of amino acid permeases in yeast. Cell *71,* 463-478.

Lodder, J. (1970). The Yeasts: a Taxonomic Study. (Amsterdam: North-Holland Publishing Co.).

McCusker, J. H., and Haber, J. E. (1990). Mutations in *Saccharomyces cerevisiae* which confer resistance to several amino acid analogs. Mol. Cell. Biol. *10,* 2941-2949.

Mortimer, R. K., and Johnston, J. R. (1986). Genealogy of principal strains of the yeast genetic stock center. Genetics *113,* 35-43.

Sherman, F., Fink, G. R., and Hicks, J. (1986). Methods in Yeast Genetics. (Cold Spring Harbor, New York: Cold Spring Harbor Laboratory Press).

Siddiqui, A. H., and Brandriss, M. C. (1988). A regulatory region responsible for proline-specific induction of the yeast *PUT2* gene is adjacent to its TATA box. Mol. Cell. Biol. *8,* 4634-4641.

Sorsoli, W. A., Spence, K. D., and Parks, L. W. (1964). Amino acid accumulation in ethionine-resistant *Saccharomyces cerevisiae*. J. Bacteriol. *88,* 20-24.

Surdin, Y., Sly, W., Sire, J., Bordes, A. M., and de Robichon-Szulmajster, H. (1965). Properties and genetic control of the amino acid accumulation system in *Saccharomyces cerevisiae*. Biochim. Biophys. Acta *107,* 546-566.

Appendix to Chapter 2:

SHR3: A Novel Component of the Secretory Pathway Specifically Required for Localization of Amino Acid Permeases in Yeast[a]

[a] My specific contributions to this paper are listed in the introduction to Chapter 2.

Cell, Vol. 71, 463–478, October 30, 1992, Copyright © 1992 by Cell Press

SHR3: A Novel Component of the Secretory Pathway Specifically Required for Localization of Amino Acid Permeases in Yeast

Per O. Ljungdahl,* Carlos J. Gimeno,*† Cora A. Styles,* and Gerald R. Fink*†
*Whitehead Institute for Biomedical Research
9 Cambridge Center
Cambridge, Massachusetts 02142
†Massachusetts Institute of Technology
Department of Biology
Cambridge, Massachusetts 02142

Summary

Mutations in *SHR3* block amino acid uptake into yeast by reducing the levels of multiple amino acid permeases within the plasma membrane. SHR3 is a novel integral membrane protein component of the endoplasmic reticulum (ER). *shr3* null mutants specifically accumulate amino acid permeases in the ER; other plasma membrane proteins, secretory proteins, and vacuolar proteins are processed and targeted correctly. Our findings suggest that SHR3 interacts with a structural domain shared by amino acid permeases, an interaction required for permease-specific processing and transport from the ER. Even in the presence of excess amino acids, *shr3* mutants exhibit starvation responses. *shr3* mutants constitutively express elevated levels of GCN4, and mutant *shr3/shr3* diploids undergo dimorphic transitions that result in filamentous growth at enhanced frequencies.

Introduction

Amino acid uptake in Saccharomyces cerevisiae is mediated by general and specific transport systems. The general amino acid permease (*GAP1*), a low affinity, high capacity permease with broad substrate specificity, is capable of transporting most amino acids, even D-amino acids (Jauniaux and Grenson, 1990; Rytka, 1975). In addition to GAP1, there are over 20 high affinity, low capacity amino acid permeases with narrow substrate specificities that have been identified biochemically and/or genetically (for reviews see Wiame et al., 1985; Horak, 1986). Three of these specific high affinity amino acid permeases have been cloned: the histidine permease (*HIP1*; Tanaka and Fink, 1985), the arginine permease (*CAN1*; Hoffmann, 1985), and the proline permease (*PUT4*; Vandenbol et al., 1989). Yeast cells differentially regulate the activity of the general and specific amino acid permeases to control amino acid uptake under a variety of environmental conditions. All four characterized permeases share extensive amino acid sequence homology (Jauniaux and Grenson, 1990; Weber et al., 1988), suggesting that the yeast permeases are members of a gene family. These permeases are structurally similar and are predicted to be integral membrane proteins comprised of 12 membrane-spanning domains. The murine ecotropic retrovirus receptor is similar to the yeast permeases and has been shown to be the principal basic L-amino acid transporter in mammalian cells (Kim et al., 1991; Wang et al., 1991).

Single mutations that block the uptake of many different amino acids into yeast have been isolated (Sorsoli et al., 1964; Surdin et al., 1965; Grenson and Hennaut, 1971; Lasko and Brandriss, 1981; McCusker and Haber, 1990). The existence of viable strains exhibiting the pleiotropic loss of multiple amino acid transport proteins, each encoded by a distinct gene, could be explained in several ways. One possible explanation is that amino acid permeases share a common pathway or maturation process required for their expression and that these pleiotropic mutations represent a defect within this pathway. Indeed, permeases are initially inserted into the endoplasmic reticulum (ER) membrane (Green et al., 1989; Green and Walter, 1992) and subsequently translocated to the plasma membrane via the yeast secretory pathway. Transport of the proline permease (PUT4) to the plasma membrane requires SEC1 (Courchesne and Magasanik, 1983), an essential protein required for vesicular transport from the Golgi apparatus to the plasma membrane (Novick and Schekman, 1979; Novick et al., 1980). The requirement for SEC1 suggests that the functional expression of amino acid permeases is dependent upon their proper entry into and progression through the entire secretory pathway. The pleiotropic effect of mutations on multiple permeases could therefore result from a block anywhere along the secretory pathway. Such *sec* mutations must represent leaky alleles because a null mutation defective in the general secretory pathway should have a lethal phenotype.

Alternatively, there may be elements of the secretory pathway that are specific to certain families of proteins and are not shared by other secreted proteins. Recent evidence supporting this notion has been found in Drosophila. Mutations in the Drosophila cyclophilin homolog ninaA specifically inhibit transport of two homologous opsins, Rh1 and Rh2 (70% sequence identity), from the ER of photoreceptor cells; consequently, ninaA mutant cells accumulate opsins in the ER membrane (Colley et al., 1991). The accumulation of opsins in the ER of ninaA mutant cells is presumed to result from improper folding as *ninaA* encodes a peptidyl-prolyl cis-trans isomerase. Proper tertiary structure has been shown to be a prerequisite for the entry of many proteins into subsequent steps of the secretory pathway (for reviews see Lodish, 1988; Hurtley and Helenius, 1989; Rose and Doms, 1988). It is clear that processing steps catalyzed by ninaA exhibit substrate specificity within the ER because opsin Rh3 (35% sequence identity with Rh1) does not depend upon ninaA function to exit from the ER (Stamnes et al., 1991). The observation that certain related membrane proteins have unique requirements for transit through the ER suggests the possibility that yeast mutations pleiotropically affecting amino acid permease function may identify components of the ER-processing machinery specific to this family of transport proteins.

Protein insertion into the membrane of the ER requires

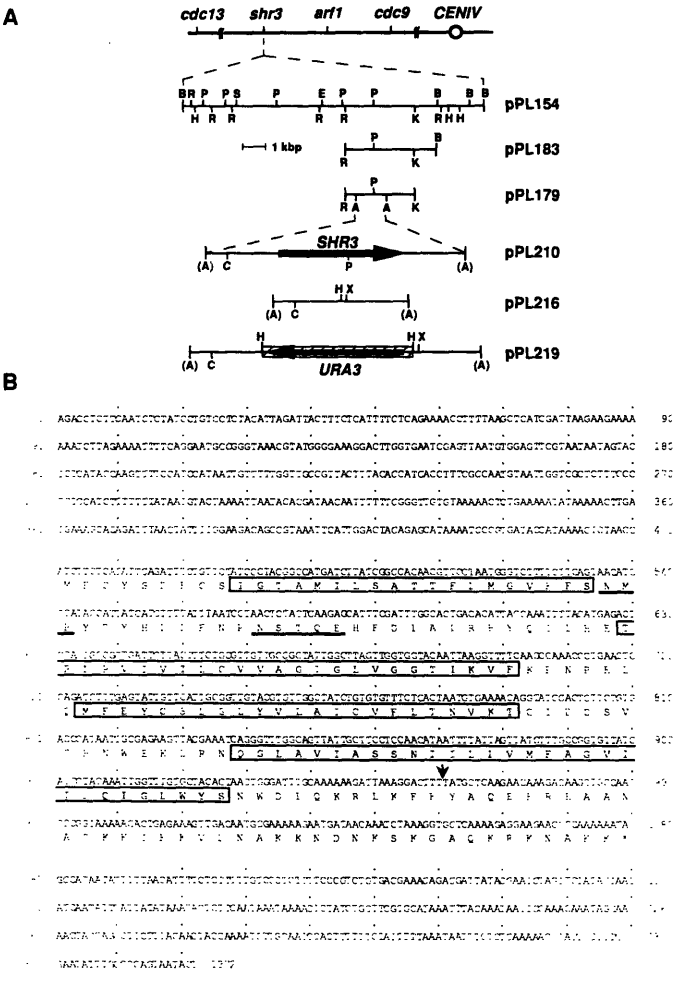

Figure 1. *SHR3* Chromosomal Location, Plasmids, and Gene Sequence

(A) A diagram showing the chromosomal location and restriction endonuclease map of the *SHR3* region and *SHR3* plasmid inserts. The map distances are *shr3–arf1*, 18.6 cM (44 parental ditype: 0 nonparental ditype: 26 tetratype); *arf1–cdc9*, 25 cM (35 parental ditype: 0 nonparental ditype: 35 tetratype); and *shr3–cdc9*, 35 cM (26 parental ditype: 1 nonparental ditype: 43 tetratype). Plasmid pPL154 contains a 13 kb *shr3*-complementing BamHI fragment. The *SHR3*-containing inserts in plasmids pPL183 and pPL179 were sequenced. Dashed lines expand the 1372 bp AccI fragment that was used to construct plasmid pPL210. The *SHR3* coding region is indicated as a closed arrow. Deletion plasmids pPL216 and pPL219 were constructed as described in the text (see Experimental Procedures). Restriction endonuclease sites are labeled as follows: A, AccI; B, BamHI; C, ClaI; E, SpeI; K, KpnI; H, HindIII; R, EcoRI; P, PstI; S, SalI; X, XhoI. The AccI sites enclosed in parentheses were inactivated during subcloning.

(B) Nucleotide and deduced amino acid sequence of the *SHR3* gene. The four segments of amino acids predicted to comprise membrane-spanning domains are highlighted within boxes (Klein et al., 1985). Putative ER retention elements are underlined (Poruchynsky and Atkinson, 1988). The position at which the hemagglutinin epitope tag (*SHR3::FLU2*) was inserted is indicated with an arrow.

the participation of several proteins. Gene fusion experiments utilizing the amino-terminal portion of the arginine permease (CAN1) identified several novel proteins, SEC70, SEC71, and SEC72, that are required for proper insertion of this permease into the membrane of the ER (Green et al., 1989, 1992; Green and Walter, 1992). Insertion of CAN1 fusion proteins also requires previously identified components of the secretory pathway, SEC61 and SEC63 (Deshaies and Schekman, 1987; Rothblatt et al., 1989). SEC61 and SEC63 are integral membrane proteins that assemble together with another protein, SEC62, and at least two additional proteins to form a complex within the ER membrane (Stirling et al., 1992; Deshaies and Schekman, 1989; Sadler et al., 1989; Deshaies et al., 1991). Despite the involvement of SEC62 in this complex, CAN1 constructs do not appear to require SEC62 for insertion into the ER membrane (Green et al., 1992). However, mutations in *SEC62* have been shown to block the translocation across the ER membrane of a variety of soluble protein precursors and the membrane insertion of the endopeptidase KEX2 (Rothblatt et al., 1989; Stirling et al., 1992). These results suggest that yeast cells possess multiple pathways for protein insertion into the ER membrane. Consistent with this conclusion are the findings that genes encoding core components of the yeast signal recognition particle (SRP) are not essential for growth (Hann and Walter, 1991; Stirling and Hewitt, 1992).

In this paper we describe the isolation and characterization of *SHR3*, a gene that encodes a novel protein located in the ER membrane. SHR3 is required for the function of multiple amino acid permeases, each encoded by a different gene. In cells lacking SHR3, amino acid permeases accumulate in the ER and fail to be transported to the plasma membrane. The ER export block exerted by *shr3* null mutations is specific for this class of permeases, as other plasma membrane proteins, secretory proteins, and vacuolar proteins are targeted correctly to their proper intracellular locations. The amino acid transport defects of

shr3 mutants result in amino acid starvation, which is reflected in elevated levels of GCN4 expression and enhanced pseudohyphal growth.

Results

Isolation of Super High Histidine-Resistant Yeast Mutants

We isolated spontaneous mutants resistant to 30 mM histidine (see Experimental Procedures). Characterization of these spontaneous super high histidine-resistant (*shr*) mutants showed that resistance resulted from recessive mutations in single genes defining nine complementation groups. Mutant representatives of five complementation groups, including *shr3* mutants, are sensitive to hyperosmotic culture conditions and high Ca^{2+} concentrations. Histidine and arginine uptake into wild-type and mutant *shr* strains was assayed using saturating concentrations of amino acids, i.e., 12 mM histidine and 4 mM arginine, respectively. All three members of the *shr3* complementation group (*shr3-3*, *shr3-16*, and *shr3-23*) exhibited less than 10% of wild-type histidine transport, whereas arginine uptake appeared relatively unaffected. None of the representatives of the other complementation groups exhibited a defect in histidine uptake as severe as that shown by *shr3* mutants. Apparently, the decreased rates of histidine uptake into these *shr3* mutants is sufficient to support the growth of His^- auxotrophs but insufficient to permit internal histidine concentrations to reach toxic levels. Studies on null alleles of *shr3* suggested that the viability of $Shr3^- His^-$ double mutants is characteristic only of leaky mutant alleles of *SHR3* (see subsequent section). Strains carrying *shr3* mutations in either a His^+ or His^- background fail to grow well on SPD plus 1 mM histidine but grow well on SPD plus 30 mM histidine. (SPD is a nonstandard synthetic medium that contains 6.7 g/l yeast nitrogen base without amino acids and ammonium sulfate [Difco Laboratories], 1.0 g/l L-proline as the sole nitrogen source, 20 g/l D-glucose.) Although we do not understand the poor growth on 1 mM histidine, we used this phenotype to clone the *SHR3* gene.

Isolation and Mapping of *SHR3*

The *SHR3* gene was cloned by complementation of the poor growth on SPD plus 1 mM histidine phenotype exhibited by *shr3-23*. Strain PLAS23-4B was transformed with a plasmid library (Rose et al., 1987). When transferred onto SPD plus 1 mM histidine, 4 out of 8000 Ura^+ transformants grew, and when subsequently tested, these transformants were no longer resistant to 30 mM histidine. Plasmids pPL152, pPL153, pPL154, and pPL155 were recovered from these strains. Each plasmid complemented all three *shr3* alleles. Restriction endonuclease analysis of the plasmid insert DNA identified a common 8.4 kb fragment (Figure 1A).

SHR3 was mapped by hybridization to separated chromosomes (Carle and Olson, 1985) and chromosomes digested with NotI and SfiI (Link and Olson, 1991). The *SHR3* probe hybridized to sequences located on the extreme left arm of chromosome IV. Data from these chromoblots and additional Southern blot experiments at both low and high stringency indicate that the *SHR3* gene is present as a single copy in the haploid yeast genome. Three point crosses involving known markers on the left arm of chromosome IV were carried out to establish the gene order and map distances for *cdc9–arf1–shr3* (Figure 1A).

SHR3 Null Mutations Are Synthetic Lethals in Combination with Several Amino Acid Auxotrophies

A precise deletion of *SHR3* was created by removal of the entire protein coding sequence and replacement of this segment with the selectable marker *URA3* (see Experimental Procedures; Figure 1A). This construct, *shr3Δ1::URA3*, was transformed into diploid yeast strain AA305 (*HIS3/his3Δ200*, *LEU2/leu2-3,112*, *ura3-52/ura3-52*, *lys2Δ201/lys2Δ201*, *ade2/ade2*). Stable Ura^+ transformants were selected and sporulated. Tetrads were dissected on both YPD and synthetic mininal dextrose (SD) media (minimal media supplemented only with auxotrophic requirements). Spore viability was excellent on SD media. Resistance to 30 mM histidine segregated 2:2 and was 100% linked to the *URA3* marker, showing that the deletion of *SHR3* leads to the resistance phenotype. The disruption of the *SHR3* locus was confirmed by Southern blot analysis. When transferred to YPD, spore-derived colonies containing the *shr3* deletion and auxotrophies for either histidine or leucine did not grow. The synthetic lethality of *shr3* null mutations in combination with these auxotrophic alleles was reflected in the pattern of spore inviability observed on YPD. These results show that on YPD amino acid auxotrophic strains require *SHR3* function during both spore germination and vegetative growth. Similar synthetic lethality was observed when auxotrophic *shr3* null mutant strains were transferred to synthetic complete (SC) medium, a medium with high concentrations of all amino acids. A summary of our results regarding combinations of amino acid auxotrophic alleles and synthetic lethality with *shr3* null mutations is presented in Table 1. These genetic data indicate that SHR3 is required for the uptake of amino acids other than histidine.

The viability of auxotrophic *shr3* null mutant strains on SD medium must reflect the uptake of required amino acids through residual permeases present in greatly reduced amounts or by nonspecific uptake systems. We surmise that the observed synthetic lethality on both YPD and

Table 1. Synthetic Lethality on Complex Media

Double Mutant	Viability
shr3Δ1::URA3 leu2	−
shr3Δ1::URA3 his3	−
shr3Δ1::URA3 trp1	−
shr3Δ1::URA3 ilv1	+
shr3Δ1::URA3 lys2	+
shr3Δ1::URA3 arg4	+
shr3Δ1::URA3 ade2	+

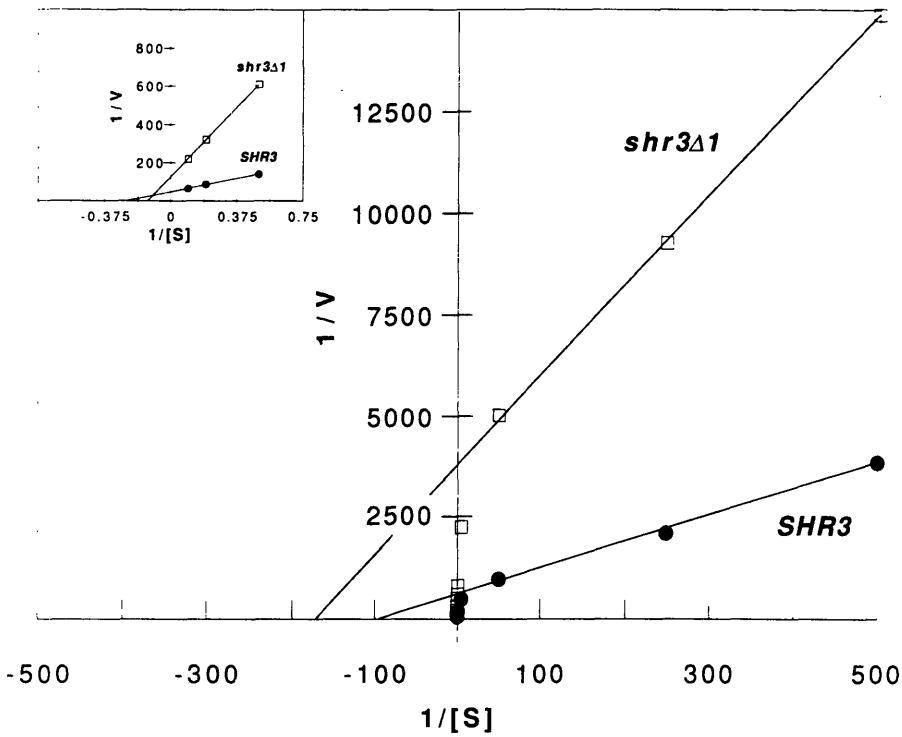

Figure 2. Kinetic Analysis of Histidine Uptake into *SHR3* and *shr3* Cells

SHR3 (PLY143) and *shr3Δ1::URA3* (PLY152) cells were grown in SUD (plus adenine, lysine, and uracil). Histidine uptake was assayed as described in Experimental Procedures. Uptake rates were determined at histidine concentrations ranging from 0.002 to 10 mM. These data were analyzed by linear regression in two data sets: high affinity, 0.002–0.02 mM; low affinity, 1–10 mM. Closed circles, *SHR3*; open squares, *shr3Δ1::URA3* cells. Insert panel is an expanded scale showing the kinetics of low affinity histidine uptake.

SC media is due to their high amino acid content. On these media, the overabundance of competing amino acids must interfere with the residual uptake mechanisms, effectively inhibiting uptake of the required amino acid. Thus, when grown on either YPD or SC, auxotrophic *shr3* null mutants cannot synthesize required amino acids nor can they import them from the external environment. Similar YPD synthetic lethality has previously been observed for mutations that pleiotropically affect amino acid uptake (Garrett, 1989; McCusker and Haber, 1990). Synthetic lethality was not observed with the original *shr3* mutant alleles isolated (*shr3-3*, *shr3-16*, and *shr3-23*), suggesting that these mutations are not complete loss of function alleles.

SHR3 Is Required for Amino Acid Transport

We examined the kinetics of histidine uptake into isogenic wild-type and *shr3Δ1::URA3* mutant strains (see Experimental Procedures). Strains were pregrown in media containing urea as the sole nitrogen source (called SUD, a medium that is the same as SPD except that 1.0 g/l urea is substituted for proline as the sole nitrogen source); both wild-type (PLY143) and *shr3Δ1::URA3* mutant (PLY152) strains grow at similar rates in this media (2.5 hr doubling time). Urea is a nonrepressing nitrogen source, and cells express maximal levels of amino acid permeases. Figure 2 shows a double reciprocal plot of the histidine uptake data. The plot is clearly nonlinear, indicating, as expected from previous work, that histidine uptake is mediated by multiple permeases with different affinities. At every concentration examined, the initial rate of histidine uptake was significantly reduced in the *shr3* deletion mutant as compared with the wild-type strain. These data indicate that in the complete absence of SHR3, the amino acid transport activity of multiple permeases is reduced. Similar kinetic data were obtained for proline, citrulline, and arginine.

The analysis of the high and low affinity components of uptake indicates that the deletion of *SHR3* did not result in large changes in the apparent affinity constant for transport (K_t) of either the high or low affinity transport systems (high affinity, *SHR3* K_t = 10 μM versus *shr3Δ1* K_t = 6 μM; low affinity, *SHR3* K_t = 4 mM versus *shr3Δ1* K_t = 8 mM). These data suggest that the decreased rates of amino acid uptake in *shr3* null mutants are not due to altered affinities of the permeases but rather result from a reduction in the concentration of functional permeases.

Table 2 provides a summary of the amino acid transport and adenine uptake rates determined for wild-type and

Table 2. Amino Acid and Adenine Uptake into *SHR3* and *shr3* Null Mutant Strains

Substrate	High Substrate Concentration (10 mM)[a]			Low Substrate Concentration (0.004 mM)[b]		
	SHR3	*shr3Δ1*	Fold Decrease	*SHR3*	*shr3Δ1*	Fold Decrease
Citrulline	0.113	0.064	1.8	0.572	0.0156	37.0
Glutamate	4.490	0.618	7.3	25.0	1.20	20.8
Leucine	3.795	0.834	4.6	15.0	0.790	19.4
Proline	0.124	0.023	5.4	0.135	0.0198	6.8
Histidine	1.504	0.397	3.8	51.0	10.0	5.1
Lysine	0.279	0.191	1.5	9.05	3.62	2.5
Arginine	0.494	0.157	3.2	102.0	45.0	2.3
Adenine	0.122	0.116	1.1	12.0	8.94	1.3

[a] Rate = nmol/min per milligram of protein.
[b] Rate = pmol/min per milligram of protein.

shr3 null mutant strains grown in SUD. The uptake rates were determined at two substrate concentrations. At high substrate concentrations (10 mM), amino acid uptake occurs predominantly through GAP1; at low substrate concentrations (0.004 mM), uptake occurs via the specific amino acid permeases. The data clearly show the pleiotropic effect of the *shr3* null mutation on both general and specific amino acid uptake systems. The uptake of each of the amino acids we examined was reduced in *shr3* null mutant strains. Adenine uptake was relatively unaffected, indicating that the expression of the purine–cytosine permease (FCY2), which is not a member of the yeast amino acid permease gene family (Weber et al., 1988, 1990), is not dependent upon SHR3 function.

Previously isolated mutations known as *aap* and *apf* pleiotropically affect amino acid uptake in yeast (Surdin et al., 1965; Grenson and Hennaut, 1971). The *apf* and *aap* mutations are presumed to be allelic (Grenson and Hennaut, 1971). Mutant *apf* strains, initially isolated as being DL-parafluorophenylalanine resistant, were subsequently found to be resistant to a variety of other toxic amino acid analogs. This resistance was shown to result from a reduction in transport activity of multiple amino acid permeases, including the general amino acid permease (GAP1) and many specific high affinity amino acid permeases. We found that *apf* mutant strains grew well on SPD media containing 30 mM histidine. A complementation test of the *apf* mutation and a *shr3* mutation was carried out. Strain CGAS53-2E (*MATa*, *apf*, *ura3-52*) was mated to strains PLAS16-4B (*MATα*, *shr3-16*, *ade2Δ1::URA3*, *ura3-52*, *his4Δ29*) and PLAS16-6C (*MATα*, *SHR3*, *ade2Δ1::URA3*, *ura3-52*, *his4Δ29*). PLAS16-4B and PLAS16-6C are isogenic except at the *SHR3* locus. Diploids derived from CGAS53-2E × PLAS16-4B were resistant to 30 mM histidine and grew poorly on 1 mM histidine, indicating that these two mutations do not complement. Transformants of strain CGAS53-2E transformed with a plasmid containing the *SHR3* gene (pPL210) were unable to grow on SPD plus 30 mM histidine but grew well on SPD plus 1 mM histidine. These results show that the *apf* and *shr3* mutations are allelic.

Based on our genetic analysis (Table 1) and amino acid uptake studies (Table 2) with *shr3* null mutant strains and on previous studies with *apf* strains (Grenson and Hennaut, 1971), at least 11 genetically distinct amino acid permeases require SHR3 for functional expression. The permeases affected by mutations in *SHR3* are the general amino acid permease (GAP1), histidine (HIP1), proline (PUT4), arginine (CAN1), glutamate (dicarboxylic amino acid permease), lysine, leucine, methionine, serine, valine, and tryptophan.

SHR3 Is a Component of the ER

The *SHR3* open reading frame beginning with the initiation codon ATG is comprised of 626 bp (see Figure 1B). The *SHR3* open reading frame encodes a protein comprised of 209 amino acids with a molecular mass of 23.5 kd and a pI equaling 10.04 (Finer-Moore et al., 1989). The SHR3 protein is predicted to be an integral membrane protein comprised of four membrane-spanning domains and an extremely hydrophilic carboxy-terminal domain (see Figure 1B). Of the last 47 amino acids in the carboxy-terminal domain, 24 are charged: 8 acidic residues and 16 basic residues. The carboxy-terminal domain is predicted to be exposed to the cytoplasm (Hartmann et al., 1989) and to adopt an α-helical secondary structure (Finer-Moore et al., 1989). SHR3 showed no significant homology with any proteins in the PIR, SwissProt, and GenPept (translated GenBank) data bases (see Experimental Procedures).

Based on the prediction that SHR3 is an integral membrane protein, we anticipated that the intracellular localization of SHR3 could be unambiguously determined and that this information would provide insight into its in vivo function. The intracellular location of SHR3 was determined by immunolocalization of a functional epitope-tagged SHR3 protein (see Experimental Procedures). Strain PLAS23-4B (*shr3-23*, *ura3-52*, *his4Δ29*) was transformed with a centromere-based plasmid containing the epitope-tagged *SHR3* construct (pPL230). The Ura$^+$ transformants containing this plasmid were no longer histidine resistant and grew well on SPD plus 1 μM histidine, indicating that the epitope-tagged SHR3 protein fully complements the *shr3* mutation. Control cells transformed with untagged *SHR3* (pPL210) were prepared in parallel for microscopic evaluation.

Cells transformed with the epitope-tagged *SHR3* con-

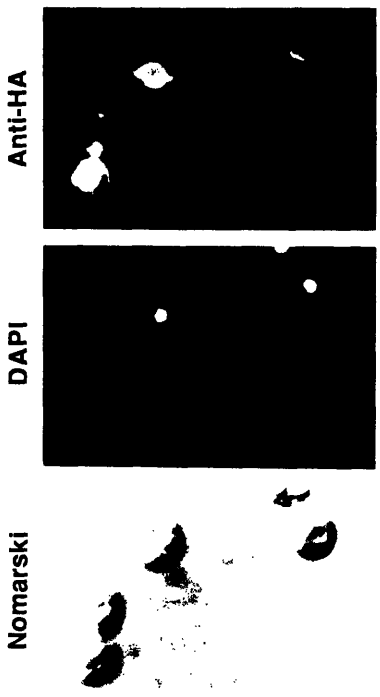

Figure 3. Localization of Epitope-Tagged SHR3 Using an Anti-Hemagglutinin Monoclonal Antibody

Strain PLAS23-4B harboring plasmid pPL230 (a CEN plasmid containing the *SHR3::FLU2* construct) was grown for 5 hr in YPD. Indirect immunofluorescence was performed using anti-hemagglutinin monoclonal antibody 12CA5 (1:5 dilution of salt-fractionated hybridoma supernatant) as described in Experimental Procedures. Top panel, DTAF staining observed with anti-hemagglutinin (Anti-HA) monoclonal antibody. Middle panel, DAPI staining. Bottom panel, cells viewed by Nomarski optics.

struct, but not with the control plasmid, showed bright perinuclear rim staining that often extended in a filamentous manner into the cytoplasm (Figure 3). The SHR3 immunofluorescence staining pattern is the same in both *SHR3* and *shr3* null mutant strains. The observed staining pattern of SHR3 is essentially identical to that reported for the lumenal ER protein KAR2 (Rose et al., 1989) and the ER membrane protein SEC62 (Deshaies and Schekman, 1990). Presumably this staining pattern reflects the continuity between the ER and nuclear envelope in sections of yeast observed by electron microscopy (Novick et al., 1980).

Null *shr3* Mutants Accumulate GAP1 in the ER

The intracellular location of SHR3 in the ER suggested a possible role for SHR3 in processing of amino acid permeases within the ER. To test this hypothesis, we constructed functional epitope-tagged versions of the general amino acid permease (*GAP1::FLU1* and *GAP1::FLU2*; see Experimental Procedures) and compared the intracellular location of GAP1 in wild-type and *shr3* deletion strains. In wild-type cells (Figure 4), GAP1 showed a plasma membrane rim staining pattern, the result expected for a plasma membrane protein (see PMA1 staining in subsequent section), whereas in the *shr3* deletion strain, GAP1 staining was perinuclear, a pattern identical to that of SHR3 (see Figure 3). These results indicate that in the absence of SHR3, GAP1 fails to localize to the plasma membrane and has an intracellular distribution consistent with localization in the ER.

Analysis of membrane preparations from *SHR3* and *shr3* strains provides important insights into the nature of the defect in *shr3* strains. Membranes were isolated from *SHR3* and *shr3* strains (see Experimental Procedures) containing GAP1 tagged with an epitope near its amino terminus (*GAP1::FLU1*). The levels of GAP1 in total cell extracts and in the isolated membranes were the same in *SHR3* and *shr3* strains (less than 15% variation) as estimated by quantitative immunoblots. The membrane preparations from *SHR3* and *shr3* strains were treated with a variety of reagents to ascertain the nature of the association between GAP1 and the membranes. The results (Figure 5A) show that GAP1 is not extracted by reagents known to extract peripherally associated membrane proteins (Figure 5A, lanes 3–5 and 8–10) but is extracted in both *SHR3* and *shr3* by a nonionic detergent known to solubilize integral membrane proteins (Figure 5A, lanes 2 and 7). These results show that roughly equivalent amounts of GAP1 are localized to membranes in *SHR3* and *shr3* and suggest that SHR3 does not alter the insertion of GAP1 into those membranes. The topology of GAP1 within the membrane preparations obtained from wild-type and *shr3* deletion strains was examined by limited protease digestion (Figure 5B). In the membranes obtained from *shr3*, GAP1 is more susceptible to trypsin digestion (compare lanes 3 and 8 in Figure 5B) and, at dilute trypsin concentrations, gives a digestion pattern different from GAP1 in *SHR3* strains. In *SHR3* membranes, fragment a predominates (Figure 5B, lanes 4 and 5), whereas in mutant membranes trypsin digestion products b and d predominate. Similar results were obtained with membrane preparations obtained from strains expressing *GAP1::FLU2*, a GAP1 protein epitope tagged near the carboxy terminus. The increased protease sensitivity of GAP1 in *shr3* deletion strains suggests that in the absence of SHR3 permeases have an altered topology. The observed variation in protease sensitivity could be due to altered folding or to different local environments; that is, in wild-type strains, GAP1 is primarily associated with the plasma membrane, whereas in *shr3* deletion strains GAP1 is in the ER membrane.

The ER Block in *shr3* Mutants Is Specific for Amino Acid Permeases

To ascertain whether the observed ER export block was general or restricted to amino acid permeases, we examined the intracellular distribution and processing state of several proteins that require passage through the secretory pathway. We compared the intracellular location of the plasma membrane [H^+]ATPase (PMA1) in wild-type and *shr3* null mutant strains by immunofluorescence mi-

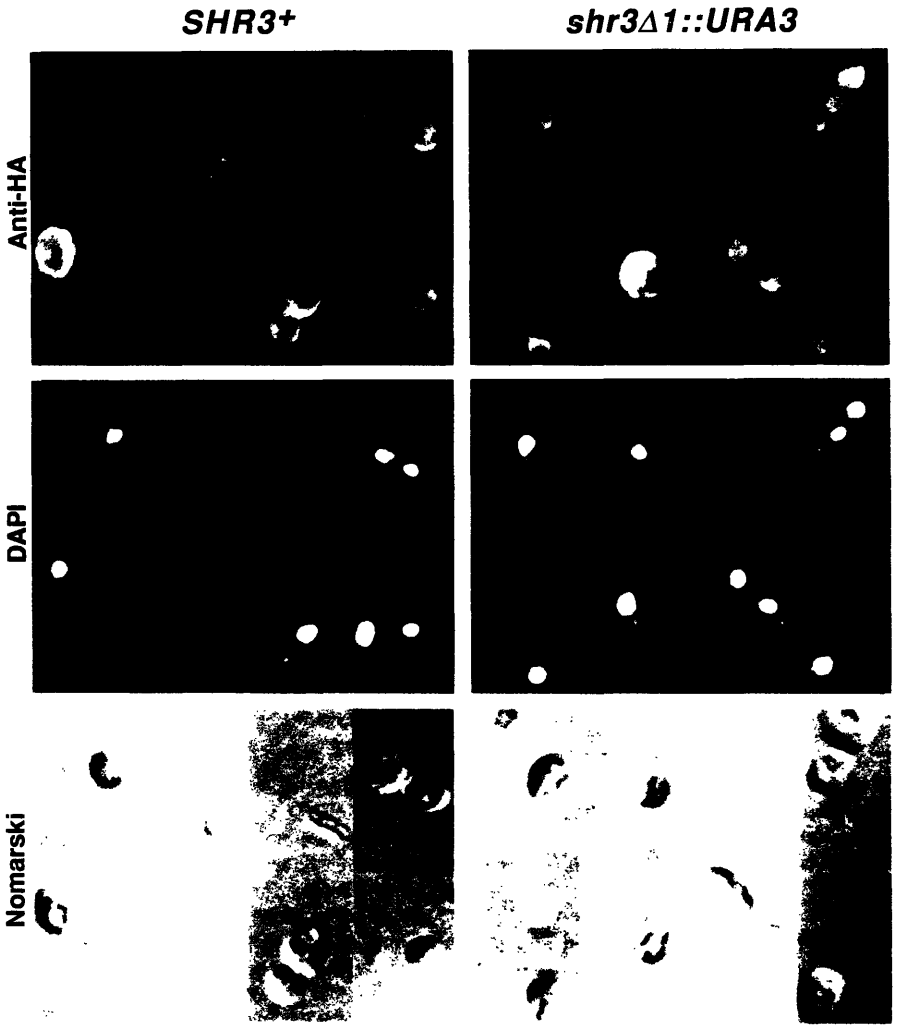

Figure 4. Localization of Epitope-Tagged GAP1 in *SHR3* and *shr3* Strains

SHR3 (PLY129) and *shr3Δ1::URA3* (PLY134) were transformed with plasmid pPL269 (a CEN plasmid containing the *GAP1::FLU1* construct), and transformants were grown in SUD (plus adenine and uracil). Indirect immunofluorescence was performed using anti-hemagglutinin monoclonal antibody 12CA5 as described in the legend to Figure 3. Top panels, DTAF staining observed with anti-hemagglutinin monoclonal antibody. Middle panels, DAPI staining. Lower panels, cells viewed by Nomarski optics.

croscopy. PMA1 is an integral polytopic membrane protein component of the plasma membrane comprised of at least eight transmembrane domains (Serrano et al., 1986). The immunolocalization of PMA1 in *SHR3* and *shr3* strains was indistinguishable; in both strains, a faint stain highlighting the external surface of the cells was observed (Figure 6). SHR3 is apparently not required for the processing and correct intracellular targeting of PMA1 to the plasma membrane.

The intracellular processing state and secreted amounts of α factor in *MATα* wild-type and *shr3* null mutant cells are the same (Figure 7A, Internal and Secreted Fractions). These results are consistent with bioassays analyzing halo sizes on tester lawns of *MAT***a** cells. Additionally, *MAT***a** *shr3* null mutant cells secrete similar levels of **a** factor and are equally sensitive to α factor as isogenic *MAT***a** *SHR3* cells. These results indicate that *shr3* mutations do not have a general effect on secretion or membrane internalization. These conclusions are supported by studies examining the processing of invertase in *shr3* mutants (Figure 7B). In wild-type cells, invertase becomes extensively glycosylated as it passes through the various Golgi compartments. As a consequence of extensive outer chain glycosylation, invertase runs as a heterogeneous high molecular weight smear upon electrophoresis. After treatment with endoglycosidase H, the resulting unglycosylated form

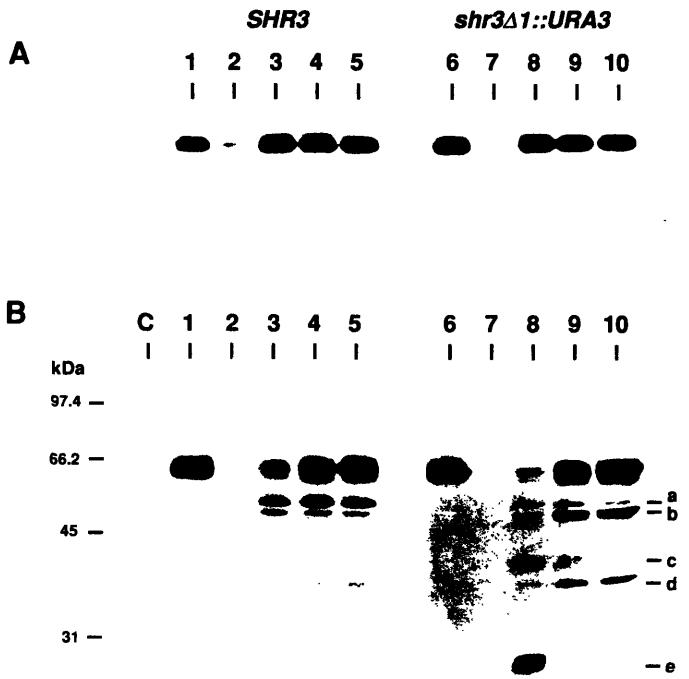

Figure 5. Behavior of Membrane-Associated GAP1 in *SHR3* and *shr3* Strains

The membrane association of GAP1 was examined in cell-free extracts as described in Experimental Procedures using total cell membranes isolated from *SHR3* (PLY129) and *shr3Δ1::URA3* (PLY134) strains transformed with plasmid pPL269 (*GAP1::FLU1*).

(A) Membranes were diluted with M buffer (lanes 1 and 6) or adjusted to a final concentration of 0.5% Triton X-100 (lanes 2 and 7), 0.1 M sodium carbonate (pH 11) (lanes 3 and 8), 1.6 M urea (lanes 4 and 9), or 0.6 M NaCl (lanes 5 and 10). After 15 min incubation at 4°C, samples were centrifuged at 100,000 g, supernatants were removed, and pellets were dissolved in SDS–PAGE sample buffer and resolved by SDS–PAGE in a 12.5% polyacrylamide gel, immunoblotted, and analyzed as described in Experimental Procedures.

(B) Membranes were treated with 0 μg (lanes 1 and 6), 5 μg (lanes 2 and 7), 1 μg (lanes 3 and 8), 0.5 μg (lanes 4 and 9), or 0.25 μg (lanes 5 and 10) of trypsin. Digests were resolved by SDS–PAGE in a 12.5% polyacrylamide gel, immunoblotted, and analyzed as described in Experimental Procedures. The major proteolytic fragments (a–e) are indicated. Lane c contains membranes isolated from strain PLY129 (*SHR3*) transformed with a *GAP1* plasmid without the epitope in GAP (pPL262).

runs as a single band (Franzusoff and Schekman, 1989). Our results indicate that invertase processing is the same in wild-type and *shr3* null mutant cells and that the addition of outer chain glycosylation occurs in an SHR3-independent manner.

The processing and intracellular targeting of the vacuolar protease carboxypeptidase Y (CPY) in wild-type and *shr3* null mutant cells is also identical. In wild-type cells, prepro-CPY enters the secretory pathway by translocation across the ER membrane. In the ER, the signal sequence is cleaved and pro-CPY becomes core-glycosylated, resulting in the 67 kd P1 form. Outer chain glycosylation occurs within the Golgi, generating a 69 kd P2 form. Finally, the mature 61 kd CPY is formed after proteolytic processing in the vacuole (Stevens et al., 1982). Our results (Figure 7C, Internal Fraction) show that there is no detectable difference between the intracellular processing or vacuolar targeting of CPY in wild-type and *shr3* null mutant cells. Additionally, CPY was exclusively targeted to the vacuole; no extracellular CPY was detected in either wild-type or *shr3* null mutant culture supernatants (Figure 7C, Secreted Fraction). These results are consistent with our observations that mutations in *SHR3* do not affect the vacuolar pH or vacuolar morphology (Preston et al., 1989).

Cellular Consequences of a General Block in Amino Acid Transport

To examine the effect of *shr3* mutations on general amino acid control, we determined the level of *GCN4* expression in isogenic histidine auxotrophic Shr$^+$ (PLAS1-7B) and Shr$^-$ (PLAS23-4B) strains. Amino acid starvation induces the expression of GCN4, the general transcriptional activator of genes in several amino acid biosynthetic pathways (Hinnebusch, 1988). Strains were transformed with a reporter plasmid construct (p180) containing *GCN4–lacZ* with the natural leader sequence that places GCN4 under general control (Hinnebusch, 1985). Under repressing conditions, in the presence of all amino acids, mutant *shr3* strains express 2-fold more β-galactosidase activity than wild-type cells (Figure 8A, Repressing). These results indicate that *shr3* mutant cells sense starvation conditions even when grown in the presence of excess amino acids. Under conditions of histidine starvation (derepressing), *shr3* strains express GCN4–LacZ at very high levels (Figure 8A, DR −his). The high levels of GCN4 expression are comparable with those found for *gcd1* mutations (Hinnebusch, 1985), an observation demonstrating that *shr3* mutants are hypersensitive to amino acid starvation. In parallel control experiments, with strains transformed with a constitutively expressed *gcn4–lacZ* construction (p227) (Mueller and Hinnebusch, 1986), both wild-type and mutant strains expressed similar levels of GCN4–LacZ activity (Figure 8B). These control experiments indicate that *shr3* mutations do not enhance the stability of GCN4–LacZ.

Mutant *shr3* cells exhibit greatly reduced growth rates in media containing proline as the sole nitrogen source: exponentially growing Shr$^+$ cells double every 10 hr, whereas the doubling time of *shr3* null mutants is increased to over 25 hr. The slower growth of *shr3* mutants on proline medium must reflect nitrogen source limitation

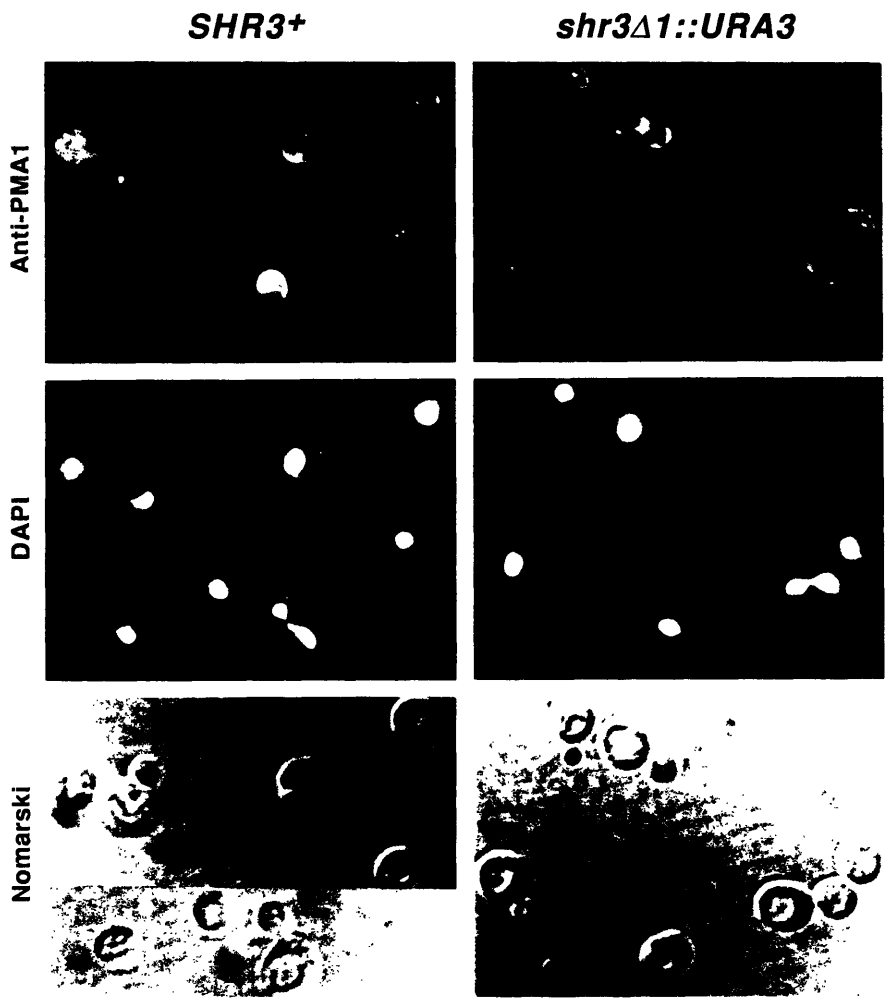

Figure 6. Localization of Plasma Membrane [H+]ATPase (*PMA1*) in *SHR3* and *shr3* Strains

SHR3 (PLY143) and *shr3Δ1::URA3* (PLY152) were grown in YPD, and indirect immunofluorescence was performed using affinity-purified rabbit anti-PMA1 antibody diluted 1:100 as described in Experimental Procedures. Top panels, DTAF staining observed with anti-PMA1 antibody. Middle panels, DAPI staining. Lower panels, cells viewed by Nomarski optics.

since mutant cells transport proline at greatly diminished rates (Table 2). Diploid strains of S. cerevisiae undergo dimorphic transitions (Gimeno et al., 1992; Gimeno and Fink, 1992). Compared with isogenic wild-type diploids, homozygous *shr3* diploids growing on proline medium undergo dimorphic transitions at enhanced frequencies. Since *shr3* mutations impair proline transport and induce starvation responses (Figure 8), the observation that these mutations enhance pseudohyphal growth strongly suggested that nitrogen source availability regulates the dimorphic transition. This model was proven by the observation that wild-type diploids could be stimulated to undergo dimorphic transitions when grown in media containing limiting concentrations of ammonia as the sole nitrogen source (Gimeno et al., 1992). The enhanced pseudohyphal growth, like the elevated GCN4 levels, is an indication of the in vivo consequences of reduced amino acid uptake.

Discussion

The evidence presented in this paper strongly suggests that SHR3 is essential for the efficient transport of structurally related but genetically distinct amino acid permeases from the ER to the plasma membrane. Yeast strains lacking a functional *SHR3* gene exhibit dramatic reductions in the activities of the general amino acid permease and in at least ten specific high affinity amino acid permeases. It is clear, based on a kinetic analysis of arginine, citrulline, histidine, and proline uptake, that the observed decrease in amino acid uptake is due to a reduction in the concentra-

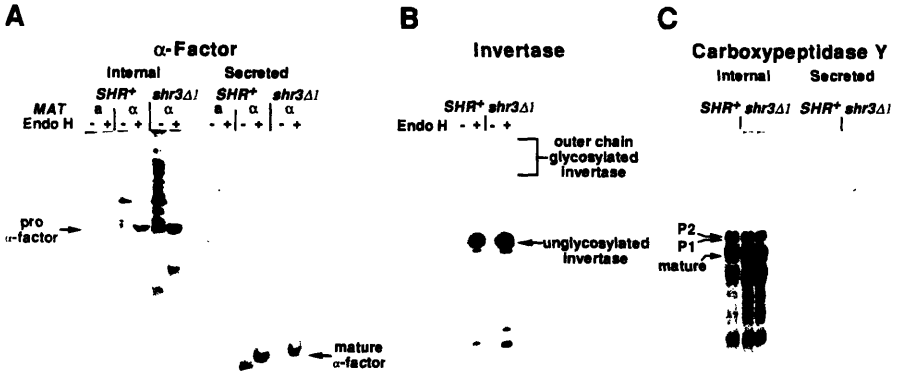

Figure 7. α Factor, Invertase, and CPY Processing and Targeting in *SHR3* and *shr3* Strains

(A) α Factor processing and secretion. *MATα SHR3* (PLY148) and *shr3Δ1::URA3* (PLY158) strains and a *MATa SHR3* (PLY145) strain were metabolically labeled with Tran^{35}S-Label for 30 min at 30°C. α Factor was immunoprecipitated from whole cell extracts (Internal) and culture supernatants (Secreted). Samples were treated with endoglycosidase H (Endo H) as indicated and resolved by SDS–PAGE in a 17% polyacrylamide gel. The positions of unglycosylated pro-α factor (18.5 kd) and mature α factor are labeled. Although there may be some quantitative differences between internal forms of α factor, the processing patterns are the same in *SHR3* and *shr3* upon longer exposure times.

(B) Invertase processing. *SHR3* (PLY148) and *shr3Δ1::URA3* (PLY158) strains were grown in low glucose media, and whole-cell protein was extracted. Samples were treated with endoglycosidase H (Endo H) as indicated. Proteins, resolved by SDS–PAGE in a 7.5% polyacrylamide gel, were transferred to nitrocellulose, and blots were probed with anti-invertase antibody as described in Experimental Procedures.

(C) CPY processing and vacuolar targeting. *MATα SHR3* (PLY148) and *shr3Δ1::URA3* (PLY158) strains were metabolically labeled as described above. CPY immunoprecipitated from whole cell extracts (Internal) and culture supernatants (Secreted) was resolved by SDS–PAGE in a 9% polyacrylamide gel.

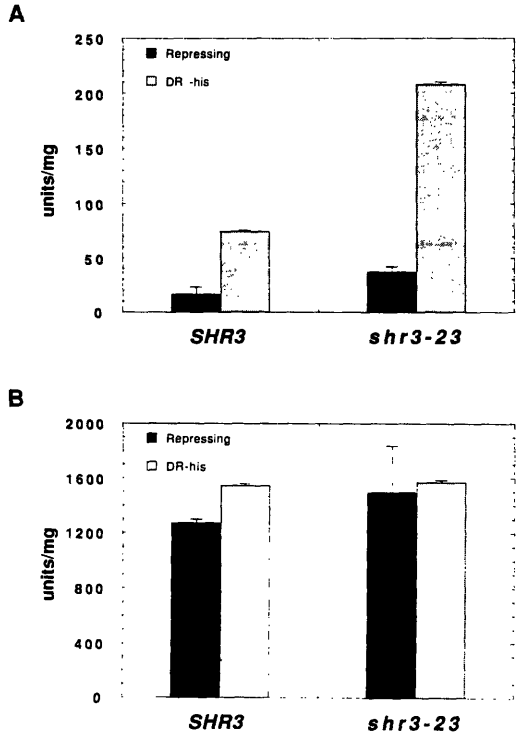

tion of functional permeases within the plasma membrane. We have shown that SHR3 is an integral membrane protein component of the ER. In *shr3* null mutants, the transport of GAP1 from the ER to the plasma membrane is inhibited, leading to accumulation of GAP1 in the ER membrane. This export block of GAP1 from the ER explains the reduced permease levels in the plasma membrane and the decreased rates of amino acid uptake. We surmise that in the absence of SHR3, the high affinity amino acid permeases affected by *shr3* mutations are also retained in the ER.

The ER export block observed in *shr3* null mutants appears to be specific for permeases. The general secretory and vacuolar targeting pathways are unaffected by *shr3* null mutations. The plasma membrane [H$^+$]ATPase (PMA1), a polytopic membrane protein comprised of multiple membrane-spanning domains, is correctly localized to

Figure 8. GCN4–LacZ Activity in *SHR3* and *shr3-23* Strains

β-Galactosidase activity in *SHR3* (PLAS1-7D) and *shr3-23* (PLAS23-4B) strains transformed with *GCN4–lacZ* plasmids with *GCN4–lacZ* under general control (p180) (A) and *gcn4–lacZ* constitutively expressed (p227) (B). β-Galactosidase activities were determined in transformants grown in complete synthetic media minus uracil for repressing conditions (Repressing) and in strains grown under derepressing conditions in complete synthetic media minus uracil and histidine (DR −his).

the plasma membrane in a SHR3-independent manner. Null *shr3* mutant strains are equally sensitive to mating pheromones as compared with wild-type strains, indicating that the integral membrane pheromone receptors are also correctly targeted to the plasma membrane in the absence of SHR3. Null *shr3* mutants correctly process and target CPY to the vacuole. Additionally, we have found that mutations in *SHR3* do not affect the vacuolar pH or vacuolar morphology, an indication that most vacuolar proteins reach their correct intracellular location. Null *shr3* mutant strains also secrete correctly processed proteins, including invertase and mating pheromones (both α factor and **a** factor), at levels indistinguishable from wild-type strains.

The finding that GAP1 is an integral membrane protein even in the complete absence of SHR3 (Figure 5A) suggests that SHR3 functions to catalyze specific folding or translocation reactions that occur subsequent to initial membrane association and insertion. For example, SHR3 may provide chaperone-like interactions that enable amino acid permeases to attain the proper three-dimensional conformation necessary for their sorting and subsequent transport from the ER. The increased protease sensitivity of GAP1 in strains lacking SHR3 (Figure 5B) is in agreement with this model. Recently, SEC70 has been shown to be required for translocation of internal carboxy-terminal transmembrane domains of the yeast arginine permease (CAN1) but not for the first three transmembrane domains (Green et al., 1992). It is possible that there is a permease-specific pathway in which SHR3 and SEC70 function together or in sequence, i.e., SHR3 being required for translocation of some permease domains and SEC70 for others. One or more of the regions of sequence identity shared by the yeast permeases could represent a signature domain recognized by SHR3 in carrying out this function. This model for SHR3 is similar to that suggested as an explanation for the function of ninaA in Drosophila. Mutations in ninaA, a cyclophilin homolog, inhibit transport of two homologous opsins from the ER of photoreceptor cells, leading to opsin accumulations in the ER membrane (Colley et al., 1991).

Alternatively, a possible function of SHR3 is suggested by the structural similarity of SHR3 with SEC62. Both of these proteins exhibit similar hydropathy profiles, and, like SHR3, SEC62 has an extremely hydrophilic carboxy-terminal domain (Deshaies and Schekman, 1989). Using sequence comparison algorithms (BESTFIT, IALIGN), we found sequence similarity between these two proteins; an alignment score of 5.5 standard deviations above the mean was calculated for 100 randomizations. The similarity was found within the carboxy-terminal 130 amino acids of both these proteins, a region that encompasses the last two transmembrane domains and extends throughout the hydrophilic carboxy-terminal domain. These proteins share 46% similarity and 18% identity within this region. The hydrophilic carboxy-terminal domains of both SHR3 and SEC62 are predicted to form α-helical secondary structures that may be important for protein–protein interactions.

The degree of similarity between SHR3 and SEC62 suggests that SHR3 may function as a permease-specific "adapter" molecule that functions in conjunction with the recently identified SEC62/SEC63 complex. SEC62 has recently been shown to be a component of a multimeric protein complex that includes SEC63 and at least two other unidentified proteins within the ER membrane (Deshaies et al., 1991). SEC61, which is present within the ER membrane in 10-fold higher amounts than SEC62, appears to be transiently associated with this SEC62/SEC63 complex. Results from biochemical cross-linking experiments have demonstrated that prepro-α factor becomes bound to microsomal membranes in an ATP-independent reaction that enables contact with SEC62 (Müsch et al., 1992). In subsequent interactions that require the presence of ATP, translocation intermediates become intimately associated with SEC61 (Müsch et al., 1992; Sanders et al., 1992). Thus, it appears that SEC62 functions at an early point in membrane insertion; however, the precise function of SEC62 has not fully been defined, and it is possible that SEC62 functions at additional stages during membrane protein assembly. Since arginine permease (CAN1) fusion constructs are inserted into the ER membrane in a SEC62 independent manner (Green et al., 1992), perhaps SHR3 performs a SEC62-like function during the processing of amino acid permeases.

The specificity of SHR3 for the expression of amino acid permeases raises some interesting questions. Does SHR3 function solely to facilitate permease processing, and, if so, why do amino acid permeases require unique factors for their functional expression? We have shown that mutant *shr3* strains are unable to extract amino acids efficiently from their extracellular environment and that amino acid auxotrophs carrying *shr3* defects experience starvation even in the presence of excess nutrients. When grown on proline medium, homozygous *shr3* mutant diploid strains ($Shr3^-$) undergo a dimorphic transition that results in filamentous pseudohyphal growth at greatly enhanced frequencies compared with $Shr3^+$ strains (Gimeno et al., 1992). Filamentous growth appears to be the manifestation of a diploid-specific developmental pathway that is induced under conditions of nutrient limitation. The observation that $Shr3^-$ strains enter this pathway at enhanced frequencies, even in the presence of excess proline, suggests that cells require a minimum concentration of permeases in the plasma membrane to assess accurately the extracellular nutrient levels. If the concentration of permeases in the plasma membrane is too low, as is the case for *shr3* mutants, cells enter the pseudohyphal pathway inappropriately. Yeast cells may, therefore, require SHR3 to expedite the processing of permeases to ensure their rapid expression at the plasma membrane in response to changing environmental conditions.

Experimental Procedures

Strains, Media, and Microbiological Techniques

Yeast strains are listed in Table 3, and the plasmids utilized are in Table 4. PLY4 was constructed from PLY1; the mating type was switched by transformation with plasmid pGAL–*HO* (Herskowitz and Jensen, 1991).

Table 3. S. cerevisiae Strains

Strain	Genotype	Source or Reference
RA68	*MATα apf*	Grenson and Hennaut, 1971
F35	*MATa/α HO/HO apf(shr3-101)/apf(shr3-101)*[a]	This work
MB758-5B	*MATa ho ura3-52*	Siddiqui and Brandriss, 1988
CGDY53	*MATa/α HO/ho apf(shr3-101)/APF(SHR3) ura3-52/URA3*	This work
CGAS53-2E	*MATa ho apf(shr3-101) ura3-52*	This work
Isogenic Derivatives of PLY1		
PLY1	*MATa his4Δ29 ura3-52*	This work
PLY4	*MATα his4Δ29 ura3-52 ade2Δ1::URA3*	This work
PLAS1-7D	*MATa ura3-52 his4Δ29*	This work
PLAS3-4A	*MATa shr3-3 ura3-52 his4Δ29*	This work
PLAS16-6B	*MATα shr3-16 ade2Δ1::URA3 ura3-52 his4Δ29*	This work
PLAS16-6C	*MATα SHR3 ade2Δ1::URA3 ura3-52 his4Δ29*	This work
PLAS23-4B	*MATα shr3-23 ura3-52 his4Δ29*	This work
Isogenic Derivatives of AA280		
AA280	*MATα ura3-52 his3Δ200 lys2Δ201 ade2*	Antebi and Fink, 1992
AA288	*MATa ura3-52 leu2-3,112 lys2Δ201 ade2*	Antebi and Fink, 1992
AA305	*MATa/α HIS3/his3Δ200 LEU2/leu2-3,112 ura3-52/ura3-52 lys2Δ201/lys2Δ201 ade2/ade2*	Antebi and Fink, 1992
PLY129	*MATa ura3-52 leu2-3,112 lys2Δ201 ade2 gap1Δ::LEU2*	This work
PLY134	*MATa ura3-52 leu2-3,112 lys2Δ201 ade2 gap1Δ::LEU2 shr3Δ1::URA3*	This work
PLY143	*MATa ura3-52 lys2Δ201 ade2*	This work
PLY145	*MATa ura3-52 lys2Δ201 ade2*	This work
PLY148	*MATα ura3-52 lys2Δ201 ade2*	This work
PLY152	*MATa ura3-52 lys2Δ201 ade2 shr3Δ1::URA3*	This work
PLY158	*MATα ura3-52 lys2Δ201 ade2 shr3Δ1::URA3*	This work

[a] The *apf* allele of F35 was renamed *shr3-101* to conform with standardized yeast genetic nomenclature.

Table 4. Plasmids

Plasmids	Description	Source or Reference
pPL130	6.2 kb fragment containing *ADE2* in pUC19	This work
pPL132	*ade2Δ1::URA3* in pUC19	This work
pPL152	9.6 kb fragment containing *SHR3* inYCp50	This work
pPL153	9.6 kb fragment containing *SHR3* in YCp50 (pPL153 appears to be identical to pPL152)	This work
pPL154	13 kb fragment containing *SHR3* in YCp50	This work
pPL155	12 kb fragment containing *SHR3* in YCp50	This work
pPL164	11 kb BamHI fragment containing *SHR3* in pRS316	This work
pPL179	3 kb KpnI–EcoRI fragment containing *SHR3* in pRS316	This work
pPL183	4 kb EcoRI–BamHI fragment containing *SHR3* in pRS316	This work
pPL202	1.4 kb AccI fragment containing *SHR3* in pBSII SK(+)	This work
pPL210	1.4 kb AccI fragment containing *SHR3* in pRS316	This work
pPL216	*shr3Δ3* in pBSII SK(+)	This work
pPL219	*shr3Δ1::URA3* in pBSII SK(+)	This work
pPL230	*SHR3::FLU2* in pRS316	This work
pPL247	3.5 kb SalI–SpeI fragment containing *GAP1* in pRS316	This work
pPL257	*GAP1::FLU1* in pRS316	This work
pPL258	*GAP1::FLU2* in pRS316	This work
pPL262	3.5 kb SalI–SpeI fragment containing *GAP1* in YCp405	This work
pPL269	*GAP1::FLU1* in YCp405	This work
pPL289	*GAP1::FLU2* in YCp405	This work
pGAL-*HO*	*HO* gene under control of *GAL10* promoter	Herskowitz and Jensen, 1991
pMS16	6.0 kb BamHI–SalI fragment containing *GAP1* in pBS KS(+)	M. Stanbrough, unpublished data
pMS20	*GAP1Δ::LEU2* in pBS KS(+)	M. Stanbrough, unpublished data
p180	*GCN4–lacZ* in YCp50 (regulated expression)	Hinnebusch, 1985
p227	*gcn4–lacZ* in YCp50 (constitutive expression)	Mueller and Hinnebusch, 1986

and the *ADE2* gene was deleted and replaced with the selectable marker *URA3* by transformation with BamHI-digested plasmid pPL132. F35 (*MATa/α HO/HO apf/apf*) is a spontaneous diploid derivative of strain RA68 (*MATα apf*) originally obtained from M. Grenson. F35 was sporulated and mated with MB758-5B (*MATa ho ura3-52*). The resulting diploid CGDY53 (*MATa/α HO/ho apf/APF ura3-52/URA3*) was sporulated, and a stable mating segregant CGAS53-2E (*MATa, ho apf ura3-52*) was obtained.

Standard yeast media were prepared and yeast genetic manipulations were performed as described by Sherman et al. (1986). Where required, SPD was supplemented with either 1 mM or 30 mM L-histidine; appropriate volumes of a filter sterilized 0.5 M L-histidine stock

solution were added, and the pH was adjusted to 5.5 with 10 N NaOH. The concentration of yeast nitrogen base in SPD is 4-fold higher than the amount used in other standard synthetic media because this amount was found to enhance the toxicity of histidine and to reduce background growth of wild-type strains during *shr* mutant screens. Solid SPD and SUD media were prepared as follows. The nitrogen sources (4 g/l) and the yeast nitrogen base (26.8 g/l) were combined to make 4 × stock solutions that were filter sterilized. Other components were autoclaved as separate stock solutions (40% glucose and 4% Difco Bacto agar). Stock solutions and sterile water were mixed to make a 2 × solution, and an equal volume of molten 4% agar was added. Yeast transformations were performed as described by Ito et al. (1983) using 50 μg of heat-denatured calf thymus DNA. Transformants were selected on solid SC media lacking appropriate auxotrophic supplements.

Genetic Analysis

Histidine is a noncatabolizable nitrogen source that is toxic at media concentrations greater than 1 mM. Spontaneous *shr* mutants were selected on SPD media supplemented with 30 mM histidine. The starting strain PLY1 (*MATa his4Δ29 ura3-52*) is a nonreverting histidine auxotroph and must therefore obtain its histidine exogenously. On SPD media, histidine enters the cell through several genetically distinct systems including the general amino acid permease (*GAP1*), the histidine specific permease (*HIP1*) and the arginine permease (*CAN1*). It is important to note that neither *gap1* nor *hip1* mutant strains grow on selective SPD plus 30 mM histidine media.

PLY1 cells pregrown in YPD media were harvested at a cell density of 2 × 10^7 cells per milliliter, washed twice, and resuspended in sterile water. Cells were spread on SPD plus 30 mM histidine at cell densities between 10^5 and 10^7 cells per plate. Putative histidine-resistant mutant colonies occurred at a frequency of 5 per 10^8 cells. Resistant colonies were picked and streaked for single colonies on SPD plus 30 mM histidine. Selected for subsequent characterization were 23 mutants giving rise to streaks of colonies of similar size and exhibiting uniform histidine resistance. These strains were backcrossed to PLY4 (*MATα his4Δ29 ura3-52 ade2Δ1::URA3*). All of the isolated *shr* mutations were recessive; heterozygous diploid strains did not grow on SPD plus 30 mM histidine. Tetrad analysis indicated that the mutant phenotypes segregated 2:2. Complementation was examined in diploids resulting from all possible combinations of pairwise mutant-by-mutant crosses.

Plasmid Construction

Plasmids with inserts derived from pPL154 capable of complementing *shr3* mutations were constructed as follows (Figure 1A). Plasmid pPL164 was constructed by inserting the 11 kb BamHI fragment from pPL154 into BamHI-digested pRS316 (Sikorski and Hieter, 1989). Plasmid pPL164 was digested with EcoRI and religated. The resulting plasmid (pPL183) contains a 4 kb insert. Plasmid pPL179 was constructed by inserting the 3 kb EcoRI–KpnI fragment from pPL183 into EcoRI–KpnI-digested pRS316. Plasmids pPL183 and pPL179 have the insert DNA cloned in opposite orientations. The 1.4 kb AccI fragment containing the *SHR3* gene was isolated from pPL179; the ends were filled in with Klenow fragment and inserted into EcoRV-digested pBSIISK(+) (Stratagene), creating plasmid pPL202. Plasmid pPL210 was constructed by inserting the 1.4 kb SalI–EcoRI from pPL202 into SalI–EcoRI-digested pRS316.

A precise deletion allele of *SHR3* with the entire protein-coding region excised was constructed in two steps using the polymerase chain reaction (PCR). A 36 base synthetic single-stranded DNA PCR primer (3′-5′ΔH) that included 9 bases to create a HindIII site and 27 bases complementary to positions −24 through +3 with respect to the initiation ATG was synthesized. The 3′-5′ΔH primer, in conjunction with the T7 primer, was used to prime a PCR using plasmid pPL202 as template DNA. The amplified 450 bp fragment was digested with HindIII and XhoI and ligated into HindIII–XhoI-digested pBSIISK(+), resulting in plasmid p5′Δ3. A second 53 base synthetic primer (3′-3′ΔHX) that included 15 bases to create a HindIII and an adjacent XhoI site and 38 bases homologous to the termination codon and the 35 bases 3′ to the coding region was synthesized. The 3′-3′ ΔHX primer and the T3 primer were used to prime a second PCR reaction using pPL202 as template DNA. The amplified 350 bp fragment was digested with HindIII and EcoRI and ligated into HindIII–EcoRI-digested p5′Δ3, creating pPL216 (*shr3Δ3*). Plasmid pPL219 (*shr3Δ1::URA3*) was constructed by inserting a 1.1 kb HindIII fragment containing the *URA3* gene into the HindIII site of plasmid pPL216.

Plasmid pPL130 was constructed by inserting a 6.2 kb BamHI fragment containing the *ADE2* gene into BamHI-digested pUC19 (Vieira and Messing, 1987). Plasmid pPL132 containing the *ade2Δ1::URA3* deletion allele was constructed by inserting the *URA3* selectable marker into BglII-digested pPL130.

DNA Sequence Analysis

The nucleotide sequence of the *SHR3* gene was determined by DNA sequence analysis of the 2.7 kb genomic EcoRI–KpnI fragment. Nested deletions of the insert fragments of plasmids pPL183 and pPL179 were generated by digestion with ExoIII as described by Henikoff (1984) except that ExoVII was substituted for S1 nuclease. Double-stranded DNA was prepared as described by Haltiner et al. (1985) and sequenced by the dideoxy chain termination method of Sanger et al. (1977). Protein homology searches were performed at the National Center for Biotechnology Information using the BLAST network service (Altschul et al., 1990).

Epitope Tagging

Epitope tagging of *SHR3* was performed as described by Kolodziej and Young (1991) using site-directed insertion mutagenesis (Kunkel et al., 1987). A 9 amino acid epitope from the influenza virus hemagglutinin protein HA1 (Wilson et al., 1984) was introduced into the SHR3 sequence between amino acid residues 171 and 172 (*SHR3::FLU2*). A synthetic oligomer with 27 nt encoding the HA1 epitope flanked on each side by 20 bases of complementary *SHR3* sequence was synthesized. This oligomer was annealed to single-stranded pPL210 DNA prepared with helper phage M13K07 (Vieira and Messing, 1987) in the *dut⁻ ung⁻* Escherichia coli host, RZ1032 (Kunkel et al., 1987). After elongation, ligation, and transformation into a *dut⁺ ung⁺* host, plasmid DNAs were screened for the presence of a new AatII restriction site diagnostic for successful mutagenesis. Plasmid pPL230, containing the epitope-tagged *SHR3::FLU2* construct, complements all *shr3* mutations.

Plasmid pPL247 was constructed by inserting the 3.5 kb SalI–SpeI fragment containing the *GAP1* gene (isolated from pMS16) into SalI–SpeI-digested pRS316. The 9 amino acid HA1 epitope was independently introduced into two locations within the GAP1 sequence, between amino acid residues 62 and 63 (*GAP1::FLU1*) and amino acid residues 550 and 551 (*GAP1::FLU2*). The resulting plasmids, pPL257 and pPL258, containing these epitope-tagged constructs complemented the growth defects of a *gap1* null mutant strain. Plasmids pPL262, pPL269, and pPL289 were constructed by inserting the 3.5 kb SalI–XbaI inserts from pPL247, pPL257, and pPL258 into SalI–XbaI-digested YCp405, respectively (Ma et al., 1987).

Amino Acid Transport Assays

Amino acid uptake was assayed essentially as described by Ohsumi et al. (1988). Exponentially grown cells were harvested, washed twice with water, and resuspended to a density of 2 × 10^8 cells per milliliter in AAB buffer (10 mM MES–Tris [pH 6.4], 2 mM $MgCl_2$, 0.6 M sorbitol supplemented with 10 mg/ml cycloheximide). The cell suspension was equilibrated to 30°C, and uptake was initiated by the addition of radiolabeled amino acids. Subsamples (100 μl) were withdrawn, diluted into 3 ml of ice-cold AAB buffer, filtered through Whatman GF/F filters, and washed three times with 5 ml of ice-cold AAB buffer. Filter discs were allowed to dry, and radioactivity was measured by liquid scintillation counting.

For kinetic analysis of histidine, proline, arginine, and citrulline, three different ^{14}C-labeled amino acid stock solutions (0.25 mCi/mmol, 1.25 mCi/mmol, or 125 mCi/mmol [for citrulline, 55.9 mCi/mmol]) were used to obtain amino acid concentrations ranging from 10 to 0.002 mM. The uptake rates of lysine, glutamate, leucine, and adenine were determined at 10 mM and 0.004 mM substrate concentrations; two ^{14}C-labeled substrate stock solutions (0.25 mCi/mmol and 125 mCi/mmol) were required to obtain desired final concentrations. The initial uptake rates were determined at each substrate concentration; subsamples were removed at 30, 90, and 180 s, filtered, and washed as described. The uptake rate for every amino acid was linear throughout the subsampling period. Cell protein was determined by the method

of Markwell et al. (1978) in samples of cells boiled in 0.1 M NaOH. Uniformly ^{14}C-labeled L-amino acids and adenine were obtained from Amersham Corporation, Arlington Heights, Illinois; L-[Ureido-^{14}C]citrulline was obtained from New England Nuclear–Du Pont Company, Wilmington, Delaware.

Protein Manipulations, Metabolic Labeling, and Immunoprecipitations

Total yeast protein was obtained by the method of Silve et al. (1991). Samples were heated for 10 min at 37°C, and proteins were resolved by SDS–PAGE using a modified Laemmli system (Laemmli, 1970) in which SDS is omitted from the gel and lower electrode buffer. Endoglycosidase H treatment was carried out according to Orlean et al. (1991). Immunoblots were processed as described by Kim et al. (1990). Primary antibodies were used at the following dilutions: anti-HA1 mouse monoclonal 12CA5 culture supernatants, 1:50; guinea pig anti-invertase antisera (the gift of D. Preuss), 1:2500; anti-PMA1 mouse monoclonal F10-9 ascites fluid (provided by J. Teem), 1:1000; affinity-purified polyclonal rabbit anti-PMA1 antiserum (provided by A. Chang), 1:2000. Blots probed with primary rabbit or guinea pig antibodies were incubated 1–2 hr with affinity-purified ^{125}I-labeled protein A (100 μCi/ml, Amersham Corporation) diluted 1:2000. Blots probed with primary mouse antibodies were incubated 1–2 hr with affinity-purified rabbit anti-mouse immunoglobulin G (IgG) (Jackson Immunoresearch, West Grove, Pennsylvania) diluted 1:500, washed, and then incubated with protein ^{125}I-labeled protein A diluted 1:2000.

Yeast growth in low sulfate synthetic medium, invertase induction, and pulse labeling were carried out essentially as described by Rothblatt and Schekman (1989). Immunoprecipitation of CPY and α factor was carried out as described by Rothblatt and Schekman (1989). For the analysis of electrophoretically resolved ^{35}S-labeled proteins, gels were fixed, prepared for fluorography, and exposed to film as described (Rothblatt and Schekman, 1989).

Membranes were prepared from cells grown in SUD (plus adenine and uracil) essentially as described by Chang and Slayman (1991). Cells were grown to an OD_{600} of 1.5, harvested by centrifugation, washed once in BB buffer (10 mM Tris [pH 7.5], 5 mM $MgCl_2$, 0.1 M NaCl, 0.3 M sorbitol), and resuspended in BB buffer at 200 OD_{600} U/ml. Protease inhibitors were added, and cells were lysed by vortexing with glass beads (three times, 1 min pulses). The cell lysate was centrifuged at 400 g for 5 min to remove unbroken cells, and a total membrane fraction was obtained by centrifugation at 100,000 g for 1 hr. Pelleted membranes were resuspended in a minimal volume of M buffer (20 mM HEPES [pH 7.4], 250 mM sucrose) at an average protein concentration of 36 mg/ml, subdivided into small aliquots, and stored frozen at −70°C. Membrane protein was determined by the method of Markwell et al. (1978).

GAP1 membrane association was determined as described by Deshaies and Schekman (1990). Membrane protein (50 μg) was diluted into 80 μl of M buffer. Twenty microliters of either M buffer, 2.5% Triton X-100, 0.5 M Na_2CO_3 (pH 11), 8 M urea, or 3 M NaCl was added; samples were incubated at 4°C for 15 min and centrifuged at 100,000 g for 1 hr. The resulting pellets were resuspended in 50 μl of SDS–PAGE sample buffer and heated at 55°C for 10 min. Aliquots (20 μl) were resolved by SDS–PAGE, and immunoblots were analyzed using the monoclonal antibody 12CA5 as previously described. Blots were incubated 1–2 hr with affinity-purified rabbit anti-mouse IgG (Jackson Immunoresearch, West Grove, Pennsylvania) diluted 1:500, washed, and then incubated with ^{125}I-labeled protein A diluted 1:2000. The amount of radioactivity was quantitated using a Fujix Bio-Image Analyzer BAS2000 (Fuji Photo Film Company, Japan).

GAP1 protease sensitivity was examined by limited trypsin digestion. Membrane protein (50 μg) suspended in 50 μl of M buffer was digested with varying trypsin concentrations for 90 min at 4°C. After digestion was terminated by the addition of 2 μl of freshly prepared 0.1 M phenylmethylsulfonyl fluoride, the samples were incubated an additional 10 min at 4°C. Twenty microliters of 5 × SDS–PAGE sample buffer was added, and samples were heated at 55°C for 10 min. Aliquots (35 μl) were resolved by SDS–PAGE, and the resulting immunoblots were analyzed using the monoclonal antibody 12CA5 as previously described. GAP1 was visualized either with ^{125}I-labeled protein A as previously described or with chemiluminescence detection reagents (ECL Western Blotting Detection System, Amersham International).

Fluorescence Microscopy

Staining of fixed yeast cells by indirect immunofluorescence was carried out essentially as described by Davis and Fink (1990). Cells transformed with epitope-tagged plasmid constructions were pregrown to a density of 1 × 10^7 cells per milliliter in SC minus uracil or in SUD to select for plasmid maintenance. Cells were then diluted to a density of 2 × 10^6 cells per milliliter in either YPD or fresh SUD medium as indicated and grown for an additional 5 hr. Freshly prepared 40% formaldehyde was added directly to the cells in growth medium to a final concentration of 4%. Cells were fixed overnight on ice, washed twice in solution B (0.1 M potassium phosphate buffer [pH 7.5] in 1.2 M sorbitol), and resuspended to 1 × 10^8 cells per milliliter in solution B containing 30 μM β-mercaptoethanol. Oxalolyticase (Enzogenetics, Corvallis, Oregon) was added to a final concentration of 0.1 mg/ml, and cells were incubated at 30°C. Spheroplasting was stopped by dilution of cells into 15 ml of ice-cold solution B. Spheroplasts were collected by centrifugation, resuspended to 1 × 10^8 cells per milliliter in solution B, and pipetted onto polylysine-coated round coverslips. After 30 min, the cell suspension was gently aspirated away, and coverslips were covered with incubation buffer (solution B containing 4% instant milk) and incubated an additional 15 min. The coverslips were washed twice with solution B, covered with 100% methanol (incubated for 5 min at −20°C), and washed three more times with solution B. The coverslips were incubated in incubation buffer for 2 hr at 30°C. Primary antisera incubations were done at 30°C for 2 hr in incubation buffer (see figure legends for dilutions). Subsequent washes, secondary antibody incubations, DAPI staining, microscopy, and photography were carried out as described (Davis and Fink, 1990). The secondary antibodies were affinity-purified fluorescent DTAF-conjugated antibodies (Jackson Labs, West Grove, Pennsylvania; DTAF: 5-[(4,6-dichlorotriazin-2-y)amino]fluorescein) diluted 1:50 in incubation buffer. Either DTAF-conjugated goat anti-mouse IgG or DTAF-conjugated donkey anti-rabbit IgG was used.

β-Galactosidase Assays

Overnight cultures of histidine auxotrophic strains transformed with β-galactosidase (LacZ) vectors p180 and p227 were grown in complete synthetic media lacking uracil. Cells were diluted 1:5 with either SC minus uracil for repressing conditions or SC lacking both uracil and histidine for derepressing histidine starvation conditions. Freshly diluted cultures were allowed to grow for an additional 5 hr at 30°C, and LacZ activity was determined as described by Rose et al. (1981). Enzymatic activities were normalized to soluble protein concentrations determined for each extract by the method of Bradford (1976).

Acknowledgments

The authors thank M. Stanbrough for providing plasmids containing the *GAP1* gene and *gap1Δ::LEU2* deletion allele, A. G. Hinnebusch for providing the *GCN4–lacZ* plasmids, and M. Grenson for providing strain RA68. We are grateful to A. Chang and J. L. Teem for their generous gifts of polyclonal and monoclonal anti-PMA1 antibodies, respectively. We thank D. Preuss for providing anti-invertase antisera and R. W. Schekman for providing anti-α factor and anti-CPY antibodies. We are grateful to R. A. Preston for measuring the vacuolar pH of our strains. We thank C. Kaiser for comments on the manuscript and all members of the Fink laboratory for helpful discussions, particularly H. Rudolf, D. Miller, L. Davis, A. Antebi, and A. Chang, as well as F. Dietrich, who provided the OFAGE blot. This work was supported by National Institutes of Health (NIH) postdoctoral fellowship GM12038 to P. O. L., a Howard Hughes Medical Institute predoctoral fellowship to C. J. G., and NIH grants GM40266 and GM35010 to G. R. F. G. R. F. is an American Cancer Professor of Genetics.

The costs of publication of this article were defrayed in part by the payment of page charges. This article must therefore be hereby marked "*advertisement*" in accordance with 18 USC Section 1734 solely to indicate this fact.

Received June 5, 1992; revised August 11, 1992.

References

Altschul, S. F., Gish, W., Miller, W., Myers, E. W., and Lipman, D. J. (1990). Basic local alignment search tool. J. Mol. Biol. *215*, 403–410.

Antebi, A., and Fink, G. R. (1992). The yeast Ca^{2+}-ATPase homologue, PMR1, is required for normal Golgi function and localizes in a novel Golgi-like distribution. Mol. Biol. Cell *3*, 633–654.

Bradford, M. (1976). A rapid and sensitive method for the quantification of microgram quantities of protein utilizing the principle of protein-dye binding. Anal. Biochem. *72*, 248–254.

Carle, G. F., and Olson, M. V. (1985). An electrophoretic karyotype for yeast. Proc. Natl. Acad. Sci. USA *82*, 3756–3760.

Chang, A., and Slayman, C. W. (1991). Maturation of the yeast plasma membrane [H^+]ATPase involves phosphorylation during intracellular transport. J. Cell Biol. *115*, 289–295.

Colley, N. J., Baker, E. K., Stamnes, M. A., and Zuker, C. S. (1991). The cyclophilin homolog ninaA is required in the secretory pathway. Cell *67*, 255–263.

Courchesne, W. E., and Magasanik, B. (1983). Ammonia regulation of amino acid permeases in *Saccharomyces cerevisiae*. Mol. Cell. Biol. *3*, 672–683.

Davis, L. I., and Fink, G. R. (1990). The *NUP1* gene encodes an essential component of the yeast nuclear pore complex. Cell *61*, 965–978.

Deshaies, R. J., and Schekman, R. W. (1987). A yeast mutant defective at an early stage in import of secretory protein precursors into the endoplasmic reticulum. J. Cell Biol. *105*, 633–645.

Deshaies, R. J., and Schekman, R. W. (1989). *SEC62* encodes a putative membrane protein required for protein translocation into the yeast endoplasmic reticulum. J. Cell Biol. *109*, 2653–2664.

Deshaies, R. J., and Schekman, R. W. (1990). Structural and functional dissection of Sec62p, a membrane-bound component of the yeast endoplasmic reticulum protein import machinery. Mol. Cell. Biol. *10*, 6024–6035.

Deshaies, R. J., Sanders, S. L., Feldheim, D. A., and Schekman, R. W. (1991). Assembly of yeast Sec proteins involved in translocation into the endoplasmic reticulum into a membrane-bound multisubunit complex. Nature *349*, 806–808.

Finer-Moore, J., Bazan, J. F., Rubin, J., and Stroud, R. M. (1989). Identification of membrane proteins and soluble protein secondary structural elements, packing arrangements by Fourier-transform and amphipathic analysis. In Prediction of Protein Structure and the Principles of Protein Conformation, G. Fasman, ed. (New York: Plenum Press), 719–759.

Franzusoff, A., and Schekman, R. W. (1989). Functional compartments of the yeast Golgi apparatus are defined by the *sec7* mutation. EMBO J. *8*, 2695–2702.

Garrett, J. M. (1989). Characterization of *AAT1*: a gene involved in the regulation of amino acid transport in *Saccharomyces cerevisiae*. J. Gen. Microbiol. *135*, 2429–2437.

Gimeno, C. J., and Fink, G. R. (1992). The logic of cell division in the life cycle of yeast. Science *257*, 626.

Gimeno, C. J., Ljungdahl, P. O., Styles, C. A., and Fink, G. R. (1992). Unipolar cell divisions in the yeast S. cerevisiae lead to filamentous growth: regulation by starvation and *RAS*. Cell *68*, 1077–1090.

Green, N., and Walter, P. (1992). C-terminal sequences can inhibit the insertion of membrane proteins into the endoplasmic reticulum of *Saccharomyces cerevisiae*. Mol. Cell. Biol. *12*, 276–282.

Green, N., Hansen, W., and Walter, P. (1989). The use of gene-fusions to determine membrane protein topology in *Saccharomyces cerevisiae*. J. Cell Sci. (Suppl.) *11*, 109–113.

Green, N., Fang, H., and Walter, P. (1992). Mutants in three novel complementation groups inhibit membrane protein insertion into and soluble protein translocation across the endoplasmic reticulum membrane of *Saccharomyces cerevisiae*. J. Cell Biol. *116*, 597–604.

Grenson, M., and Hennaut, C. (1971). Mutation affecting activity of several distinct amino acid transport systems in *Saccharomyces cerevisiae*. J. Bacteriol. *105*, 477–482.

Haltiner, M., Kempe, T., and Tjian, R. (1985). A novel strategy for constructing clustered point mutations. Nucl. Acids Res. *13*, 1015–1025.

Hann, B. C., and Walter, P. (1991). The signal recognition particle in S. cerevisiae. Cell *67*, 131–144.

Hartmann, E., Rapoport, T. A., and Lodish, H. F. (1989). Predicting the orientation of eukaryotic membrane-spanning proteins. Proc. Natl. Acad. Sci. USA *86*, 5786–5790.

Henikoff, S. (1984). Unidirectional digestion with exonuclease III creates targeted breakpoints for DNA sequencing. Gene *28*, 351–359.

Herskowitz, I., and Jensen, R. E. (1991). Putting the *HO* gene to work: practical uses for mating-type switching. Meth. Enzymol. *194*, 132–146.

Hinnebusch, A. G. (1985). A hierarchy of trans-acting factors modulates translation of an activator of amino acid biosynthetic genes in *Saccharomyces cerevisiae*. Mol. Cell. Biol. *5*, 2349–2360.

Hinnebusch, A. G. (1988). Mechanisms of gene regulation in the general control of amino acid biosynthesis in *Saccharomyces cerevisiae*. Microbiol. Rev. *52*, 248–273.

Hoffmann, W. (1985). Molecular characterization of the *CAN1* locus in *Saccharomyces cerevisiae*. J. Biol. Chem. *260*, 11831–11837.

Horak, J. (1986). Amino acid transport in eukaryotic microorganisms. Biochim. Biophys. Acta *864*, 223–256.

Hurtley, S. M., and Helenius, A. (1989). Protein oligomerization in the endoplasmic reticulum. Annu. Rev. Cell Biol. *5*, 277–307.

Ito, H., Fukuda, Y., Murata, K., and Kimura, A. (1983). Transformation of intact yeast cells treated with alkali cations. J. Bacteriol. *153*, 163–168.

Jauniaux, J. C., and Grenson, M. (1990). *GAP1*, the general amino acid permease gene of *Saccharomyces cerevisiae*: nucleotide sequence, protein similarity with the other bakers yeast amino acid permeases, and nitrogen catabolite repression. Eur. J. Biochem. *190*, 39–44.

Kim, J. W., Ljungdahl, P. O., and Fink, G. R. (1990). *kem* mutations affect nuclear fusion in *Saccharomyces cerevisiae*. Genetics *126*, 799–812.

Kim, J., Closs, E. I., Albritton, L. M., and Cunningham, J. M. (1991). Transport of cationic amino acids by the mouse ecotropic retrovirus receptor. Nature *352*, 725–728.

Klein, P., Kanehisa, M., and DeLisi, C. (1985). The detection and classification of membrane spanning proteins. Biochim. Biophys. Acta *815*, 468–476.

Kolodziej, P. A., and Young, R. A. (1991). Epitope tagging and protein surveillance. Meth. Enzymol. *194*, 508–519.

Kunkel, T. A., Roberts, J. D., and Zakour, R. A. (1987). Rapid and efficient site-specific mutagenesis without phenotypic selection. Meth. Enzymol. *154*, 367–382.

Laemmli, U. K. (1970). Cleavage of structural proteins during the assembly of the head of bacteriophage T4. Nature *227*, 680–685.

Lasko, P. F., and Brandriss, M. C. (1981). Proline transport in *Saccharomyces cerevisiae*. J. Bacteriol. *148*, 241–247.

Link, A. J., and Olson, M. V. (1991). Physical map of the *Saccharomyces cerevisiae* genome at 110-kilobase resolution. Genetics *127*, 681–698.

Lodish, H. F. (1988). Transport of secretory and membrane glycoproteins from the rough endoplasmic reticulum to the Golgi: a rate-limiting step in protein maturation and secretion. J. Biol. Chem. *263*, 2107–2110.

Ma, H., Kunes, S., Schatz, P. J., and Botstein, D. (1987). Plasmid construction by homologous recombination in yeast. Gene *58*, 201–216.

Markwell, M. K., Haas, S. M., Bieber, L. L., and Tolbert, N. E. (1978). A modification of the Lowery procedure to simplify protein determination in membrane and lipoprotein samples. Anal. Biochem. *87*, 206–210.

McCusker, J. H., and Haber, J. E. (1990). Mutations in *Saccharomyces cerevisiae* which confer resistance to several amino acid analogs. Mol. Cell. Biol. *10*, 2941–2949.

Mueller, P. P., and Hinnebusch, A. G. (1986). Multiple upstream AUG codons mediate translational control of *GCN4*. Cell *45*, 201–207.

Müsch, A., Wiedmann, M., and Rapoport, T. A. (1992). Yeast Sec proteins interact with polypeptides traversing the endoplasmic reticulum membrane. Cell *69*, 343–352.

Novick, P., and Schekman, R. W. (1979). Secretion and cell-surface growth are blocked in temperature-sensitive mutants of *Saccharomyces cerevisiae*. Proc. Natl. Acad. Sci. USA *76*, 1858–1862.

Novick, P., Field, C., and Schekman, R. W. (1980). Identification of 23 complementation groups required for post-translational events in the yeast secretory pathway. Cell *21*, 205–215.

Ohsumi, Y., Kitamoto, K., and Anraku, Y. (1988). Changes induced in the permeability barrier of the yeast plasma membrane by cupric ion. J. Bacteriol. *170*, 2676–2682.

Orlean, P., Kuranda, M. J., and Albright, C. F. (1991). Analysis of glycoproteins from *Saccharomyces cerevisiae*. Meth. Enzymol. *194*, 682–697.

Poruchynsky, M. S., and Atkinson, P. H. (1988). Primary sequence domains required for the retention of rotavirus VP7 in the endoplasmic reticulum. J. Cell Biol. *107*, 1697–1706.

Preston, R. A., Murphy, R. F., and Jones, E. W. (1989). Assay of vacuolar pH in yeast and identification of acidification-defective mutants. Proc. Natl. Acad. Sci. USA *86*, 7027–7031.

Rose, J. K., and Doms, R. W. (1988). Regulation of protein export from the endoplasmic reticulum. Annu. Rev. Cell Biol. *4*, 257–288.

Rose, M. D., Casadaban, M. J., and Botstein, D. (1981). Yeast genes fused to β-galactosidase in *Escherichia coli* can be expressed normally in yeast. Proc. Natl. Acad. Sci. USA *78*, 2460–2464.

Rose, M. D., Novick, P., Thomas, J. H., Botstein, D., and Fink, G. R. (1987). A *Saccharomyces cerevisiae* genomic plasmid bank based on a centromere-containing shuttle vector. Gene *60*, 237–243.

Rose, M. D., Misra, L. M., and Vogel, J. P. (1989). *KAR2*, a karyogamy gene, is the yeast homolog of the mammalian BiP/GRP78 gene. Cell *57*, 1211–1221.

Rothblatt, J. A., and Schekman, R. W. (1989). A hitchhiker's guide to analysis of the secretory pathway in yeast. Meth. Cell Biol. *32*, 3–36.

Rothblatt, J. A., Deshaies, R. J., Sanders, S. L., Daum, G., and Schekman, R. W. (1989). Multiple genes are required for proper insertion of secretory proteins into the endoplasmic reticulum in yeast. J. Cell Biol. *109*, 2641–2652.

Rytka, J. (1975). Positive selection of general amino acid permease mutants in *Saccharomyces cerevisiae*. J. Bacteriol. *121*, 562–570.

Sadler, I., Chiang, A., Kurihara, T., Rothblatt, J. A., Way, J., and Silver, P. (1989). A yeast gene important for protein assembly into the endoplasmic reticulum and the nucleus has homology to DnaJ, an *Escherichia coli* heat shock protein. J. Cell Biol. *109*, 2665–2675.

Sanders, S. L., Whitfield, K. M., Vogel, J. P., Rose, M. D., and Schekman, R. W. (1992). Sec61p and BiP directly facilitate polypeptide translocation into the ER. Cell *69*, 353–365.

Sanger, F. S., Nicklen, S., and Coulson, A. R. (1977). DNA sequencing with chain-terminating inhibitors. Proc. Natl. Acad. Sci. USA *74*, 5463–5467.

Serrano, R., Kielland-Brandt, M. C., and Fink, G. R. (1986). Yeast plasma membrane ATPase is essential for growth and has homology with $(Na^+ + K^+)$, K^+- and Ca^{2+}-ATPases. Nature *319*, 689–693.

Sherman, F., Fink, G. R., and Hicks., J. (1986). Methods in Yeast Genetics (Cold Spring Harbor, New York: Cold Spring Harbor Laboratory).

Siddiqui, A. H., and Brandriss, M. C. (1988). A regulatory region responsible for proline-specific induction of the yeast *PUT2* gene is adjacent to its TATA box. Mol. Cell. Biol. *8*, 4634–4641.

Sikorski, R. S., and Hieter, P. (1989). A system of shuttle vectors and yeast host strains designed for efficient manipulation of DNA in *Saccharomyces cerevisiae*. Genetics *122*, 19–27.

Silve, S., Volland, C., Garnier, C., Jund, R., Chevallier, M. R., and Haguenauer-Tsapis, R. (1991). Membrane insertion of uracil permease, a polytopic yeast plasma membrane protein. Mol. Cell. Biol. *11*, 1114–1124.

Sorsoli, W. A., Spence, K. D., and Parks, L. W. (1964). Amino acid accumulation in ethionine-resistant *Saccharomyces cerevisiae*. J. Bacteriol. *88*, 20–24.

Stamnes, M. A., Shieh, B.-H., Chuman, L., Harris, G. L., and Zuker, C. S. (1991). The cyclophilin homolog ninaA is a tissue-specific integral membrane protein required for the proper synthesis of a subset of Drosophila rhodopsins. Cell *65*, 219–227.

Stevens, T., Esmon, B., and Schekman, R. W. (1982). Early stages in the yeast secretory pathway are required for transport of carboxypeptidase Y to the vacuole. Cell *30*, 439–448.

Stirling, C. J., and Hewitt, E. W. (1992). The *S. cerevisiae SEC65* gene encodes a component of yeast signal recognition particle with homology to human SRP19. Nature *356*, 534–537.

Stirling, C. J., Rothblatt, J. A., Hosobuchi, M., Deshaies, R. J., and Schekman, R. W. (1992). Protein translocation mutants defective in the insertion of integral membrane proteins into the endoplasmic reticulum. Mol. Biol. Cell *3*, 129–142.

Surdin, Y., Sly, W., Sire, J., Bordes, A. M., and de Robichon-Szulmajster, H. (1965). Properties and genetic control of the amino acid accumulation system in *Saccharomyces cerevisiae*. Biochim. Biophys. Acta *107*, 546–566.

Tanaka, J., and Fink, G. R. (1985). The histidine permease gene (*HIP1*) of *Saccharomyces cerevisiae*. Gene *38*, 205–214.

Vandenbol, M., Jauniaux, J. C., and Grenson, M. (1989). Nucleotide sequence of the *Saccharomyces cerevisiae PUT4* proline-permease-encoding gene: similarities between CAN1, HIP1 and PUT4 permeases. Gene *83*, 153–159.

Vieira, J., and Messing, J. (1987). Production of single-stranded plasmid DNA. Meth. Enzymol. *153*, 3–11.

Wang, H., Kavanaugh, M. P., North, R. A., and Kabat, D. (1991). Cell-surface receptor for ecotropic murine retroviruses is a basic amino-acid transporter. Nature *352*, 729–731.

Weber, E., Chevallier, M. R., and Jund, R. (1988). Evolutionary relationship and secondary structure predictions in four transport proteins of *Saccharomyces cerevisiae*. J. Mol. Evol. *27*, 341–350.

Weber, E., Rodriguez, C., Chevallier, M. R., and Jund, R. (1990). The purine-cytosine permease gene of *Saccharomyces cerevisiae*: primary structure and deduced protein sequence of the *FCY2* gene product. Mol. Microbiol. *4*, 585–596.

Wiame, J. M., Grenson, M., and Arst, H. N., Jr. (1985). Nitrogen catabolite repression in yeasts and filamentous fungi. Adv. Microb. Physiol. *26*, 1–88.

Wilson, I. A., Niman, H. L., Houghten, R. A., Cherenson, A. R., Connolly, M. L., and Lerner, R. A. (1984). The structure of an antigenic determinant in a protein. Cell *37*, 767–778.

GenBank Accession Number

The accession number for the sequence reported in this paper is L01264.

Chapter 3:

Unipolar Cell Divisions in the Yeast *S. cerevisiae* Lead to Filamentous Growth: Regulation by Starvation and *RAS*[a]

[a] My specific contributions to this paper are listed in the introduction to Chapter 2.

Cell, Vol. 68, 1077–1090, March 20, 1992, Copyright © 1992 by Cell Press

Unipolar Cell Divisions in the Yeast S. cerevisiae Lead to Filamentous Growth: Regulation by Starvation and *RAS*

Carlos J. Gimeno, Per O. Ljungdahl, Cora A. Styles, and Gerald R. Fink
Whitehead Institute for Biomedical Research and
Department of Biology
Massachusetts Institute of Technology
Cambridge, Massachusetts 02142

Summary

Diploid S. cerevisiae strains undergo a dimorphic transition that involves changes in cell shape and the pattern of cell division and results in invasive filamentous growth in response to starvation for nitrogen. Cells become long and thin and form pseudohyphae that grow away from the colony and invade the agar medium. Pseudohyphal growth allows yeast cells to forage for nutrients. Pseudohyphal growth requires the polar budding pattern of a/α diploid cells; haploid axially budding cells of identical genotype cannot undergo this dimorphic transition. Constitutive activation of *RAS2* or mutation of *SHR3*, a gene required for amino acid uptake, enhance the pseudohyphal phenotype; a dominant mutation in *RSR1/BUD1* that causes random budding suppresses pseudohyphal growth.

Introduction

The polarity of cell division is critical in determining the size and shape of organisms. A cell that undergoes polarized cell division specifically orients its division axis or plane of division with respect to some reference point; a site on the surface of the cell, the position of sibling or ancestral cells, and/or the position of other tissues, organs or structures. For example, oriented cell division is critical in the embryogenesis of both the mouse (Johnson and Maro, 1986; Sutherland et al., 1990) and the nematode Caenorhabditis elegans (Hyman and White, 1987; Hyman, 1989). The mechanism of directional root growth in higher plants also involves polarized cell division (Gunning, 1982).

The yeast Saccharomyces cerevisiae divides mitotically by budding (Pringle and Hartwell, 1981). The bud emerges from a site on the surface of the cell and enlarges while the mother remains relatively constant in size. The mitotic spindle forms along the mother–bud axis and, after a set of chromosomes is distributed into the bud, the mother and the bud separate. A chitin plug termed the bud scar is deposited at the site of cell separation and conveniently marks the sites of previous budding events. A single cell can bud many times. The polarity of cell division is defined with respect to the position on the cell surface of previous budding events. Polarized cell division is manifested as two genetically programmed spatial patterns of cell division, axial for **a** or α cells and polar for **a**/α cells (Freifelder, 1960; Hicks et al., 1977; Chant and Herskowitz, 1991). In the axial pattern, the mother and daughter cells bud adjacent to their cell pole that defined the previous mother–daughter junction (see Table 1 for illustration). In the polar pattern, a virgin mother's first several buds emerge at the pole opposite the one that defined the junction to its mother (we refer to this initial pattern as unipolar budding); subsequent buds emerge at either this or the opposite pole (Freifelder, 1960; Hicks et al., 1977) (we refer to this latter pattern as bipolar budding). The biological function of axial haploid budding for mating has been discussed (Nasmyth, 1982), but to date the function of diploid bipolar budding has remained obscure.

Polar cell division is controlled genetically in S. cerevisiae (reviewed by Drubin, 1991). The current model proposes that budding pattern genes represented by *RSR1/BUD1* and *BUD2-BUD5* (Bender and Pringle, 1989; Chant and Herskowitz, 1991; Chant et al., 1991; Powers et al., 1991) are required for selection of the proper bud site and consequently for establishing the proper axis of cell division. *RSR1/BUD1*, *BUD2*, and *BUD5* convert the default random budding pattern to bipolar, and subsequent action of *BUD3* and *BUD4* convert bipolar to axial. To explain the observed cell type specificity (diploids are bipolar, haploids axial) an elegant model was proposed (Chant and Herskowitz, 1991) that either or both *BUD3* and *BUD4* are repressed by the repressor a1α2 found only in **a**/α cells. Neither lethality nor alterations in colony morphology were observed in strains that had lost *BUD* gene function; random, bipolar, and axial budding all lead to the formation of a smooth, hemispherical colony. We call this the unpolarized colonial growth pattern. In summary, dramatic differences in budding pattern seemed to have no effect on growth or colony morphology. Why then does yeast have such an elaborate system for determining budding pattern?

In this report, we define a dimorphic transition in the life cycle of S. cerevisiae: pseudohyphal growth. The term dimorphic has been used to define fungi that can grow vegetatively in either a yeast or filamentous form (Shepherd, 1988). A pseudohypha is defined as a "fragile chain of cells (usually yeasts, which have arisen by budding and have elongated without detaching from adjacent cells), with morphological characteristics intermediate between a chain of yeast cells and a hypha" (Evans and Richardson, 1989). This dimorphic transition is induced by starvation for a nitrogen source and is controlled directly or indirectly by the *RAS* signal transduction pathway. Pseudohyphal growth in S. cerevisiae is a unique type of polarized cell division that requires unipolar budding and a change in cellular morphology that results in the formation of macroscopic structures emanating away from the colony into unpopulated substrate. Reiteration of unipolar cell division by pseudohyphal cells leads to the formation of an asymmetric polarized colony. We propose that the role of the diploid budding pattern is to permit otherwise sessile cells to forage for nutrients and substrate at a distance from their initial colonization site.

Table 1. Budding Pattern of Pseudohyphal and Sated a/α Shr3⁻ Cells

	First Buds		Second Buds	
	Pseudohyphal	Sated	Pseudohyphal	Sated
Cell Divisions	90	69	90	69
Free End	100%	100%	90%	73%
Birth End	0%	0%	10%	27%

Time lapse photography was used to determine bud site selection in both pseudohyphal and sated cells as described in Experimental Procedures.

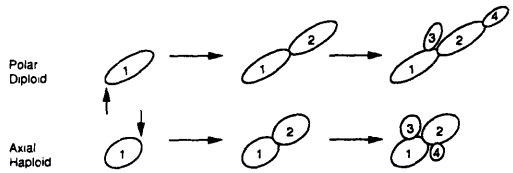

The polar budding pattern most often observed in diploid virgin pseudohyphal and sated cells as well as the axial budding pattern of haploid cells is shown in the drawing. In the 159 cell divisions reported, axial haploid budding was never observed. In all cases cell 1 is a virgin cell. The vertical arrows indicate the birth end of cell 1. Cell 2 and cell 3 are the first and second daughters, respectively, of cell 1. Cell 4 is the first daughter of cell 2.

Results

A yeast cell grown on standard media multiplies until it forms a visible structure, an approximately hemispherical colony with a smooth circular outline. This morphology is strikingly homogeneous, with little variation from colony to colony. We have found that yeast has a second distinct mode of proliferation, pseudohyphal growth. Pseudohyphal growth results from a reiterated pattern of unipolar cell division to form the chain of cells that constitute the pseudohypha. In polarized colonies, which resemble colonies formed by filamentous fungi, the pseudohyphae radiate outward in all directions (Figure 1).

The Dimorphic Switch to Pseudohyphal Growth Is Induced by Nitrogen Starvation

The transition from unpolarized colonial growth to pseudohyphal growth occurs on agar-based synthetic growth medium deficient in nitrogen. Wild-type cells form pseudohyphae on standard minimal medium containing low levels of ammonia (synthetic low ammonia histidine dextrose [SLAHD]) or proline as sole nitrogen source (synthetic proline histidine dextrose [SPHD]). On the low ammonia medium, all of the wild-type colonies form pseudohyphae (CGX31, Figures 2A and 2E), whereas on proline medium (SPHD), small regions of pseudohyphal growth are apparent in about a quarter of the colonies (CGX31, Figures 2B and 2F). CGX31 does not form pseudohyphae when grown on standard ammonia-based medium (SD) (Sherman et al., 1986) or media with the same composition as SPHD but containing as sole nitrogen source(s) standard levels of ammonia (synthetic ammonia histidine dextrose [SAHD]), arginine (synthetic arginine histidine dextrose [SRHD]), proline and ammonium sulfate (synthetic proline ammonia histidine dextrose [SPAHD]), or proline and arginine (synthetic proline arginine histidine dextrose [SPRHD]) (data not shown).

Of all strains tested, those with the Σ1278b background undergo the most uniform and easily controlled transition from unpolarized to pseudohyphal growth on both low ammonia and proline medium. Many laboratories commonly use strains derived from this background (Grenson et al., 1966; Brandriss and Magasanik, 1979) because they are extremely sensitive to the ammonia repression of nitrogen assimilation pathways (Rytka, 1975; Wiame et al., 1985). Σ1278b and its derivatives cross well with other standard laboratory strains such as S288C (Siddiqui and Brandriss, 1988) and make up part of the set of interbreeding laboratory isolates known collectively as S. cerevisiae.

Mutations in the *SHR3* Gene Enhance Pseudohyphal Growth

Diploid strains homozygous for mutant loss-of-function *SHR3* alleles produce a more uniform, prolific, and extended transition to the pseudohyphal growth pattern on SPHD medium than wild-type strains (compare Figures 2B and 2F with Figures 2C and 2G). Mutations in the *SHR3* gene lead to reduced uptake of many amino acids, including proline (Ljungdahl et al., unpublished data). This reduction in proline uptake probably starves the cell for nitrogen and accounts for the reduced growth on SPHD of *shr3* strains as compared with *SHR3* strains. Strains containing *shr3* mutations also show more extensive and exaggerated pseudohyphal growth than wild type on low ammonia medium (data not shown). The enhanced pseudohyphal growth of a Shr3⁻ strain (CGX19) on low ammonia can be explained if ammonia uptake, like amino acid uptake, is

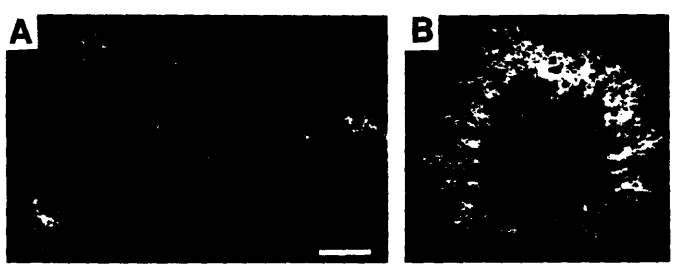

Figure 1. Morphology of Polarized Colonies Produced by Pseudohyphally Growing S. cerevisiae

(A) CGX19 (*MATa/α* Shr3⁻) or (B) F35 (*MATa/α* Shr3⁻) were streaked for single cells on SPHD plus uracil and SPHD plates, respectively, grown at 24°C for 11 and 14 days, respectively, and representative colonies were photographed. The colony in (B) was in a zone of low colony density, whereas the colonies in (A) were in a zone of high colony density. The scale bar is for both panels and represents 0.2 mm.

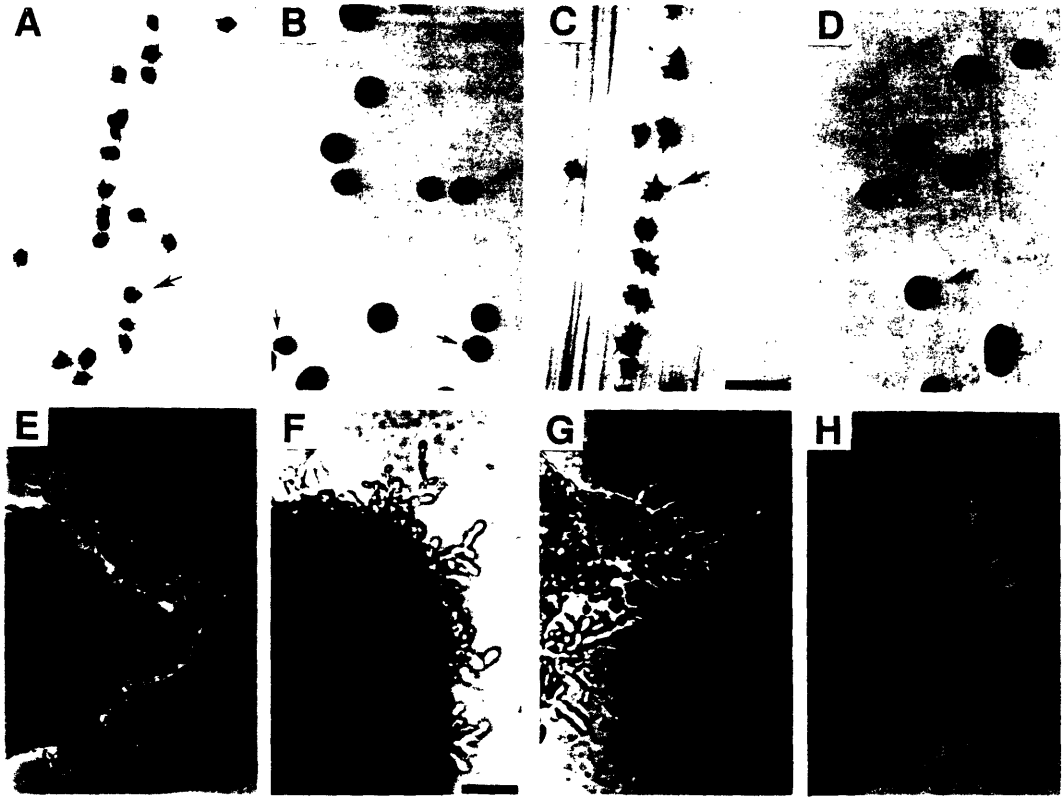

Figure 2. Genetic and Physiological Characterization of S. cerevisiae Pseudohyphal Growth

MATa/α ura3-52/ura3-52 (CGX31) and *MATa/α ura3-52/ura3-52 shr3-102/shr3-102* (CGX19) were streaked for single cells on SLAHD plus uracil, SPHD plus uracil, or SAHD plus uracil plates, incubated at 30°C for 48 hr, and the resulting colonies were photographed. (A), (B), (C), and (D) show low magnification views of colonies of: (A) strain CGX31 growing on SLAHD plus uracil, (B) CGX31 growing on SPHD plus uracil, (C) CGX19 growing on SPHD plus uracil, and (D) CGX19 growing on SAHD plus uracil. In (B) the three colonies with pseudohyphae are designated with arrows. (E), (F), (G), and (H) show high magnification views of the colonies marked by large arrows in (A), (B), (C), and (D). (A), (B), (C), and (D) have the same scale, with the scale bar in (C) representing 0.5 mm. (E), (F), and (G) have the same scale, with the scale bar in (F) representing 30 μm. The scale bar in (H) represents 30 μm.

impaired. On medium containing standard levels of ammonium sulfate as sole nitrogen source, Shr3$^+$ (CGX31) and Shr3$^-$ (CGX19) cells grow at similar rates, and neither strain forms pseudohyphae (data not shown and Figures 2D and 2H). The fact that CGX19 fails to form pseudohyphae when proline medium (SPHD) contains ammonia (SPAHD) supports the contention that it is nitrogen starvation that induces pseudohyphal growth. To prove it is loss of function of *SHR3* that is responsible for enhancing pseudohyphal growth we transformed CGX19 (*MATa/α shr3-102/shr3-102 ura3-52/ura3-52*) with a centromere-based plasmid containing either no insert (pRS306) or the *SHR3* gene (pPL210). Transformants containing pRS306 (CG64) showed pseudohyphal growth identical to that exhibited by CGX19, whereas the pPL210 transformants (CG62) did not. Only a minority of colonies of diploid cells homozygous for *shr3* in a S288C backround have pseudohyphae, and the number of pseudohyphae per colony is much lower than that observed in a comparable Shr3$^-$ Σ1278b strain. Diploid cells derived from a *shr3* S288C parent and a *shr3* Σ1278b parent show the pseudohyphal growth characteristic of Σ1278b Shr3$^-$ diploids.

Activation of the RAS2 Protein Enhances Pseudohyphal Growth

Strains carrying the dominant *RAS2^{val19}* mutation show greatly enhanced pseudohyphal growth. The *RAS2^{val19}* mutation results in a constitutively activated *RAS* signal transduction pathway and consequent elevated intracellular cAMP levels (Toda et al., 1985). Strains with an activated *RAS*/cAMP pathway are very sensitive to nitrogen starvation (Toda et al., 1987). Since the *RAS2^{val19}* mutation is dominant (Kataoka et al., 1984; Powers et al., 1989), its effects on growth could be tested by introducing it into our standard Ras2$^+$ Σ1278b strains by transformation. CGX31 transformed with a plasmid containing *RAS2^{val19}* (YCpR2V, kindly provided by M. Wigler) exhibits greatly enhanced pseudohyphal growth (Figure 3A). The same Shr3$^+$ strain

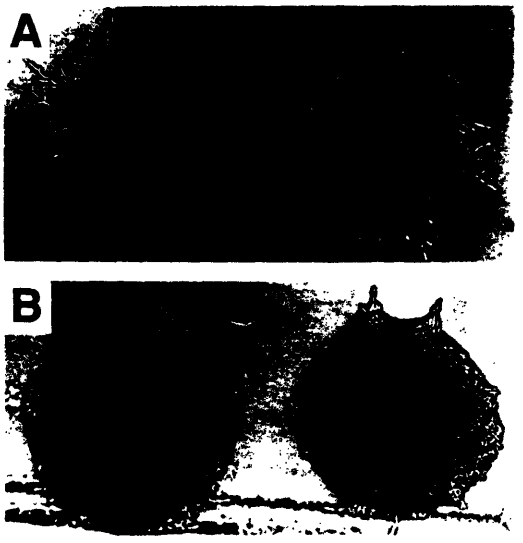

Figure 3. *RAS2*^{val19} Induction of Pseudohyphal Growth

A wild-type strain *MATa/α ura3-52/ura3-52* (CGX31) was transformed with YCpR2V or YCp50 generating (A) CG69 and (B) CG71, respectively. These strains were streaked for single cells on SPHD medium, and resulting colonies were photographed after 33 hr of growth at 30°C. The scale bar represents 60 μm.

(CGX31) transformed with vector (YCp50) alone shows only low frequency pseudohyphal growth on SPHD medium (Figure 3B). The pseudohyphal growth of CGX31 carrying the *RAS2*^{val19} mutation occurs in a Shr3$^+$ background where growth on SPHD is much better than that of Shr3$^-$ strains. Thus, it is not simply the poor growth of Shr3$^-$ strains on SPHD that results in pseudohyphal development.

Pseudohyphal Growth Is a Diploid-Specific Pathway

Diploid but not haploid S. cerevisiae strains give rise to pseudohyphae. To study the effect of ploidy and the genotype at the mating type locus on pseudohyphal growth, we have constructed a congenic set of yeast strains carrying a mutant allele of *SHR3*. Figure 4 compares the morphology of the diploid strain CGX19 (Figure 4A) with its two haploid parents (Figures 4B and 4C) carrying the *shr3-102* mutation. No *shr3-102* haploids we have analyzed manifest pseudohyphal growth; all form typical hemispherical unpolarized colonies on SPHD. *MATa/a shr3-102/shr3-102* (CG85) and *MATα/α shr3-102/shr3-102* (CG67) isogenic derivatives of CGX19 (*MATa/α shr3-102/shr3-102*) also do not form pseudohyphae on SPHD; instead they form hemispherical colonies identical to those shown in Figure 2D. In addition, **a** and α haploid strains carrying the *RAS2*^{val19} allele (CG73 and CG75, respectively) do not form pseudohyphae, whereas the **a**/α diploid resulting from crossing these haploids does. The cell type specificity of pseudohypal growth is controlled in part by the alleles of the mating type locus.

Pseudohyphal Growth Results from Unipolar Cell Division

The unipolar cell divisions that characterize polar diploid budding are critical for the elaboration of pseudohyphal growth. We define virgin cells as those that have had no daughters and sated cells as those growing vegetatively on rich medium. We observed the budding pattern of virgin sated CGX19 cells or of virgin CGX19 cells growing in pseudohyphae by time lapse photomicroscopy. Figure 5 shows the results of a time lapse experiment where the development of a pseudohypha was monitored for 6 hr, with interpretative drawings summarizing the results. From this sequence it can be seen that serial reiteration of unipolar budding by terminal pseudohyphal cells results in polarized chain elongation. It can be seen also that the second bud of a virgin terminal cell initiates a new lateral chain oriented at an angle from the main lineage.

We assayed budding pattern quantitatively by determining the site of emergence of the first and second buds of

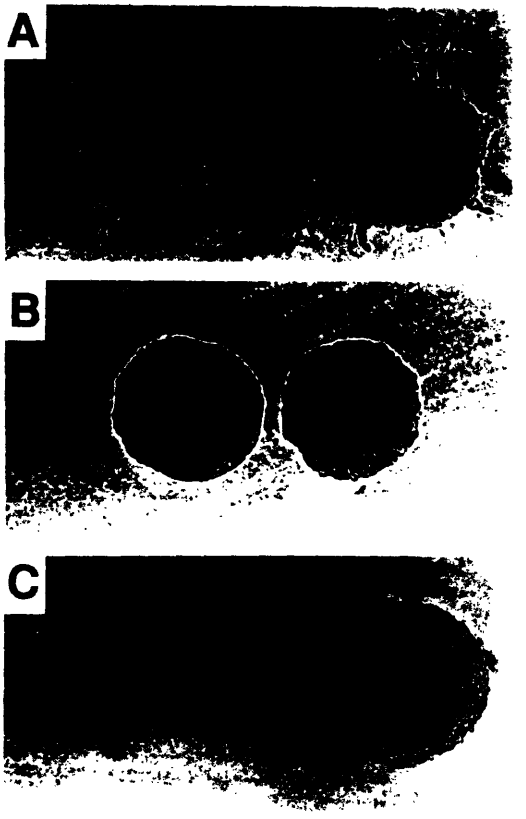

Figure 4. Effect of Ploidy on Pseudohyphal Growth

(A) CGX19 (*MATa/α ura3-52/ura3-52 shr3-102/shr3-102*) and its two haploid parents, (B) CG41 (*MATα ura3-52 shr3-102*) and (C) CG25 (*MATa ura3-52 shr3-102*), were streaked for single cells on the same SPHD plus uracil plate, incubated at 30°C for 49 hr, and the resulting colonies were photographed. The scale bar represents 60 μm.

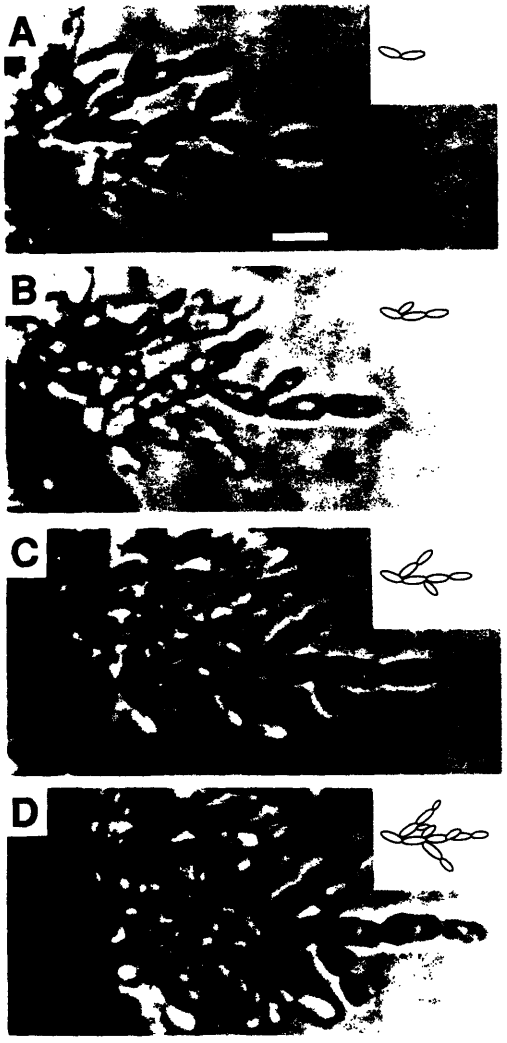

Figure 5. Time Lapse Photographic Analysis of Pseudohyphal Growth

Strain CGX19 *MATa/α ura3-52/ura3-52 shr3-102/shr3-102* was streaked for single cells on SPHD plus uracil medium. After 3 days of growth at 30°C, a visible pseudohypha was chosen and photographed at 2 hr intervals while growing at 30°C. (A) is the initial time point. An interpretative drawing of the elongating pseudohypha appears in the upper right hand corner of each panel. The scale bar represents 10 μm.

virgin pseudohyphal and sated cells by time lapse observation (Table 1). Following the conventions of Freifelder (1960), the pole of a bud that contacts its mother cell is called the birth end and the opposite pole the free end. The first bud of 90 virgin terminal pseudohyphal cells and 69 virgin sated cells of strain CGX19 emerged without exception on the free end of its mother cell. The first bud of a diploid is therefore a good marker for the free end of this cell. The second bud of 90 virgin terminal pseudohyphal cells emerged in 90% of the cases again on the free end of its mother cell after two doubling times had elapsed. The shape of these cells together with their immobility in the agar matrix permitted easy identification of a cell's poles. The proliferation of ancestral cells prevented us from scoring events at the birth end in the other 10% of the cases where no bud was present at the free end after two doubling times. The second bud of each of 69 sated cells emerged from the mother cell's free end, which we identify in this case as the same cell pole from which the first bud emerged 73% of the time and from the birth end, defined as the opposite pole, 27% of the time. Clearly the first bud of virgin CGX19 cells emerges in a unipolar manner from the free end regardless of the cell's growth mode. The second bud also emerges unipolarly in the majority of cell divisions.

It is important to note that in some lineages lateral budding was completely absent, whereas apical growth continued (see Figure 8B). In other words, daughters divided for several divisions while the mother cells did not, suggesting that in these lineages cell division may be repressed after a cell gives birth to its first daughter. In the fungal literature, this phenomenon is known as apical dominance (Rayner, 1991).

The Cells of the Pseudohypha Are a Morphologically Distinct Cell Type

We compared the dimensions of pseudohyphal and sated cells of the same genotype. In the first experiment, we grew Shr3$^-$ (CGX19) cells on YPD or SPHD plus uracil media. We then prepared cells taken from the surface of the agar for scanning electron microscopy (SEM). Figure 6 shows SEM micrographs of a typical ellipsoidal CGX19 cell from the YPD plate as well as a CGX19 pseudohyphal cell from the SPHD plus uracil plate. To be certain that the surface grown cells in SEM micrographs were representative of cells in invasive pseudohyphae, we also measured the dimensions of the latter by light photomicroscopy (Table 2). Given the difference in imaging methods, the two sets of measurements agree well and give similar axial ratios. Pseudohyphal cells that contain *RAS2^{val19}* are even longer and have even larger axial ratios than CGX19 or CGX31 pseudohyphal cells (data not shown). We have not observed pseudohyphal growth for our strains (*shr3* or *RAS2^{val19}*) when grown in liquid medium (SPHD).

The Daughter of a Pseudohyphal Cell Can Be a Pseudohyphal Cell or a Blastospore-Like Cell

The elongated pseudohyphal cells have been observed to give rise to either of two cell types. Elongated cells may divide to produce an elongated daughter with roughly the same final dimensions as the mother cell or alternatively a spheroidal blastospore-like cell with roughly the dimensions of a sated yeast cell (Table 2). Blastospores are defined as round or oval budding yeast cells arising from pseudohyphae (Lodder, 1970). Both the elongate pseudohyphal cell and the blastospore-like cell can be produced either apically or laterally. The blastospore-like cells produced by the pseudohyphal cell may be a new cell type or they may be identical to vegetative cells. When monitored by time lapse photomicroscopy, pseudohyphae are often observed to invade the agar and subsequently

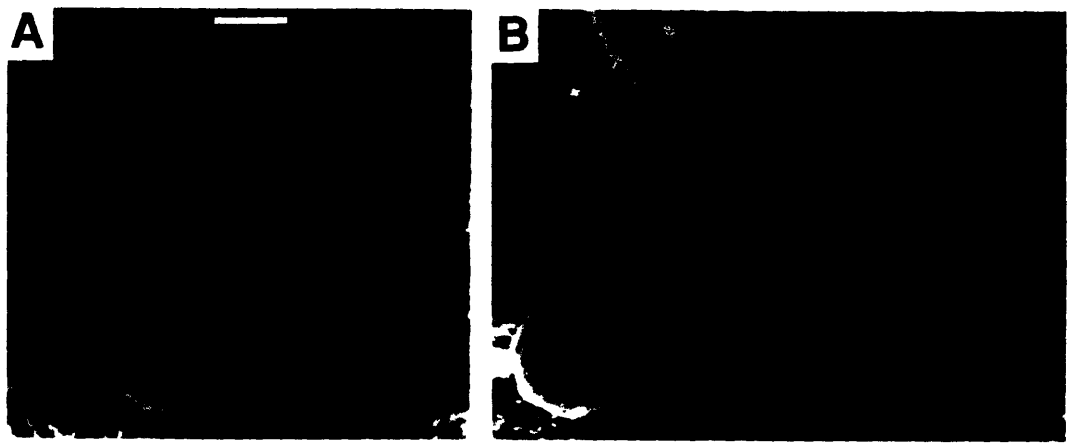

Figure 6. SEM Analysis of Starvation-Induced Cell Morphology Changes

CGX19 *MATa/α ura3-52/ura3-52 shr3-102/shr3-102* growing vegetatively at 30°C was streaked for single colonies on prewarmed (A) YPD and (B) SPHD plus uracil plates. These plates were incubated at 30°C for 31 hr and then prepared for SEM as described in Experimental Procedures. (A) shows a representative YPD-grown sated yeast cell that has been budding in a bipolar manner. The budding pattern of the cell can be deduced from the positions of the bud scars, the protrusions visible on the surface of the cell. (B) shows a pseudohyphal cell with two bud scars visible at one pole, a conformation predicted by polar budding. (A) and (B) have the same scale, with the scale bar in (A) representing 1 μm.

begin budding blastospore-like cells at the base of the pseudohypha. When pseudohyphae stop growing, they typically become covered with blastospore-like cells (Figure 7). These blastospore-like cells can divide, showing that at least some of them are actively proliferating.

Pseudohyphal Cells Invade the Semisolid Agar Growth Medium

Pseudohyphal cells penetrate the surface of the agar plate and grow down into the medium. Shr3⁻ diploids as well as other standard strains growing in the sated mode on rich medium grow by spreading out on the surface of the agar. Even on SPHD medium, most strains grow on the surface. By contrast, Shr3⁻ diploids on SPHD medium are invasive and grow into the agar, presumably in search of nutrients. Columns within the agar have about the same number of members as those on the surface, so the agar represents no deterrent to their exploration. The invasive growth is easily observed in a dissecting microscope and is further demonstrated by the observation that a microneedle must pierce the agar to reach the cells of many pseudohyphae. The mothers and daughters within the chain appear to be physically attached because they often can be manipulated as a unit. Figure 8 shows both pseudohyphae emanating from a microcolony beginning to penetrate the agar and an older pseudohypha that has invaded extensively.

A Mutation in *RSR1/BUD1* Causing Random Bud Site Selection Suppresses Pseudohyphal Growth

To test the hypothesis that the polar budding pattern of diploids is required for pseudohyphal growth, we studied the growth pattern of strains that budded either in the polar or the random pattern. A dominant mutation of the *RSR1/BUD1* gene (Bender and Pringle, 1989; Ruggieri et al., 1992) *rsr1*^{asn16} (kindly provided by A. Bender) that causes random budding even in the presence of *RSR1/BUD1* enabled us to examine the role of budding pattern in pseudohyphal growth. We constructed isogenic diploid strains containing either the *rsr1*^{asn16} gene on a centromere vector (YCp[rsr1^{asn16}]) or the vector alone (YCp50). We examined the budding pattern of our strains by fluorescence microscopy after staining with Calcofluor (Pringle et al., 1989).

Table 2. Dimensions of Pseudohyphal Cells, Sated Cells, and Blastospore-Like Cells

Strain	Cell Type	Medium	Cell Length (μm)	Cell Width (μm)	Axial Ratio Length/Width
CGX19	Pseudohyphal (SEM)	SPHD+U	6.7 ± 1.0 (3)	1.9 ± 0.1 (3)	3.5
CGX19	Sated (SEM)	YPD	4.2 ± 0.4 (7)	3.0 ± 0.2 (7)	1.4
CGX19	Pseudohyphal (LM)	SPHD+U	9.2 ± 1.7 (11)	2.7 ± 0.3 (11)	3.4
CGX19	Sated (LM)	YPD	5.7 ± 0.8 (19)	3.9 ± 0.4 (19)	1.5
CGX19	Blastospore-like (LM)	SPHD+U	5.6 ± 0.5 (10)	4.4 ± 0.4 (10)	1.3

CGX19 cells (*MATa/α ura3-52/ura3-52 shr3-102/shr3-102*) were measured in all cases. Cell dimensions are based on scanning electron and light photomicrographs as described in Experimental Procedures. Cell length is the length of the longest axis of the cell. Cell width is the width of the cell at the midpoint of its longest axis. The axial ratio is the average cell length divided by the average cell width. The tabulated values are averages with standard deviations listed. The number of cells measured for each table entry appears in parentheses after the standard deviation.

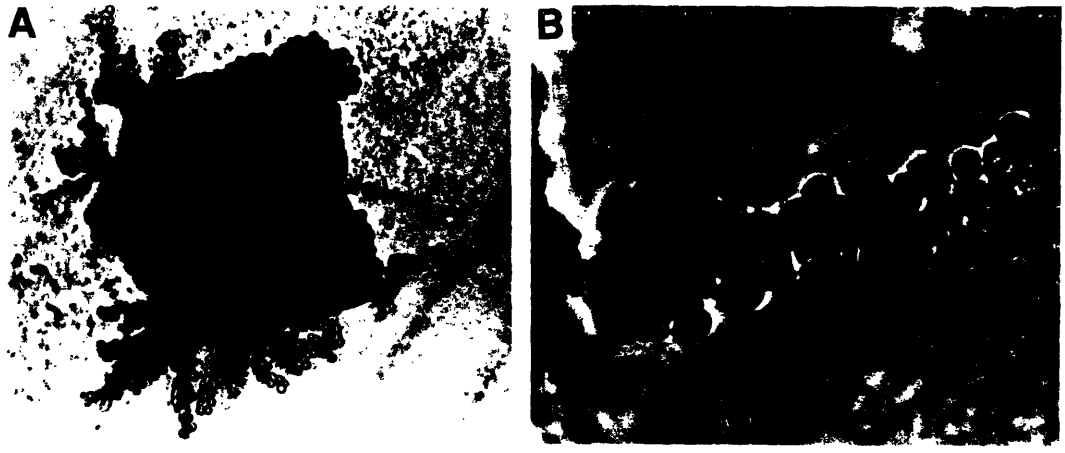

Figure 7. Production of Blastospore-Like Cells by S. cerevisiae Pseudohyphal Cells

A MAT**a**/α Shr3⁻ strain (F35) was streaked for single cells on SPHD medium. After 3 days, microcolonies like the one shown in (A) existed in the dense part of the streakout. In these colonies the pseudohyphae were covered with small spherical blastospore-like cells. (B) shows an enlarged view of the pseudohypha at the right of the colony shown in (A). The scale bar is for (B) only and represents 10 μm.

Calcofluor stains the chitin in the bud scars and indicates the pattern of previous bud sites on the surface of cells. Both wild-type Shr3⁺ (CGX31) and Shr3⁻ (CGX19) strains containing the plasmid with the *rsr1*^{asn16} gene show a random budding pattern, whereas the isogenic CGX31 and CGX19 strains carrying the vector alone show the bipolar budding pattern (data not shown). We examined the consequences of random budding on colony morphology and pseudohyphal growth. The presence of the *rsr1*^{asn16} allele suppresses pseudohyphal growth of CGX31 and CGX19 on both SPHD (Figure 9) and on low ammonia medium (data not shown).

The examination of the cells growing at the fringes of the colonies suggests that the random budding pattern caused by *rsr1*^{asn16} suppresses pseudohyphal growth. At the fringes of the CGX19 *rsr1*^{asn16} colonies (Figure 9) there are a few long cells protruding away from the mass of cells. Their shape, though not as long and thin, resembles that of pseudohyphal Bud⁺ cells. Their distinguishing feature is that the first daughters of these cells often bud at the middle of their mother rather than at her distal tip and grow in a direction perpendicular to the mother's long axis. Thus, despite having an appropriate long cell shape, the disorientation of the daughters prevents cell lineages from

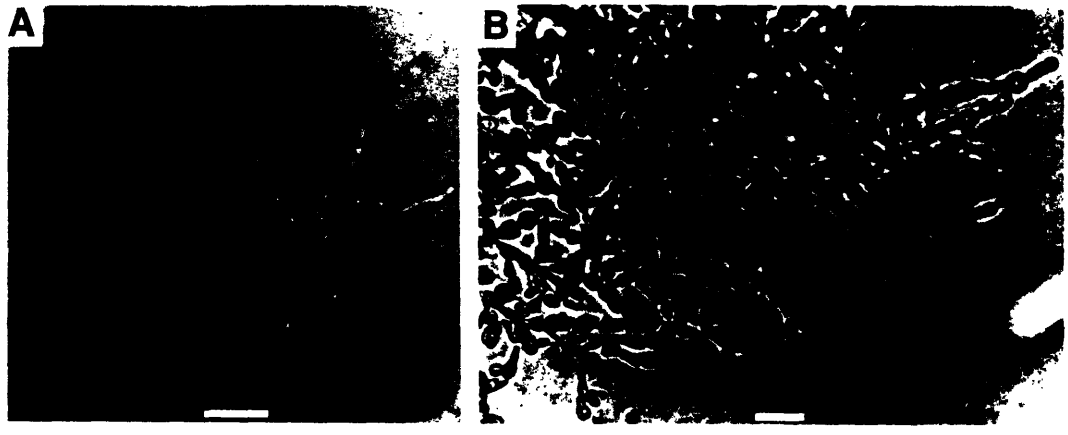

Figure 8. Invasiveness of S. cerevisiae Pseudohyphae

A MAT**a**/α Shr3⁻ strain (F35) was streaked for single colonies on SPHD medium. After 2 days of growth at 30°C (A), a microcolony was photographed. In (B) after 21 days of growth, pseudohyphae of a macrocolony were photographed. The pseudohyphae in (B) also represent a subclass of pseudohyphae that have unusually long cells. The scale bars in (A) and (B) represent 20 μm.

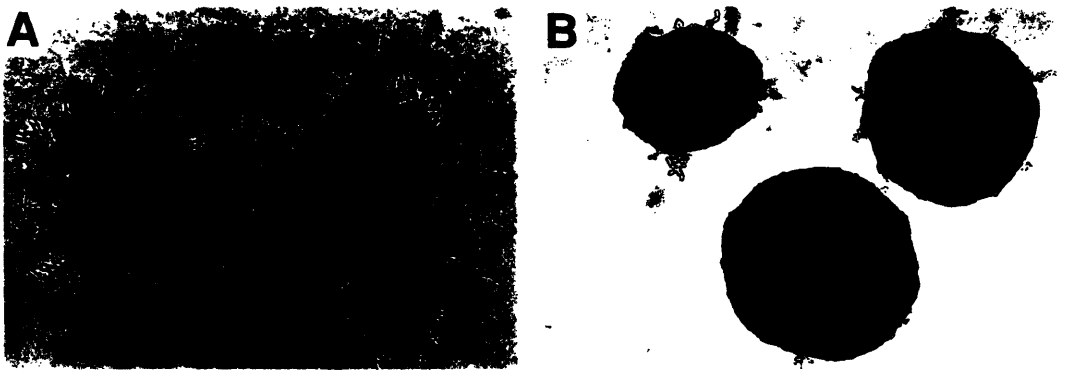

Figure 9. Mutation of *RSR1/BUD1* Suppresses Pseudohyphal Growth

A Shr3 strain *MATa/α ura3-52/ura3-52 shr3-102/shr3-102* (CGX19) was transformed with YCp50 or YCp(rsr1^{asn16}) generating (A) CG133 and (B) CG134, respectively. These strains were streaked for single cells on SPHD medium, and the resulting colonies were photographed after 5 days growth at 30°C. The scale bar represents 0.1 mm.

developing into pseudohyphal structures that extend beyond the colony margin.

Discussion

The Dimorphic Transition to Pseudohyphal Growth Permits Foraging for Nutrients

We have described pseudohyphal growth, a dimorphic transition in the life cycle of S. cerevisiae. The pseudohypha in Saccharomyces consists of a lineage of first daughters associated in a chain. There have been anecdotal references to pseudohyphal growth for this yeast (Guilliermond, 1920; Brown and Hough, 1965; Lodder, 1970; Eubanks and Beuchat, 1982; and references in these sources) but no detailed description of the conditions required for its induction. Figure 10 diagrams our current view of the S. cerevisiae life cycle. The radial pattern and invasive character of cell proliferation into the growth substrate clearly is a mechanism that permits cells to forage for nutrients at a distance from their initial position. The unipolar growth pattern manifest by yeast pseudohyphae is the major mechanism by which filamentous fungi proliferate (Rayner, 1991; and references therein).

The Requirements for Pseudohyphal Growth

Starvation for Nitrogen

Growth on low ammonia or proline as sole nitrogen source (SPHD) induces pseudohyphal growth. Growth on high amounts of ammonium sulfate or a mixture of proline and ammonium sulfate suppresses pseudohyphal growth. Proline is known to be a poor nitrogen source for wild-type cells (Cooper, 1982) and is an even poorer source for Shr3$^-$ cells, because of their impaired proline uptake ability.

Diploidy and the BUD Genes

Only **a**/α diploids and not **a** or α haploids or **a**/**a** or α/α diploids show pseudohyphal growth, indicating that the mating type locus controls this dimorphic transition. Cells expressing both *MATa* and *MATα* bud in a polar manner, whereas those expressing only *MATa* or *MATα* bud in the axial pattern (Freifelder, 1960; Hicks et al., 1977, Chant and Herskowitz, 1991). The simplest explanation for the control of pseudohyphal growth by the mating type locus is that the polar budding pattern of **a**/α diploid cells permits linear chains of cells to form; the axial pattern leads to budding at the junction of two cells and cannot extend the column (Freifelder, 1960).

The budding pattern of diploids is controlled by five *BUD* genes. *RSR1/BUD1*, *BUD2*, and *BUD5* convert the random pattern into a bipolar pattern, and the bipolar pattern is converted into axial by *BUD3* and *BUD4* (Chant and Herskowitz, 1991, Chant et al., 1991; Powers et al., 1991). The polar budding of *MATa/α* diploids is explained by a1/α2 repression of *BUD3* and/or *BUD4*. Based on this model,

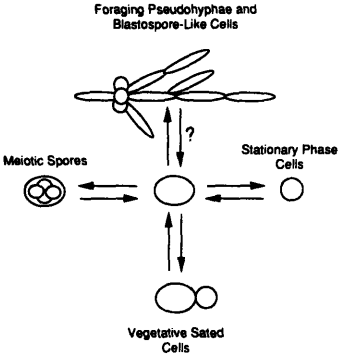

Figure 10. Developmental Pathways of Diploid Yeast Cells

Under favorable environmental conditions, yeast cells grow vegetatively by budding. Environmental stresses can cause diploid yeast to enter the pseudohyphal pathway, differentiate into a growth-arrested stationary phase cell, or undergo meiosis and sporulation, with the resulting production of an ascus with its four dormant spores. We presume that either pseudohyphal cells or their blastospores can resume vegetative growth. Stationary phase cells and diploid cells formed after germination and mating of ascospores both resume vegetative growth under favorable environmental conditions.

we expected that mutations in *RSR1/BUD1*, *BUD2*, and *BUD5* should interfere with the polar cell divisions required for pseudohyphal growth. In agreement with this expectation, **a**/α cells that bud randomly because of the *rsr1*^{asn16} (Bud1$^-$) mutation are unable to form pseudohyphae (see Figure 9). On the basis of these experiments, we propose that one role of the *BUD* genes in yeast biology is to enable cells in the diploid phase to forage for nutrients under conditions of nitrogen starvation.

Cell Shape Changes

Pseudohyphal cells are longer and thinner than sated cells growing on rich medium. As cells become longer and thinner, their axial ratio becomes greater, and therefore the tip of the cell becomes more defined. The ellipsoidal shape of a sated diploid yeast cell confers upon it a low surface area. We surmise that when the growth medium is deficient, the ellipsoidal shape provides insufficient surface area for the cell to extract the diminishing nutrients. A dimorphic transition is induced to adapt to the new environmental conditions, and new daughters develop an elongated morphology. This differentiation creates a shape that increases the surface area and consequently the absorptive surface of the cells.

This change in cell shape has two additional consequences. The first is that the change in cell shape may constrain the plane of cell division along the longitudinal axis of the pseudohyphal cell so that the buds come out very close to the tip (see Figure 6B). In a sense the wall of the cell becomes part of the structure orienting the plane of cell division. We contrast this with polarized growth of sated cells where the buds come out only near to the end, not exactly at the end (see Figure 6A). This constraint could occur in much the same way that the shape of the ascus in Neurospora crassa leads to linear asci; in this fungus, the direction of meiotic cell division is confined to the longitudinal plane by the extreme axial ratio of the ascus. The second consequence is that cell growth is polarized along the same axis as cell division. This dual polarity of cell growth and cell division enhances the ability of the growing chain of cells to escape the colony, because the growth of each new individual unit of the chain of cells along the axis of cell division incrementally moves the column along. The velocity of pseudohyphal elongation is proportional to the length of the cells that comprise the chain.

Unipolar Cell Division

Cell division in the pseudohypha is polarized in one direction, the direction away from the mass of cells in the colony and out into the substrate. This polarization is achieved by four constraints on cell division. First, a terminal pseudohyphal cell always buds at its free end, the one opposite the junction with its mother. Second, the site of bud emergence on the daughter is close to 180° from that junction. Third, daughters stay juxtaposed to their mothers exactly along the axis of cell division, either because they are physically connected or because they are constrained by the agar. Fourth, the first daughter of the founding mother cell (the cell that gives rise to the column) divides in a direction away from the mass of cells in the colony. This initial division coupled with the three other constraints leads to the polarized extension of pseudohyphae away from the colony into unpopulated substrate.

Sated cells, like pseudohyphal cells, initially bud in a unipolar fashion. The first bud of a virgin sated cell (one that has no prior daughters) as well as the majority of the second buds from these cells, emerge from the pole opposite the junction of the virgin with its mother. If sated diploid cells can bud in a unipolar pattern then why don't they form pseudohyphae? The answer is that subsequent steps in the budding and growth of sated cells create asymmetries that preclude the formation of a pseudohypha. First, the buds of sated cells generally separate from their mothers. The detachment of mother and daughter is often associated with movement of the cell that changes the orientation of the daughter with respect to the mother cell. This displacement of the mother–daughter division axes when reiterated in subsequent divisions ultimately leads to randomization of the division planes of an individual mother with respect to any founding cell or starting point. Second, although the buds on sated cells arise on the surface opposite the mother–daughter junction, the position of the new bud is not always 180° from that junction. The sated cells are ellipsoidal, so the poles are less defined than in the elongate pseudohyphal cells. Any changes in the angle of the bud with respect to the axis of the previous mother–daughter junction contribute to unpolarized growth. An extreme example of the effect of bud angle is demonstrated by the *rsr1*^{asn16} mutation, which, by randomizing the sites of bud formation, prevents diploids from forming pseudohyphae.

Previous workers have noted that sated mother cells that have divided at least once (nonvirgin) show bipolar cell division (Freifelder, 1960; Chant and Herskowitz, 1991). In bipolar cell division, buds can emerge on either the birth or free ends of mother cells that are not virgin. It is not known how many divisions must occur before the unipolar pattern is replaced by the bipolar pattern. We have observed that when cells in the pseudohypha bud for a second time they bud in a unipolar pattern about 90% of the time. When sated cells bud for a second time, they also generally bud unipolarly, although about 20% less frequently than pseudohyphal cells. This phenomenon suggests that nutritional factors may regulate the budding pattern of diploid cells.

Invasiveness

Pseudohyphal cells are invasive and grow into the agar, presumably foraging for nutrients. Some of the foraging columns of cells have as many as 10 members in the main chain. Columns within the agar have about the same number of cells as those on the surface, so the agar is no deterrent to their exploration. The invasiveness of pseudohyphal cells can be explained in several ways. One might imagine that the force of unipolar cell division by thin pseudohyphal cells is sufficient to propel a column through the agar. In the pseudohyphal cycle, cell separation, a late step in cell division, may be delayed, leaving the daughters attached to the mother. This linked structure might be able to generate more force than a single cell because the previous generations could act as an anchor for the cell at the apex. Although this mechanical model may be correct, we

know that the connection between the apical cell in the pseudohyphal column and its mother can sometimes be broken by mechanical agitation with a microneedle. Furthermore, flocculent strains and cell-cycle mutants defective in cell separation do not grow invasively, showing that cell separation defects alone do not cause invasiveness.

The secretion of hydrolytic enzymes is likely to be an important factor permitting invasive growth. Lytic enzymes capable of hydrolyzing polysaccharides may be secreted by strains capable of pseudohyphal growth. The secretion of proteases is common to many invading pathogens such as Candida albicans (Macdonald and Odds, 1983). Hydrolytic enzymes in C. albicans are important in creating a pathway for penetration into the host tissue. By analogy, the invasive habit of pseudohyphal S. cerevisiae cells may be a growth pattern used in nature to penetrate natural substrates such as grapes.

Conclusions

S. cerevisiae Undergoes a Dimorphic Transition

S. cerevisiae possesses the latent capacity to undergo a dimorphic transition to pseudohyphal growth. In this pathway, yeast cells give rise to elongated pseudohyphal cells that eventually give rise to blastospore-like cells (see Figure 7 and Table 2). This dimorphic pathway seems similar to that found in C. albicans (Odds, 1988). C. albicans gives rise to blastospores and to chlamydospores, true spores with a chemical composition and structure different from the vegetative yeast cells. So far, we have no evidence for this cell type in S. cerevisiae.

Proline Medium Mimics the Natural Habitat of Yeast Cells

Early workers reported that when some S. cerevisiae strains are inoculated into grape juice and allowed to complete primary fermentation without agitation, they form pseudohyphae (Guilliermond, 1920). In grapes, an important natural substrate for S. cerevisiae (Lodder, 1970), proline is the predominant amino acid, and its concentration often exceeds 1 gram/liter, a concentration that is 10 to 100 times the concentration of other amino acids in grapes (Huang and Ough, 1989; Ough and Stashak, 1974). The histidine concentration of grapes is low and roughly that found in our SPHD medium (Huang and Ough, 1989). The other abundant amino acid in grapes is arginine (Huang and Ough, 1989; Bisson, 1991), whose catabolism requires its conversion to proline (Brandriss and Magasanik, 1980). Only once the ammonia, arginine, and other nitrogen sources in grape juice are exhausted do the cells use the remaining proline as the sole nitrogen source (Bisson, 1991). In addition, proline may be catabolized in grape juice only under aerobic conditions (Ingledew et al., 1987).

The ascomycete Ceratocystis ulmi, the dimorphic yeast that causes Dutch elm disease, also regulates its dimorphic transition in response to proline (Kulkarni and Nickerson, 1981). In this fungus, by contrast with S. cerevisiae, proline supports the yeast phase, and ammonium sulfate supports the invasive mycelial form. Nutritional regulation by proline may be related to disease, because elms resistant to infection contain high proline levels in their xylem sap, while susceptible elms do not (Singh and Smalley, 1969). Proline levels also regulate the development of the human pathogen Candida albicans (Land et al., 1975; Dabrowa et al., 1976; Holmes and Shepherd, 1987). In C. albicans, as in S. cerevisiae, proline supports filamentous growth while high ammonium sulfate supports yeast phase growth.

The RAS Pathway Regulates Pseudohyphal Growth

An activated *RAS* pathway in S. cerevisiae either directly or indirectly results in enhanced pseudohyphal growth. *MATa/α* wild-type diploids carrying the *RAS2*^{val19} mutation (analogous to the missense mutation found in some transforming alleles of mammalian *ras* [Barbacid, 1987; Powers et al., 1989]) undergo enhanced pseudohyphal growth on proline medium and exhibit pseudohyphal growth on rich YPD medium (C. J. G., unpublished data). *RAS2* mutants have perturbed responses to environmental stresses (Kataoka et al., 1984; Tatchell et al., 1984, 1985). The *RAS* pathway is thought to regulate certain stress responses in yeast (reviewed by Broach and Deschennes, 1990). Our results suggest that one role of the *RAS* pathway may be to regulate the dimorphic transition of S. cerevisiae to pseudohyphal growth. We favor a model where nitrogen starvation induces the *RAS* pathway and signals the cell to enter the pseudohyphal pathway. Alternatively, a constitutively activated *RAS* pathway may perturb nitrogen assimilation pathways in a way that enhances pseudohyphal growth. Our result suggests but does not prove that cAMP regulates S. cerevisiae dimorphism because *RAS* is thought to modulate other signaling pathways in yeast (Kaibuchi et al., 1986). Evidence exists that cAMP plays a role in the regulation of the dimorphism of several fungi (Shepherd, 1988).

Implications of Dimorphic Growth and Diploidy for Pathogenesis

The interconversion of a yeast form and a filamentous form is typical of many pathogenic fungi (Shepherd, 1988). In C. albicans, a human pathogen, the ability to undergo a dimorphic transition is critical for pathogenesis (Soll, 1991). In tissue infected with Candida, yeast cells, pseudohyphae, and true hyphae are found (Odds, 1988). Diploid S. cerevisiae (Freifelder, 1960) and C. albicans (Chaffin, 1984) cells possess a unipolar budding pattern that is important for pseudohyphal growth. The requirement of unipolar diploid budding for pseudohyphal growth could explain why Candida is found only as a diploid (no haploid form or sexual cycle has been observed; Odds, 1988). Perhaps Candida once had a haploid phase, but with time and selection, genes required for meiosis and therefore the generation of haploid cells were lost.

Ustilago maydis, the causitive agent of corn smut, is pathogenic only in its dikaryotic filamentous form. The haploid phase of this fungus grows exclusively in a yeast form and is nonpathogenic (Schulz et al., 1990). Although Saccharomyces, an ascomycete and Ustilago, a basidiomycete, are quite distant on a phylogenetic scale, the major morphogenetic event in each species, conversion of the yeast to a filamentous form, has similar genetic control. Both Saccharomyces and Ustilago haploids grow as yeast cells unable to develop into their filamentous form. Saccharomyces diploids and Ustilago dikaryons heterozy-

Table 3. Saccharomyces cerevisiae Strains[a]

Strain	Genotype	Reference and/or Comments
F35	*MATa/α HO/HO shr3-101/shr3-101*	Ljungdahl et al., (unpublished data)
MB1000	*MATα*	Brandriss and Magasanik, (1979)
MB758-5B	*MATa ura3-52*	Siddiqui and Brandriss, (1988)
CG25	*MATa ura3-52 shr3-102*	This work, MB758-5B derivative
CGX15	*MATa/α ura3-52/URA3 shr3-102/SHR3*	MB1000 × CG25
CG41	*MATα ura3-52 shr3-102*	Ascospore from CGX15
CG46	*MATa ura3-52*	Ascospore from CGX15
CG48	*MATα ura3-52*	Ascospore from CGX15
CGX19	*MATa/α ura3-52/ura3-52 shr3-102/shr3-102*	CG25 × CG41
CGX31	*MATa/α ura3-52/ura3-52*	CG46 × CG48
CG67	*MATα/α ura3-52/ura3-52 shr3-102/shr3-102*	*MATα/α derivative of CGX19*
CG85	*MATa/a ura3-52/ura3-52 shr3-102/shr3-102*	*MATa/a derivative of CGX19*
CG62	*MATa/α ura3-52/ura3-52 shr3-102/shr3-102* (pPL210)	CGX19 + pPL210
CG64	*MATa/α ura3-52/ura3-52 shr3-102/shr3-102* (pRS306)	CGX19 + pRS306
CG69	*MATa/α ura3-52/ura3-52* (YCpR2V)	CGX31 + YCpR2V
CG71	*MATa/α ura3-52/ura3-52* (YCp50)	CGX31 + YCp50
CG73	*MATa ura3-52* (YCpR2V)	CG46 + YCpR2V
CG75	*MATα ura3-52* (YCpR2V)	CG48 + YCpR2V
CG132	*MATa/α ura3-52/ura3-52* (YCp[rsr1^{asn16}])	CGX31 + YCp(rsr1^{asn16})
CG133	*MATa/α ura3-52/ura3-52 shr3-102/shr3-102* (YCp50)	CGX19 + YCp50
CG134	*MATa/α ura3-52/ura3-52 shr3-102/shr3-102* (YCp[rsr1^{asn16}])	CGX19 + YCp(rsr1^{asn16})

[a] All S. cerevisiae strains are congenic to the Σ1278b genetic background (Grenson et al., 1966)

Plasmids

Name	Description	Source or Reference
pPL210	1.4 kb fragment containing *SHR3* in pRS306	Ljungdahl et al., (unpublished data)
pRS306	*URA3* marked centromere vector	Sikorski and Hieter, (1989)
YCpR2V	*RAS2^{val19}* in YCp50	*RAS2^{val19}* is described in Kataoka et al., (1984). This unpublished plasmid was obtained from M. Wigler.
YCp(rsr1^{asn16})	*rsr1^{asn16}* in YCp50	Ruggieri et al., (1992). Obtained from A. Bender.

gous for mating type loci undergo a dimorphic transition to filamentous growth. In Saccharomyces diploids (*MATa/α*), the heterodimeric repressor a1α2 (Goutte and Johnson, 1988; reviewed by Herskowitz, 1989) encoded by the mating type loci must be required for the conversion because isogenic *MATα/α* or *MATa/a* strains do not undergo the dimorphic transition. We surmise that a1α2 repression of *BUD3* and/or *BUD4*, two genes that convert the diploid to the haploid budding pattern, is required for conversion to the pseudohyphal growth mode. In Ustilago, where the mating type loci are also thought to encode transcription factors (Schulz et al., 1990), heterozygosity at the mating type loci may also be required to repress haploid-specific cell division patterns because dikaryons homozygous at the mating type loci cannot undergo the dimorphic transition and are nonpathogenic. These transcription factors and the genes they regulate could form the targets for antifungal agents.

Experimental Procedures

Strains, Media, and Microbiological Techniques

Yeast strains are listed in Table 3. Standard yeast media were prepared, and yeast genetic manipulations were performed as described in Sherman et al. (1986). Departures from standard media are all variations of SPHD medium that contains 6.7 grams/liter Yeast Nitrogen Base without amino acids and ammonium sulfate (Difco Laboratories), 1.0 gram/liter L-proline as sole nitrogen source (Sigma Grade Sigma), 2% anhydrous D-glucose (J. T. Baker), and 0.2 mM L-histidine hydrochloride (Sigma). In SAHD and SRHD, the proline was replaced with 1.0 gram/liter ammonium sulfate (J. T. Baker) and 1.0 gram/liter L-arginine (Sigma) respectively. SPAHD and SPRHD media contain, respectively, 0.5 grams/liter L-proline plus 0.5 grams/liter ammonium sulfate or 0.5 grams/liter L-proline plus 0.5 grams/liter L-arginine as sole nitrogen sources. SLAHD (low ammonia) contains only 0.05 mM ammonium sulfate as sole nitrogen source and is made with washed agar.

The nitrogen sources, the 0.5 M L-histidine hydrochloride solution, and the concentrated (4×) stock solution of the Yeast Nitrogen Base were filter sterilized. Other components were autoclaved as separate stock solutions (20 mM uracil, 40% glucose, and 4% Difco Bacto agar). Stock solutions and sterile water were mixed to make a 2× solution to which an equal volume of molten 4% agar was added. Standard 100 × 15 mm plastic petri dishes were filled with 25 ml of medium. These plates yielded uniform and consistent results only when used during the first week following preparation. This period could be lengthened to 2–3 weeks by washing the agar a few times with water before autoclaving. Yeast transformations were performed by the lithium acetate method of Ito et al. (1983) using ~30 μg of sonicated calf thymus DNA as carrier and selecting for transformants on solid SC medium lacking uracil.

Yeast Strain Construction

Several different mutant alleles of *SHR3* gave rise to enhanced pseudohyphal growth on SPHD. These include both an in vitro constructed null allele *shr3Δ1::URA3* (Ljungdahl et al., unpublished data) and a

spontaneously isolated allele *shr3-102*. Each of these, when homozygous in a *MATa/α* diploid, gives rise to pseudohyphal growth. As indicated in the Results section, strains from the Σ1278b background give the most extensive pseudohyphae, so we carried out our experiments in this background. S. cerevisiae strains MB1000 (*MATα*, Brandriss and Magasanik, 1979) and MB758-5B (*MATa ura3-52*, Siddiqui and Brandriss, 1988) were obtained from M. Brandriss. MB1000 is also known in the literature as Σ1278b (Grenson et al., 1966). The *ura3-52* mutation in MB758-5B originates from strain DBY785 and was introduced by a cross with MB1000. A *ura3-52* segregant from this cross was made congenic to Σ1278b by performing 10 backcrosses to MB1000, resulting in MB758-5B (Siddiqui and Brandriss, 1988).

We obtained a *ura3-52* Shr3⁻ mutant strain in the Σ1278b backround by obtaining a spontaneous mutant of MB758-5B resistant to 30 mM histidine. These conditions allow the positive selection of Shr3⁻ mutants (Ljungdahl et al., unpublished data). The particular allele we chose (*shr3-102* in CG25) was shown to be an allele of *SHR3* by the following tests: it was recessive to *SHR3* and failed to complement the 30 mM histidine growth or the enhanced pseudohyphal growth of a known loss-of-function Shr3⁻ allele; it was complemented for both the growth at 30 mM histidine and enhanced pseudohyphal growth phenotypes by a plasmid containing a 1.4 kb genomic fragment (pPL210) that contained only the *SHR3* coding region; and when it was crossed by an *SHR3* strain, the 30 mM histidine growth phenotype segregated in a Mendelian fashion in tetrads. We called this mutant allele *shr3-102*.

CG25 (*MATa ura3-52 shr3-102*) was backcrossed to MB1000 (*MATα*) and segregants with the following genotypes were identified and isolated: *MATα ura3-52 shr3-102* (CG41), *MATa ura3-52* (CG46), *MATα ura3-52* (CG48). A *MATa/α ura3-52/ura3-52 shr3-102/shr3-102* diploid (CGX19) was constructed by crossing CG25 × CG41. A *MATa/α ura3-52/ura3-52* diploid (CGX31) was constructed by crossing CG46 × CG48. Spontaneous *MATa/a* and *MATα/α ura3-52/ura3-52 shr3-102/shr3-102* derivatives of CGX19, CG85, and CG67, respectively, were isolated by obtaining spontaneous mitotic recombinants homozygous at the *MAT* locus from CGX19 cells. Isogenic pairs of diploid strains that differ only in their *SHR3*, *RAS2*, or *RSR1/BUD1* alleles were produced by transformation with centromere plasmids and selection of transformants on solid SC (without uracil) medium (Table 3).

Bud Site Selection Assay

Photomicrographs of developing pseudohyphae in colonies of CGX19 (a/α Shr3⁻) that had been growing for 1 to 3 days on SPHD plus uracil medium at 30°C were taken at time intervals. All lineages in which the origin of the terminal 3 cells could be determined by time lapse observation were used. Emergence of the first bud of the virgin mother's first daughter was scored as from the free or birth end. Following the conventions of Freifelder (1960), the pole of a bud that contacts its mother cell is called the birth end and the opposite pole the free end. Emergence of the virgin mother's second bud after the time required for two cell divisions was scored as either occurring at the free end or not occurring at the free end. There were 11 instances where no second bud emerged on the free end of the mother cell. In each of these cases the birth end was obscured by neighboring cells, so the presence of a bud at the birth pole could not be scored. These 11 events were tabulated as birth end buds. This scoring strategy was used because it allowed the incorporation of all cell divisions visible by time lapse photomicroscopy into the data set.

The budding pattern of sated virgin CGX19 cells was analyzed by patching out CGX19 on YPD medium supplemented with 20 milligrams/liter adenine sulfate, pregrowing the cells for two days at 30°C, and then micromanipulating cells with small buds onto a YPD plate in a grid pattern. After 7–9 hr of growth at 24°C, all cells except for virgin cells with a small bud (one per cell originally placed on plate if this cell grew normally) were micromanipulated away from the grid. The positions of the virgin cell and its first bud were recorded at the beginning of the experiment and at time intervals. All virgin cells that gave rise to microcolonies of four cells within a 6 hr period at 24°C were scored. Emergence of the first bud produced by the original virgin cell's first daughter was scored as emerging from its free or birth end. Emergence of the virgin mother's second bud was scored as either from the free or birth end, assuming that the pole from which the first bud emerged is the free end as discussed.

SEM Methods

Yeast cells proliferating on agar growth medium were transferred with a toothpick to small squares of wet Schleicher and Schuell #576 filter paper. The cells on the paper were then fixed in 2.5% glutaraldehyde in 0.1 M sodium cacodylate (pH 7.2) at 24°C for 60 min and dehydrated in a graded ethanol series at 24°C. This material was critical point dried in liquid carbon dioxide, mounted on SEM stubs, and then sputter coated with gold and palladium. SEM was performed on the upper stage of an ISI-DS130 scanning electron microscope and the images were photographed on Polaroid 55 film.

Light Microscopic Techniques

Light microscopy of single cells and microcolonies was done with a Zeiss WL light microscope using bright field optics. Petri plates were placed directly on the microscope stage. A 40 × short working distance objective and 32 × and 2.5 × long working distance objectives, all from Zeiss, were used to visualize cells or colonies. Some light microscopy of macrocolonies was done with a Wild M5A stereomicroscope with a transmitted light console base. Light photomicroscopy for quantitation of single cell dimensions was done with a Zeiss Axioskop using Nomarski optics. Either 40 × (for pseudohyphae) or 100 × (for single cells) objectives were used.

Quantitation of Yeast Cell Dimensions

Measurements of pseudohyphal and sated cell dimensions were based on photomicrographs of cells from colonies obtained by streaking CGX19 (*MATa/α ura3-52/ura3-52 shr3-102/shr3-102*) for single cells on agar plates. Sated and pseudohyphal cells used for quantitation by SEM were, respectively, from YPD and SPHD plus uracil plates incubated at 30°C for 31 hr. The pseudohyphal cells and blastospore-like cells used for light photomicroscopic quantitation were from the same SPHD plus uracil plate incubated at 30°C for 7 days. Blocks of agar 1.0 cm × 0.5 cm containing several polarized colonies were lifted from the plate with a scalpel. A thin piece of agar from the surface 0.2–0.3 cm thick containing the colonies and their associated invasive pseudohyphae was removed from the block, transferred to a slide, and a cover slip was applied to it without pressure. Photomicrographs of invasive pseudohyphae and their associated blastospore-like cells were made with a 40 × objective with Nomarski optics. The sated cells used for light photomicrographic quantitation were from YPD plates incubated at 30°C for 26 hr. To reproduce the optical conditions of the invasive pseudohyphae and blastospore-like cells, sated cells from a colony on the agar surface were suspended in a 37°C solution of 0.6 M sorbitol, 5% glucose, and 1% low melting point agarose and dropped onto a slide. A coverslip was quickly applied and pressed down to form a thin layer of agar-suspended cells. Photomicrographs were taken after the agar had solidified with a 100 × oil immersion objective with Nomarski optics. All measurements were converted to μm.

Acknowledgments

The authors thank S. Penman for helping with the SEM experiment and M. Brandriss for providing yeast strains. We thank A. Bender and M. Wigler for providing plasmids. We thank L. Bisson, N. Gow, B. Magasanik, D. Pfister, D. Soll, and members of the Fink lab for helpful conversations. We thank C. Kaiser, D. Pellman, D. Pfister, and A. Sachs for comments on the manuscript. We thank the staff of the Farlow Reference Library of Cryptogamic Botany at Harvard University for their assistance. This work was supported by a Howard Hughes Medical Institute Predoctoral Fellowship to C. J. G., National Institutes of Health Research Fellowship GM12038-01 to P. O. L., and National Institutes of Health Research Grants GM40266 and GM35010 to G. R. F. G. R. F. is an American Cancer Society Professor of Genetics.

The costs of publication of this article were defrayed in part by the payment of page charges. This article must therefore be hereby marked "*advertisement*" in accordance with 18 USC Section 1734 solely to indicate this fact.

Received November 13, 1991; revised January 13, 1992.

References

Barbacid, M. (1987). *ras* genes. Annu. Rev. Biochem. *56*, 779–827.

Bender, A., and Pringle, J. R. (1989). Multicopy suppression of the *cdc24* budding defect in yeast by *CDC42* and three newly identified genes including the *ras*-related gene *RSR1*. Proc. Natl. Acad. Sci. USA *86*, 9976–9980.

Bisson, L. F. (1991). Influences of nitrogen on yeast and fermentation of grapes. In Proceedings of the International Symposium on Nitrogen in Grapes and Wine, June 18–19, 1991, Seattle, WA (American Society for Enology and Viticulture), 136–147.

Brandriss, M. C., and Magasanik, B. (1979). Genetics and physiology of proline utilization in *Saccharomyces cerevisiae*: enzyme induction by proline. J. Bacteriol. *140*, 498–503.

Brandriss, M. C., and Magasanik, B. (1980). Proline: an essential intermediate in arginine degradation in *Saccharomyces cerevisiae*. J. Bacteriol. *143*, 1403–1410.

Broach, J. R., and Deschennes, R. J. (1990). The function of *RAS* genes in *Saccharomyces cerevisiae*. Adv. Cancer Res. *54*, 79–139.

Brown, C. M., and Hough, J. S. (1965). Elongation of yeast cells in continuous culture. Nature *206*, 676–678.

Chaffin, W. L. (1984). Site selection for bud and germ tube emergence in *Candida albicans*. J. Gen. Microbiol. *130*, 431–440.

Chant, J., and Herskowitz, I. (1991). Genetic control of bud site selection in yeast by a set of gene products that constitute a morphogenetic pathway. Cell *65*, 1203–1212.

Chant, J., Corrado, K., Pringle, J. R., and Herskowitz, I. (1991). Yeast *BUD5*, encoding a putative GDP–GTP exchange factor, is necessary for bud site selection and interacts with bud formation gene *BEM1*. Cell *65*, 1213–1224.

Cooper, T. G. (1982). Nitrogen metabolism in *Saccharomyces cerevisiae*. In The Molecular Biology of the Yeast *Saccharomyces*: Metabolism and Gene Expression, J. N. Strathern, E. W. Jones, and J. R. Broach, eds. (Cold Spring Harbor, New York: Cold Spring Harbor Laboratory), pp. 39–99.

Dabrowa, N., Taxer, S. S. S., and Howard, D. H. (1976). Germination of *Candida albicans* induced by proline. Infect. Immun. *13*, 830–835.

Drubin, D. G. (1991). Development of cell polarity in budding yeast. Cell *65*, 1093–1096.

Evans, E. G. V., and Richardson, M. D., eds. (1989). Medical Mycology: a Practical Approach (Oxford: Information Press Ltd.).

Eubanks, V. L., and Beuchat, L. R. (1982). Effects of antioxidants on growth, sporulation, and pseudomycelium production by *Saccharomyces cerevisiae*. J. Food Sci. *47*, 1717–1722.

Freifelder, D. (1960). Bud position in *Saccharomyces cerevisiae*. J. Bacteriol. *80*, 567–568.

Goutte, C., and Johnson, A. D. (1988). a1 protein alters the DNA binding specificity of α2 repressor. Cell *52*, 875–882.

Grenson, M., Mousset, M., Wiame, J. M., and Bechet, J. (1966). Multiplicity of the amino acid permeases in *S. cerevisiae*. I. Evidence for a specific arginine transporting system. Biochim. Biophys. Acta *127*, 325–338.

Guilliermond, A. (1920). The Yeasts (New York: John Wiley and Sons, Inc.).

Gunning, B. E. S. (1982). The root of the water fern Azolla: cellular basis of development and multiple roles for cortical microtubules. In Developmental Order: Its Origin and Regulation (New York: Alan R. Liss), pp. 379–421.

Herskowitz, I. (1989). A regulatory hierarchy for cell specialization in yeast. Nature. *342*, 749–757.

Hicks, J. B., Strathern, J. N., and Herskowitz, I. (1977). Interconversion of yeast mating types III. Action of the homothallism (*HO*) gene in cells homozygous for the mating type locus. Genetics *85*, 395–405.

Holmes, A. R., and Shepherd, M. G. (1987). Proline-induced germ-tube formation in *Candida albicans*: role of proline uptake and nitrogen metabolism. J. Gen. Microbiol. *133*, 3219–3228.

Huang, Z., and Ough, C. S. (1989). Effect of vineyard locations, varieties, and rootstocks on the juice amino acid composition of several cultivars. Am. J. Enol. Vitic. *40*, 135–139.

Hyman, A. A., and White, J. G. (1987). Determination of cell division axes in the early embryogenesis of *Caenorhabditis elegans*. J. Cell Biol. *105*, 2123–2135.

Hyman, A. A. (1989). Centrosome movement in the early divisions of *Caenorhabditis elegans*: a cortical site determining centrosome position. J. Cell Biol. *109*, 1185–1193.

Ingledew, W. M., Magnus, C. A., and Sosulski, F. W. (1987). Influence of oxygen on proline utilization during the wine fermentation. Am. J. Enol. Vitic. *38*, 246–248.

Ito, H., Fukada. Y., Murata, K., and Kimura, A. (1983). Transformation of intact yeast cells with alkali cations. J. Bacteriol. *153*, 163–168.

Johnson, M. H., and Maro, B. (1986). Time and space in the mouse early embryo: a cell biological approach to cell diversification. In Experimental Approaches to Mammalian Embryonic Development, J. Rossant and R. A. Pedersen, eds. (New York: Cambridge University Press), pp 35–65.

Kaibuchi, K., Miyajima, A., Arai, K.-I., and Matsumoto, K. (1986). Possible involvement of *RAS*-encoded proteins in glucose-induced inositol phospholipid turnover in *Saccharomyces cerevisiae*. Proc. Natl. Acad. Sci. USA *83*, 8172–8176.

Kataoka, T., Powers, S., McGill, C., Fasano, O., Strathern, J., Broach, J., and Wigler, M. (1984). Genetic analysis of yeast *RAS1* and *RAS2* genes. Cell *37*, 437–445.

Kulkarni, R. K., and Nickerson, K. W. (1981). Nutritional control of dimorphism in *Ceratocystis ulmi*. Exp. Mycol. *5*, 148–154.

Land, G. A., McDonald, W. C., Stjernholm, R. L., and Friedman, L. (1975). Factors affecting filamentation in *Candida albicans*: relationship of the uptake and distribution of proline to morphogenesis. Infect. Immun. *11*, 1014–1023.

Lodder, J., ed. (1970). The Yeasts: a Taxonomic Study (Amsterdam: North-Holland Publishing Co.).

Macdonald, F., and Odds, F. C. (1983). Virulence for mice of a proteinase-secreting strain of *Candida albicans* and a proteinase deficient mutant. J. Gen. Microbiol. *129*, 431–438.

Nasmyth, K. A. (1982). Molecular genetics of yeast mating type. Annu. Rev. Genet. *16*, 439–500.

Odds, F. C., ed. (1988). Candida and Candidosis (London: Bailliere Tindal).

Ough, C. S., and Stashak, R. M. (1974). Further studies on proline concentration in grapes and wines. Amer. J. Enol. Vitic. *25*, 7–12.

Powers, S., O'Neill, K., and Wigler, M. (1989). Dominant yeast and mammalian *RAS* mutants that interfere with the *CDC25*-dependent activation of wild-type *RAS* in *Saccharomyces cerevisiae*. Mol. Cell. Biol. *9*, 390–395.

Powers, S., Gonzales, E., Christensen, T., Cubert, J., and Broek, D. (1991). Functional cloning of *BUD5*, a *CDC25*-related gene from S. cerevisiae that can suppress a dominant-negative *RAS2* mutant. Cell *65*, 1225–1231.

Pringle, J. R., and Hartwell, L. H. (1981). The *Saccharomyces cerevisiae* cell cycle. In The Molecular Biology of the Yeast *Saccharomyces*: Life Cycle and Inheritance, J. N. Strathern, E.W. Jones, and J. R. Broach, eds. (Cold Spring Harbor, New York: Cold Spring Harbor Laboratory), pp. 97–142.

Pringle, J. R., Preston, R. A., Adams, A. E. M., Stearns, T., Drubin, D. G., Haarer, B. K., and Jones, E. W. (1989). Fluorescence microscopy methods for yeast. Meth. Cell Biol. *31*, 357–435.

Rayner, A. D. M. (1991). The challenge of the individualistic mycelium. Mycologia *83*, 48–71.

Ruggieri, R., Bender, A., Matsui, Y., Powers, S.. Takai, Y., Pringle, J. R., and Matsumoto, K. (1992). *RSR1*, a *ras*-like gene homologous to K*rev-1*/*smg*21A/*rap*1A: role in the development of cell polarity and interactions with the Ras pathway in *Saccharomyces cerevisiae*. Mol. Cell Biol. *12*, 758–766.

Rytka, J. (1975). Positive selection of general amino acid permease mutants in *Saccharomyces cerevisiae*. J. Bacteriol. *121*, 562–570.

Schulz, B., Banuett, F., Dahl, M., Schlesinger, R., Schäfer, W., Martin, T., Herskowitz, I., and Kahmann, R. (1990). The *b* alleles of *U. maydis*, whose combinations program pathogenic development, code for polypeptides containing a homeodomain-related motif. Cell *60*, 295–306.

Shepherd, M. G. (1988). Morphogenetic transformation of fungi. Curr. Top. Med. Mycol. *2*, 278–304.

Sherman, F., Fink, G. R., and Hicks, J. B. (1986). Methods in Yeast Genetics (Cold Spring Harbor, New York: Cold Spring Harbor Laboratory).

Siddiqui, A. H., and Brandriss, M. C. (1988). A regulatory region responsible for proline-specific induction of the yeast *PUT2* gene is adjacent to its TATA box. Mol. Cell. Biol. *8*, 4634–4641.

Sikorski, R. S., and Hieter, P. (1989). A system of shuttle vectors and yeast host strains designed for efficient manipulation of DNA in *Saccharomyces cerevisiae*. Genetics *122*, 19–27.

Singh, D., and Smalley, E. B. (1969). Nitrogenous compounds in the xylem sap of American elms with Dutch elm disease. Canad. J. Bot. *47*, 1061–1065.

Soll, D. R. (1991). Current status of the molecular basis of *Candida* pathogenicity. In The Fungal Spore and Disease Initiation in Plants and Animals, G. T. Cole and H. C. Hoch, eds. (New York, New York: Plenum Press), pp. 503–540.

Sutherland, A. E., Speed, T. P., and Calarco, P. G. (1990). Inner cell allocation in the mouse morula: the role of oriented division during fourth cleavage. Dev. Biol. *137*, 13–25.

Tatchell, K., Chaleff, D. T., DeFeo-Jones, D., and Scolnick, E.M. (1984). Requirement of either of a pair of *ras*-related genes of *Saccharomyces cerevisiae* for spore viability. Nature *309*, 523–527.

Tatchell, K., Robinson, L. C., and Breitenbach, M. (1985). *RAS2* of *Saccharomyces cerevisiae* is required for gluconeogenic growth and proper response to nutrient limitation. Proc. Natl. Acad. Sci. USA *82*, 3785–3789.

Toda, T., Uno, I., Ishikawa, T., Powers, S., Kataoka, T., Broek, D., Cameron, S., Broach, J., Matsumoto, K., and Wigler, M. (1985). In yeast, *RAS* proteins are controlling elements of adenylate cyclase. Cell *40*, 27–36.

Toda, T., Cameron, S., Sass, P., Zoller, M., Scott, J. D., McMullen, B., Hurwitz, M., Krebs, E. G., and Wigler, M. (1987). Cloning and characterization of *BCY1*, a locus encoding a regulatory subunit of the cyclic AMP-dependent protein kinase in *Saccharomyces cerevisiae*. Mol. Cell. Biol. *7*, 1371–1377.

Wiame, J.-M., Grenson, M., and Arst Jr., H. N. (1985). Nitrogen catabolite repression in yeasts and filamentous fungi. Adv. Microb. Physiol. *26*, 1–88.

Chapter 4:

Induction of Pseudohyphal Growth by Overexpression of *PHD1*, a *Saccharomyces cerevisiae* Gene Related to Transcriptional Regulators of Fungal Development

MOLECULAR AND CELLULAR BIOLOGY, Mar. 1994, p. 2100–2112
0270-7306/94/$04.00+0

Vol. 14, No. 3

Induction of Pseudohyphal Growth by Overexpression of *PHD1*, a *Saccharomyces cerevisiae* Gene Related to Transcriptional Regulators of Fungal Development†

CARLOS J. GIMENO AND GERALD R. FINK*

Whitehead Institute for Biomedical Research and Department of Biology, Massachusetts Institute of Technology, Cambridge, Massachusetts 02142

Received 3 November 1993/Returned for modification 7 December 1993/Accepted 29 December 1993

When starved for nitrogen, *MAT*a/*MAT*α cells of the budding yeast *Saccharomyces cerevisiae* undergo a dimorphic transition to pseudohyphal growth. A visual genetic screen, called PHD (pseudohyphal determinant), for *S. cerevisiae* pseudohyphal growth mutants was developed. The PHD screen was used to identify seven *S. cerevisiae* genes that when overexpressed in *MAT*a/*MAT*α cells growing on nitrogen starvation medium cause precocious and unusually vigorous pseudohyphal growth. *PHD1*, a gene whose overexpression induced invasive pseudohyphal growth on a nutritionally rich medium, was characterized. *PHD1* maps to chromosome XI and is predicted to encode a 366-amino-acid protein. PHD1 has a SWI4- and MBP1-like DNA binding motif that is 73% identical over 100 amino acids to a region of *Aspergillus nidulans* StuA. StuA regulates two pseudohyphal growth-like cell divisions during conidiophore morphogenesis. Epitope-tagged PHD1 was localized to the nucleus by indirect immunofluorescence. These facts suggest that PHD1 may function as a transcriptional regulatory protein. Overexpression of *PHD1* in wild-type haploid strains does not induce pseudohyphal growth. Interestingly, *PHD1* overexpression enhances pseudohyphal growth in a haploid strain that has the diploid polar budding pattern because of a mutation in the *BUD4* gene. In addition, wild-type diploid strains lacking *PHD1* undergo pseudohyphal growth when starved for nitrogen. The possible functions of *PHD1* in pseudohyphal growth and the uses of the PHD screen to identify morphogenetic regulatory genes from heterologous organisms are discussed.

The baker's yeast, *Saccharomyces cerevisiae*, is a dimorphic fungus that interconverts between multicellular filamentous and unicellular growth modes (29, 31, 36, 65). *S. cerevisiae* grows mitotically by budding (37) as individual ellipsoidal cells or as filamentous chains of elongated cells termed pseudohyphae. The switch from unicellular to filamentous growth is a *MAT*a/*MAT*α diploid-specific dimorphic transition triggered by nitrogen starvation (31). There are at least three distinct phases that proceed in chronological sequence during the development of a pseudohypha. In the first phase, an ellipsoidal mother cell divides to produce an elongated daughter cell (32). In the second phase, the elongated daughters produce identical elongated daughters that compose the backbone of the filament (31). In the third phase, the elongated cells of the pseudohypha, with the exception of those very near the growing tip of the filament, bud vegetative ellipsoidal cells (31, 32). The net result is that pseudohyphal growth disperses asexually produced vegetative ellipsoidal yeast cells to new and otherwise inaccessible growth substrates.

The filamentous phase in *S. cerevisiae* consists of at least four processes, polar budding, cell elongation, incomplete cell separation, and invasive growth (31). Except for polar budding, which is a property of *MAT*a/*MAT*α diploids (15), these processes are induced by nitrogen starvation (31). The *MAT* and *RSR1*/*BUD1* genes affect pseudohyphal growth because they regulate one of these processes, polar budding (8, 14, 15, 62). Cells of the *MAT*a/*MAT*α genotype have the polar budding pattern that permits pseudohyphal growth, whereas *MAT*a and *MAT*α haploids and *MAT*a/*MAT*a and *MAT*α/*MAT*α diploids have the axial pattern that precludes pseudohyphal growth (31). The *RSR1*/*BUD1* gene is also required for the polar budding pattern; a Rsr1$^-$ diploid has a random budding pattern that impairs pseudohyphal growth (14, 31). It is not known whether these genes affect other component processes of pseudohyphal growth.

The *SHR3* gene indirectly regulates pseudohyphal growth by a mechanism understood in some molecular detail. Shr3$^-$ strains inappropriately induce pseudohyphal growth when grown on proline as the sole nitrogen source (31, 32). SHR3, a component of the endoplasmic reticulum, is required for amino acid permeases, including the proline permease PUT4, to exit the endoplasmic reticulum and reach the plasma membrane (47). Thus, Shr3$^-$ strains have impaired proline uptake that results in nitrogen starvation, which consequently leads to induction of pseudohyphal growth when proline is the sole nitrogen source (31, 47).

Recently, it has been shown that *MAT*a/*MAT*α diploid strains homozygous for mutations in the *STE7*, *STE11*, *STE12*, and *STE20* genes have impaired pseudohyphal growth (46). STE7, STE11, STE12, and STE20 are part of a signal transduction pathway that transcriptionally regulates mating-specific genes (72) and some genes linked to either transposon Ty (16, 25) or the repeated element sigma (78). In addition, a number of other genes including *CDC55*, *ELM1*, *ELM2*, *ELM3*, *PPZ1*, *PPZ2*, and *RAS2* have been reported to regulate pseudohyphal growth (9, 31, 44). The mechanism by which these genes affect pseudohyphal growth is not yet clear.

Here we report the development of a visual genetic screen, called PHD (pseudohyphal determinant), for pseudohyphal growth mutants and its use in identifying genes that when

* Corresponding author. Mailing address: Whitehead Institute for Biomedical Research, Nine Cambridge Center, Cambridge, MA 02142. Fax: (617) 258-9872.

† C.J.G. dedicates this article to his parents, Joaquín and Rosalie Gimeno.

TABLE 1. *S. cerevisiae* strains and plasmids

Strain or plasmid	Genotype or description	Reference, source, or derivation
S. cerevisiae strains[a]		
CGX69	*MATa/MATα ura3-52/ura3-52*	CGX66 (32) derivative
10480-5C	*MATa ura3-52*	Fink laboratory collection
10480-5D	*MATα ura3-52*	Fink laboratory collection
L5366	*MATa/MATα ura3-52/ura3-52*	10480-5C × 10480-5D
CGX133	*MATa/MATα phd1Δ1::hisG-URA3-hisG/PHD1 ura3-52/ura3-52*	L5366 derivative
CGX134	*MATa/MATα phd1Δ1::hisG-URA3-hisG/PHD1 ura3-52/ura3-52*	L5366 derivative
CGX135	*MATa/MATα phd1Δ1::hisG-URA3-hisG/phd1Δ1::hisG-URA3-hisG ura3-52/ura3-52*	CGX134 derivative
CGX137	*MATa/MATα phd1Δ1::hisG-URA3-hisG/phd1Δ1::hisG-URA3-hisG ura3-52/ura3-52*	CGX133 derivative
CGX160	*MATa/MATα phd1Δ1::hisG/phd1Δ1::hisG ura3-52/ura3-52*	CGX133 derivative
CGX161	*MATa/MATα phd1Δ1::hisG/phd1Δ1::hisG ura3-52/ura3-52*	CGX134 derivative
CG737	*MATa/MATα phd1Δ1::hisG/phd1Δ1::hisG ura3-52/ura3-52* (pCG38)	CGX160 + pCG38
CG739	*MATa/MATα phd1Δ1::hisG/phd1Δ1::hisG ura3-52/ura3-52* (pCG37)	CGX160 + pCG37
CGX155	*MATa/MATα phd1Δ1::hisG-URA3-hisG/phd1Δ1::hisG-URA3-hisG shr3Δ1::URA3-hisG/shr3Δ1::URA3 ura3-52/ura3-52*	CGX134 derivative
CGX157	*MATa/MATα shr3Δ1::URA3/shr3Δ1::URA3 ura3-52/ura3-52*	CGX134 derivative
CG934	*MATa/MATα ura3-52/ura3-52* (pCG38)	L5366 + pCG38
CG936	*MATa/MATα ura3-52/ura3-52* (pRS202)	L5366 + pRS202
CG937	*MATa ura3-52* (pCG38)	10480-5C + pCG38
CG939	*MATa ura3-52* (pRS202)	10480-5C + pRS202
CG940	*MATα ura3-52* (pCG38)	10480-5D + pCG38
CG942	*MATα ura3-52* (pRS202)	10480-5D + pRS202
CG953	*MATa/MATα ura3-52/ura3-52* (pRS316)	L5366 + pRS316
SS3-2B	*MATa bud4 ura3-52*	63
Plasmids		
pCG36	7.0-kb fragment with *phd1Δ1::hisG-URA3-hisG* in pBluescriptII KS+	This work
pCG37	2.6-kb fragment with *PHD1::FLU1* in pRS202	This work
pCG38	2.6-kb fragment with *PHD1* in pRS202	This work
pBluescriptII KS+	*E. coli* vector	73
pDE1	*FUP1* overexpression plasmid	22
pEY312C	*MSN1* overexpression plasmid	26
pNKY1009	*TRP1* disruption vector	1
pPL219	*shr3Δ1::URA3* in pBluescriptII SK+	47
pRS202	*URA3*-marked 2μm vector	18
pRS316	*URA3*-marked *CEN* vector	71
pSE1076	5.0-kb *hisG-URA3-kan*^{r}*-hisG* fragment in vector	23

[a] All strains are congenic to the Σ1278b genetic background (34).

overexpressed in a *MATa/MATα* strain cause precocious and unusually vigorous pseudohyphal growth. This study focuses on one of these genes, *PHD1*, that is related to transcriptional regulators of fungal development and whose overexpression causes constitutive pseudohyphal growth. *PHD1* may be a transcriptional regulator of pseudohyphal growth that controls structural genes involved in this process.

MATERIALS AND METHODS

Yeast strains, media, and microbiological techniques. Yeast strains used in experiments are listed in Table 1 except for strains used in the genetic mapping of *PHD1*, which are given below. Standard yeast media were prepared and yeast genetic manipulations were performed as previously described (69). Yeast transformations were performed by standard protocols (28, 39). Plasmids were isolated from yeast strains by a standard method (38). SLAHD and SPHD media were prepared as previously described (31, 47). SLAD medium is SLAHD medium without histidine.

The following method is used to induce *MATa/MATα* strains overexpressing *PHD1* (for instance, CG934) to undergo pseudohyphal growth in liquid medium. The culture is prepared by pregrowing the yeast strain for 2 days on a nitrogen starvation (SLAD medium) plate, resuspending it at a density of 10^4 cells per ml in liquid SLAD medium, and then adding 10 ml of the resulting cell suspension to a 10-ml SLAD agar plate. Most cells remain in the liquid phase of the culture and do not settle onto the surface of the plate. The culture is grown without agitation at 30°C, and after 16 h, pseudohyphal microcolonies are observed growing in the liquid phase of the culture and about 50% of the cells in the culture have a pseudohyphal morphology. When this experiment is repeated with a wild-type *MATa/MATα* strain (for instance, CG936), pseudohyphal microcolonies are not observed and about 5% of the cells in the culture have a pseudohyphal morphology.

Yeast strain construction. Construction of yeast strains is shown in tabular form (Table 1) and described below. All strains not used in the genetic mapping of *PHD1* are congenic to the Σ1278b genetic background and are derived from either MB758-5B (*MATa ura3-52*) (70) or MB1000 (*MATα*) (10) or both. For this work, the *trp1::hisG* (1) auxotrophic marker was introduced into the Σ1278b genetic background (34) by using a previously described method (1) and plasmid pNKY1009 (Table 1). The *shr3Δ1* allele was introduced into Σ1278b strains with pPL219 (47).

Physical mapping of *PHD1* to *PHD7*. All DNA probes for hybridizations were purified from agarose gels using the Geneclean kit (Bio 101) and then labeled with ^{32}P using the Prime Time C kit (IBI), unless otherwise specified. Manufacturer's

TABLE 2. Results of *S. cerevisiae* PHD screen[a]

Gene	Plasmid[b]	No. of independent isolations of plasmid	Location of gene on chromosome	Prime λ clone(s)[c]
PHD1	pCG7	2	XI	4326
	pCG19	1		
PHD2	pCG6	1	XV	1697, 2399
PHD3	pCG5	1	VII or XV	
	pCG20	1		
PHD4	pCG4	2	VII or XV	
	pCG10	1		
PHD5	pCG11	1	XIII	
PHD6	pCG8	1	X	
PHD7	pCG9	3	XIV	

[a] *PHD2* is probably allelic to *MSN1/FUP1*.
[b] Plasmids are from the 2μm genomic library described in Materials and Methods (18).
[c] The prime λ clone numbers of the phage DNAs to which a DNA probe derived from the relevant plasmid insert hybridized are listed.

instructions were followed for the use of both kits. *S. cerevisiae* chromosome blots were obtained from Clontech. DNA sequencing of the left end of the pCG6 insert was primed with the T3 primer, while sequencing of the right end was primed with the T7 primer. These primers are described elsewhere (73).

PHD3 to *PHD7* were mapped physically by first liberating the yeast genomic DNA inserts from the pRS202-based multicopy genomic library plasmid isolates with a *Sal*I-*Sac*I double digestion. Digests were electrophoresed on 0.7% agarose TAE (40 mM Tris acetate-1 mM EDTA) gels and DNA fragments that originated from the insert were ^{32}P labeled and used to probe chromosome blots (Table 2). DNA fragments used were the ≈9-kb fragment of pCG20, the ≈7-kb fragment of pCG4, the ≈7-kb fragment of pCG11, the ≈3- and ≈4-kb fragments of pCG8, and the ≈6-kb fragment of pCG9. The pCG9 fragment chromosome blot was performed with an ECL direct nucleic acid labeling and detection system (Amersham) following the manufacturer's directions.

Genetic mapping of *PHD1*. Genetic mapping of *PHD1* was initiated by the construction of suitable mapping strains. Strains 10053-3A (*MAT***a** *cdc16-1 his4-619 ura3-52*) and CG245 (*MATα phd1Δ1::hisG-URA3-hisG trp1::hisG ura3-52*) were crossed and sporulated, cells from two robust ascospore colonies were crossed and sporulated, and once more cells from two robust ascospore colonies, CG343 (*MAT***a** *ura3-52 trp1::hisG cdc16-1 phd1Δ1::hisG-URA3-hisG*) and CG344 (*MATα ura3-52 his4-619*), were crossed. Diploid CGX94 resulted from this final mating and was sporulated and analyzed by tetrad analysis.

Qualitative pseudohyphal growth assay. The qualitative pseudohyphal growth assay was performed essentially as described previously (31, 32). Strains to be tested were patched onto plates containing synthetic complete medium lacking uracil (SC-ura), grown overnight at 30°C, and then streaked to obtain single cells on fresh SC-ura (30-ml) or SLAD (25-ml) plates. Four strains were always streaked on one plate. The streaking technique was such that a gradient of colony density existed in the streak, with the highest density existing in the center of the plate. Cultures were grown at 30°C, and after an appropriate period of time dictated by the specific experiment, representative colonies from the streak were photographed. In those experiments where transformants were studied, two independent transformants were assayed. In our experiments, the pairs of transformants always had the same phenotype.

Agar invasion assay. The agar invasion assay was based on observations reported previously (31). Strains to be tested were carefully patched on a SC-ura plate and grown at 30°C. The cells that did not invade the agar were washed away by rubbing the surface of the plate with a gloved hand while rinsing the plate under running water. The cells that had invaded the agar remained as visible patches on the surface of the agar after washing. Invasiveness was confirmed by microscopic examination of the remaining cells and determination that both the plane of focus required for cell visualization resided inside the agar and that a micromanipulation needle was required to penetrate the agar to reach the cells. Populations of invasive cells were prepared for light photomicroscopy by removing a piece of agar containing invasive cells with a toothpick and crushing the agar piece between a coverslip and a microscope slide. This sample preparation method did not maintain the positions of cells in the agar. In those experiments where transformants were studied, two independent transformants were assayed. In our experiments, the pairs of transformants always had the same phenotype.

Light microscopic techniques. Light microscopic techniques have been described in detail elsewhere (31). For Fig. 2C and D, yeast strains were streaked for single cells on SLAD plates as described above in "Qualitative pseudohyphal growth assay" and incubated at 30°C for an appropriate period of time. Invasive pseudohyphae from well-separated colonies were isolated in small agar blocks. The agar blocks were placed on a microscope slide and covered with a coverslip, which was lightly pressed down. Photomicrographs of invasive pseudohyphae were made with a 100× oil immersion objective using Nomarski optics.

Plasmid construction. Recombinant DNA methods were performed by established protocols (48). Plasmids used in experiments reported in this study are listed in Table 1, with the following exceptions. Plasmids isolated from the genomic *S. cerevisiae* library described below containing *PHD1* to *PHD7* are listed in Table 2. Plasmids used only to map the location of *PHD1* on the pCG7 insert are shown in Fig. 3. Plasmids constructed for *PHD1* epitope tagging or deletion are discussed below. Plasmids pCG7 and pCG19 (see Fig. 3 and Table 2) were identified in the PHD screen, contain *PHD1*, and originate from a high-copy-number *S. cerevisiae* genomic library. This library was made in pRS202, a derivative of pRS306 (71) that contains the 2μm origin of replication. The library was made by cloning 6- to 8-kb fragments of genomic *S. cerevisiae* DNA into pRS202 (18).

Deletions of parts of the pCG7 insert were made by removing various restriction fragments from its insert and religating the resulting plasmids (see Fig. 3). pCG13 is pCG7 lacking the 5.5-kb *Eco*RI fragment (one *Eco*RI site is in the polylinker). pCG14 is pCG7 lacking the 0.9-kb *Kpn*I fragment (one *Kpn*I site is in the polylinker). pCG15 is pCG7 lacking the 3.5-kb *Bam*HI fragment (one *Bam*HI site is in the polylinker). pCG16 is pCG7 lacking the 2.0-kb *Bgl*II fragment. pCG17 is pCG7 lacking the 5.3-kb *Bam*HI-*Bgl*II fragment (the *Bam*HI site is in the polylinker).

Other pCG7 derivatives were constructed by subcloning restriction fragments into vectors. pCG27 is the 2.2-kb *Bgl*II-*Cla*I fragment of pCG16 cloned into *Bam*HI-*Cla*I-digested pRS202. pCG28 is the 1.1-kb *Eco*RI-*Eag*I fragment of pCG27

cloned into *Eco*RI-*Eag*I-digested pRS202. pCG31 is the 3.1-kb *Bgl*II-*Sac*I fragment of pCG16 cloned into *Bam*HI-*Sac*I-digested pBluescriptII KS +. pCG38 is the 2.6-kb *Hin*dIII fragment from pCG31 cloned into *Hin*dIII-digested pRS202 in the same orientation as that of pCG31.

DNA sequence analysis of *PHD1*. Double-stranded DNA for use as a sequencing template was prepared by the method of Haltiner et al. (35) and sequenced by the dideoxy-chain termination method of Sanger et al. (64). Protein and DNA homology searches were performed at the National Center for Biotechnology Information using the BLAST network service (2).

Epitope tagging of *PHD1*. *PHD1* was tagged with an epitope as described by Kolodziej and Young (41) by site-directed insertion mutagenesis (42). A 9-amino-acid epitope from the influenza virus hemagglutinin protein HA1 (81) was introduced into the *PHD1* sequence between amino acid residues 355 and 356 (*PHD1::FLU1*). This position was chosen because amino acid residues 354 to 366 are not required for high-copy-number *PHD1* enhancement of pseudohyphal growth (pCG27 in Fig. 3). Oligonucleotide PHD1EPI (5'-GCTCTACTTGTT TGGGCAGCGTAGTCTGGGACGTCGTATGGGTACTC AGTATCGATATGGTTG) was synthesized with 27 nucleotides (nt) encoding the HA1 epitope (in the noncoding orientation) flanked on the 5' side with 17 nt and on the 3' side with 19 nt complementary to the *PHD1* sequence. This oligonucleotide was annealed to single-stranded pCG31 DNA prepared with helper phage M13K07 (79) in the *dut ung Escherichia coli* host RZ1032 (42). After elongation, ligation, and transformation into a *dut*$^+$ *ung*$^+$ host, a plasmid which had acquired the *Aat*II restriction site diagnostic for successful mutagenesis was saved and called pCG35. The 2.6-kb *Hin*dIII fragment from pCG35 was cloned into *Hin*dIII-digested pRS202 in the same orientation as in pCG31, and the resulting construct was called pCG37. pCG37, which contains *PHD1::FLU1*, enhanced pseudohyphal growth to a similar degree as pCG38, which contains *PHD1* (data not shown).

Immunofluorescence of *PHD1::FLU1*. Staining of fixed cells for indirect immunofluorescence was carried out essentially as described previously (47). Experimental and control strains were grown to a density of 10^7 cells per ml in SC-ura to select for plasmid maintenance. Cells were then diluted to a density of 2×10^6 cells per ml in YPD medium (69) and grown for an additional 6 h. Formaldehyde (37%) (0.11 volume) was then added to the culture, which was kept on ice overnight. Cells were washed three times with solution A (0.1 M potassium phosphate buffer [pH 7.5] in 1.2 M sorbitol) and resuspended at a density of 10^8 cells per ml in solution A containing 2 μl of β-mercaptoethanol per ml. Oxalolyticase was added to a final concentration of 0.1 mg/ml, and the cells were incubated at 30°C for 15 min. Spheroplasting was stopped by diluting the cells in 1 ml of cold solution A. Spheroplasts were collected by centrifugation, washed once with 1 ml of cold solution A, resuspended in cold solution A at a density of 2×10^8 cells per ml, and pipetted onto polylysine-coated round coverslips. After 5 min, the cell suspension was gently aspirated away, and the coverslips were incubated at 24°C for 15 min. The coverslips were washed twice with solution A, covered with 100% methanol (incubated for 5 min at −20°C), and washed three more times with solution A. The coverslips were then covered with incubation buffer (solution A containing 4% instant milk) and incubated for 30 min at 30°C. The primary antibody was anti-hemagglutinin monoclonal antibody 12CA5. Salt-fractionated hybridoma supernatant was diluted 1:5 in incubation buffer and was added to coverslips which were incubated overnight at 4°C. Subsequent washes, secondary antibody incubations, 4',6-diamidino-2-phenylindole (DAPI) staining, microscopy, and photography were carried out as previously described (19). The secondary antibody was an affinity-purified fluorescent 5-[(4,6-dichlorotriazin-2-yl)amino] fluorescein (DTAF)-conjugated goat anti-mouse immunoglobulin G (19).

Construction of a precise *PHD1* deletion. A precise deletion of the *PHD1* open reading frame (*phd1Δ::hisG-URA3-hisG*) was constructed by oligonucleotide-directed mutagenesis (42). The oligonucleotide PHD1KO (5'-GAGCAAAGAGTTAAC GGATTATGTTATGTGCAGATCTATTTTCTGCTTAAT GAATTATGAATTCCAGC) used for mutagenesis is arrayed in the following order (5' to 3'), the 31 nt that immediately follow the *PHD1* terminator, the hexanucleotide sequence recognized by the *Bgl*II restriction endonuclease, and the 31 nt that immediately precede the putative ATG initiator codon of *PHD1*. As in the construction of pCG35, the oligonucleotide was annealed to single-stranded pCG31 DNA. After elongation, ligation, and transformation into a *dut*$^+$ *ung*$^+$ host, plasmid DNAs were screened for the absence of the 1.1-kb *PHD1* coding sequence and the presence in its place of a unique new *Bgl*II site diagnostic of a successful mutagenesis. pCG34 was one of these plasmids. pCG36 was constructed by cloning the 5-kb *Bgl*II-*Bam*HI fragment of pSE1076 (23), a derivative of pNKY51 (1) which contains within its two *hisG* repeats the *kan*^{r} gene 3' to the *URA3* gene, into *Bgl*II-digested pCG34 in the orientation *Eco*RI (at bp 674 in Fig. 4)-*Bgl*II-*hisG-URA3-kan*^{r}*-hisG*-(*Bam*HI-*Bgl*II).

Deletion of *PHD1*. pCG36 (10 μg) was digested with both *Sal*I and *Sac*I, extracted once with an equal volume of 1:1 mixture of phenol and 24:1 chloroform-isoamyl alcohol, extracted again with an equal volume of 24:1 chloroform-isoamyl alcohol, ethanol precipitated, and used to transform L5366 as described previously (28). Stable Ura$^+$ transformants were selected on SC-ura plates. Deletion of the *PHD1* gene by homologous recombination was confirmed by hybridization to a genomic Southern blot. CGX133 and CGX134 were constructed in this manner and were independently derived. CGX133 and CGX134 were sporulated, and two Ura$^+$ (*phd1*) sister ascospore segregants from each cross were confirmed to be *phd1Δ1::hisG-URA3-hisG* by Southern analysis. These ascospore segregants were crossed to generate CGX137 and CGX135 (*phd1/phd1*), respectively.

Strains with unmarked deletions of *PHD1* were generated by a standard method (1) by screening for Ura$^-$ segregants of the haploid parents of CGX137 and CGX135 and then by genomic Southern analysis confirming that they had lost the *URA3* gene by mitotic recombination. Haploid strains of opposite mating types generated in this way from the parents of CGX137 and CGX135 were crossed to generate CGX160 and CGX161, respectively.

Nucleotide sequence accession number. The GenBank accession number of the *PHD1* DNA sequence reported in this paper is U05241.

RESULTS

A gene overexpression screen identifies multicopy enhancers of pseudohyphal growth. We carried out a screen (called PHD for pseudohyphal determinant) for genes that enhanced pseudohyphal growth when present in high copy number. The PHD screen was carried out by using a 2μm plasmid-based genomic library because genes cloned in 2μm-based plasmids are typically maintained at high copy numbers (11). The extra copies of a gene often lead to higher levels of the encoded protein (61).

The wild-type Σ1278b strain CGX69 (*MAT***a**/*MAT*α *ura3-52*/

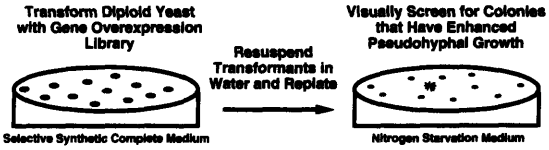

FIG. 1. PHD screen. A *MATa*/*MATα* diploid *S. cerevisiae* strain was transformed with a *S. cerevisiae* gene overexpression library. Transformants were selected on selective SC medium. Transformants were resuspended in water and plated on nitrogen starvation medium (SLAHD) at a density of 2,000 colonies per plate (not to scale). In the 1 to 3 days after plating, microcolonies were screened visually with the aid of a dissecting microscope for those colonies exhibiting enhanced pseudohyphal growth. Normal colonies were round, and symmetrical while colonies with enhanced pseudohyphal growth had a striking rough and filamentous appearance. Cells from enhanced colonies were picked and the plasmid causing the enhanced phenotype was recovered from these colonies.

ura3-52) was transformed with a genomic *S. cerevisiae* library (18) constructed in a *URA3*-marked 2μ-based high-copy-number vector (pRS202). Because Σ1278b strains have a low transformation efficiency, it was necessary to use a high-efficiency transformation protocol (28). A total of 15,000 transformants were obtained in 20 independent pools by selection on SC-ura plates. After 5 days, transformants from each pool were resuspended in water, and plated at a density of 2,000 CFU per 9-cm-diameter petri plate containing solid SLAHD (nitrogen starvation) medium. This high colony density was chosen because it allowed the efficient screening of relatively large numbers of transformants on a moderate number of petri plates. During the next 3 days, the SLAHD plates were screened under a dissecting microscope. Most microcolonies were symmetrical and smooth, but colonies with rough outlines caused by pseudohyphal filaments were observed (Fig. 1) at a frequency of about 0.5%. These colonies containing plasmids that potentially conferred enhanced pseudohyphal growth were purified, and plasmids that enhanced pseudohyphal growth were isolated from some colonies. Restriction enzyme mapping, DNA sequencing, and cross-hybridization analysis (data not shown) demonstrated that they represented seven different genes, *PHD1* to *PHD7* (Table 2).

Overexpression of *PHD1* gave the strongest enhanced pseudohyphal growth phenotype, so it was chosen for further study. *PHD1* was subjected to secondary screens to determine whether it was genetically similar to *RAS2* or *SHR3*, two other genes that enhance pseudohyphal growth when appropriately mutated. The $RAS2^{Val-19}$ and *shr3Δ1* mutations cause enhanced pseudohyphal growth (31) and other phenotypes, such as heat shock sensitivity for $RAS2^{Val-19}$ and super high histidine resistance for *shr3Δ1* (12, 47). *MATa*/*MATα* diploid strains carrying multicopy *PHD1* were tested for these two phenotypes to determine whether multicopy *PHD1* phenotypically copies $RAS2^{Val-19}$ or *shr3Δ1* for phenotypes other than pseudohyphal growth enhancement. Strains with multicopy *PHD1* have normal heat shock sensitivity and do not have super high histidine resistance (data not shown).

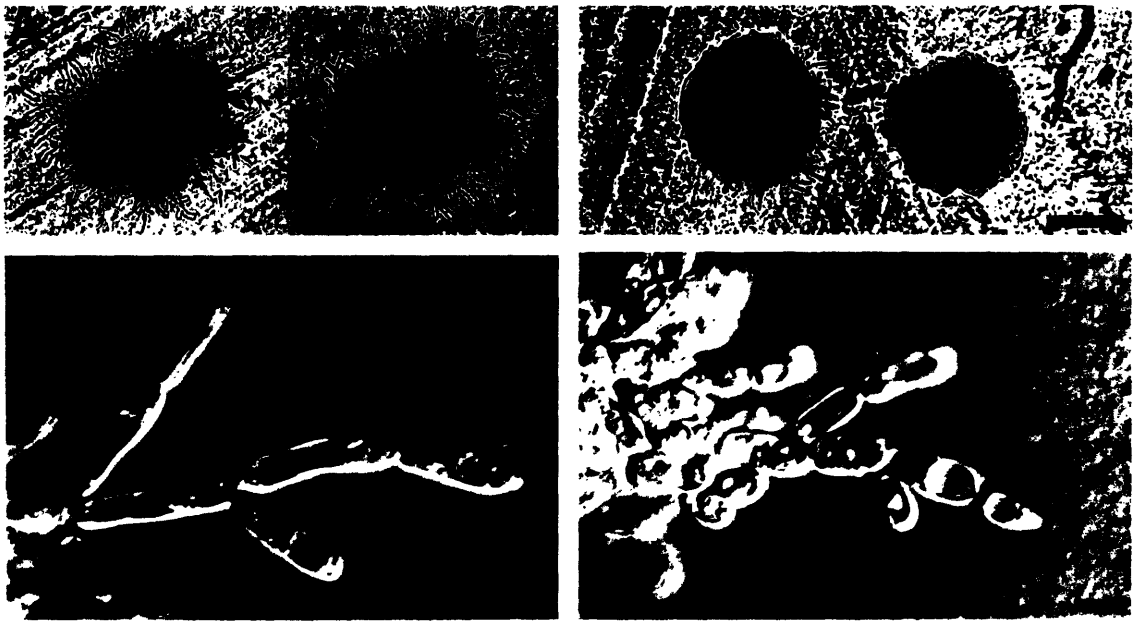

FIG. 2. Pseudohyphal growth enhancement by overexpression of *PHD1*. CG934 (A and C), a *MATa*/*MATα* *PHD1*-overexpressing strain, and CG936 (B) and CG953 (D), *MATa*/*MATα* wild-type control strains, were patched on SC-ura medium, grown overnight at 30°C, and then streaked to obtain single cells on nitrogen starvation (SLAD) medium. Plates were incubated at 30°C, and for panels A and B, representative microcolonies were photographed after 45 h of growth. The scale bar in panel B applies to panels A and B and represents 100 μm. Invasive pseudohyphae from CG934 and CG953 were visualized under the microscope with Nomarski optics and photographed after 2 (C) and 5 (D) days. The scale bar in panel D applies to panels C and D and represents 5 μm.

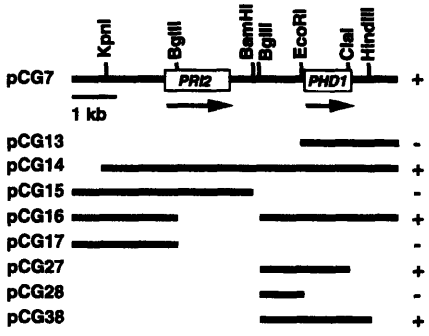

FIG. 3. Localization of pseudohyphal growth enhancement activity to *PHD1*. DNA fragments from the pCG7 insert were subcloned into pRS202 and assayed for their ability to enhance pseudohyphal growth in strain L5366 (*MATa/MATα ura3-52/ura3-52*). Plasmid designations are shown to the left of their DNA inserts, which are represented by dark lines. Plasmids that cause (+) enhanced pseudohyphal growth, such as pCG38 in Fig. 2A, and plasmids that did not cause (−) enhanced pseudohyphal growth, such as pRS202 in Fig. 2B, are indicated. Open reading frames are shown by rectangles, and their orientation is indicated by an arrow. Plasmid pCG19 contains the *PHD1* gene in a 4.5-kb insert that begins at the end of *PRI2* at nt 2036 (numbered as in reference 27). Only those restriction sites used in subcloning are shown.

We compared the pseudohyphal growth of strains growing on nitrogen starvation medium carrying either *PHD1* on a 2μm plasmid or the vector without an insert (Fig. 2). Interestingly, *PHD1* overexpression also vigorously enhances pseudohyphal growth in liquid SLAD cultures prepared as described in Materials and Methods. *PHD1* overexpression causes cells growing on nitrogen starvation medium to enter the pseudohyphal growth mode earlier than their wild-type counterparts. Moreover, pseudohyphal cells produced by *PHD1*-overexpressing strains are more elongated than those produced by wild-type strains. Therefore, *PHD1* regulates the timing of initiation of pseudohyphal growth as well as the size of the cells composing the pseudohyphae.

Mapping *PHD1* to *PHD7* to the *S. cerevisiae* genome. Restriction mapping and DNA sequencing experiments (Fig. 3) demonstrated that *PHD1* is adjacent to the *PRI2* gene, which has been mapped to chromosome XI by hybridization to a chromosome blot (27). The 1.1-kb *Eco*RI-*Cla*I fragment of pCG27 was hybridized to the prime λ clones, a panel of λ clones that contain *S. cerevisiae* genomic DNA inserts and represent most of this organism's genome (59, 60), and one hybridizing phage containing DNA from chromosome XI predicted to be near *CDC16* was identified (Table 2).

This position was confirmed by genetic mapping. Diploid CGX94 (*MATa/MATα PHD1/phd1Δ1::hisG-URA3-hisG CDC16/cdc16-1 TRP1/trp1::hisG HIS4/his4-619 ura3-52/ura3-52*) was sporulated and analyzed by tetrad analysis. Segregation of the two alleles of *PHD1* in this cross was followed by scoring uracil prototrophy. The two alleles of *CDC16* were followed by scoring growth at 36°C. *CEN11* was followed by scoring tryptophan prototrophy (*trp1::hisG* is tightly centromere linked). Analysis of 53 tetrads in which all five markers in the cross segregated in a Mendelian fashion revealed that the distance between *phd1* and *cdc16* is 15.1 centimorgans (37 parental ditypes, 0 nonparental ditypes, and 16 tetratypes) and that the distance between *cdc16* and *CEN11* is 19.8 centimorgans (11 parental ditypes, 21 nonparental ditypes, and 21 tetratypes). *phd1* was not detectably linked to *CEN11* (8 parental ditypes, 11 nonparental ditypes, and 34 tetratypes).

Mapping of *PHD2* was initiated by sequencing the DNA at the two ends of the pCG6 insert. DNA sequencing revealed that the *MSN1/FUP1* gene encoding a putative transcription factor implicated in carbon and iron metabolism as well as in mating (22, 26, 58) was at its left end and that part of the first copy of the gene for ribosomal proteins rp28 and S16A, which has been mapped genetically to chromosome XV (55), was at the insert's right end. To test whether *PHD2* was allelic to *MSN1/FUP1*, pEY312C (26), a multicopy vector with a 2-kb DNA insert containing the 1.1-kb *MSN1/FUP1* open reading frame, was tested for its ability to enhance pseudohyphal growth in a *MATa/MATα* strain on SLAD medium. pEY312C enhanced pseudohyphal growth, but not as well as pCG6, consistent with the report that pEY312C probably lacks some of the *MSN1/FUP1* promoter (26). pDE1, a multicopy *MSN1/FUP1* plasmid isolated from a library (22), enhanced pseudohyphal growth to a similar degree as pCG6 on SLAD plates. Thus, *PHD2* is probably allelic to *MSN1/FUP1*. The 1.2-kb *Mlu*I-*Bam*HI fragment from pEY312C (26), containing most of the *MSN1/FUP1* open reading frame, was hybridized to the prime λ clones, and two phages containing overlapping DNA fragments from chromosome XV were identified (Table 2).

PHD3 to *PHD7* were mapped physically by hybridizing the inserts of the library plasmids to *S. cerevisiae* chromosome blots. In this way, *PHD3* to *PHD7* were mapped to yeast chromosomes (Table 2).

DNA and predicted amino acid sequences of *PHD1*. The segment of pCG7 that encodes *PHD1* was defined by subcloning fragments of the yeast segment of pCG7 into the 2μm plasmid pRS202, transforming these constructs into a *MATa/MATα* diploid, and assaying their ability to enhance pseudohyphal growth (Fig. 3). The smallest segment that enhanced pseudohyphal growth in multicopy was sequenced and an open reading frame was found (Fig. 4) terminated by a TAA codon, the most common terminator in *S. cerevisiae* (80). The first ATG codon of the *PHD1* open reading frame has at position −3 the conserved adenine residue that is present in 75% of *S. cerevisiae* initiator ATG codons (21). The open reading frame of 1,098 bp is predicted to encode a protein of 366 amino acids. Overexpression of this open reading frame from the inducible *GAL1* promoter (58) in a diploid enhanced pseudohyphal growth on nitrogen starvation medium (30). PHD1 is predicted to have a molecular mass of 40.6 kDa and an isoelectric point of 8.99. PHD1 is proline rich (9.3%) relative to 891 yeast proteins (34 of 366, 4.4%) in the GenBank data base surveyed (80). The amino-terminal 145 amino acids of PHD1 contain 21 prolines.

PHD1 is related to transcriptional regulators of fungal development. Four proteins with amino acid sequence similarity to one region of PHD1 were identified by the BLAST program (2) in data bases, *Aspergillus nidulans* StuA (53), the *Schizosaccharomyces pombe* transcription factors Cdc10 (6) and Res1 (Sct1) (13, 74), and the *S. cerevisiae* transcription factor SWI4 (4) (Fig. 5). In addition, the same region of PHD1 is also similar to the recently described (40) *S. cerevisiae* MBP1 transcription factor (Fig. 5) and its *Kluyveromyces lactis* homolog K.l.MBP1 (data not shown). Thus, PHD1 may be a member of a family of transcriptional regulators of fungal development (5).

At the amino acid sequence level, PHD1 is most closely related to the StuA protein. PHD1 and StuA share about 70% identity over 100 amino acids. MBP1, SWI4, Cdc10, and Res1

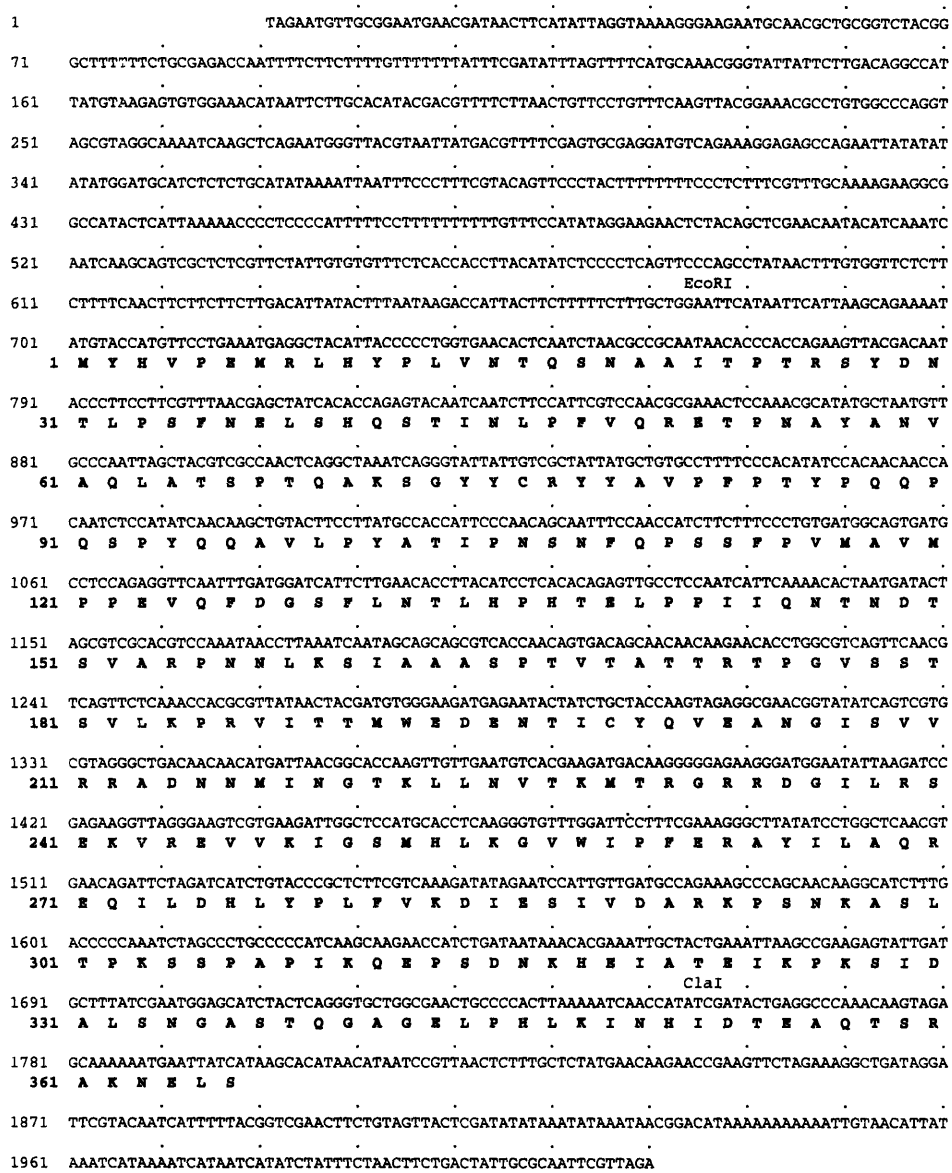

FIG. 4. DNA and predicted amino acid sequences of *PHD1*. The nucleotide sequence of the *PHD1* gene is shown. The predicted 366-amino-acid protein product of *PHD1* is shown in the one-letter amino acid code. The *Eco*RI and *Cla*I sites shown in Fig. 3 are indicated.

also share similarity with the same 100-amino-acid region of PHD1 (Fig. 5). This 100-amino-acid region functions as a DNA binding domain in MBP1 and SWI4 (40, 57), and it probably also serves this function in PHD1 and StuA. The amino termini of PHD1 and StuA are both proline rich, which may have functional significance because some transcription factors have proline-rich regions as their activation domains (51, 54). The DNA binding motifs of MBP1, SWI4, Cdc10, and Res1 are all located at their amino termini (40). By contrast, the DNA binding motifs of PHD1 and StuA are not located in the amino termini of these proteins (Fig. 5). The ankyrin repeats located in the central domain of MBP1, SWI4, Cdc10, and Res1 are not found in either PHD1 or StuA. Therefore, PHD1 and StuA represent one class of proteins containing SWI4-like DNA binding motifs, while SWI4, MBP1, K.l.MBP1, Cdc10, and Res1 represent another. In addition to their amino acid sequence similarities, PHD1 and StuA appear to have related biological functions: PHD1 regulates pseudo-

FIG. 5. PHD1 contains a DNA binding motif present in fungal transcriptional regulators. Alignments of five proteins similar to PHD1 are shown. The name of the protein whose amino acid sequence is shown is to the left of the sequence. When an amino acid in PHD1 is identical to the corresponding amino acid in a similar protein, both amino acids are designated by a white letter in a black rectangle. To the right of the sequence is the position of the amino acid sequence with respect to the amino terminus of the protein from which it originates. The lower section shows schematic representations of the six proteins, with amino termini to the left; the amino acid sequences shown in the upper portion of the figure are aligned and represented as black rectangles. The number of amino acids identical between PHD1 and its homologs in the regions shown in this figure is listed to the right.

hyphal growth in *S. cerevisiae*, while StuA participates in conidiophore morphogenesis in *A. nidulans*.

Immunolocalization of functionally epitope-tagged PHD1 protein to the nucleus. PHD1 protein was localized with a FLU epitope-tagged construct (*PHD1::FLU1*) that appeared to be fully functional. Multicopy *PHD1::FLU1* enhanced pseudohyphal growth to the same degree as multicopy *PHD1* (data not shown). A diploid strain lacking both endogenous copies of *PHD1* and overexpressing *PHD1::FLU1* (CG739) was subjected to indirect immunofluorescence. *PHD1::FLU1*-specific immunofluorescence always colocalized with the nuclear stain 4′,6-diamidino-2-phenylindole (Fig. 6). A control strain overexpressing a nontagged version of *PHD1* (CG737) exhibited no immunofluorescence above background levels (data not shown). Nuclear localization of PHD1 protein is consistent with the idea that PHD1 functions as a transcriptional regulatory protein.

***PHD1* overexpression induces pseudohyphal growth on rich medium.** Strains were constructed to determine whether the effects of *PHD1* overexpression were restricted to the conditions of nitrogen starvation required for pseudohyphal growth in wild-type cells. Diploid strains containing either a *PHD1* overexpression plasmid (pCG38) or a control plasmid with no insert (pRS202) were streaked for single cells on high-nitrogen medium (SC-ura), and microcolonies were photographed after 17 h (Fig. 7). This time of growth was chosen because soon after 17 h, rapidly growing ellipsoidal yeast cells overgrow the pseudohyphae and make it difficult to see their development (31, 32). Overexpression of *PHD1* vigorously induces pseudohyphal growth on rich medium.

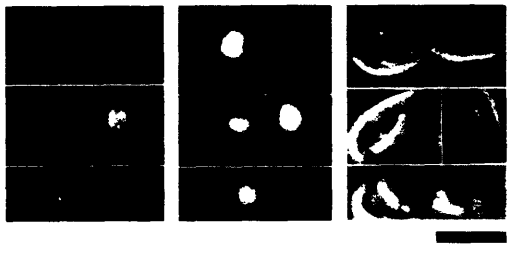

FIG. 6. Immunolocalization of epitope-tagged PHD1 to the nucleus. Strain CGX160 harboring plasmid pCG37 (a multicopy plasmid containing the *PHD1::FLU1* construct) was subjected to indirect immunofluorescence as described in Materials and Methods. (Left panel) DTAF staining observed with anti-hemagglutinin monoclonal antibody; (middle panel) 4′, 6-diamidino-2-phenylindole staining; (right panel) cells viewed by Nomarski optics. Bar, 5 μm.

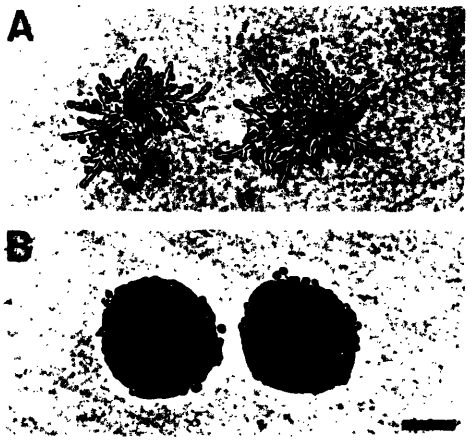

FIG. 7. *PHD1* overexpression activates pseudohyphal growth on rich medium. CG934 (A), a *MATa/MATα PHD1*-overexpressing strain, and CG936 (B), a *MATa/MATα* wild-type strain, were patched on SC-ura, grown overnight at 30°C, and then streaked to obtain single cells on SC-ura plates which were incubated at 30°C. Microcolonies were photographed after 17 h. Bar, 40 μm.

To test whether the pseudohyphae induced on rich medium by overexpression of *PHD1* invaded the agar, the *PHD1*-overexpressing and wild-type strains were patched on SC-ura. After about 2 days of growth, the patches on the plate were photographed (Fig. 8A). Cells that had not invaded the agar were rinsed off the plate, and the plate was rephotographed (Fig. 8B). The *PHD1*-overexpressing strain vigorously invaded the agar (upper patch), whereas the wild-type strain did not (lower patch) (Fig. 8A and B). The morphology of invasive cells was determined by light microscopy. Invasive pseudohyphae were observed (Fig. 8C), and invasive cells were predominantly pseudohyphal (Fig. 8D). *PHD1* overexpression inappropriately induces vigorous pseudohyphal growth on rich medium and the pseudohyphae produced on rich medium, like those produced on nitrogen starvation medium (SLAD), invade the growth substrate.

Analysis of pseudohyphal growth in haploids overexpressing *PHD1*. Pseudohyphal growth is a *MATa/MATα* diploid-specific dimorphic transition regulated by the mating-type locus (31). Wild-type haploid cells do not undergo pseudohyphal growth when starved for nitrogen because the haploid-specific axial budding pattern precludes linear growth of a filament. To determine whether *PHD1* overexpression induces pseudohyphal growth in *MATa* and *MATα* wild-type haploid strains, haploid strains were transformed with a *PHD1* overexpression plasmid or a control plasmid with no insert. The resulting transformants were streaked for single cells on nitrogen starvation medium (SLAD), which induces pseudohyphal growth in *MATa/MATα* diploid strains (Fig. 2B). Colonies produced by all strains in this experiment were smooth and round and had no pseudohyphae emanating from them (Fig. 9).

Although overexpression of *PHD1* does not cause wild-type haploid strains to enter the pseudohyphal pathway, it does alter their morphology. When grown on SC-ura, haploid colonies composed of *PHD1*-overexpressing cells (CG937 and CG940) have a higher proportion of elongated cells than haploid colonies composed of cells containing a control vector (CG939 and CG942).

Recent studies show that some haploid mutants that have the diploid polar budding pattern undergo pseudohyphal growth when starved for nitrogen (63, 82). We tested whether *PHD1* overexpression enhances pseudohyphal growth in one of these, a *bud4* mutant strain (SS3-2B) (*MATa bud4 ura3-52*) (63). This haploid strain has the diploid polar budding pattern because it is Bud4$^-$ (14, 63), and undergoes modest pseudohyphal growth when starved for nitrogen (63). As judged by the qualitative pseudohyphal growth assay described in Materials and Methods performed on a SLAD plate, this haploid *bud4* mutant strain transformed with a *PHD1* overexpression plasmid (pCG38) exhibits enhanced pseudohyphal growth (data not shown).

Deletion of *PHD1*. Tetrad analysis of independently derived strains (CGX133 and CGX134) heterozygous for a *PHD1* null allele (*phd1Δ1::hisG-URA3-hisG*) revealed four viable spores per ascus, showing that *PHD1* is not required for cell viability on rich medium. *PHD1/PHD1* and *phd1/phd1* strains grew at similar rates on rich medium (SC-ura plates). As determined by the qualitative pseudohyphal growth assay described in Materials and Methods, *PHD1/PHD1* and *phd1/phd1* strains (CGX135 and CGX137) underwent similar pseudohyphal growth on nitrogen starvation medium (SLAD) and *PHD1/PHD1 shr3/shr3* (CGX157) and *phd1/phd1 shr3/shr3* (CGX155) double mutants underwent similar pseudohyphal growth on proline medium (SPHD) (data not shown). By a qualitative plate sporulation assay (69), *PHD1/PHD1* and *phd1/phd1* strains exhibited similar levels of sporulation.

DISCUSSION

Function of *PHD1*. On the basis of its similarity to the MBP1 and SWI4 DNA binding domains and its nuclear localization, it is reasonable to propose that PHD1 is a transcription factor. The phenotypes resulting from *PHD1* overexpression, enhancement of pseudohyphal growth on nitrogen starvation medium, and induction of pseudohyphal growth on rich medium are also consistent with this assumption. These phenotypes could be explained by positing that *PHD1* regulates pseudohyphal growth by responding to an inductive signal, such as nitrogen starvation, and activates the transcription of downstream genes responsible for the pseudohyphal growth program. Overexpression of *PHD1* could enhance pseudohyphal growth by largely bypassing the requirement for that signal.

The only complication with this hypothesis is that diploids homozygous for a null allele of *PHD1* form pseudohyphae in response to nitrogen starvation. This result can be explained if *S. cerevisiae* has one or more genes that are functionally redundant with *PHD1*. This explanation is reasonable because many examples of genetic redundancy exist among genes encoding *S. cerevisiae* signal transduction pathway components (12). Another intriguing explanation is that *PHD1* induces pseudohyphal growth in response to a signal other than nitrogen starvation. It is also possible that *PHD1* does not normally function in pseudohyphal growth but that its overexpression leads indirectly to pseudohyphal growth enhancement by, for instance, a transcriptional "squelching" mechanism, where overexpressed PHD1 protein would titrate a negative regulator of pseudohyphal growth. Alternatively, *phd1 phd1* strains may undergo defective pseudohyphal growth which is not detectable by the qualitative assays used in this study.

***PHD1* is related to four transcription factors which regulate the cell cycle.** PHD1 contains the DNA binding motif present in several fungal transcriptional regulators: SWI4 and MBP1 from *S. cerevisiae* (4) and Cdc10 and Res1 from *S. pombe* (6,

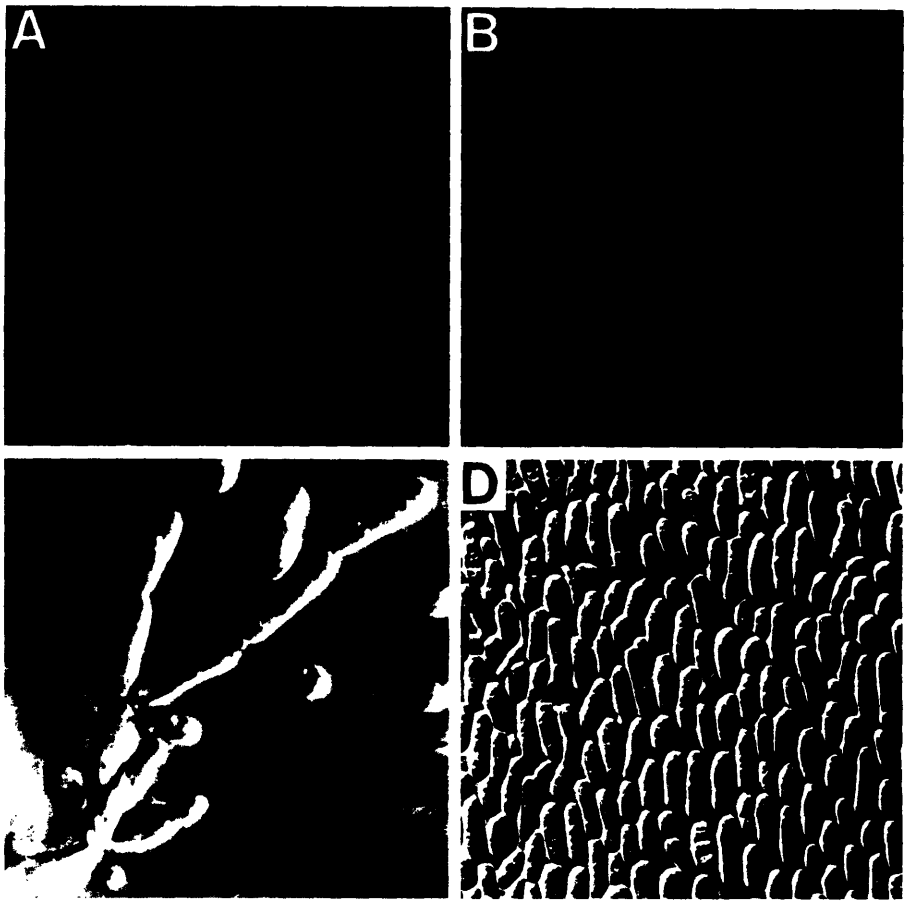

FIG. 8. Agar invasion by a *PHD1*-overexpressing strain. CG934 (upper patch), a *MATa*/*MATα PHD1*-overexpressing strain, and CG936 (lower patch), a *MATa*/*MATα* wild-type strain, were grown overnight at 30°C on SC-ura, patched onto a SC-ura plate, and grown for 44 h at 30°C. The plate was then photographed (A), rinsed with water to remove noninvasive cells, and rephotographed (B). Thin agar slices cut from the edge of the CG934 patch in panel B containing invasive cells were then placed under coverslips. The cells in the agar were examined and photographed under the microscope using Nomarski optics. An invasive pseudohypha (C) and a population of invasive cells (D) are shown. The scale bar in panel C applies to panels C and D and represents 5 μm for panel C and 10 μm for panel D.

13, 74). In SWI4 and MBP1, this DNA binding motif is known to function as a DNA binding domain (40, 57). In view of the fact that PHD1 overexpression permits pseudohyphal growth on rich medium, it is interesting that Res1 may be involved in the transduction of starvation signals (13, 74).

These four PHD1 homologs have similar functions: they regulate the expression of genes whose transcription is limited to discrete portions of the cell cycle by binding to related DNA sequences that are present in their promoters. These DNA sequences, the SCB (SWI4-SWI6 cell cycle box) and MCB (*Mlu*I cell cycle box) elements, are present in the promoters of many Start-specific genes (3, 13, 74). PHD1 has a DNA binding motif in common with these cell cycle regulatory proteins and may therefore bind either SCB or MCB or both sequences to regulate Start-specific transcription. The properties of PHD1 make it a candidate for an MCB-binding protein in *S. cerevisiae*, distinct from MBP1, whose existence was inferred from genetic experiments (40). If PHD1 is a cell cycle regulator, it could control pseudohyphal growth by affecting cell cycle-regulated processes such as cell wall biosynthesis and cell separation. Potential targets relevant for pseudohyphal growth include *CTS1*, which encodes a chitinase (20, 43), and several cyclin genes that have possible roles in morphogenesis (24, 45, 56, 66).

Implications of the relationship between *S. cerevisiae* PHD1 and *A. nidulans* StuA. The amino acid sequence of PHD1 is most closely related to that of *A. nidulans* StuA. The SWI4-like DNA binding motifs present in these two proteins are about 70% identical over 100 amino acids. This sequence similarity between PHD1 and StuA is especially interesting because these proteins affect respectively pseudohyphal growth, as described here, and conidiophore morphogenesis (17, 52, 53), which are functionally and morphologically analogous biological processes.

Both conidiophore morphogenesis and pseudohyphal growth facilitate the dispersal of asexually produced cells.

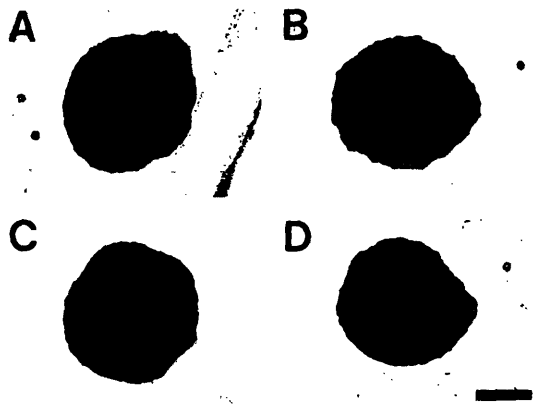

FIG. 9. *PHD1* overexpression does not induce pseudohyphal growth in wild-type haploids. (A) CG937 (C), a *MAT***a** *PHD1*-overexpressing strain; (B) CG939, a *MAT***a** wild-type strain; (C) CG940, a *MAT*α *PHD1*-overexpressing strain, and (D) CG942, a *MAT*α wild-type strain. These four strains were patched on SC-ura, grown overnight at 30°C, and then streaked to obtain single cells on nitrogen starvation (SLAD) medium. Representative microcolonies were photographed after 45 h of growth. Panels A and B of Fig. 2 are appropriate positive controls for this experiment. Bar, 100 μm.

Conidiophore morphogenesis positions conidia outside a spent growth substrate and permits their dispersal by air to new substrates (75, 76). In a similar sense, pseudohyphal growth can be interpreted as a mechanism to deliver ellipsoidal yeast cells to new and otherwise inaccessible substrates (32). During conidiophore morphogenesis in *A. nidulans*, the formation of elongated metula and phialide cells by polar budding (75–77) closely resembles the polar budding of pseudohyphal cells observed in *S. cerevisiae*. These polar cell divisions in *A. nidulans* are regulated by *StuA* because *stuA* mutants typically do not form metulae or phialides (17, 52). Thus, PHD1 and StuA show regions of structural identity and appear to be involved in functionally analogous processes.

PHD screen as a method to identify morphogenetic regulators from heterologous organisms. The PHD screen described here is a facile method for identifying any gene capable of inducing filamentous growth in *S. cerevisiae*. Some of the genes involved in polarized growth and development in *S. cerevisiae* are likely to be conserved in plants and animals, and the PHD screen could be used to identify them.

The PHD screen should be especially effective in identifying functionally conserved genes involved in dimorphism from heterologous fungi. The identification of dimorphism genes from pathogenic fungi will be interesting because dimorphism appears to be involved in the virulence of several fungal pathogens of animals and plants (7, 67). For instance, the unicellular growth mode of the human pathogen *Histoplasma capsulatum* is associated with disease, while the filamentous phase appears to be avirulent (49, 50). A drug that could lock *H. capsulatum* in its avirulent filamentous state might be an effective antifungal agent. Dimorphism genes from pathogenic fungi, cloned using the PHD screen, could provide new antifungal drug targets. The identification of heterologous dimorphism genes and their comparison with those of *S. cerevisiae* should provide important insights into the evolution of this unique fungal developmental pathway.

A PHD screen can be performed on an organism of interest once a cDNA library, or in some cases a genomic library, constructed in a *S. cerevisiae* overexpression vector has been generated. This library would then be screened as described in this article, with minor modifications if necessary. The PHD screen permits one to screen a sufficiently large number of transformants so that even genomes considerably larger than that of *S. cerevisiae* can be assayed. PHD screens have been successfully used on libraries from human cells (33) and the plant *Arabidopsis thaliana* (68). The PHD screen promises to be a generally useful tool for the analysis of morphogenesis and development.

ACKNOWLEDGMENTS

We thank Cora Styles for performing the *bud4* and pseudohyphal growth in liquid medium experiments. We are grateful to Marian Carlson, David Eide, Steven Elledge, Phillip Hieter, and Nancy Kleckner for providing plasmids. We thank Marjorie Brandriss, Ira Herskowitz, Sylvia Sanders, and Cora Styles for providing yeast strains. We are grateful to Maynard Olson and Linda Riles for providing the prime λ clone filters and *S. cerevisiae* genome physical map information. We thank Ira Herskowitz, Bruce Miller, and Sylvia Sanders for sharing information prior to publication. We thank George Kobayashi, Alan Lambowitz, and William Timberlake for helpful discussions. We thank Fink laboratory members for helpful conversations. Kyle Cunningham, Ruth Hammer, Stephen Kron, and Per Ljungdahl are thanked for critically reviewing the manuscript.

This work was supported by a Howard Hughes Medical Institute predoctoral fellowship to C.J.G. and NIH research grants GM40266 and GM35010 to G.R.F. G.R.F. is an American Cancer Society Professor of Genetics.

REFERENCES

1. **Alani, E., L. Cao, and N. Kleckner.** 1987. A method for gene disruption that allows repeated use of *URA3* selection in the construction of multiply disrupted yeast strains. Genetics **116**:541–545.
2. **Altschul, S. F., W. Gish, W. Miller, E. W. Myers, and D. J. Lipman.** 1990. Basic local alignment search tool. J. Mol. Biol. **215**:403–410.
3. **Andrews, B. J.** 1992. Dialogue with the cell cycle. Nature (London) **355**:393–394.
4. **Andrews, B. J., and I. Herskowitz.** 1989. The yeast SWI4 protein contains a motif present in developmental regulators and is part of a complex involved in cell-cycle-dependent transcription. Nature (London) **342**:830–833.
5. **Andrews, B. J., and S. W. Mason.** 1993. Gene expression and the cell cycle: a family affair. Science **261**:1543–1544.
6. **Aves, S. J., B. Durkacz, A. Carr, and P. Nurse.** 1985. Cloning, sequencing and transcriptional control of the *Schizosaccharomyces pombe cdc10* 'start' gene. EMBO J. **4**:457–463.
7. **Banuett, F.** 1992. *Ustilago maydis*, the delightful blight. Trends Genet. **8**:174–180.
8. **Bender, A., and J. R. Pringle.** 1989. Multicopy suppression of the *cdc24* budding defect in yeast by *CDC42* and three newly identified genes including the *ras*-related gene *RSR1*. Proc. Natl. Acad. Sci. USA **86**:9976–9980.
9. **Blacketer, M. J., C. M. Koehler, S. G. Coats, A. M. Myers, and P. Madaule.** 1993. Regulation of dimorphism in *Saccharomyces cerevisiae*: involvement of the novel protein kinase homolog Elm1p and protein phosphatase 2A. Mol. Cell. Biol. **13**:5567–5581.
10. **Brandriss, M. C., and B. Magasanik.** 1979. Genetics and physiology of proline utilization in *Saccharomyces cerevisiae*: enzyme induction by proline. J. Bacteriol. **140**:498–503.
11. **Broach, J. R.** 1981. The yeast plasmid 2μ circle, p. 445–470. *In* J. N. Strathern, E. W. Jones, and J. R. Broach (ed.), The molecular biology of the yeast *Saccharomyces*, life cycle and inheritance. Cold Spring Harbor Laboratory Press, Cold Spring Harbor, N.Y.
12. **Broach, J. R., and R. J. Deschennes.** 1990. The function of *RAS* genes in *Saccharomyces cerevisiae*. Adv. Cancer Res. **54**:79–139.
13. **Caligiuri, M., and D. Beach.** 1993. Sct1 functions in partnership with Cdc10 in a transcription complex that activates cell cycle START and inhibits differentiation. Cell **72**:607–619.

14. **Chant, J., and I. Herskowitz.** 1991. Genetic control of bud site selection in yeast by a set of gene products that constitute a morphogenetic pathway. Cell **65**:1203–1212.
15. **Chant, J., and J. R. Pringle.** 1991. Budding and cell polarity in *Saccharomyces cerevisiae*. Curr. Opin. Genet. Dev. **1**:342–350.
16. **Ciriacy, M., K. Freidel, and C. Lohning.** 1991. Characterization of trans-acting mutations affecting Ty and Ty-mediated transcription in *Saccharomyces cerevisiae*. Curr. Genet. **20**:441–448.
17. **Clutterbuck, A. J.** 1969. A mutational analysis of conidial development in *Aspergillus nidulans*. Genetics **63**:317–327.
18. **Connelly, C., and P. Hieter.** Personal communication.
19. **Davis, L. I., and G. R. Fink.** 1990. The *NUP1* gene encodes an essential component of the yeast nuclear pore complex. Cell **61**:965–978.
20. **Dohrmann, P. R., G. Butler, K. Tamai, S. Dorland, J. R. Greene, D. J. Thiele, and D. J. Stillman.** 1992. Parallel pathways of gene regulation: homologous regulators *SWI5* and *ACE2* differentially control transcription of *HO* and chitinase. Genes Dev. **6**:93–104.
21. **Donahue, T. F., and A. M. Cigan.** 1990. Sequence and structure requirements for efficient translation in yeast. Methods Enzymol. **185**:366–372.
22. **Eide, D., and L. Guarente.** 1992. Increased dosage of a transcriptional activator gene enhances iron-limited growth of *Saccharomyces cerevisiae*. J. Gen. Microbiol. **138**:347–354.
23. **Elledge, S. J.** Personal communication.
24. **Epstein, C. B., and F. R. Cross.** 1992. *CLB5*: a novel B cyclin from budding yeast with a role in S phase. Genes Dev. **6**:1695–1706.
25. **Errede, B., and G. Ammerer.** 1989. STE12, a protein involved in cell-type-specific transcription and signal transduction in yeast, is part of protein-DNA complexes. Genes Dev. **3**:1349–1361.
26. **Estruch, F., and M. Carlson.** 1990. Increased dosage of the *MSN1* gene restores invertase expression in yeast mutants defective in the SNF1 protein. Nucleic Acids Res. **18**:6959–6964.
27. **Foiani, M., C. Santocanale, P. Plevani, and G. Lucchini.** 1989. A single essential gene, *PRI2*, encodes the large subunit of DNA primase in *Saccharomyces cerevisiae*. Mol. Cell. Biol. **9**:3081–3087.
28. **Gietz, D., J. A. St. Jean, R. A. Woods, and R. H. Schiestl.** 1992. Improved method for high efficiency transformation of intact yeast cells. Nucleic Acids Res. **20**:1425.
29. **Gimeno, C. J., and G. R. Fink.** 1992. The logic of cell division in the life cycle of yeast. Science **257**:626.
30. **Gimeno, C. J., and G. R. Fink.** Unpublished data.
31. **Gimeno, C. J., P. O. Ljungdahl, C. A. Styles, and G. R. Fink.** 1992. Unipolar cell divisions in the yeast *S. cerevisiae* lead to filamentous growth: regulation by starvation and *RAS*. Cell **68**:1077–1090.
32. **Gimeno, C. J., P. O. Ljungdahl, C. A. Styles, and G. R. Fink.** 1993. Characterization of *Saccharomyces cerevisiae* pseudohyphal growth, p. 83–103. *In* H. Vanden Bossche, F. C. Odds, and D. Kerridge (ed.), Dimorphic fungi in biology and medicine. Plenum, New York.
33. **Golemis, E. A.** Personal communication.
34. **Grenson, M., M. Mousset, J. M. Wiame, and J. Bechet.** 1966. Multiplicity of the amino acid permeases in *Saccharomyces cerevisiae*. I. Evidence for a specific arginine-transporting system. Biochim. Biophys. Acta **127**:325–338.
35. **Haltiner, M., T. Kempe, and R. Tjian.** 1985. A novel strategy for constructing clustered point mutations. Nucleic Acids Res. **13**: 1015–1025.
36. **Hansen, E. C.** 1886. Recherches sur la physiologie et la morphologie des ferments alcooliques. V. Méthodes pour obtenir des cultures pures de *Saccharomyces* et de microorganismes analogues. C. R. Trav. Lab. Carlsberg Ser. Physiol. **2**:92–136.
37. **Hartwell, L. H.** 1974. *Saccharomyces cerevisiae* cell cycle. Bacteriol. Rev. **38**:164–198.
38. **Hoffman, C. S., and F. Winston.** 1987. A ten-minute DNA preparation from yeast efficiently releases autonomous plasmids for transformation of *Escherichia coli*. Gene **57**:267–272.
39. **Ito, H., Y. Fukuda, K. Murata, and A. Kimura.** 1983. Transformation of intact yeast cells treated with alkali cations. J. Bacteriol. **153**:163–168.
40. **Koch, C., T. Moll, M. Neuberg, H. Ahorn, and K. Nasmyth.** 1993. A role for the transcription factors Mbp1 and Swi4 in progression from G1 to S phase. Science **261**:1551–1557.
41. **Kolodziej, P. A., and R. A. Young.** 1991. Epitope tagging and protein surveillance. Methods Enzymol. **194**:508–519.
42. **Kunkel, T. A., J. D. Roberts, and R. A. Zakour.** 1987. Rapid and efficient site-specific mutagenesis without phenotypic selection. Methods Enzymol. **154**:367–382.
43. **Kuranda, M. J., and P. W. Robbins.** 1991. Chitinase is required for cell separation during growth of *Saccharomyces cerevisiae*. J. Biol. Chem. **266**:19758–19767.
44. **Lee, K. S., L. K. Hines, and D. E. Levin.** 1993. A pair of functionally redundant yeast genes (*PPZ1* and *PPZ2*) encoding type 1-related protein phosphatases function within the *PKC1*-mediated pathway. Mol. Cell. Biol. **13**:5843–5853.
45. **Lew, D. J., and S. I. Reed.** 1993. Morphogenesis in the yeast cell cycle: regulation by Cdc28 and cyclins. J. Cell Biol. **120**:1305–1320.
46. **Liu, H., C. A. Styles, and G. R. Fink.** 1993. Elements of the yeast pheromone response pathway required for filamentous growth of diploids. Science **262**:1741–1744.
47. **Ljungdahl, P. O., C. J. Gimeno, C. A. Styles, and G. R. Fink.** 1992. SHR3: a novel component of the secretory pathway specifically required for localization of amino acid permeases in yeast. Cell **71**:463–478.
48. **Maniatis, T., E. F. Fritsch, and J. Sambrook.** 1982. Molecular cloning: a laboratory manual. Cold Spring Harbor Laboratory Press, Cold Spring Harbor, N.Y.
49. **Maresca, B., and G. S. Kobayashi.** 1989. Dimorphism in *Histoplasma capsulatum*: a model for the study of cell differentiation in pathogenic fungi. Microbiol. Rev. **53**:186–209.
50. **Medoff, G., M. Sacco, B. Maresca, D. Schlessinger, A. Painter, G. S. Kobayashi, and L. Carratu.** 1986. Irreversible block of the mycelial-to-yeast phase transition of *Histoplasma capsulatum*. Science **231**:476–479.
51. **Mermod, N., E. A. O'Neill, T. J. Kelly, and R. Tjian.** 1989. The proline-rich transcriptional activator of CTF/NF-1 is distinct from the replication and DNA binding domain. Cell **58**:741–753.
52. **Miller, K. Y., T. M. Toennis, T. H. Adams, and B. L. Miller.** 1991. Isolation and transcriptional characterization of a morphological modifier: the *Aspergillus nidulans stunted* (*stuA*) gene. Mol. Gen. Genet. **227**:285–292.
53. **Miller, K. Y., J. Wu, and B. L. Miller.** 1992. *StuA* is required for cell pattern formation in *Aspergillus*. Genes Dev. **6**:1770–1782.
54. **Mitchell, P. J., and R. Tjian.** 1989. Transcriptional regulation in mammalian cells by sequence-specific DNA binding proteins. Science **245**:371–378.
55. **Molenaar, C. M., L. P. Woudt, A. E. Jansen, W. H. Mager, R. J. Planta, D. M. Donovan, and N. J. Pearson.** 1984. Structure and organization of two linked ribosomal protein genes in yeast. Nucleic Acids Res. **12**:7345–7358.
56. **Nasmyth, K.** 1993. Control of the yeast cell cycle by the Cdc28 protein kinase. Curr. Opin. Cell Biol. **5**:166–179.
57. **Primig, M., S. Sockanathan, H. Auer, and K. Nasmyth.** 1992. Anatomy of a transcription factor important for the start of the cell cycle in *Saccharomyces cerevisiae*. Nature (London) **358**:593–597.
58. **Ramer, S. W., S. J. Elledge, and R. W. Davis.** 1992. Dominant genetics using a yeast genomic library under the control of a strong inducible promoter. Proc. Natl. Acad. Sci. USA **89**:11589–11593.
59. **Riles, L., J. E. Dutchik, A. Baktha, B. K. McCauley, E. C. Thayer, M. P. Leckie, V. V. Braden, J. E. Depke, and M. V. Olson.** 1993. Physical maps of the 6 smallest chromosomes of *Saccharomyces cerevisiae* at a resolution of 2.6-kilobase pairs. Genetics **134**:81–150.
60. **Riles, L., and M. Olson.** Personal communication.
61. **Rine, J.** 1991. Gene overexpression in studies of *Saccharomyces cerevisiae*. Methods Enzymol. **194**:239–251.
62. **Ruggieri, R., A. Bender, Y. Matsui, S. Powers, Y. Takai, J. R. Pringle, and K. Matsumoto.** 1992. *RSR1*, a *ras*-like gene homologous to *Krev-1* (*smg21A*/*rap1A*): role in the development of cell polarity and interactions with the Ras pathway in *Saccharomyces cerevisiae*. Mol. Cell. Biol. **12**:758–766.
63. **Sanders, S., and I. Herskowitz.** Personal communication.
64. **Sanger, F. S., S. Nicklen, and A. R. Coulson.** 1977. DNA sequencing with chain-terminating inhibitors. Proc. Natl. Acad. Sci. USA **74**:5463–5467.

65. **Scherr, G. H., and R. H. Weaver.** 1953. The dimorphism phenomenon in yeasts. Bacteriol. Rev. **17**:51–92.
66. **Schwob, E., and K. Nasmyth.** 1993. *CLB5* and *CLB6*, a new pair of B cyclins involved in DNA replication in *Saccharomyces cerevisiae*. Genes Dev. **7**:1160–1175.
67. **Shepherd, M. G.** 1988. Morphogenetic transformation of fungi. Curr. Top. Med. Mycol. **2**:278–304.
68. **Sherman, A., and G. R. Fink.** Unpublished data.
69. **Sherman, F., G. R. Fink, and J. Hicks.** 1986. Methods in yeast genetics. Cold Spring Harbor Laboratory Press, Cold Spring Harbor, N.Y.
70. **Siddiqui, A. H., and M. C. Brandriss.** 1988. A regulatory region responsible for proline-specific induction of the yeast *PUT2* gene is adjacent to its TATA box. Mol. Cell. Biol. **8**:4634–4641.
71. **Sikorski, R. S., and P. Hieter.** 1989. A system of shuttle vectors and yeast host strains designed for efficient manipulation of DNA in *Saccharomyces cerevisiae*. Genetics **122**:19–27.
72. **Sprague, G. F., and J. W. Thorner.** 1992. Pheromone response and signal transduction during the mating process of *Saccharomyces cerevisiae*, p. 657–744. *In* E. W. Jones, J. R. Pringle, and J. R. Broach (ed.), The molecular and cellular biology of the yeast *Saccharomyces*: gene expression. Cold Spring Harbor Laboratory Press, Cold Spring Harbor, N.Y.
73. **Stratagene.** 1991. Product catalog. Stratagene, La Jolla, Calif.
74. **Tanaka, K., K. Okazaki, N. Okazaki, T. Ueda, A. Sugiyama, H. Nojima, and H. Okayama.** 1992. A new *cdc* gene required for S phase entry of *Schizosaccharomyces pombe* encodes a protein similar to the cdc 10+ and SWI4 gene products. EMBO J. **11**:4923–4932.
75. **Timberlake, W. E.** 1990. Molecular genetics of *Aspergillus* development. Annu. Rev. Genet. **24**:5–36.
76. **Timberlake, W. E.** 1991. Temporal and spatial controls of *Aspergillus* development. Curr. Opin. Genet. Dev. **1**:351–357.
77. **Timberlake, W. E.** 1993. Molecular controls of conidiogenesis in *Aspergillus nidulans*, p. 13–22. *In* H. Vanden Bossche, F. C. Odds, and D. Kerridge (ed.), Dimorphic fungi in biology and medicine. Plenum, New York.
78. **Van Arsdell, S. W., G. L. Stetler, and J. Thorner.** 1987. The yeast repeated element sigma contains a hormone-inducible promoter. Mol. Cell. Biol. **7**:749–759.
79. **Vieira, J., and J. Messing.** 1987. Production of single-stranded plasmid DNA. Methods Enzymol. **153**:3–11.
80. **Wada, K., Y. Wada, F. Ishibashi, T. Gojobori, and T. Ikemura.** 1992. Codon usage tabulated from GenBank genetic sequence data. Nucleic Acids Res. **20**(Suppl.):2111–2118.
81. **Wilson, I. A., H. L. Niman, R. A. Houghton, A. R. Cherenson, M. L. Connolly, and R. A. Lerner.** 1984. The structure of an antigenic determinant in a protein. Cell **37**:767–778.
82. **Wright, R. M., T. Repine, and J. E. Repine.** 1993. Reversible pseudohyphal growth in haploid *Saccharomyces cerevisiae* is an aerobic process. Curr. Genet. **23**:388–391.

Chapter 5:

Isolation and Characterization of Genes Induced by *PHD1* Overexpression

Introduction

Chapter 4 of this thesis describes the isolation and characterization of *PHD1*, a *Saccharomyces cerevisiae* gene encoding a putative transcription factor that enhances pseudohyphal growth when overexpressed (Gimeno and Fink, 1994). In addition, overexpression of *PHD1* induces pseudohyphal growth in *MAT**a**/MAT*α strains growing on rich medium. The PHD1 protein is homologous to *Aspergillus nidulans* StuA, a regulator of two pseudohyphal growth-like cell divisions during conidiophore morphogenesis (Miller et al., 1991; Miller et al., 1992; Timberlake, 1991). PHD1 overexpression may enhance pseudohyphal growth by increasing the expression of genes that affect the pseudohyphal growth program, are important to the physiology of pseudohyphal cells, or both. Identification of these downstream target genes is important because they may be involved in pseudohyphal growth and give insights into the cellular function of PHD1.

A genetic screen identified 5 genes that are induced by *PHD1* overexpression. These 5 genes may be normally regulated by PHD1. Two of these genes are probably nonessential for yeast cell viability. One of these is a previously uncharacterized gene (*IPO1*) and the other is *DAL81*, a transcriptional regulator of nitrogen catabolic genes (Bricmont and Cooper, 1989; Bricmont et al., 1991; Coornaert et al., 1991). *MAT**a**/MAT*α strains homozygous for mutations in *IPO1* and *DAL81* likely to be null alleles undergo normal nitrogen starvation-induced pseudohyphal growth and also exhibit enhanced pseudohyphal growth when overexpressing *PHD1*. Interestingly, *DAL81* was found to be induced by nitrogen starvation conditions and by *RAS2*^{val19}, two conditions that induce pseudohyphal growth. These results raise the possibility that PHD1 may be involved in nitrogen metabolism.

Three of the *PHD1*-induced genes are essential for yeast cell viability. These 3 include two previously uncharacterized genes (*IPO2 and IPO3*) and *POL2*, encoding a DNA polymerase involved in chromosomal DNA replication and DNA repair (Budd and Campbell, 1993; Morrison et al., 1990; Wang et al., 1993). As discussed in the Results section, *IPO3* may be identical to the unpublished gene *CDC91*. Interestingly, *POL2* is regulated by MBP1, a transcription factor whose DNA binding domain is homologous the the DNA binding motif present in PHD1 (Araki et al., 1992; Gimeno and Fink, 1994; Johnston and Lowndes, 1992; Koch et al., 1993). MBP1 is an important cell cycle regulator because it induces *POL2* and a battery of other genes involved in DNA metabolism during the G1 to S phase transition in the cell cycle. PHD1 overexpression may inappropriately activate genes of the MBP1 regulon. However, if PHD1 normally regulates genes of the MBP1 regulon, this raises the interesting possibility that PHD1 may be involved in cell cycle regulation. This possibility is attractive because MBP1 regulates genes involved in morphogenesis and cell separation, two of the component processes of pseudohyphal growth (Dohrmann et al., 1992; Gimeno and Fink, 1994; Lew and Reed, 1993; Nasmyth, 1993).

Materials and Methods

Yeast Strains, Media, and Microbiological Techniques

Yeast strains are listed in Table 5.1. Standard yeast media including synthetic complete medium lacking uracil and leucine (SC-ura-leu) were prepared and yeast genetic manipulations were performed as described (Sherman et al., 1986). SC-ura-leu galactose medium is identical to SC-ura-leu medium except that it contains 2% weight per volume D-galactose (Sigma Grade, Sigma) as sole carbon source. For clarity, SC-ura medium is sometimes referred to as SC-ura glucose medium. 5-fluoroorotic acid (5-FOA) plates (Boeke et al., 1984) were SC plates with 1 mg/ml 5-FOA. SLAD medium was prepared as previously described (Gimeno and Fink, 1994). SLAG medium is identical to SLAD except that it contains 2% weight per volume D-galactose as sole carbon source. Yeast transformations were performed by standard protocols (Gietz et al., 1992; Ito et al., 1983). Genomic DNAs were isolated from yeast strains by a standard method (Hoffman and Winston, 1987).

Yeast Strain Construction

Construction of yeast strains is shown in tabular form (Table 5.1). All *S. cerevisiae* strains used in this study are congenic to the Σ1278b genetic background and are derived from MB758-5B (*MATa ura3-52*) (Siddiqui and Brandriss, 1988), MB1000 (*MATα*) (Brandriss and Magasanik, 1979), or both. The *leu2::hisG* auxotrophic marker was introduced into the Σ1278b background by using a previously described method and plasmid pNKY85

Table 5.1 Yeast Strain List

Strain Name[a]	Genotype	Derivation
CGX179	*MATa/MATα leu2::hisG/leu2::hisG ura3-52/ura3-52*	10480-6DX10480-2C
CG814	*MATa/MATα leu2::hisG/leu2::hisG ura3-52/ura3-52* (pCG70)	CGX179 + pCG70
CG824	*MATa/MATα leu2::hisG/leu2::hisG ura3-52/ura3-52* (pRS315 and pRS316)	CGX179 + pRS315 and pRS316
CG930	*MATa/MATα leu2::hisG/leu2::hisG ura3-52/ura3-52* (pRS315 and pCG38)	CGX179 + pRS315 and pCG38
GL4	*MATa/MATα IPO1-lacZ::LEU2/IPO1 leu2::hisG/leu2::hisG ura3-52/ura3-52* (pCG70)	CG814 derivative
GL53	*MATa/MATα POL2-lacZ::LEU2/POL2 leu2::hisG/ leu2::hisG ura3-52/ura3-52* (pCG70)	CG814 derivative
GL74	*MATa/MATα IPO2-lacZ::LEU2/IPO2 leu2::hisG/leu2::hisG ura3-52/ura3-52* (pCG70)	CG814 derivative
GL78	*MATa/MATα DAL81-lacZ::LEU2/DAL81 leu2::hisG/ leu2::hisG ura3-52/ura3-52* (pCG70)	CG814 derivative
GL123	*MATa/MATα IPO3-lacZ::LEU2/IPO3 leu2::hisG/leu2::hisG ura3-52/ura3-52* (pCG70)	CG814 derivative
GLE4	*MATa/MATα IPO1-lacZ::LEU2/IPO1 leu2::hisG/leu2::hisG ura3-52/ura3-52*	GL4 derivative
GLE53	*MATa/MATα POL2-lacZ::LEU2/POL2 leu2::hisG/ leu2::hisG ura3-52/ura3-52*	GL53 derivative
GLE74	*MATa/MATα IPO2-lacZ::LEU2/IPO2 leu2::hisG/leu2::hisG ura3-52/ura3-52*	GL74 derivative

GLE78	*MATa/MATα DAL81-lacZ::LEU2/DAL81 leu2::hisG/ leu2::hisG ura3-52/ura3-52*	GL78 derivative
GLE123	*MATa/MATα IPO3-lacZ::LEU2/IPO3 leu2::hisG/leu2::hisG ura3-52/ura3-52*	GL123 derivative
CG858	*MATa/MATα IPO1-lacZ::LEU2/IPO1 leu2::hisG/leu2::hisG ura3-52/ura3-52* (pDAD2)	GLE4 transformant
CG859	*MATa/MATα IPO1-lacZ::LEU2/IPO1 leu2::hisG/leu2::hisG ura3-52/ura3-52* (pCG70)	GLE4 transformant
CG898	*MATa/MATα POL2-lacZ::LEU2/POL2 leu2::hisG/ leu2::hisG ura3-52/ura3-52* (pDAD2)	GLE53 transformant
CG899	*MATa/MATα POL2-lacZ::LEU2/POL2 leu2::hisG/ leu2::hisG ura3-52/ura3-52* (pCG70)	GLE53 transformant
CG904	*MATa/MATα IPO2-lacZ::LEU2/IPO2 leu2::hisG/leu2::hisG ura3-52/ura3-52* (pDAD2)	GLE74 transformant
CG905	*MATa/MATα IPO2-lacZ::LEU2/IPO2 leu2::hisG/leu2::hisG ura3-52/ura3-52* (pCG70)	GLE74 transformant
CG886	*MATa/MATα DAL81-lacZ::LEU2/DAL81 leu2::hisG/ leu2::hisG ura3-52/ura3-52* (pDAD2)	GLE78 transformant
CG887	*MATa/MATα DAL81-lacZ::LEU2/DAL81 leu2::hisG/ leu2::hisG ura3-52/ura3-52* (pCG70)	GLE78 transformant
CG892	*MATa/MATα IPO3-lacZ::LEU2/IPO3 leu2::hisG/leu2::hisG ura3-52/ura3-52* (pDAD2)	GL123 transformant
CG893	*MATa/MATα IPO3-lacZ::LEU2/IPO3 leu2::hisG/leu2::hisG ura3-52/ura3-52* (pCG70)	GL123 transformant
CJ3	*MATa/MATα DAL81-lacZ::LEU2/DAL81 leu2::hisG/ leu2::hisG ura3-52/ura3-52* (YCpR2V)	GLE78 transformant
CG878	*MATa IPO1-lacZ::LEU2 leu2::hisG ura3-52*	GLE4 ascospore

CG879	*MATα IPO1-lacZ::LEU2 leu2::hisG ura3-52*	GLE4 ascospore
CGX184	*MATa/MATα IPO1-lacZ::LEU2/IPO1-lacZ::LEU2 leu2::hisG/leu2::hisG ura3-52/ura3-52*	CG878XCG879
CG926	*MATa/MATα IPO1-lacZ::LEU2/IPO1-lacZ::LEU2 leu2::hisG/leu2::hisG ura3-52/ura3-52* (pRS316)	CGX184 transformant
CG928	*MATa/MATα IPO1-lacZ::LEU2/IPO1-lacZ::LEU2 leu2::hisG/leu2::hisG ura3-52/ura3-52* (pCG38)	CGX184 transformant
CG909	*MATa DAL81-lacZ::LEU2 leu2::hisG ura3-52*	GLE78 ascospore
CG911	*MATα DAL81-lacZ::LEU2 leu2::hisG ura3-52*	GLE78 ascospore
CGX190	*MATa/MATα DAL81-lacZ::LEU2/DAL81-lacZ::LEU2 leu2::hisG/leu2::hisG ura3-52/ura3-52*	CG909XCG911
CG927	*MATa/MATα DAL81-lacZ::LEU2/DAL81-lacZ::LEU2 leu2::hisG/leu2::hisG ura3-52/ura3-52* (pRS316)	CGX190 transformant
CG929	*MATa/MATα DAL81-lacZ::LEU2/DAL81-lacZ::LEU2 leu2::hisG/leu2::hisG ura3-52/ura3-52* (pCG38)	CGX190 transformant

[a] All strains are congenic to the ∑1278b genetic background.

(Alani et al., 1987). Derivatives of GL4, GL53, GL74, GL78, and GL123 lacking pCG70 were isolated in the following way. Patches of cells of these 5 strains were grown for 2 days at 30°C on nonselective rich YPAD medium. Cells from the patches were then streaked to obtain single cells on YPAD plates. After 2 days of growth at 30°C, the streakouts were replica plated to SC-ura medium. Strains derived from segregants that had lost *URA3*-marked pCG70 did not grow on this medium and were isolated from the YPAD master plate. These strains were named GLE4, GLE53, GLE74, GLE78, and GLE123.

Qualitative Pseudohyphal Growth Assay

This assay was performed as described previously (Gimeno and Fink, 1994). In those experiments where transformants were studied, two independent transformants were assayed. In the experiments reported here, the pairs of transformants always had the same phenotype.

Light Microscopic Techniques

These techniques have been described in detail elsewhere (Gimeno et al., 1992).

Plasmid Construction

Recombinant DNA methods were performed using established protocols (Maniatis et al., 1982). Plasmids used in this study are listed in Table 5.2. The DNA immediately adjacent to *lacZ* in the 5 *PHD1* inducible fusion genes was cloned essentially as described by M. Snyder (Snyder, 1994). First, GLE4,

Table 5.2 Plasmid List

Plasmid Name	Description	Source or Derivation
pCG19	*PHD1* 2μm overexpression plasmid	(Gimeno and Fink, 1994)
pCG38	*PHD1* 2μm overexpression plasmid	(Gimeno and Fink, 1994)
pDAD2	*URA3*-marked 2μm *GAL1-10* promoter vector	(Pellman et al., 1994)
pNKY85	*LEU2* disruption vector	(Alani et al., 1987)
pRS202	*URA3*-marked 2μm vector	(Connelly and Hieter, 1994)
pRS315	*LEU2*-marked *CEN* vector	(Sikorski and Hieter, 1989)
pRS316	*URA3*-marked *CEN* vector	(Sikorski and Hieter, 1989)
pBluescriptII SK+	*E. coli* cloning vector	(Stratagene, 1991)
pCG70	*GAL1-10-PHD1* in pDAD2	This study
pCG80	*IPO1* fragment in YIp5 derivative	This study
pCG85	*POL2* fragment in YIp5 derivative	This study
pCG88	*IPO2* fragment in YIp5 derivative	This study
pCG90	*DAL81* fragment in YIP5 derivative	This study
pCG91	*IPO3* fragment in YIp5 derivative	This study
pCG93	NsiI-SalI fragment of pCG85 in PstI-SalI digested pBluescriptII SK+	This study
pCG94	NsiI-SalI fragment of pCG91 in PstI-SalI digested pBluescriptII SK+	This study
pCG95	NsiI-SalI fragment of pCG80 in PstI-SalI digested pBluescriptII SK+	This study
pCG96	NsiI-SalI fragment of pCG88 in PstI-SalI digested pBluescriptII SK+	This study

pCG97	NsiI-SalI fragment of pCG90 in PstI-SalI digested pBluescriptII SK+	This study
YCpR2V	*URA3*-marked *RAS2*^{val19} vector	(Gimeno et al., 1992)
YIp5	*URA3*-marked integrative vector	(Struhl et al., 1979)

GLE53, GLE74, GLE78, and GLE123 were transformed with PvuI disgested YIp5 which integrates into the transposon at the ampicillin-resistance gene. Genomic DNA of these transformants was prepared as described by Hoffman and Winston (Hoffman and Winston, 1987) and digested with NsiI to release a linear fragment containing the bacterial origin of DNA replication, *lacZ*, and a fragment of the *S. cerevisiae* DNA that is fused to *lacZ*. NsiI-digested genomic DNA was circularized in a dilute ligation reaction and transformed into *E. coli*. The 5 plasmids derived in this manner are pCG80, pCG85, pCG88, pCG90, and pCG91. NsiI-SalI digestion of these 5 plasmids liberates one DNA fragment that contains the recovered *S. cerevisiae* genomic DNA fragment fused to *lacZ* and another DNA fragment containing the vector backbone. The NsiI-SalI fragments containing the yeast DNA and *lacZ* from pCG80, pCG85, pCG88, pCG90, and pCG91 were subcloned into PstI-SalI digested pBluesciptII SK+ for more facile analysis (pCG93-pCG97).

DNA Sequencing

Double stranded DNA was prepared by the method of Haltiner et al. (Haltiner et al., 1985) and sequenced by the dideoxy chain termination method of Sanger et al. (Sanger et al., 1977). The *lacZ*-fusion junctions of the 5 *PHD1* inducible genes were sequenced using oligonucleotide primer ZLP (5'-CGTTGTAAAACGACGGGATCCCC) which is complementary to sequences in the transposon. Plasmids pCG93-pCG97 were the template DNAs in these sequencing reactions. Protein and DNA homology searches were performed at the National Center for Biotechnology Information using the BLAST network service (Altschul et al., 1990).

Construction of a Plasmid Containing *PHD1* Under the Control of the *GAL1-10* Promoter

A *GAL1-10-PHD1* plasmid was constructed using PCR. Primers were designed to allow the amplification and subcloning of the 1.1 kb *PHD1* open reading frame (Gimeno and Fink, 1994) into pDAD2, a *GAL1-10* promoter and *PHO5* terminator containing 2μm based *URA3* marked plasmid. pDAD2 was constructed in the same way as pDAD1 except that the polylinker is in the opposite orientation (Davis and Fink, 1990). Oligonucleotide PCR1 (5'-AGGGAATTCATGTACCATGTTCCTGAAATGAGGC) has the hexanucleotide sequence recognized by EcoRI after the first 3 nucleotides and then 25 bases identical to the first 25 nucleotides of the *PHD1* open reading frame. Oligonucleotide PCR2 (5'-AGGGGATCCTTGTTCATAGA GCAAAGAGTTAACGG) was synthesized, which has the hexanucleotide sequence recognized by BamHI after the first 3 nucleotides followed by 26 bases complementary to nucleotides 1841 to 1816 in the *PHD1* sequence reported previously (Gimeno and Fink, 1994) which occur shortly after the end of the *PHD1* open reading frame. PCR1 and PCR2 were used to prime a PCR using pCG19 as template and $Vent_R$ DNA polymerase (NEB, Inc.). The amplified 1.1 kb fragment was digested with EcoRI and BamHI and ligated into EcoRI-BamHI digested pDAD2. pCG70 was constructed in this manner. *MAT**a**/MAT*α strains carrying pCG70 and growing on nitrogen starvation galactose medium (SLAG) undergo dramatically enhanced pseudohyphal growth.

ß-Galactosidase Assays

The filter disk ß-galactosidase (ß-gal) assay was performed essentially as previously described (Brill et al., 1994). Briefly, strains to be tested were grown as patches of cells on appropriate medium dictated by the experiment at 30°C overnight. The patches of cells were then replica plated to Whatman #50 paper disks (Schleicher & Schuell, #576) that had been placed on the test medium in the petri dishes. After growth overnight at 30°C, the paper disks were removed from the plates and the cells on them were permeabilized by immediately immersing them in liquid nitrogen for 30 seconds. After this treatment, the paper disks were thawed at room temperature for 20 seconds and then placed in petri dishes that contained a disk of Whatman #3 paper (Schleicher & Schuell, #593) saturated with 2.5 ml of Z buffer containing 37 μl of 2% weight per volume of the chromogenic ß-gal substrate 5-bromo-4-chloro-3-indolyl-ß-D-galactoside (X-gal). The permeabilized strains on the paper disks were incubated at 30°C and inspected at timed intervals for the blue color diagnostic of ß-gal activity in this assay. The assay was stopped by removing the paper disk containing the patches of cells and air drying it. In those experiments where transformants were studied, two independent transformants were assayed. In the experiments reported here, the pairs of transformants always had the same phenotype.

Results

A Genetic Screen Identifies Genes Induced by *PHD1* Overexpression

We carried out a screen (called IPO for Induced by PHD1 Overexpression) for genes that are induced by overexpression of the putative transcription factor PHD1. First, a 2μm (high copy number) plasmid containing *PHD1* under the control of the *GAL1-10* promoter was constructed (pCG70). A Σ1278b *MAT**a**/MATα leu2::hisG/leu2::hisG ura3-52/ura3-52* diploid strain carrying this plasmid was then generated (CG814). In CG814, *PHD1* expression is repressed when glucose is the sole carbon source and induced when galactose is the sole carbon source.

The logic of the IPO screen was to identify genes that are induced when CG814 is grown on galactose, and in this way identify genes that are induced by *PHD1* overexpression (Fig. 5.1). The protocol began by transforming CG814 with a *S. cerevisiae* genomic library that had been mutagenized in *E. coli* with a mini-Tn3::*LEU2* transposon in which one of the transposon's 38-base pair terminal repeats extends in frame into *lacZ*. In this transposon, *lacZ* lacks both an initiator ATG codon and a promoter so *lacZ* expression in yeast only occurs when the transposon resides in frame in a gene (Snyder, 1994). Because Σ1278b strains have a low transformation efficiency, it was necessary to use a high efficiency transformation protocol (Gietz et al., 1992). A total of 70,000 transformants were selected on 100 9-cm-diameter SC-ura-leu plates at a density of 700 transformants per plate. After 2 days of growth at 30°C, transformants were replica plated to paper disks on both SC-ura-leu glucose plates and paper disks on SC-ura-leu galactose plates. These 200 plates were incubated at 30°C overnight and then their paper disks, on which

Figure 5.1 IPO screen. A *MAT**a**/MAT*α diploid *S. cerevisiae* strain carrying a *GAL1-10-PHD1* construct, which is repressed by glucose and induced by galactose, was transformed with an integrative library of random *lacZ*-fusions to yeast genes. Transformants were selected on SC-ura-leu glucose medium at a density of 700 colonies per plate. Transformants were replica plated to paper disks on selective SC glucose and SC galactose plates and grown overnight. The paper disks were then processed for paper disk ß-gal assays. The colonies on the processed paper disks were examined visually for colonies that had turned blue on the SC galactose plates but not on the SC glucose plates. 5 of the colonies identified in this way contained *PHD1*-inducible *lacZ*-fusion genes.

TRANSFORM DIPLOID
GAL1-PHD1 STRAIN
WITH INTEGRATIVE
lacZ-FUSION LIBRARY

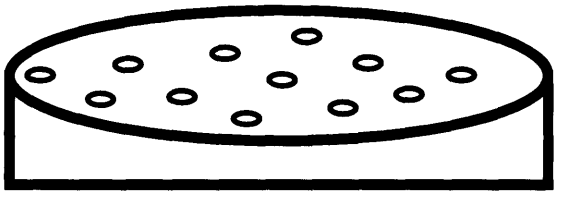

SELECTIVE GLUCOSE MEDIUM

REPLICA PLATE

VISUALLY SCREEN FOR
COLONIES WHICH ARE
BLUE ON GALACTOSE
AND WHITE ON GLUCOSE

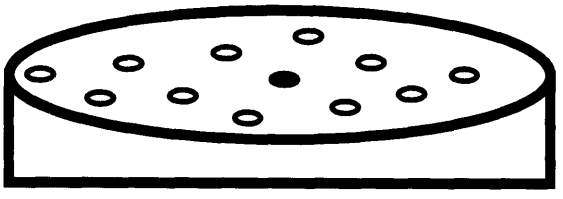

SELECTIVE GALACTOSE MEDIUM

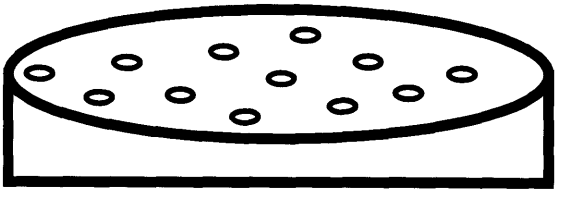

SELECTIVE GLUCOSE MEDIUM

the transformant colonies had grown, were removed and processed for paper disk ß-gal assays.

The colonies were assayed by incubation in ß-gal assay buffer containing X-gal at room temperature for 2 hours to 3 days and examined visually to identify those that had turned blue, an indication that they were expressing ß-gal. About 70 colonies out of the 700 on each filter were blue. Cells from 178 fusion gene containing strains that appeared to express more ß-gal when grown on galactose than when grown on glucose were isolated directly from the processed paper disks.

These 178 strains were rescreened by the paper disk ß-gal assay after growth as patches on SC-ura-leu glucose and SC-ura-leu galactose plates. Of these strains, 141 were found to contain fusion genes that were either not induced or weakly induced by galactose and these strains were not characterized further. The remaining 37 candidate strains were patched on nonselective YPAD medium, grown overnight at 30°C, and streaked to obtain single cells on 5-FOA plates to select for strains that had lost the *PHD1*-containing *URA3*-marked plasmid pCG70. Cells from colonies growing on 5-FOA plates were screened by the paper disk ß-gal assay after 2 days of growth at 30°C as patches on SC-leu glucose and SC-leu galactose plates. Of these strains, 30 contained fusion genes that were induced by galactose and these strains were classified as containing galactose-inducible but *PHD1*-independent fusion genes and were not characterized further. The remaining 7 candidate strains were patched on nonselective YPAD medium, grown for 2 days at 30° C, and streaked to obtain single cells on YPAD plates. The resulting colonies were replica plated to SC-leu plates and the 2 strains that segregated Leu^- clones were classified as containing unstable fusion genes and not characterized further.

The remaining 5 strains (GL4, GL53, GL74, GL78, and GL123) contained fusion genes that were induced by galactose in a pCG70-dependent fashion and were subjected to one final experiment. Derivatives of these 5 strains lacking plasmid pCG70 were isolated (GLE4, GLE53, GLE74, GLE78, and GLE123) and retransformed with pCG70 and pDAD2 (the vector backbone of pCG70 that has no insert). The resulting 10 strains were assayed by the paper disk ß-gal assay after overnight growth at 30°C as patches on SC-ura glucose and SC-ura galactose plates (Fig. 5.2). The fusion genes in the 5 strains carrying pDAD2 were not inducible by galactose whereas the fusion genes in the 5 strains carrying pCG70 were galactose-inducible. Thus, the 5 fusion genes were shown to be galactose-inducible in a *PHD1*-dependent fashion.

Sequence Analysis of the 5 *PHD1*-Inducible Fusion Genes

To obtain information about the functions and identities of the 5 *PHD1*-inducible fusion genes, I cloned and sequenced the DNA immediately adjacent to *lacZ*. Two of the fusions were to known genes, *POL2* encoding a DNA polymerase (Budd and Campbell, 1993; Morrison et al., 1990; Wang et al., 1993) and *DAL81* encoding a positive transcriptional regulator of genes involved in the catabolism of several nitrogen sources (Bricmont and Cooper, 1989; Bricmont et al., 1991; Coornaert et al., 1991). The fusion to *POL2* was at nucleotide 2176 (Morrison et al., 1990) while the fusion to *DAL81* was at nucleotide 2948 (Coornaert et al., 1991). Only 20 base pairs of yeast DNA from the *IPO3-lacZ* fusion gene were recovered from the genome. Interestingly, 19/20 of these base pairs are identical to the sequence of bases 3396-3415 of the *CDC91* gene (Genbank accession number L31649). This

Figure 5.2 Regulation of *PHD1*-inducible genes. The 5 *MATa/MATα* strains that have *PHD1*-inducible *lacZ*-fusion genes (GLE4 with *IPO1-lacZ*, GLE53 with *POL2-lacZ*, GLE74 with *IPO2-lacZ*, GLE78 with *DAL81-lacZ*, and GLE123 with *IPO3-lacZ*) were transformed with the *GAL1-10-PHD1* plasmid pCG70 (CG859, CG899, CG905, CG887, and CG893) and with the control plasmid pDAD2 (CG858, CG898, CG904, CG886, and CG892). These 10 transformed strains were patched onto a SC-ura plate (A) and grown at 30°C for 18.5 hours and then replica plated to paper disks on SC-ura glucose (B) and SC-ura galactose plates (C). Replica plated strains were grown for 23.5 hours, subjected to the paper disk ß-gal assay, and developed at 30°C for 5 hours. GLE53 was transformed with the activated *RAS2* (*RAS2*^{val19}) plasmid YCpR2V (CJ3) and a control plasmid (CG886). These two strains were patched onto a SC-ura glucose plate (D) and grown at 30°C for 18.5 hours and then replica plated to paper disks on SC-U glucose (E) and nitrogen starvation (SLAD) (F) plates. Strains that had been replica plated were grown for 23.5 hours, subjected to the paper disk ß-gal assay, and developed at 30°C for 5 hours.

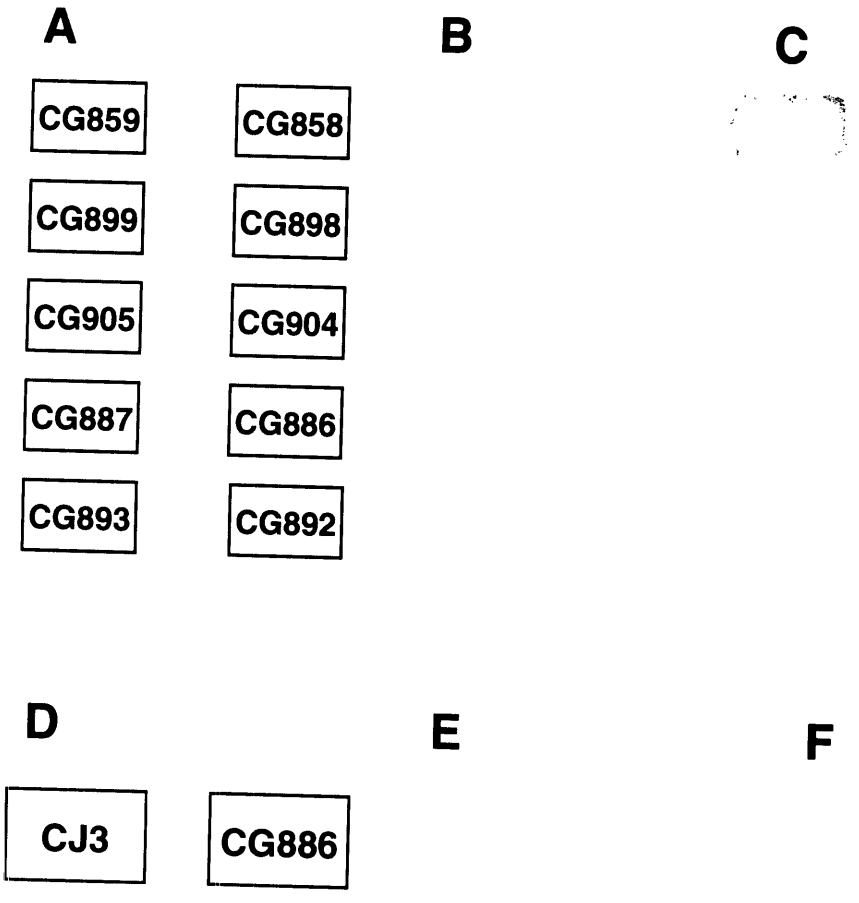
A
B
C
CG859
CG858
CG899
CG898
CG905
CG904
CG887
CG886
CG893
CG892
D
E
F
CJ3
CG886

means that *IPO3* may be identical to *CDC91*. This unpublished gene is essential for yeast cell viability and encodes a 394 amino acid protein that is not significantly related to known proteins. *CDC91* has a perfect MBP1 binding site about 460 base pairs upstream of its initiator ATG codon, suggesting that it may be under MBP1 control. MBP1 is a transcriptional regulator of a battery of genes involved in S phase and has a DNA binding domain that is related to the DNA binding motif present in PHD1. Interestingly, *POL2* also has an MBP1 binding site in its promoter and is known to be a target of MBP1 (Araki et al., 1992). These results suggest that PHD1 may be able to activate transcription via MBP1 binding sites as proposed previously (Gimeno and Fink, 1994). Sequencing of fragments of the other 2 *PHD1*-inducible yeast genes revealed that they had not been previously characterized. DNA sequence tags of these 2 novel genes are listed (Table 5.3). These 2 novel genes were named *IPO1* and *IPO2*.

Analysis of Strains Carrying Disruptions of *PHD1*-Inducible Genes

The 5 transformants containing *PHD1*-inducible *lacZ* fusions are heterozygous for insertion mutations in these genes. After I segregated off the pCG70 plasmid, the resulting strains from each of these 5 transformants were sporulated and subjected to tetrad analysis (10 tetrads each). The haploid ascospore segregants that had received the disrupted genes could be identified because they were $Leu2^+$ (the transposon carries *LEU2*) and produced ß-gal activity detectable in the paper disk ß-gal assay. As expected, disruption of *POL2* was lethal (lethality segregated 2:2 in the cross and viable spores were always $Leu2^-$ and never produced ß-gal activity). As previously reported, disruption of *DAL81* was not lethal but caused slow growth on plates

Table 5.3 DNA sequence tags of *IPO1* and *IPO2*

pCG95-ZLP	5' agatcggggttctttgagaaaagcatcataccagcgaat
IPO1	
pCG96-ZLP	5' aataccacgttctgtcagcttacctgtcgatattggg
IPO2	ttactttgtagtgcattatttccatcaatattagcagtgtc

DNA sequence tags of the *IPO1* and *IPO2* genes determined using pCG95 and pCG96 as templates and primer ZLP are shown.

where allantoin was the sole nitrogen source. This phenotype occurs because *DAL81* is required for the induction of the enzymes that catabolize allantoin. Disruption of *IPO1* was not lethal whereas disruption of *IPO2* and *IPO3* was lethal.

Analysis of Pseudohyphal Growth in Strains that Have Disruption Alleles of *IPO1* and *DAL81*

*MAT**a**/MAT*α diploid strains homozygous for disruption alleles of *IPO1* (CGX184) and *DAL81* (CGX190)were constructed. The *DAL81-lacZ* allele is a partial loss of function allele because, as expected for *dal81* mutants (Bricmont and Cooper, 1989), *DAL81-lacZ* strains grow more slowly on a medium where allantoin is the sole nitrogen source than do wild-type strains. CGX184 and CGX190 were made prototrophic by transformation with the *URA3*-marked centromeric plasmid pRS316 resulting in CG926 and CG927, respectively. CG926, CG927, and the wild-type control strain CG824 were grown on nitrogen starvation medium (SLAD) for 46 hours at 30°C and observed to undergo similar levels of pseudohyphal growth. CGX184 and CGX190 were then transformed with the *PHD1*-overexpression plasmid pCG38 creating CG928 and CG929, respectively. CG928, CG929, and a *PHD1*-overexpressing wild-type control strain, CG930, were grown on nitrogen starvation medium (SLAD) for 46 hours at 30°C and observed to undergo similar enhanced pseudohyphal growth. The qualitative pseudohyphal growth assays performed in this section were carried out as described in Materials and Methods.

Analysis of *DAL81* Regulation

As a secondary screen it was determined if any of the 5 fusion genes were induced by nitrogen starvation, the signal that induces pseudohyphal growth. GLE4, GLE53, GLE74, GLE78, and GLE123 were transformed with pRS316, a *URA3* marked centromeric plasmid, and the resulting 5 transformed strains (CG862, CG901, CG907, CG889, and CG895) were patched on a SC-ura-leu plate. After growth at 30°C overnight, the 5 strains were replica plated to paper disks on SC-ura-leu and nitrogen starvation (SLAD) plates. These 2 plates were incubated at 30°C overnight and then the paper disks were removed and processes for the paper disk ß-gal assay. The *DAL81* gene fusion to *lacZ* was clearly induced by nitrogen starvation (SLAD) medium (Figs. 5.2E and 5.2F). *IPO1* appeared to be moderately induced by SLAD medium.

I then determined whether the $RAS2^{val19}$ mutation that induces pseudohyphal growth (Gimeno et al., 1992) could induce expression of *DAL81-lacZ*. GLE78 was transformed with a $RAS2^{val19}$ plasmid (YCpR2V) giving rise to CJ3. The expression of *DAL81-lacZ* in CJ3 and in a wild-type *DAL81-lacZ* strain (CG886) grown on both rich SC-ura medium and nitrogen starvation (SLAD) medium was determined (Figs. 5.2E and 5.2F). $RAS2^{val19}$ did not affect the expression of *DAL81-lacZ* on SC-ura medium. However, $RAS2^{val19}$ dramatically induces *DAL81-lacZ* on SLAD medium. Thus, $RAS2^{val19}$ induces *DAL81-lacZ* in a nitrogen starvation-dependent manner.

Discussion

PHD1 Overexpression Induces *POL2*

It is very interesting that *PHD1* overexpression induces *POL2* because this gene is regulated by MBP1 (Araki et al., 1992). MBP1 is a cell cycle-regulatory transcription factor that induces S phase-specific genes (Johnston and Lowndes, 1992; Koch et al., 1993). The DNA binding domain of MBP1 is related to the PHD1 DNA binding motif suggesting that these two proteins may bind to the same or related DNA sequences and thus regulate the same genes (Gimeno and Fink, 1994). This connection also raises the possibility that PHD1 may have a role in cell cycle regulation, an attractive idea because MBP1 regulates genes involved in morphogenesis and cell separation, two of the component processes of pseudohyphal growth (Dohrmann et al., 1992; Gimeno and Fink, 1994; Lew and Reed, 1993; Nasmyth, 1993). This issue is discussed in more detail in Chapter 4. Alternatively, PHD1 may not normally control MBP1-regulated genes: in this case PHD1 overexpression would fortuitously activates genes of the MBP1 regulon because the DNA binding motif present in PHD1 is similar to the MBP1 DNA binding domain.

PHD1 Overexpression Induces *DAL81*

DAL81 is required for the induced expression of genes encoding enzymes that catabolize allantoin, 4-aminobutyric acid, arginine, and urea (Coornaert et al., 1991). These enzymes are induced when yeast cells exhaust their preferred nitrogen sources and then begin to utilize poor nitrogen sources. *DAL81* is also induced by three different pseudohyphal growth activating

conditions, *PHD1* overexpression, nitrogen starvation and *RAS2^{val19}*. These results raise the possibility that PHD1 may be involved in the transduction of the nitrogen starvation signal, the *RAS2^{val19}* signal, or both to *DAL81*.

The loss of function *DAL81-lacZ* allele affects neither nitrogen starvation induced pseudohyphal growth nor *PHD1*-overexpression enhanced pseudohyphal growth. These results should be interpreted with caution because the *DAL81-lacZ* allele may not be a null allele and are most easily explained by postulating that *DAL81* is not required for cell elongation, agar invasion, or incomplete cell separation. In this model, *DAL81* is required for pseudohyphal cells to express the nitrogen catabolic enzymes that enable them to utilize the poor nitrogen sources they are likely to encounter while foraging. If *PHD1* directly regulates pseudohyphal growth and *DAL81*, and *DAL81* is only required for nitrogen catabolic enzyme induction in pseudohyphal cells, then there must be other *PHD1* targets that are involved in cell elongation, agar invasion, and incomplete cell separation. The identification of *IPO* genes whose disruption blocks pseudohyphal growth would support the idea that *PHD1* plays a direct role in pseudohyphal growth control.

Conclusions

The IPO screen identified 5 genes that are induced by *PHD1* overexpression. These genes may or may not be normally regulated by *PHD1*. The IPO screen is clearly not saturated and many more *PHD1*-induced genes could be readily isolated with it. The work in this chapter raises the interesting possibilities that *PHD1* may be involved in cell cycle regulation and nitrogen metabolism, two processes that have obvious connections to pseudohyphal growth. The work in this chapter also raises the possibility that PHD1 may bind

to the MBP1 binding site which is called a MluI cell cycle box (Nasmyth, 1993) or to a related DNA sequence. This hypothesis could be tested with standard transcription factor biochemistry experiments.

Literature Cited

Alani, E., Cao, L., and Kleckner, N. (1987). A method for gene disruption that allows repeated use of *URA3* selection in the construction of multiply disrupted yeast strains. Genetics *116,* 541-545.

Altschul, S. F., Gish, W., Miller, W., Myers, E. W., and Lipman, D. J. (1990). Basic local alignment search tool. J. Mol. Biol. *215,* 403-410.

Araki, H., Ropp, P. A., Johnson, A. L., Johnston, L. H., Morrison, A., and Sugino, A. (1992). DNA polymerase II, the probable homolog of mammalian DNA polymerase ε, replicates chromosomal DNA in the yeast *Saccharomyces cerevisiae*. EMBO J. *11,* 733-740.

Boeke, J., Lacroute, F., and Fink, G. R. (1984). A positive selection for mutants lacking orotidine-5' phosphate decarboxylase activity in yeast: 5-fluoro-orotic acid resistance. Mol. Gen. Genet. *197,* 345-346.

Brandriss, M. C., and Magasanik, B. (1979). Genetics and physiology of proline utilization in *Saccharomyces cerevisiae*: enzyme induction by proline. J. Bacteriol. *140,* 498-503.

Bricmont, P. A., and Cooper, T. G. (1989). A gene product needed for induction of allantoin system genes in *Saccharomyces cerevisiae* but not for their transcriptional activation. Mol. Cell. Biol. *9,* 3869-3877.

Bricmont, P. A., Daugherty, J. R., and Cooper, T. G. (1991). The *DAL81* gene product is required for induced expression of two differently regulated nitrogen catabolic genes in *Saccharomyces cerevisiae*. Mol. Cell. Biol. *11,* 1161-1166.

Brill, J. A., Elion, E. A., and Fink, G. R. (1994). A role for autophosphorylation revealed by activated alleles of *FUS3*, the yeast MAP kinase homolog. Mol. Biol. Cell *5,* 297-312.

Budd, M. E., and Campbell, J. L. (1993). DNA polymerases ∂ and ε are required for chromosomal replication in *Saccharomyces cerevisiae*. Mol. Cell. Biol. *13,* 496-505.

Connelly, C., and Hieter, P. (1994). Personal communication.

Coornaert, D., Vissers, S., and André, B. (1991). The pleiotropic *UGA35* (*DURL*) regulatory gene of *Saccharomyces cerevisiae*: cloning, sequence, and identity with the *DAL81* gene. Gene *97,* 163-171.

Davis, L. I., and Fink, G. R. (1990). The *NUP1* gene encodes an essential component of the yeast nuclear pore complex. Cell *61,* 965-978.

Dohrmann, P. R., Butler, G., Tamai, K., Dorland, S., Greene, J. R., Thiele, D. J., and Stillman, D. J. (1992). Parallel pathways of gene regulation: homologous regulators *SWI5* and *ACE2* differentially control transcription of *HO* and chitinase. Genes Dev. *6,* 93-104.

Gietz, D., St. Jean, J. A., Woods, R. A., and Schiestl, R. H. (1992). Improved method for high efficiency transformation of intact yeast cells. Nucleic Acids Res. *20,* 1425.

Gimeno, C. J., and Fink, G. R. (1994). Induction of pseudohyphal growth by overexpression of *PHD1*, a *Saccharomyces cerevisiae* gene related to transcriptional regulators of fungal development. Mol. Cell. Biol. *14,* 2100-2112.

Gimeno, C. J., Ljungdahl, P. O., Styles, C. A., and Fink, G. R. (1992). Unipolar cell divisions in the yeast *S. cerevisiae* lead to filamentous growth: regulation by starvation and *RAS*. Cell *68,* 1077-1090.

Haltiner, M., Kempe, T., and Tjian, R. (1985). A novel strategy for constructing clustered point mutations. Nucleic Acids Res. *13,* 1015-1025.

Hoffman, C. S., and Winston, F. (1987). A ten-minute DNA preparation from yeast efficiently releases autonomous plasmids for transformation of *Escherichia coli*. Gene *57,* 267-272.

Ito, H., Fukuda, Y., Murata, K., and Kimura, A. (1983). Transformation of intact yeast cells treated with alkali cations. J. Bacteriol. *153,* 163-168.

Johnston, L. H., and Lowndes, N. F. (1992). Cell cycle control of DNA synthesis in budding yeast. Nucleic Acids Res *20,* 2403-2410.

Koch, C., Moll, T., Neuberg, M., Ahorn, H., and Nasmyth, K. (1993). A role for the transcription factors Mbp1 and Swi4 in progression from G1 to S phase. Science *261,* 1551-1557.

Lew, D. J., and Reed, S. I. (1993). Morphogenesis in the yeast cell cycle: regulation by Cdc28 and cyclins. J. Cell. Biol. *120,* 1305-1320.

Maniatis, T., Fritsch, E. F., and Sambrook, J. (1982). Molecular Cloning. (Cold Spring Harbor, New York: Cold Spring Harbor Laboratory Press).

Miller, K. Y., Toennis, T. M., Adams, T. H., and Miller, B. L. (1991). Isolation and transcriptional characterization of a morphological modifier: the *Aspergillus nidulans* stunted (*stuA*) gene. Mol. Gen. Genet. *227,* 285-292.

Miller, K. Y., Wu, J., and Miller, B. L. (1992). *StuA* is required for cell pattern formation in *Aspergillus*. Genes Dev. *6,* 1770-1782.

Morrison, A., Araki, H., Clark, A. B., Hamatake, R. K., and Sugino, A. (1990). A third essential DNA polymerase in *S. cerevisiae*. Cell *62,* 1143-1151.

Nasmyth, K. (1993). Control of the yeast cell cycle by the Cdc28 protein kinase. Curr. Opin. Cell Biol. *5,* 166-179.

Pellman, D., Miller, D., and Fink, G. R. (1994). Personal communication.

Sanger, F. S., Nicklen, S., and Coulson, A. R. (1977). DNA sequencing with chain-terminating inhibitors. Proc. Natl. Acad. Sci. USA *74,* 5463-5467.

Sherman, F., Fink, G. R., and Hicks, J. (1986). Methods in Yeast Genetics. (Cold Spring Harbor, New York: Cold Spring Harbor Laboratory Press).

Siddiqui, A. H., and Brandriss, M. C. (1988). A regulatory region responsible for proline-specific induction of the yeast *PUT2* gene is adjacent to its TATA box. Mol. Cell. Biol. *8,* 4634-4641.

Sikorski, R. S., and Hieter, P. (1989). A system of shuttle vectors and yeast host strains designed for efficient manipulation of DNA in *Saccharomyces cerevisiae*. Genetics *122,* 19-27.

Snyder, M. (1994). Personal communication.

Stratagene. (1991). Product catalog. (La Jolla, Calif: Stratagene).

Struhl, K., Stinchcomb, D. T., Scherer, S., and Davis, R. W. (1979). High-frequency transformation of yeast: autonomous replication of hybrid DNA molecules. Proc. Natl. Acad. Sci. USA *76,* 1035-1039.

Timberlake, W. E. (1991). Temporal and spatial controls of *Aspergillus* development. Curr. Opin. Genet. Dev. *1,* 351-357.

Wang, Z., Wu, X., and Friedberg, E. C. (1993). DNA repair synthesis during base excision repair in vitro is catalyzed by DNA polymerase ε and is influenced by DNA polymerases α and ∂ in *Saccharomyces cerevisiae*. Mol. Cell. Biol. *13,* 1051-1058.

Chapter 6:

Investigation of the Role of PHD1 Homolog SOK2 in the Regulation of *Saccharomyces cerevisiae* Pseudohyphal Growth

Introduction

Chapter 4 of this thesis describes the isolation and characterization of *PHD1*, a *Saccharomyces cerevisiae* gene encoding a putative transcription factor that ectopically activates pseudohyphal growth upon overexpression (Gimeno and Fink, 1994). PHD1 has an 100 amino acid DNA binding motif that is 70% identical to a region of StuA, an *Aspergillus nidulans* protein. This identity is especially interesting because StuA regulates conidiophore morphogenesis, a process with striking functional and morphological similarities to pseudohyphal growth (Miller et al., 1991; Miller et al., 1992; Timberlake, 1990; Timberlake, 1991).

A *S. cerevisiae* gene called *SOK2*, whose product is also related to PHD1, was recently identified and may act in the RAS-cAMP pathway downstream of cAMP-dependent protein kinase (Ward and Garrett, 1994). A detailed explanation of the carbon source signal transmitted by the RAS-cAMP pathway and the role of this pathway in the control of carbon metabolism is presented in Chapter 1. Readers are encouraged to review this information because in the Discussion section of this chapter it is integrated with the data presented in this chapter to form a model for how the RAS-cAMP pathway might regulate pseudohyphal growth.

In *S. cerevisiae*, the 3 *TPK* genes encode the 3 functionally redundant catalytic subunits of cAMP-dependent protein kinase (Cannon and Tatchell, 1987; Toda et al., 1987). Mutant yeast strains lacking any single *TPK* gene or any pair of *TPK* genes are viable, whereas *tpk1*$^-$ *tpk2*$^-$ *tpk3*$^-$ yeast strains are inviable. When the RAS-cAMP pathway is inactive, two TPK proteins associate with two BCY1 proteins, the regulatory subunits of cAMP-dependent protein kinase (Toda et al., 1987), to form a catalytically inactive

heterotetramer (Broach and Deschennes, 1990). When the RAS-cAMP pathway is active, cellular cAMP levels rise causing cAMP molecules to bind specifically to the BCY1 proteins. When BCY1 proteins bind cAMP, they release the TPK proteins, which are then catalytically active as serine-threonine protein kinases. These kinases then phosphorylate substrate proteins in the cell which mediate the varied physiological effects of an active RAS-cAMP pathway.

Yeast cells downregulate the RAS-cAMP pathway at the level of cAMP dependent protein kinase by having two cAMP phosphodiesterases, PDE1 (Nikawa et al., 1987) and PDE2 (Sass et al., 1986), that hydrolyze cAMP to AMP. The consequence is a lowering the intracellular concentration of cAMP and the reassociation of BCY1 proteins with TPK proteins. The second messenger, cAMP, is synthesized by an adenylate cyclase which in turn is activated by two proteins called RAS1 and RAS2 (Kataoka et al., 1984; Powers et al., 1984; Toda et al., 1985). Interestingly, a constitutively active version of the RAS2 protein called $RAS2^{val19}$ (Kataoka et al., 1984) causes inappropriate activation of the pseudohyphal growth program (Gimeno et al., 1992), the first evidence suggesting that the RAS-cAMP pathway might directly regulate pseudohyphal growth.

SOK2 was isolated by Mary Ward and Stephen Garrett as a high copy number suppressor of the temperature-sensitive growth defect of a *tpk1⁻ tpk2(ts) tpk3⁻* mutant (Ward and Garrett, 1994). Subsequently, deletion of *SOK2* was found to exacerbate the temperature sensitivity of the *tpk2(ts)* mutation. Together, these results suggest that SOK2 may function in the RAS-cAMP pathway downstream of cAMP-dependent protein kinase. *SOK2* is predicted to encode a 470 amino acid protein that contains a DNA binding motif that is 81.7% identical to the DNA binding motif found in PHD1. Because

PHD1 and the RAS-cAMP pathway have been implicated in pseudohyphal growth control, SOK2 was a good candidate for another pseudohyphal growth regulatory gene. For this reason its possible role in pseudohyphal growth was studied.

To determine whether *SOK2* plays a role in the control of pseudohyphal development, the pseudohyphal growth phenotypes of *MAT**a**/α sok2/sok2*, *MAT**a**/α SOK2*-2μm, *MAT**a**/α phd1/phd1 sok2/sok2*, and *MAT**a**/α PHD1*-2μm *SOK2*-2μm yeast strains were determined. The results of these experiments led to the conclusion that SOK2 is a pseudohyphal growth regulatory protein and that it interacts genetically with PHD1. Therefore, it became important to determine whether the RAS-cAMP pathway is involved at the level of cAMP in pseudohyphal growth control. This experiment was done by determining the pseudohyphal growth phenotypes of *MAT**a**/α PDE2*-2μm and *MAT**a**/α RAS2*^{val19} *PDE2*-2μm strains. Yeast strains that are *PDE2*-2μm overexpress a cAMP phosphodiesterase and have greatly reduced levels of cAMP. The results of these experiments strongly suggest that cAMP is an important regulator of pseudohyphal growth. These experiments show that the related putative transcription factors PHD1 and SOK2 control pseudohyphal growth and that they may do so as components of the RAS-cAMP pathway.

Materials and Methods

Yeast Strains, Plasmids, Media, and Microbiological Techniques

Yeast strains and plasmids are listed in Table 6.1. Standard yeast media, including synthetic complete medium (SC) lacking specific components, were prepared and yeast genetic manipulations were performed as described (Sherman et al., 1986). SLAD medium was prepared as described previously (Gimeno and Fink, 1994). Yeast transformations were performed by standard protocols (Gietz et al., 1992; Ito et al., 1983). Genomic DNAs were isolated from yeast strains by a standard method (Hoffman and Winston, 1987).

Yeast Strain Construction

Construction of yeast strains is shown in tabular form (Table 6.1). All *S. cerevisiae* strains used in this study are congenic to the Σ1278b genetic background and are derived from MB758-5B (*MATa ura3-52*) (Siddiqui and Brandriss, 1988), MB1000 (*MAT*α) (Brandriss and Magasanik, 1979), or both.

Qualitative Pseudohyphal Growth Assay

This assay was performed as described previously (Gimeno and Fink, 1994). In those experiements where transformants were studied, two independent transformants from each transformation were assayed. In the experiments presented here, the pairs of transformants always had the same phenotypes.

Table 6.1 Yeast Strain and Plasmid List

Strain or Plasmid	Genotype or Description	Reference, Source, or Derivation
***S. cerevisiae* strains**[a]		
L5366	*MATa/MATα ura3-52/ura3-52*	(Gimeno and Fink, 1994)
10480-2C	*MATα leu2::hisG ura3-52*	Fink lab collection
10480-6D	*MATa leu2::hisG ura3-52*	Fink lab collection
CGX179	*MATa/MATα leu2::hisG/leu2::hisG ura3-52/ura3-52*	10480-2CX10480-6D
CJ24	*MATa/MATα sok2::URA3/SOK2 ura3-52/ura3-52*	L5366 transformant
CJ14	*MATa sok2::URA3 ura3-52*	CJ24 ascospore
CJ15	*MATα sok2::URA3 ura3-52*	CJ24 ascospore
CGX210	*MATa/MATα sok2::URA3/sok2::URA3 ura3-52/ura3-52*	CJ14XCJ15
CJ26	*MATa/MATα sok2::URA3/SOK2 ura3-52/ura3-52*	L5366 transformant
CJ22	*MATa sok2::URA3 ura3-52*	CJ26 ascospore
CJ23	*MATα sok2::URA3 ura3-52*	CJ26 ascospore
CGX218	*MATa/MATα sok2::URA3/sok2::URA3 ura3-52/ura3-52*	CJ22XCJ23
CGX134	*MATa/MATα phd1Δ1::hisG-URA3-hisG/PHD1 ura3-52/ura3-52*	(Gimeno and Fink, 1994)
CG611	*MATα phd1Δ1::hisG-URA3-hisG ura3-52*	CGX134 ascospore
CGX214	*MATa/MATα phd1Δ1::hisG-URA3-hisG/PHD1 sok2::URA3/SOK2 ura3-52/ura3-52*	CJ14XCG611
CJ27	*MATa phd1Δ1::hisG-URA3-hisG sok2::URA3 ura3-52*	CGX214 ascospore
CJ28	*MATα phd1Δ1::hisG-URA3-hisG sok2::URA3 ura3-52*	CGX214 ascospore
CGX217	*MATa/MATα phd1Δ1::hisG-URA3-hisG/ phd1Δ1::hisG-URA3-hisG sok2::URA3/sok2::URA3 ura3-52/ura3-52*	CJ27XCJ28

CGX219	*MATa/MATα phd1Δ1::hisG-URA3-hisG/PHD1 sok2::URA3/SOK2 ura3-52/ura3-52*	CJ22XCG611
CJ46	*MATa or MATα phd1Δ1::hisG-URA3-hisG sok2::URA3 ura3-52*	CGX219 ascospore
CJ47	*MATa or MATα phd1Δ1::hisG-URA3-hisG sok2::URA3 ura3-52*	CGX219 ascospore
CGX224	*MATa/MATα phd1Δ1::hisG-URA3-hisG/ phd1Δ1::hisG-URA3-hisG sok2::URA3/sok2::URA3 ura3-52/ura3-52*	CJ46XCJ47
CJ48	*MATa or MATα phd1Δ1::hisG-URA3-hisG sok2::URA3 ura3-52*	CGX219 ascospore
CJ49	*MATa or MATα phd1Δ1::hisG-URA3-hisG sok2::URA3 ura3-52*	CGX219 ascospore
CGX225	*MATa/MATα phd1Δ1::hisG-URA3-hisG/ phd1Δ1::hisG-URA3-hisG sok2::URA3/sok2::URA3 ura3-52/ura3-52*	CJ48XCJ49
CG953	*MATa/MATα ura3-52/ura3-52* (pRS316)	(Gimeno and Fink, 1994)
CGX137	*MATa/MATα phd1Δ1::hisG-URA3-hisG/ phd1Δ1::hisG-URA3-hisG ura3-52/ura3-52*	(Gimeno and Fink, 1994)
CG934	*MATa/MATα ura3-52/ura3-52* (pCG38)	(Gimeno and Fink, 1994)
CG995	*MATa/MATα ura3-52/ura3-52* (pMW61)	L5366 transformant
CJ52	*MATa/MATα leu2::hisG/leu2::hisG ura3-52/ura3-52* (pCG41 & pMW61)	CGX179 transformant
CJ53	*MATa/MATα leu2::hisG/leu2::hisG ura3-52/ura3-52* (pRS3052μ & pMW61)	CGX179 transformant
CJ54	*MATa/MATα leu2::hisG/leu2::hisG ura3-52/ura3-52* (pCG41 & YEp195)	CGX179 transformant

CJ55	*MATa/MATα leu2::hisG/leu2::hisG ura3-52/ura3-52* (pRS3052*μ* & YEp195)	CGX179 transformant
CJ56	*MATa/MATα leu2::hisG/leu2::hisG ura3-52/ura3-52* (YEpPDE2-1 & pRS316)	CGX179 transformant
CJ57	*MATa/MATα leu2::hisG/leu2::hisG ura3-52/ura3-52* (pRS3052*μ* & pRS316)	CGX179 transformant
CJ58	*MATa/MATα leu2::hisG/leu2::hisG ura3-52/ura3-52* (pRS3052*μ* & YCpR2V)	CGX179 transformant
CJ59	*MATa/MATα leu2::hisG/leu2::hisG ura3-52/ura3-52* (YEpPDE2-1 & YCpR2V)	CGX179 transformant

[a] All strains are congenic to the ∑1278b genetic background.

Plasmids

pCG38	*PHD1* cloned into pRS202	(Gimeno and Fink, 1994)
pCG41	*PHD1* cloned into pRS3052*μ*	This study
pMW52	*sok2::URA3* disruption construct	(Ward and Garrett, 1994)
pMW61	*SOK2* cloned into YEplac195	(Ward and Garrett, 1994)
pRS202	*URA3*-marked 2*μ*m vector	(Connelly and Hieter, 1994)
pRS3052*μ*	*LEU2*-marked 2*μ*m vector	(Miller and Fink, 1994)
pRS316	*URA3*-marked *CEN* vector	(Sikorski and Hieter, 1989)
YCpR2V	*URA3*-marked $RAS2^{val19}$ vector	(Gimeno et al., 1992)
YEplac195	2 *μ*m plasmid	(Gietz and Sugino, 1988)
YEpPDE2-1	*LEU2*-marked *PDE2*-2*μ*m vector	(Sass et al., 1986)

Light Microscopic Techniques

These techniques have been described in detail elsewhere (Gimeno et al., 1992).

Disruption of *SOK2*

SOK2 was disrupted in a Σ1278b strain using pMW52 which contains the *sok2::URA3* disruption DNA fragment (Ward and Garrett, 1994). Briefly, 10 μg of pMW52 were digested with PvuII and SphI, extracted once with an equal volume of a 1:1 mixture of phenol and 24:1 chloroform-isoamyl alcohol, extracted again with an equal volume of 24:1 chloroform-isoamyl alcohol, ethanol precipitated, and used to transform L5366 (*MAT**a**/MATα ura3-52/ura3-52*) as previously described (Gietz et al., 1992). Stable Ura$^+$ transformants were selected on SC-ura plates. CJ24 and CJ26 were constructed in this manner and were independently derived. CJ24 and CJ26 were sporulated, and two Ura$^+$ (*sok2::URA3*) sister ascospore segregants from each strain were confirmed to be *sok2::URA3* by genomic Southern blotting analysis. In this way CJ24 gave rise to CJ14 and CJ15 and CJ26 produced CJ22 and CJ23. CJ14 and CJ15 were mated to produce CGX210 and CJ22 and CJ23 were mated to produce CGX218. CGX210 and CGX218 are independent *MAT**a**/MATα sok2::URA3/sok2::URA3 ura3-52/ura3-52* strains. CGX210 and CGX218 behaved identically in the experiments presented here.

Construction of *phd1/phd1 sok2/sok2* Double Mutant Strains

This construction was initiated by crossing CJ14 (*MAT**a** sok2::URA3 ura3-52*) by CG611 (*MATα phd1Δ1::hisG-URA3-hisG ura3-52*) to produce strain CGX214 and CJ22 (*MAT**a** sok2::URA3 ura3-52*) by CG611 (*MATα phd1Δ1::hisG-URA3-hisG ura3-52*) to produce strain CGX219 . CGX214 and CGX219 were sporulated and subjected to tetrad analysis. Tetrads in which the Ura$^+$ phenotype segregated 2:2 were identified. Two Ura$^+$ sister ascospore-derived strains (CJ27 and CJ28) of opposite mating types from one of these tetrads derived from CGX214 were crossed to generate CGX217, a *MAT**a**/MATα phd1Δ1::hisG-URA3-hisG/phd1Δ1::hisG-URA3-hisG sok2::URA3/sok2::URA3 ura3-52/ura3-52* strain. CGX217 was confirmed to have this genotype by genomic Southern blotting analysis. Four Ura$^+$ sister ascospore-derived strains (CJ46, CJ47, CJ48, and CJ49) of opposite mating types derived from CGX219 were identified and CJ46 and CJ47 were crossed to generate CGX224 and CJ48 and CJ49 were crossed to generate CGX225, producing two more *MAT**a**/MATα phd1Δ1::hisG-URA3-hisG/phd1Δ1::hisG-URA3-hisG sok2::URA3/sok2::URA3 ura3-52/ura3-52* strains. Again, these genotypes were confirmed with genomic Southern blotting analysis. CGX217, CGX224, and CGX225 behaved identically in the experiments presented here.

Results

100 Amino Acids of SOK2 Are 80% Identical to the DNA Binding Motif Present in PHD1

I became interested in SOK2 when I learned that Mary Ward and Stephen Garrett had identified a StuA homolog as a high copy number suppressor of the temperature-sensitive growth defect of a *tpk1*$^-$ *tpk2(ts) tpk3*$^-$ yeast mutant (Ward and Garrett, 1994). After consulting with these two scientists, a collaboration was initiated: I would study the possible role of SOK2 in pseudohyphal growth and they would investigate the potential role of PHD1 in the RAS-cAMP signaling pathway.

A comparison of the 366 amino acid PHD1 sequence and the 470 residue SOK2 sequence revealed that these two proteins are significantly related only in their 104 amino acid SWI4-like DNA binding motifs which are 81.7% identical (Fig. 6.1). In addition, both the PHD1 and SOK2 DNA binding motifs are 71.2% identical to the SWI4-like DNA binding motif found in *A. nidulans* StuA. These DNA binding motifs are located in similar areas of the PHD1 and SOK2 proteins: in PHD1 the DNA binding motif begins at amino acid 184 and in SOK2 it begins at amino acid 183. The remarkable similarity between the PHD1 and SOK2 DNA binding motifs suggests that they may recognize identical or similar DNA sequences and that they may regulate the same genes.

Analysis of Pseudohyphal Growth in Strains that Have Mutant Alleles of *SOK2*

Figure 6.1 The DNA binding motif present in SOK2 is 81.7 % identical to the DNA binding motif in PHD1. Alignments of the DNA binding motifs in PHD1 and StuA with the DNA binding motif present in SOK2. The name of the protein whose amino acid sequence is shown is to the left of the sequence. When an amino acid in SOK2 is identical to the corresponding amino acid in a similar protein, both amino acids are designated by a white letter in a black rectangle. To the right of the sequence is the position of the amino acid sequence with respect to the amino terminus of the protein from which it originates. Over the region shown, SOK2 is 81.7% identical to PHD1 and both SOK2 and PHD1 are 71.2% identical to StuA.

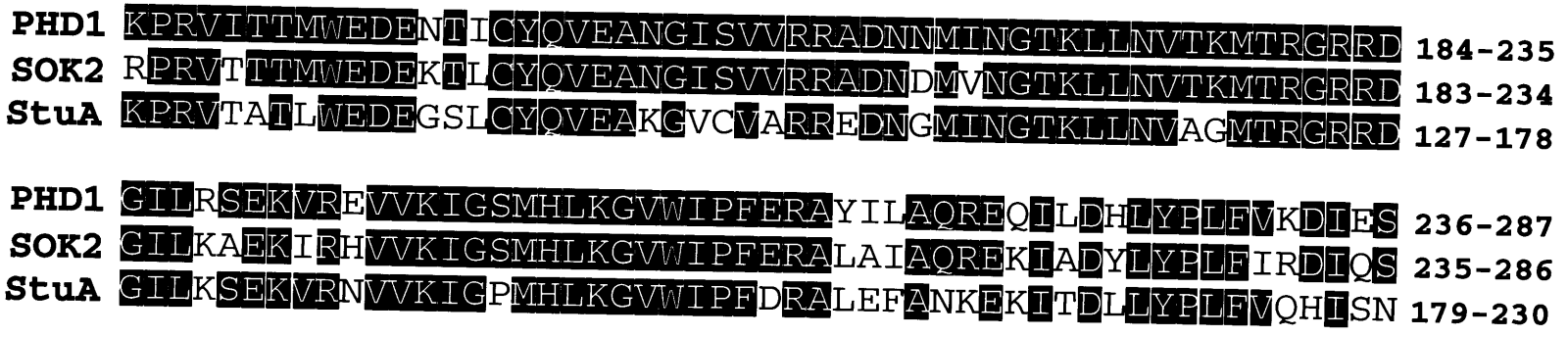
PHD1 KPRVITTMWEDENTICYQVEANGISVVRRADNNMINGTKLLNVTKMTRGRRD 184-235
SOK2 RPRVTTTMWEDEKTLCYQVEANGISVVRRADNDMVNGTKLLNVTKMTRGRRD 183-234
StuA KPRVTATLWEDEGSLCYQVEAKGVCVARREDNGMINGTKLLNVAGMTRGRRD 127-178
PHD1 GILRSEKVREVVKIGSMHLKGVWIPFERAYILAQREQILDHLYPLFVKDIES 236-287
SOK2 GILKAEKIRHVVKIGSMHLKGVWIPFERALAIAQREKIADYLYPLFIRDIQS 235-286
StuA GILKSEKVRNVVKIGPMHLKGVWIPFDRALEFANKEKITDLLYPLFVQHISN 179-230

To determine if *SOK2* plays a role in the control of pseudohyphal development, the pseudohyphal growth phenotypes of *MAT**a**/α sok2/sok2*, *MAT**a**/α SOK2*-2μm, *MAT**a**/α phd1/phd1 sok2/sok2*, and *MAT**a**/α PHD1*-2μm *SOK2*-2μm yeast strains were determined. The 2μm-based *SOK2* overexpression plasmid pMW61 was used to determine the pseudohyphal growth phenotype of *SOK2* overexpression. When grown on SLAD medium, *MAT**a**/α* pMW61-carrying strains were found to exhibit weakly enhanced pseudohyphal growth (Fig. 6.2). *MAT**a**/α* strains simultaneously overexpressing *SOK2* and *PHD1* were constructed using pMW61 and pCG41, a 2μm-based *PHD1* overexpression plasmid. These strains underwent enhanced pseudohyphal growth indistinguishable from that manifested by strains overexpressing only *PHD1* (Fig. 6.3).

The *SOK2* gene was replaced with the *sok2::URA3* disruption allele which consists of the *SOK2* gene disrupted at a SpeI site located between the nucleotides encoding amino acids 26 and 27. Evidence that *sok2::URA3* is nonfunctional is that, unlike *SOK2* overexpressed from a 2μm plasmid, *sok2::URA3* overexpressed from a 2μm plasmid does not suppress the temperature sensitive growth of a *tpk1⁻ tpk2⁻(ts) tpk3⁻* yeast strain. Interestingly, *MAT**a**/α sok2::URA3/sok2::URA3* strains were found to exhibit greatly enhanced pseudohyphal growth when grown on nitrogen starvation (SLAD) medium. For comparison, wild-type, *phd1Δ1::hisG-URA3-hisG/phd1Δ1::hisG-URA3-hisG*, and *PHD1*-overexpressing strains are also shown (Fig. 6.2). This result suggests that on SLAD medium *SOK2* inhibits pseudohyphal growth. Next, *MAT**a**/α phd1Δ1::hisG-URA3-hisG/phd1Δ1::hisG-URA3-hisG sok2::URA3/sok2::URA3* double mutant strains were constructed. These strains underwent moderately enhanced pseudohyphal growth, demonstrating that *sok2::URA3/sok2::URA3* pseudohyphal growth enhancement is a *PHD1*-dependent process.

Figure 6.2 Analysis of the effects of mutant alleles of *SOK2* on pseudohyphal growth. Wild-type (A, CG953), *phd1/phd1* (B, CGX137), *SOK2*-2μm (C, CG995), *PHD1*-2μm (D, CG934), *sok2/sok2* (E, CGX210), and *phd1/phd1 sok2/sok2* (F, CGX225) strains were subjected to the qualitative pseudohyphal growth assay. Strains were patched on SC-ura medium, grown overnight at 30°C, and then streaked to obtain single cells on nitrogen starvation (SLAD) medium. Representative microcolonies were photographed after two days. The scale bar represents 100 μm.

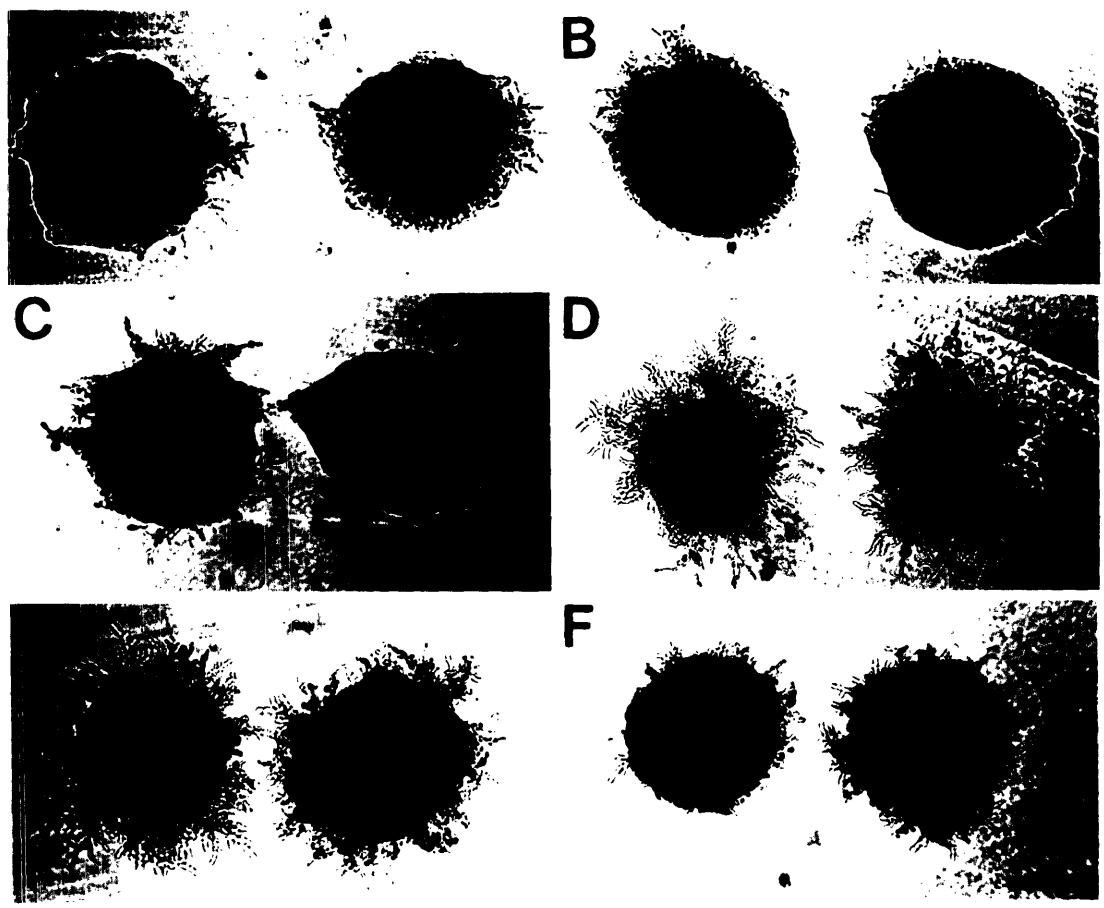
B
C
D
F

Figure 6.3 Analysis of the effect on pseudohyphal growth of simultaneously overexpressing *PHD1* and *SOK2*. Wild-type (A, CJ55), *SOK2*-2μm (B, CJ53), *PHD1*-2μm (C, CJ54), and *PHD1*-2μm *SOK2*-2μm (D, CJ52) strains were subjected to the qualitative pseudohyphal growth assay. Strains were patched on SC-ura medium, grown overnight at 30°C, and then streaked to obtain single cells on nitrogen starvation (SLAD) medium. Representative microcolonies were photographed after two days. The scale bar represents 100 μm.

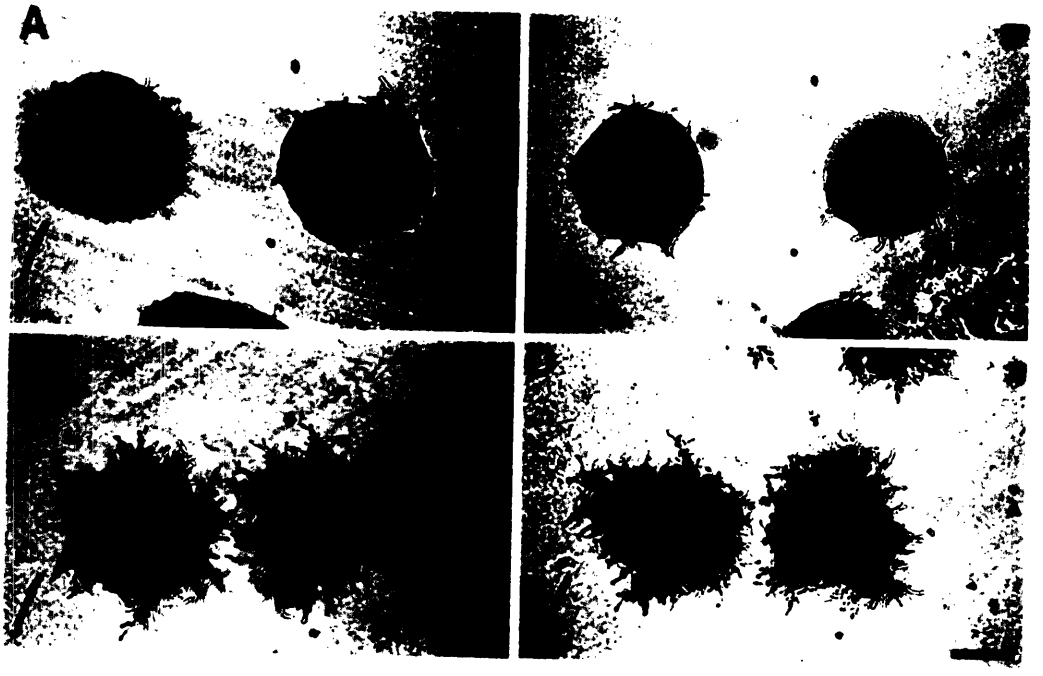
A

Overexpression of cAMP Phosphodiesterase 2 Inhibits Pseudohyphal Growth and Is Epistatic to Activated RAS2

The preceding experiments show that SOK2 has a direct or indirect role in pseudohyphal growth control. Experiments by Ward and Garrett demonstrate that SOK2 may be a component of the RAS-cAMP pathway, which functions downstream of cAMP-dependent protein kinase. To learn if SOK2 might regulate pseudohyphal growth by functioning in the RAS-cAMP pathway downstream of cAMP-dependent protein kinase, I determined whether this part of the RAS-cAMP pathway participates in pseudohyphal growth control.

It is well established that the constitutively active *RAS2*^{val19} gene strongly enhances pseudohyphal growth (Gimeno et al., 1992). *RAS2*^{val19} could enhance pseudohyphal growth either by the well characterized cAMP-dependent pathway or via a cAMP-independent pathway. To help distinguish between these two possibilities, the pseudohyphal growth phenotypes of *MAT***a**/α wild-type control strains and *MAT***a**/α *PDE2*-2μm strains were compared. *PDE2* encodes a high affinity cAMP phosphodiesterase that functions to downregulate the RAS-cAMP pathway (Sass et al., 1986) and *PDE2* overexpression suppresses the phenotypes caused by *RAS2*^{val19}. It was found that *MAT***a**/α *PDE2*-2μm strains had dramatically inhibited pseudohyphal growth when compared to *MAT***a**/α wild-type controls (Fig. 6.4). This suggests that cAMP is an important pseudohyphal growth regulatory molecule.

Next, an epistasis experiment was performed to determine if inhibition of pseudohyphal growth by *PDE2* overexpression is epistatic to enhancement of pseudohyphal growth by *RAS2*^{val19}. The pseudohyphal growth phenotypes of *MAT***a**/α wild-type control strains, *MAT***a**/α *RAS2*^{val19} strains, *MAT***a**/α *PDE2*-

Figure 6.4 Analysis of the effect of phosphodiesterase 2 overexpression on pseudohyphal growth. Wild-type (A and E, CJ57), *PDE2*-2μm (B and F, CJ56), *RAS2*^{val19} (C, CJ58), *PDE2*-2μm *RAS2val19* (D, CJ59) strains were subjected to the qualitative pseudohyphal growth assay. Strains were patched on SC-ura medium, grown overnight at 30°C, and then streaked to obtain single cells on nitrogen starvation (SLAD) medium. Representative microcolonies were photographed after 2 (A, B, C, and D) and 5 (E and F) days. The scale bar represents 100 μm.

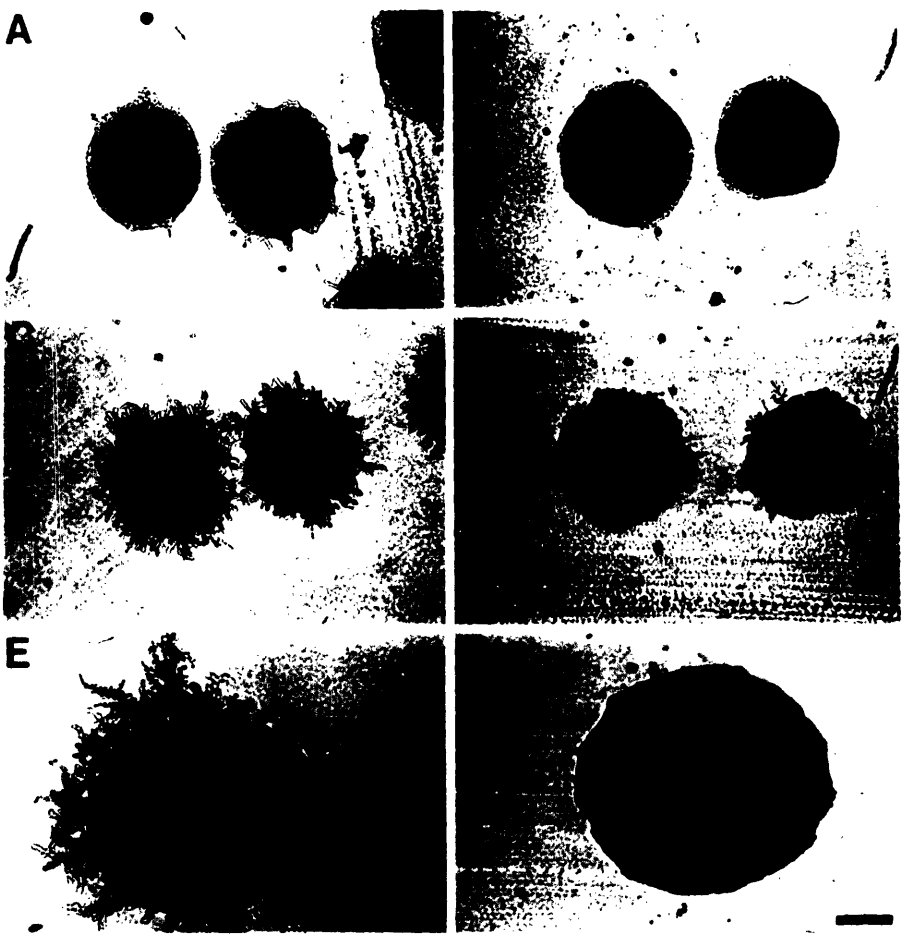
A
E

2μm strains, and *MAT**a**/α RAS2*^{val19} *PDE2*-2μm double mutant strains were compared (Fig. 6.4). The pseudohyphal growth of the *MAT**a**/α RAS2*^{val19} *PDE2*-2μm strain was far less enhanced than that of the *MAT**a**/α RAS2*^{val19} strain. The *MAT**a**/α RAS2*^{val19} *PDE2*-2μm strains exhibited more prolific pseudohyphal growth than either the *MAT**a**/α PDE2*-2μm strains or the *MAT**a**/α* wild-type control strains. This probably occurs because the elevated levels of PDE2 in the *MAT**a**/α RAS2*^{val19} *PDE2*-2μm strains are not high enough to reduce the cAMP levels in these strains to wild-type concentrations. This epistasis experiment strongly suggests that RAS2^{val19} enhances pseudohyphal growth by the well characterized cAMP-dependent mechanism that involves cAMP-dependent protein kinase. These important results suggest that diploid cells integrate RAS-cAMP pathway signals into their decision to undergo pseudohyphal growth. Thus it is possible that SOK2 may regulate pseudohyphal growth by functioning in the RAS-cAMP pathway downstream of cAMP-dependent protein kinase.

Discussion

A Model for Pseudohyphal Growth Control by *PHD1* and *SOK2*

The pseudohyphal growth phenotypes of diploid yeast strains containing mutant alleles of either or both *PHD1* and *SOK2* can be explained by first assuming that *PHD1* and *SOK2* regulate one or more genes that control or carry out the pseudohyphal growth program. In this model, PHD1 acts positively on these genes, SOK2 acts negatively on them, and PHD1 and SOK2 compete for the same regulatory binding sites in the promoters of these genes. *PHD1* overexpression enhances pseudohyphal growth because it pushes the promoter binding equilibrium between PHD1 and SOK2 to the PHD1 side. Likewise, disruption of *SOK2* enhances pseudohyphal growth because PHD1 proteins do not have to compete with SOK2 proteins for promoter binding. That *MAT**a**/α sok2/sok2 phd1/phd1* strains exhibit moderately enhanced pseudohyphal growth suggests that there is at least one positively acting PHD1 homolog. This last proposal is supported by the result that *MAT**a**/α phd1/phd1* strains undergo normal pseudohyphal growth when starved for nitrogen.

This model has a problem explaining why overexpression of *SOK2* weakly enhances pseudohyphal growth and why simultaneous overexpression of *PHD1* and *SOK2* results in the same pseudohyphal growth phenotype as overexpression of *PHD1* alone. The simplest explanation for both of these observations in the context of this model is that overexpression of *SOK2* exerts a dominant negative effect that is not unlike the pseudohyphal growth enhancing effect of *SOK2* disruption. A similar phenomenon has been documented for the *SEC12* gene (Hardwick et al., 1992).

One of the more interesting features of this model is that it predicts the presence of a gene that is functionally redundant with *PHD1* in the yeast genome. If this gene exists, its product will probably have a DNA binding motif that is very similar to both the DNA binding motifs in PHD1 and SOK2. PHD1, SOK2, and other related proteins, if they exist, may determine a cell's developmental fate by receiving and integrating information from signal transduction pathways, including the RAS-cAMP pathway, that report environmental and cellular conditions.

The Possible Role of the RAS-cAMP Pathway in Pseudohyphal Growth Control

Upregulation of the RAS-cAMP pathway promotes pseudohyphal growth and downregulation of the RAS-cAMP pathway inhibits it. Interestingly, the opposite is true for sporulation: upregulation of the RAS-cAMP pathway inhibits this process while RAS-cAMP pathway downregulation promotes it. That the RAS-cAMP pathway transmits information about a cell's carbon status (see Chapter 1) makes this reciprocal relationship especially interesting for the following reasons.

When starved for nitrogen, diploid cells decide to either sporulate or undergo pseudohyphal growth. This decision is regulated by the availability of a carbon source. Faced with both carbon and nitrogen starvation, the cells sporulate. When the nitrogen starvation occurs in the presence of an abundant carbon source like glucose, pseudohyphal growth results. The RAS-cAMP pathway may provide information about the availability and quality of a cell's carbon source that is integrated with information about the cell's nitrogen status and probably other information to determine the cell's developmental fate.

In this model, when a cell is starved for nitrogen, the upregulation of the RAS-cAMP pathway that occurs if it is also growing on an abundant and good carbon source signals for it to undergo pseudohyphal growth. Alternatively, when a cell is starved for nitrogen and is growing under conditions of carbon starvation or on a poor carbon source, downregulation of the RAS-cAMP pathway signals the cell to sporulate. To accomodate other data about the RAS-cAMP pathway, this model must stipulate that the RAS-cAMP pathway is one of several inputs into a cell's decision to sporulate or undergo pseudohyphal growth and, in a wild-type cell is capable of influencing but not determining the cell's developmental fate. Work described in this chapter suggests that SOK2 may receive pseudohyphal growth regulatory signals from the RAS-cAMP pathway. PHD1 may receive pseudohyphal growth regulatory signals from the RAS-cAMP pathway or from another pathway, for instance one that transmits information about a cell's nitrogen status. It will be very interesting to test the model that PHD1 and SOK2 receive and integrate pseudohyphal growth regulatory signals from the RAS-cAMP and other signaling pathways to determine a cell's developmental fate.

Literature Cited

Brandriss, M. C., and Magasanik, B. (1979). Genetics and physiology of proline utilization in *Saccharomyces cerevisiae*: enzyme induction by proline. J. Bacteriol. *140,* 498-503.

Broach, J. R., and Deschennes, R. J. (1990). The function of *RAS* genes in *Saccharomyces cerevisiae*. Adv. Cancer Res. *54,* 79-139.

Cannon, J. F., and Tatchell, K. (1987). Characterization of *Saccharomyces cerevisiae* genes encoding subunits of cyclic AMP-dependent protein kinase. Mol. Cell. Biol. *7,* 2653-2663.

Connelly, C., and Hieter, P. (1994). Personal communication.

Gietz, D., St. Jean, J. A., Woods, R. A., and Schiestl, R. H. (1992). Improved method for high efficiency transformation of intact yeast cells. Nucleic Acids Res. *20,* 1425.

Gietz, R. D., and Sugino, A. (1988). New yeast-*Escherichia coli* shuttle vectors constructed with in vitro mutagenized yeast genes lacking six-base pair restriction sites. Gene *74,* 527-534.

Gimeno, C. J., and Fink, G. R. (1994). Induction of pseudohyphal growth by overexpression of *PHD1*, a *Saccharomyces cerevisiae* gene related to transcriptional regulators of fungal development. Mol. Cell. Biol. *14,* 2100-2112.

Gimeno, C. J., Ljungdahl, P. O., Styles, C. A., and Fink, G. R. (1992). Unipolar cell divisions in the yeast *S. cerevisiae* lead to filamentous growth: regulation by starvation and *RAS*. Cell *68,* 1077-1090.

Hardwick, K. G., Boothroyd, J. C., Rudner, A. D., and Pelham, H. R. B. (1992). Genes that allow yeast cells to grow in the absence of the HDEL receptor. EMBO J. *11,* 4187-4195.

Hoffman, C. S., and Winston, F. (1987). A ten-minute DNA preparation from yeast efficiently releases autonomous plasmids for transformation of *Escherichia coli.* Gene *57,* 267-272.

Ito, H., Fukuda, Y., Murata, K., and Kimura, A. (1983). Transformation of intact yeast cells treated with alkali cations. J. Bacteriol. *153,* 163-168.

Kataoka, T., Powers, S., McGill, C., Fasano, O., Strathern, J., Broach, J., and Wigler, M. (1984). Genetic analysis of yeast *RAS1* and *RAS2* genes. Cell *37,* 437-445.

Miller, D., and Fink, G. R. (1994). Personal communication.

Miller, K. Y., Toennis, T. M., Adams, T. H., and Miller, B. L. (1991). Isolation and transcriptional characterization of a morphological modifier: the *Aspergillus nidulans* stunted (*stuA*) gene. Mol. Gen. Genet. *227,* 285-292.

Miller, K. Y., Wu, J., and Miller, B. L. (1992). *StuA* is required for cell pattern formation in *Aspergillus*. Genes Dev. *6,* 1770-1782.

Nikawa, J.-I., Sass, P., and Wigler, M. (1987). Cloning and characterization of the low-affinity cyclic AMP phosphodiesterase gene of *Saccharomyces cerevisiae*. Mol. Cell. Biol. *7,* 3629-3636.

Powers, S., Kataoka, T., Fasano, O., Goldfarb, M., Strathern, J., Broach, J., and Wigler, M. (1984). Genes in *S. cerevisiae* encoding proteins with domains homologous to the mammalian *ras* proteins. Cell *36,* 607-612.

Sass, P., Field, J., Nikawa, J., Toda, T., and Wigler, M. (1986). Cloning and characterization of the high-affinity cAMP phosphodiesterase of *Saccharomyces cerevisiae*. Proc. Natl. Acad. Sci. USA *83,* 9303-9307.

Sherman, F., Fink, G. R., and Hicks, J. (1986). Methods in Yeast Genetics. (Cold Spring Harbor, New York: Cold Spring Harbor Laboratory Press).

Siddiqui, A. H., and Brandriss, M. C. (1988). A regulatory region responsible for proline-specific induction of the yeast *PUT2* gene is adjacent to its TATA box. Mol. Cell. Biol. *8,* 4634-4641.

Sikorski, R. S., and Hieter, P. (1989). A system of shuttle vectors and yeast host strains designed for efficient manipulation of DNA in *Saccharomyces cerevisiae*. Genetics *122,* 19-27.

Timberlake, W. E. (1990). Molecular genetics of *Aspergillus* development. Annu. Rev. Genet. *24,* 5-36.

Timberlake, W. E. (1991). Temporal and spatial controls of *Aspergillus* development. Curr. Opin. Genet. Dev. *1,* 351-357.

Toda, T., Cameron, S., Sass, P., Zoller, M., Scott, J. D., McMullen, B., Hurwitz, M., Krebs, E. G., and Wigler, M. (1987). Cloning and characterization of *BCY1*, a locus encoding a regulatory subunit of the cyclic AMP-dependent protein kinase in *Saccharomyces cerevisiae*. Mol. Cell. Biol. *7,* 1371-1377.

Toda, T., Cameron, S., Sass, P., Zoller, M., and Wigler, M. (1987). Three different genes in *S. cerevisiae* encode the catalytic subunits of the cAMP-dependent protein kinase. Cell *50,* 277-287.

Toda, T., Uno, I., Ishikawa, T., Powers, S., Kataoka, T., Broek, D., Cameron, S., Broach, J., Matsumoto, K., and Wigler, M. (1985). In yeast, *RAS* proteins are controlling elements of adenylate cyclase. Cell *40,* 27-36.

Ward, M. P., and Garrett, S. (1994). Personal communication.

Chapter 7

Conclusions

This thesis presents the characterization of *Saccharomyces cerevisiae* pseudohyphal development. Chapters 2 and 3 include observational experiments showing that pseudohyphal cells are morphologically distinct from ellipsoidal cells, that pseudohyphae elongate by budding, that a pseudohyphal cell can bud to produce another pseudohyphal cell or a mitotic ellipsoidal cell, and that newborn pseudohyphal and sated ellipsoidal cells both have a unipolar budding pattern. This last result suggested that one role of the tightly regulated unipolar budding pattern of newborn *MAT***a**/α diploid cells is to allow pseudohyphal growth. Additional observational experiments showed that the first pseudohyphal cell of a pseudohypha is formed by budding from an ellipsoidal mother cell and that the role of pseudohyphal cells in the pseudohypha is probably to deliver vegetative ellipsoidal cells to new substrates that they subsequently colonize.

Chapter 3 also presents several physiological and genetic experiments. The most important physiological experiment is that a medium with abundant glucose as sole carbon source and starvation levels of ammonium sulfate as sole nitrogen source induces pseudohyphal growth. This and experiments with *shr3/shr3* mutants showed that nitrogen starvation induces pseudohyphal growth. Experiments with mating type locus mutants established that the mating type locus regulates pseudohyphal growth and that pseudohyphal growth is a *MAT***a**/α diploid-specific dimorphic transition. Subsequent work by others has shown that mutant haploid strains that have the diploid budding pattern undergo pseudohyphal growth when starved for nitrogen (Sanders and Herskowitz, 1994; Wright et al., 1993). This result suggests that the

mating type locus regulates pseudohyphal growth by programming the cell-type specific budding patterns of diploids and haploids

Work in Chapters 3 and 6 strongly implicates the RAS-cAMP signaling pathway as a direct regulator of pseudohyphal growth. The constitutively active *RAS2^{val19}* allele inappropriately activates pseudohyphal growth. Overexpression of the phosphodiesterase 2 gene (*PDE2*) downregulates the RAS-cAMP signaling pathway and inhibits nitrogen starvation-induced pseudohyphal growth. A model in Chapter 6 suggests that the RAS-cAMP pathway transmits carbon status signals that cells factor into their decision to undergo pseudohyphal growth.

Chapter 4 describes the isolation and characterization of the *PHD1* gene. *PHD1* activates the pseudohyphal growth program when overexpressed and probably encodes a transcription factor. PHD1 contains a DNA binding motif homologous to the DNA binding domains of the MBP1 and SWI4 cell cycle regulatory transcription factors. MBP1 and SWI4 activate the transcription of Start-specific genes by binding to related DNA sequences in their promoters. The DNA binding motif in PHD1 is about 70% identical to the DNA binding motif present in StuA. StuA is an *Aspergillus nidulans* protein that regulates a pseudohyphal growth-like process. Interestingly, *phd1/phd1* strains undergo normal pseudohyphal growth in response to nitrogen starvation. This result suggests that if *PHD1* directly regulates pseudohyphal growth one or more genes that are functionally redundant with *PHD1* exist.

As described in Chapter 5, *PHD1* overexpression activates *POL2*, a gene of the MBP1 regulon. This raises the possibility that PHD1 may activate transcription by binding to MBP1 binding sites or related DNA sequences. This possibility is attractive because genes regulated by MBP1 are involved in morphogenesis and cell separation, two of the component processes of

pseudohyphal growth. Overexpression of *PHD1* also activates *DAL81*, a positive transcriptional regulator of nitrogen catabolic genes. If *DAL81* is not required for pseudohyphal growth, as suggested by some experiments presented in Chapter 5, *PHD1* may induce it so that pseudohyphal cells have the catabolic enzymes they need to utilize the poor nitrogen sources that they are likely to encounter while foraging.

The SOK2 protein has a DNA binding motif that is 81.7% identical to the DNA binding motif present in PHD1. SOK2 may act in the RAS-cAMP pathway downstream of cAMP-dependent protein kinase. As described in Chapter 6, deletion of *SOK2* dramatically enhances pseudohyphal growth while overexpression of *SOK2* weakly enhances pseudohyphal growth. *PHD1* and *SOK2* genetically interact because *phd1/phd1 sok2/sok2* strains undergo significantly less enhanced pseudohyphal growth than *sok2/sok2* strains. A model that explains these results is that SOK2 is a repressor of pseudohyphal growth while PHD1 is an activator. In this model, SOK2 and PHD1 receive and integrate environmental and cellular signals that determine whether a cell enters the pseudohyphal growth pathway.

Prospectus

During the three years that the pseudohyphal growth field has existed, it has produced studies that report that one or more genes are directly or indirectly involved in pseudohyphal growth (Blacketer et al., 1993; Gimeno and Fink, 1994; Gimeno et al., 1992; Hu and Ronne, 1994; Liu et al., 1993). These studies tend to report that one or more genes, usually thought to be involved in signal transduction, when overexpressed or mutated inhibit or activate pseudohyphal growth. These sorts of studies are important because they identify candidate direct pseudohyphal growth regulatory genes that also can be useful tools. The list of candidate pseudohyphal growth regulatory genes is rather long, so for this class of genes the focus of the pseudohyphal growth field should begin to shift from gene identification to gene characterization.

An especially fertile area of the pseudohyphal growth field is the identification of genes involved in cell elongation, agar invasion, and incomplete cell separation, three of the component processes of pseudohyphal growth. This research area is fertile because members of this class of genes have not yet been reported. Another productive area of research is the identification of homeotic pseudohyphal growth mutants. This interesting class of mutants includes those that produce pseudohyphal cells instead of blastospore-like cells and those that produce pseudohyphae that have backbones of ellipsoidal instead of pseudohyphal cells. The defective genes in these mutants might be involved in programming cell identity.

An exciting subfield of pseudohyphal growth focuses on the genetic similarities between *A. nidulans* conidiation and pseudohyphal growth in *S. cerevisiae*. One important regulator of conidiation is StuA and it is

homologous to PHD1 and SOK2, two pseudohyphal growth regulatory genes (Chapter 6). Another important conidiation regulator, AbaA (Sewall et al., 1990), enhances pseudohyphal growth when expressed in *S. cerevisiae* (Andrianopoulos et al., 1993). *S. cerevisiae* has an AbaA homolog called TEC1 (Andrianopoulos and Timberlake, 1991; Laloux et al., 1990) and its possible role in pseudohyphal growth is being investigated. These results suggest that the genetic regulation of conidiation and pseudohyphal growth may be similar. It will be interesting to learn if *S. cerevisiae* has homologs of BrlA, WetA, and MedA, three other master regulators of conidiation (Clutterbuck, 1969; Timberlake, 1990; Timberlake, 1991), that are involved in pseudohyphal growth.

The physiology of pseudohyphal growth also promises to be a fruitful and important area of research. Basic questions like the role of carbon source in pseudohyphal growth and if starvation for nutrients other than nitrogen can induce pseudohyphal growth remain to be systematically studied. It should also be determined if GLN3, a well characterized transcription factor known to transduce nitrogen starvation signals (Minehart and Magasanik, 1991), is involved in transducing the nitrogen starvation signal that induces pseudohyphal growth.

Subsequent sections of this prospectus will describe how the role of *PHD1* and *SOK2* in pseudohyphal growth could be characterized, how genes involved in the component processes of pseudohyphal growth could be identified, and advances that would help the pseudohyphal growth field progress. The strategies discussed for elucidating the role of *PHD1* and *SOK2* in pseudohyphal growth are generalizable to any regulatory protein of interest. The basic concept of these strategies involves two lines of experimentation. The first is to identify the signals and proteins that directly

regulate the protein of interest. The second is to identify the proteins and/or genes that the protein of interest regulates. When these genes and gene products have been identified and their functions are understood, it will be clear if the protein of interest directly or indirectly regulates pseudohyphal growth. An example of this approach is the characterization of the indirect pseudohyphal growth regulatory gene *SHR3* presented in the appendix to Chapter 2.

Characterizing *PHD1* and *SOK2* and Identifying Pseudohyphal Growth Genes

Tantalizing evidence exists that *PHD1* and *SOK2* are involved in pseudohyphal growth control. The models for *PHD1* and *SOK2* function presented in this thesis predict that there is at least one gene that is functionally redundant with *PHD1.* This hypothetical gene's product will probably have a DNA binding motif that is very similar to the DNA binding motif present in PHD1. Thus, it should be possible to clone it using PCR and degenerate primers complementary to the DNA encoding the most highly conserved regions of PHD1, SOK2, and StuA. DNA probes containing the *PHD1* or *SOK2* genes might hybridize to this possible homolog under low stringency conditions. This may allow the homolog to be cloned by colony or plaque hybridization techniques. If additional PHD1 structural homologs exist, it is important that they be identified before the work described in the rest of this section is attempted, and it will be interesting to determine if they are functionally redundant with PHD1. If the search for PHD1 homologs fails, it should be determined if MBP1 and SWI4, which are relatively distantly related to PHD1 at the amino acid sequence level, are functionally redundant with PHD1.

PHD1 and *SOK2* appear to have different roles in pseudohyphal growth control: *PHD1* behaves like an activator while *SOK2* has characteristics of a repressor. It would be interesting to construct a panel of PHD1-SOK2 chimeras to determine which regions of these two proteins are responsible for their different activities. These experiments might give insights into whether PHD1 and SOK2 bind to the same DNA sequences and whether PHD1 is an activator while SOK2 is a repressor.

The genes and signals that control the activity of PHD1 and SOK2 and the direct targets of PHD1 and SOK2 must be discovered in order for the role of PHD1 and SOK2 in pseudohyphal growth to be elucidated. There is already some evidence that PHD1 and SOK2 may receive signals from the RAS-cAMP pathway. In addition, some evidence supports the interesting possibility that PHD1 may regulate Start-specific genes and nitrogen catabolic genes. These issues will be clarified with a combination of biochemical, cell biological, and genetic approaches.

It should be determined if PHD1, SOK2, or both bind to the promoters of *POL2*, *DAL81*, and *IPO1-IPO3* and if the binding sites are also regulatory loci that respond to nitrogen starvation, cAMP, or other signals. After saturation of the IPO screen, it should be systematically determined if mutations in *PHD1*, *SOK2*, or newly discovered *PHD1* homologs affect the normal environmental regulation of *IPO* genes. It should also be determined if PHD1, SOK2, or PHD1 homologs are regulated transcriptionally, translationally, or posttranslationally by signals and signaling pathways that directly or indirectly control pseudohyphal growth.

An *IPO* gene that has PHD1, SOK2, or PHD1 homolog regulatory binding sites in its promoter and whose induced expression is dependent on one or more of these gene products would be valuable tool. This reporter

gene could be used in a screen for mutations that block its induced expression. Some of these mutations would probably be in genes that encode signal transduction proteins that are upstream of PHD1. Such *IPO* genes may also encode proteins that are responsible for the agar invasion, incomplete cell separation, and cell elongation that characterize pseudohyphal growth. Characterization of these *IPO* genes would reveal such an involvement.

A genetic screen that may identify genes required for pseudohyphal growth that are regulated by *PHD1* is already in progress. In consultation with me, one of my Fink laboratory colleagues, Hans-Ulrich Mösch, constructed a haploid *MAT**a**/α PHD1*-2μm strain that undergoes enhanced pseudohyphal growth on nitrogen starvation medium. This strain was mutagenized and mutants that no longer undergo pseudohyphal growth were isolated. These mutants may be deficient in genes that are regulated by *PHD1* and are directly involved in pseudohyphal growth. This elegant screen is an excellent strategy for identifying and isolating structural genes involved in the component processes of pseudohyphal growth.

The experiments proposed in this section will determine if *PHD1* and *SOK2* are directly involved in pseudohyphal growth control and will probably also identify regulatory and structural genes directly involved in this process.

Discovering a Pseudohyphal Growth-Specific Gene

The discovery of a pseudohyphal growth-specific gene would be a major advance. Such a gene, however, may not exist because the component processes of pseudohyphal growth could be elaborated exclusively with genes that also function at other times in the life cycle. If a pseudohyphal

growth-specific gene were isolated, it could be used to identify the cis-acting sequences and the regulatory proteins that confer upon it its expression pattern. A pseudohyphal growth-specific gene would also be very useful in distinguishing between mutations that induce pseudohyphal growth and mutations that cause cell elongation or abnormal growth.

One approach to cloning a pseudohyphal growth-specific gene would be to first identify a pseudohyphal growth-specific metabolite or protein and then devise an elegant way to isolate mutants that lack it. To give an example from another system, meiotic spores have a spore-specific dityrosine-containing macromolecule that is conveniently fluorescent. Nonfluorescent mutants were isolated and one of them had spores that lacked dityrosine. This strain had a mutation in a gene encoding a cytochrome P450 homolog (*DIT2*), an excellent candidate for a dityrosine biosynthetic enzyme (Briza et al., 1990). Northern analysis showed that *DIT2* is a sporulation-specific gene.

A Quantitative Assay for Cell Elongation

The assays used up until now to study pseudohyphal growth are qualitative. These assays demonstrate large differences in pseudohyphal growth between test strains. For this reason, only genes that cause dramatic pseudohyphal growth phenotypes when overexpressed or mutated have been studied. Qualitative assays have also made epistasis analysis complicated because double mutants often have intermediate phenotypes that make it difficult to judge which mutant phenotype predominates.

One quantitative assay would be to measure the lengths of invasive pseudohyphal cells in a colony and in this way quantitate the cell elongation component of pseudohyphal growth. That wild-type invasive pseudohyphal

cells are heterogeneous with respect to their lengths and that each colony and each pseudohyphal cell exists in a unique microenvironment complicates this assay. Another sampling problem is that only the pseudohyphal cells in pseudohyphae that have extended beyond the main mass of cells in the colony can be counted. These cells may not be representative.

Data generated using this assay are shown in Table 7.1 for pairs of congenic strains (see Chapter 4 for full genotypes) and experimental details are described in a subsequent Materials and Methods section. Perhaps the most interesting feature of these data is that pseudohyphal cells have very heterogeneous lengths. This suggests that pseudohyphal cell length may be environmentally regulated. These data suggest that *phd1/phd1* pseudohyphal cells are the same length or perhaps a shorter length than wild-type cells. These data also corroborate the observation that *PHD1-2μm* strains produce longer invasive pseudohyphal cells than their wild-type counterparts. These data and the accompanying comments should give the reader a sense of the applications and limits of this assay. It is important for assay development to continue and produce improved methods of quantitating pseudohyphal growth.

Table 7.1 Lengths of Invasive Pseudohyphal Cells

Geno-type	*PHD1/ PHD1*	*PHD1/ PHD1*	*phd1/ phd1*	*phd1/ phd1*	*PHD1-2μm*	*PHD1-2μm*
Strain	CG953A	CG953B	CGX135	CGX137	CG934A	CG934B
Min.	6.6	7.3	7.1	6.8	6.1	7.3
Max.	16	15.2	13.5	12.1	19.3	18.8
N	50	50	50	50	50	50
Mean	10.1	10.7	9.7	9.1	12.5	12.3
Median	10.0	10.5	9.6	9.2	12.8	12.6
S. D.	1.9	1.8	1.3	1.1	2.8	2.1
S. E. M.	0.3	0.3	0.2	0.2	0.4	0.3

All lengths are in μm. Min. is the length of the shortest cell in the sample and Max. is the length of the longest cell in the sample. N is the sample size. Mean is the mean length and Median is the median length. S. D. is the standard deviation and S. E. M. is the standard error of the mean. CG953A and CG953B are two independent transformants isogenic to CG953 (Chapter 4) and CG934A and CG934B are two independent transformants isogenic to CG934 (Chapter 4).

Materials and Methods

Quantitation of Pseudohyphal Cell Dimensions

Strains to be tested were patched onto plates containing synthetic complete medium lacking uracil (SC-ura), grown overnight at 30°C, and then streaked to obtain single cells on fresh nitrogen starvation (SLAD) plates (25 ml). Each plate always had four streakouts on it. The streaking technique was such that a gradient of colony density existed in the streak, with the highest density existing in the center of the plate. Cultures were grown at 30°C and were analyzed after 5 days. Blocks of agar containing a colony that was well separated from its neighbors were cut out of the plates with a scalpel. A thin slice of agar containing the colony was then cut from the block and noninvasive cells were removed from it by rinsing it under a stream of water. The slice of agar containing the colony was trimmed to a 0.1 mm^2 square and placed on a microscope slide. A cover slip was then applied with gentle pressure on top of the agar slice.

Invasive intact pseudohyphae in these samples were visualized with Nomarski optics using a Zeiss Axioskop equipped with a 63X plan-apochromat objective, a 4XTV video adaptor, a Hamamatsu C2400 Newvicon video camera, a Hamamatsu Argus-10 image processor, and a Panasonic WV-5410 monochrome monitor set at moderate contrast. Images were recorded and played back using a Panasonic TQ-3031F optical memory disc recorder and cells were measured using the line measurement function on the Argus-10 image processor. This image processor was calibrated with a 20 μm scale and images were displayed at a size such that 1 μm was equal to 13 pixels. Only mature (that had budded or that were budding) pseudohyphal

cells in the linear backbones of pseudohyphae were measured. For each genotype, two independently derived yeast strains were included in the experiment. Fifty cells of each duplicate strain were measured.

Literature Cited

Andrianopoulos, A., Gimeno, C. J., Fink, G. R., and Timberlake, W. E. (1993). Unpublished data.

Andrianopoulos, A., and Timberlake, W. E. (1991). ATTS, a new and conserved DNA binding domain. Plant Cell *3,* 747-748.

Blacketer, M. J., Koehler, C. M., Coats, S. G., Myers, A. M., and Madaule, P. (1993). Regulation of dimorphism in *Saccharomyces cerevisiae*: involvement of the novel protein kinase homolog Elm1p and protein phosphatase 2A. Mol. Cell. Biol. *13,* 5567-5581.

Briza, P., Breitenbach, M., Ellinger, A., and Segall, J. (1990). Isolation of two developmentally regulated genes involved in spore wall maturation in *Saccharomyces cerevisiae.* Genes Dev. *4,* 1775-1789.

Clutterbuck, A. J. (1969). A mutational analysis of conidial development in *Aspergillus nidulans.* Genetics *63,* 317-327.

Gimeno, C. J., and Fink, G. R. (1994). Induction of pseudohyphal growth by overexpression of *PHD1*, a *Saccharomyces cerevisiae* gene related to transcriptional regulators of fungal development. Mol. Cell. Biol. *14,* 2100-2112.

Gimeno, C. J., Ljungdahl, P. O., Styles, C. A., and Fink, G. R. (1992). Unipolar cell divisions in the yeast *S. cerevisiae* lead to filamentous growth: regulation by starvation and *RAS*. Cell *68,* 1077-1090.

Hu, G.-Z., and Ronne, H. (1994). Overexpression of yeast *PAM1* gene permits survival without protein phosphatase 2A and induces a filamentous phenotype. J. Biol. Chem. *269,* 3429-3435.

Laloux, I., Dubois, E., Dewerchin, M., and Jacobs, E. (1990). *TEC1*, a gene involved in the activation of Ty1 and Ty1-mediated gene expression in *Saccharomyces cerevisiae*: cloning and molecular analysis. Mol. Cell. Biol. *10,* 3541-3550.

Liu, H., Styles, C. A., and Fink, G. R. (1993). Elements of the yeast pheromone response pathway required for filamentous growth of diploids. Science *262,* 1741-1744.

Minehart, P. L., and Magasanik, B. (1991). Sequence and expression of *GLN3*, a positive nitrogen regulatory gene of *Saccharomyces cerevisiae* encoding a protein with a putative zinc finger DNA-binding domain. Mol. Cell. Biol. *11,* 6216-6228.

Sanders, S., and Herskowitz, I. (1994). Personal communication.

Sewall, T. C., Mims, C. W., and Timberlake, W. E. (1990). *abaA* controls phialide differentiation in *Aspergillus nidulans*. Plant Cell *2,* 731-739.

Timberlake, W. E. (1990). Molecular genetics of *Aspergillus* development. Annu. Rev. Genet. *24,* 5-36.

Timberlake, W. E. (1991). Temporal and spatial controls of *Aspergillus* development. Curr. Opin. Genet. Dev. *1,* 351-357.

Wright, R. M., Repine, T., and Repine, J. E. (1993). Reversible pseudohyphal growth in haploid *Saccharomyces cerevisiae* is an aerobic process. Curr. Genet. *23,* 388-391.